

**MODEL-SCALE TESTS  
IN TURBULENT WIND**

**PART II**

**PHENOMENA DEPENDENT ON THE VELOCITY PRESSURE**

**Wind Loads on Buildings**

**MARTIN JENSEN AND NIELS FRANCK**

**The Danish Technical Press**

**COPENHAGEN**

**1965**

**MODEL-SCALE TESTS  
IN TURBULENT WIND**

**Part II**

Dedicated to Inger

**MODEL-SCALE TESTS  
IN TURBULENT WIND**

**PART II**

**PHENOMENA DEPENDENT ON THE VELOCITY PRESSURE**

**Wind Loads on Buildings**

**MARTIN JENSEN AND NIELS FRANCK**

**The Danish Technical Press  
COPENHAGEN  
1965**

## PREFACE

In 1958 a paper called "The Model-Law for Phenomena in Natural Wind" was published. It gave a short account of some of the most important findings which are now dealt with in detail in the present, Part II, and in a previous treatise, Part I.

The paper mentioned had the following introduction:

"A great many technical circumstances depend on the wind in nature and cannot, or can only with great difficulty, be analysed except through model tests.

As examples may be mentioned the wind load on buildings and structures, the contamination of the air from chimneys, and the various sheltering problems in agriculture and in living spaces between buildings.

There is an unquestionable need of model tests, and as a matter of fact, a great many model tests have been carried out in the course of time within the said fields and similar fields in the aerodynamic laboratories.

These investigations, however, are to some extent misleading, because the test procedure, especially the model-law, has been wrong. It may seem strange that within a vast research field incorrect model-laws have been applied, but the explanation is both simple and not very flattering: the model tests have practically never been checked by full-scale tests in nature.

The natural wind is turbulent, and the phenomena dealt with in this paper take place in the boundary layer of the wind, and, as should be emphasized, are highly dependent on the nature of this boundary layer.

Unfortunately, however, almost all previous tests have been carried out in wind-tunnels with as far as possible a smooth flow of air, and as for models of objects standing on the ground, it has moreover been tried earnestly to avoid the boundary layer of the wind tunnel.

The correct model test for phenomena in the wind must be carried out in a turbulent boundary layer, and the model-law requires that this boundary layer be to scale as regards the velocity profile."

The present paper deals with wind loads, that is phenomena depending on the velocity pressure of the wind. The purpose is primarily to prove that the model law, described in Model Scale Tests, Part I, is also valid for such phenomena.

The model law demands, that in model tests for pheno-

mena in the natural wind consideration must be given to the turbulence in the wind. To obtain agreement between the model test and nature the turbulence in the air flow in the model test should correspond to the turbulence in the natural wind.

Besides this demonstration of the validity of the model law for model tests concerning wind load, this treatise contains partly a description of an experimental technique that takes the model law into account, and partly the results of measurements of wind load on different models of houses and free roofs.

The experiments were carried out in the Wind Laboratory of the Technical University of Denmark during the years 1957 to 1960.

The economic support for the investigations was provided by The Institution of Danish Civil Engineers, Danish Council for Scientific and Industrial Research and The Danish National Institute of Building Research.

Mr. K. Johannessen, head of a laboratory workshop at the Technical University of Denmark, has given very valuable assistance in the construction of the models and experimental apparatus.

The translation into English was performed by Mr. J.O. Carroll, B.E.

Figures and tables are numbered according to the page on which they are printed. Thus, Figure 18 is to be found on page 18.

## CONTENTS

PREFACE	v
1. APPARATUS AND EXPERIMENTAL TECHNIQUE	1
1.1 House in nature. Pitot--static tube for measuring in nature.	1
1.2 Wind tunnel.	3
1.3 Tunnel coatings.	4
1.4 Models of houses and free roofs.	6
1.5 Turntable. Multi-manometer.	9
1.6 Model arrangement and measuring procedure.	12
2. INVESTIGATION OF THE BLOCKING-EFFECT IN THE WIND TUNNEL	14
3. THE MODEL LAW	17
3.1 Introduction.	17
3.2 Choice of $q_{ref}$ .	18
3.3 Wind load on the Albertslund house.	19
3.4 Wind load on the model of the Albertslund house.	23
3.5 Conclusion.	28
4. STREAM FLOW ABOUT A HOUSE	35
4.1 Introduction.	35
4.2 Experimental arrangement and technique.	38
4.3 Test results.	39
5. EXTERIOR WALLS	42
5.1 Key to the models.	42
5.2 Scope of the tests.	43
5.3 Test results.	43
5.4 Conclusions.	46
6. HORIZONTAL ROOFS ON HOUSES	62
6.1 Scope of the tests.	62
6.2 Test results.	62
6.3 Conclusions.	63

7. DESK ROOFS ON HOUSES	70
7.1 Scope of the tests.	70
7.2 Test results .	71
7.3 Conclusions.	73
8. SADDLE ROOFS ON HOUSES	100
8.1 Scope of the tests.	100
8.2 Test results.	100
8.3 Conclusions.	106
9. FREE DESK ROOFS	138
9.1 Scope of the tests.	138
9.2 Test results.	140
9.3 Conclusions.	150
10. FREE TROUGH AND SADDLE ROOFS	155
10.1 Scope of the tests.	155
10.2 Test results.	155
10.3 Conclusions.	167
BIBLIOGRAPHY	170

Figures and tables are numbered according to the page on which they are printed. Thus, Fig. 18 is to be found on page 18.

# 1. APPARATUS AND EXPERIMENTAL TECHNIQUE

## 1.1 House in nature. Pitot-static tube for measuring in nature

House in nature. In order to compare measurements of wind pressure on a house in nature and a corresponding model in the wind tunnel, a small house was built and placed in nature.

The house was 305 cm long, 150 cm wide and 163 cm high. It had a saddle roof with a slope of 1÷10, see Figure 2. The house was built of 3.5 mm thick masonite plates which were nailed to a framework of battens. In one gable of the house was a removable shutter.

In the plane of symmetry of the house, points for measuring the pressure or suction of the wind were placed. In all there were fourteen measuring points, five in the windward wall, three in the leeward wall, and three in each of the two roof sections. The placing is shown on the cross section of the house in Figure 2.

The measuring holes were 2 cm in diameter. At each measuring hole a 20 mm tube stub was fastened behind the masonite plate, at right angles to it. A 20 mm rubber tube was fixed to this tube stub, leading to one side of a manometer. A detail of the measuring hole is shown in Figure 2.

The house could turn in relation to the wind direction. On account of its small weight the house had to be fastened to wooden planks hammered into the ground.

Pitot-static tube for measuring in nature. For measurement of wind velocity and static pressure in nature a pitot-static tube was used as shown in Figure 3.

The pitot-static tube is hinged on a vertical axis on a closed housing of steel plate. The wind vane consists of a double plate and a head, h, interconnected by a 1" tube, open at the front end of the vane at h, and closed at the other end. At right angles and in open connection to this tube is welded another 1" tube, turning on two ball bearings, placed in the housing.

The vertical tube is connected with a U-shaped tube, ending in a stub outside the housing, by means of an oil

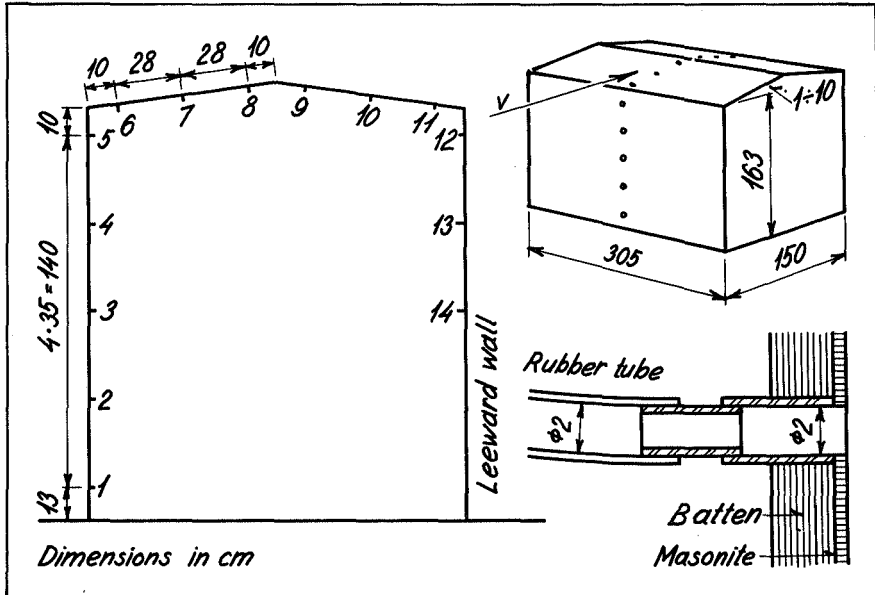


Fig. 2. The Albertslund house.

House for measuring the wind load in nature.

This is a lightweight construction with walls and roof of masonite on a framework of battens. It can easily be placed in the correct position in relation to the wind.

The measurements of pressure and suction were carried out by photographing the manometers connected to the measuring holes numbered 1 ..... 14.

trap. At this stub the total pressure of the wind is obtained.

A cylindrical mantle, c, is clamped to the vertical tube of the wind vane. This mantle is provided with two slits in the direction of the generators at the two places, where the air pressure on the cylinder is zero. By means of an oil lock, this pressure is transmitted to the housing. The upper stub on the housing is in direct connection with the inside of the housing. Here the static pressure is obtained.

The two stubs are connected with 20 mm rubber tubes to the manometer thus directly showing the difference between the two pressures, i.e. the velocity pressure.

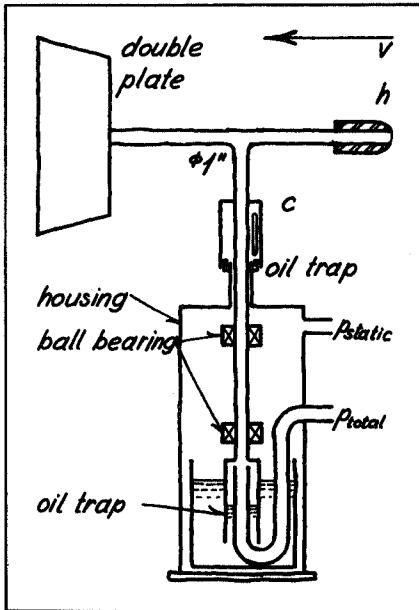


Fig. 3. Pitot-static tube for measurements in nature.

The wind vane holds the head  $h$  against the wind. The opening at  $h$  takes the total pressure of the wind, i.e. static pressure plus velocity pressure. The total pressure is conducted through the lower oil trap to the lower stub on the housing.  $c$  is a circular cylinder, having two slits in the generators where the wind pressure is zero. Here the static pressure is obtained. It is conducted via the upper oil trap to the upper stub on the housing.

The total height of the apparatus is 1.3 m.

## 1.2 Wind tunnel

In all the model tests the wind tunnel described in Part I, Section 1.2, with enclosed working section, open return flow and with 60·60 cm cross-section is used.

However, the working section of the tunnel was lengthened by 2 m for the model tests described in this paper, so that the distance from the honeycomb at the inlet end to the honeycomb after the 4th working section was 7.5 m. The additional length was inserted between section 1 and 2, see Part I, Figure 5.

The purpose of this lengthening of the tunnel was to make it possible to produce a higher turbulent boundary layer over the tunnel bottom.

### 1.3 Tunnel coatings

The tunnel coatings given in the Table were used to produce different turbulent boundary layers over the tunnel bottom.

In all cases the coating extended from the honeycomb at the inlet end to the 4th working section, i.e. over a length of 7.5 m. The coating extended over the entire width of the tunnel.

Apart from the coating no. 6, 1.1 cm lists, all the coatings given in the Table are described in Part I, Section 1.4. However, in Part I only one type of sandpaper is used, whilst here two types with different grain sizes are used.

Tunnel coating no. 6 consist of 60 cm long wooden strips, cross-section 1.1 cm, placed across the tunnel, forming an angle between  $90^\circ$  and  $70^\circ$  with the longitudinal axis, at intervals varying at random from 10 to 15 cm.

The velocity profiles for the tunnel coatings given in the Table are shown in Figure 5.

The velocity profiles shown are measured in the 4th section of the tunnel. In the Table is given the roughness parameter  $z_0$  as well as the thickness of the boundary layer in the 4th section.

For tunnel coating no. 7, 2.5.2 cm lists, the roughness parameter  $z_0$  can vary somewhat with the placing of the lists in the tunnel. Therefore in the Table the interval is given in which  $z_0$  is situated for the tests with tunnel coating no. 7 described in this paper. The velocity profile for tunnel coating no. 7 shown in Figure 5 corresponds to  $z_0 = 0.6$  cm.

Tunnel coatings	$z_0$ cm	Thickness of the boundary layer in 4th section. cm
1. Smooth masonite sheets	$1.8 \cdot 10^{-3}$	13
2. Sandpaper, fine	$0.7 \cdot 10^{-2}$	14
3. Sandpaper, coarse	$1.85 \cdot 10^{-2}$	15
4. Corrugated paper	0.047	18
5. Broken stones	0.21	20
6. 1.1 cm lists	0.21	22
7. 2.5.2 cm lists	0.4 - 0.7	28
8. 7.3 cm lists	2.3	35

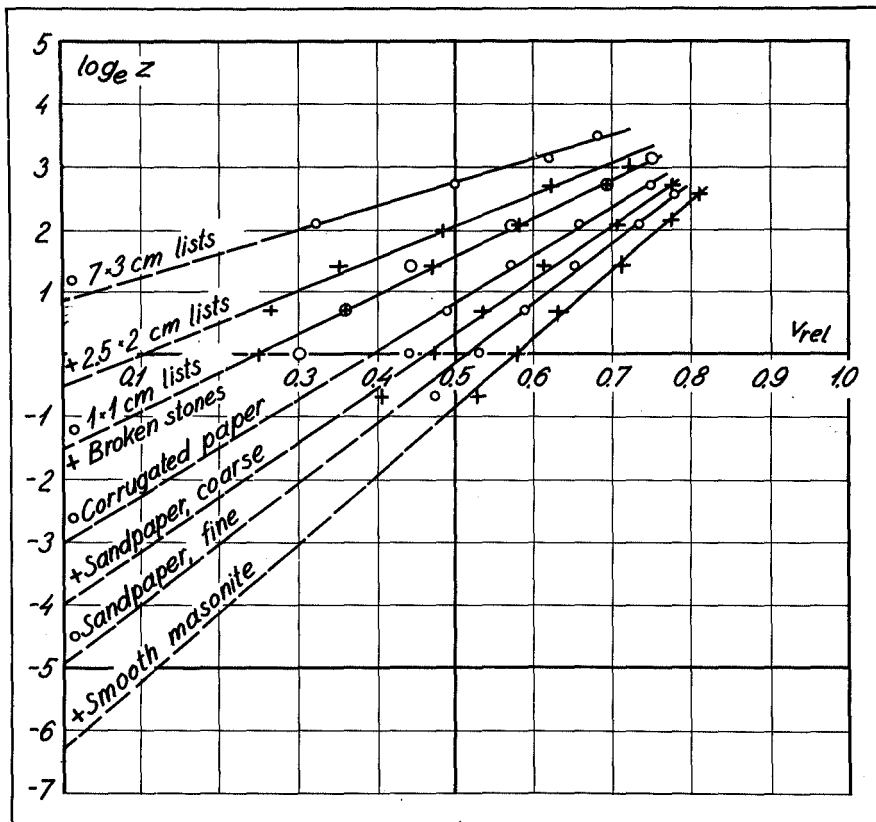


Fig. 5. Velocity profiles over different coatings of the bottom of the wind tunnel.

The abscissa is the relative speed of the wind, the speed at 100 cm level having been fixed at 1.00. The ordinate is the logarithm of the height above the surface.

For tunnel coating no. 5, broken stones, and no. 8, 7.3 cm lists, the corresponding condition asserts itself. Therefore the velocity profiles shown in Figure 5 and the corresponding  $z_0$  values are not fully identical with those given in Part I, Section 1.4.

The boundary layer thickness in the 4th section is bigger than for the corresponding coating in Part I. This is due to the 2 m longer tunnel used in all tests described in Part II.

### 1.4 Models of houses and free roofs

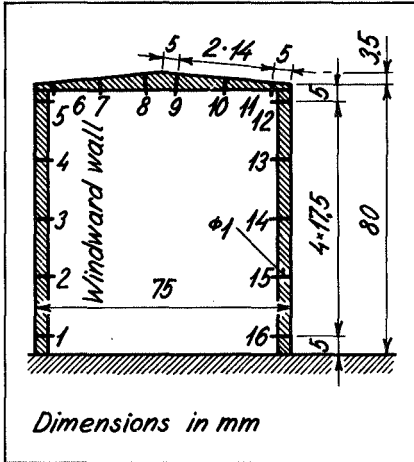


Fig. 6. Model of the Alberts-lund house.

The model, made of plywood, is in scale  $1:20$  to the house in nature. The length of the model is 152 mm.

Models of houses. In the tests in the wind tunnel house models made either of wood or brass were used. All the models were hollow and without bottom.

The wooden models were built of 3 to 6 mm plywood. Such a model is shown in Figure 6.

The brass models, Figure 7, were built of 1 to 5 mm plates, which were soldered together along the edges of the model.

All the models had smooth surfaces.

The models were placed on the bottom of the tunnel on the turntable, described in Section 1.5.

Models of different typical house shapes were used. The individual model types and their data will be described in that part of the paper where tests with the model concerned are dealt with.

The roof and walls of the models were provided with measuring holes in numbers and positions which made it possible to obtain a satisfactory picture of the distribution of pressure and suction over the model surface. The measuring holes in the roofs were placed in greatest numbers at the corners, where experience has shown the greatest suction values to occur.

In the measuring points, at right angles to the surface thin steel tubes, internal diameter 1 mm, external diameter 1.5 mm, were inserted, so that one end of the tubes lay in the plane of the model surface, as shown in

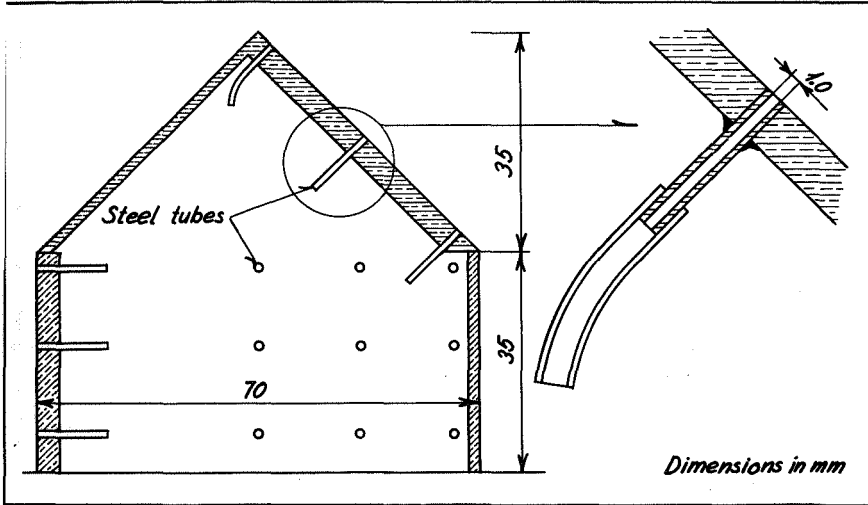


Fig. 7. Model of a house.

The model is made of brass plate. It consists of two parts, a 35 mm high lower part and the roof. Different lower parts and roofs can then be combined to give the house types desired.

Figure 7. The tubes were soldered to the brass models and glued to the wooden models.

To the end of the tube inside the model, a rubber tube, internal diameter 1.5 mm, was fastened. The rubber tube led out of the tunnel to the manometer, see Figure 11.

On all the brass models either the roof or one of the walls was fastened with screws to the remaining part of the model and could be removed whilst mounting the rubber tubes.

In the tests given in Section 2 steel tubes for the measuring holes were used which had other dimensions than those above. The conditions are more explicitly described in the section concerned.

Models of free roofs. In the tests of the wind loading on free roofs two models were used:

Model of a desk roof

model of a pitched or through roof.

The model of the desk roof consist of a 3.5 mm thick brass plate of length 60 cm and width 10 cm. The model was placed across the tunnel at right angles to the wind. The model was supported at the tunnel walls on a system of blocks and wedges, which made it possible to vary the in-

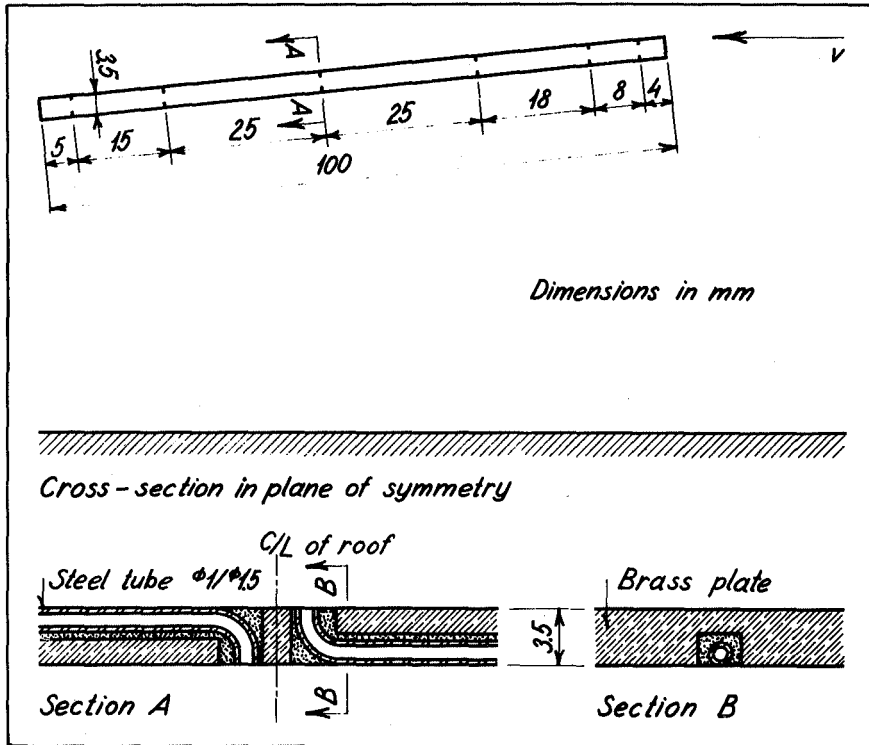


Fig. 8. Model of free, desk roof.

The model was placed across the tunnel at right angles to the wind, so that the experiments are two-dimensional.

The model was placed at different heights over the tunnel bottom and the slope of the roof was varied.

clination of the model in relation to the wind and the height over the tunnel bottom.

When the model is just exposed for wind at right angles to the longitudinal axis only measuring holes in the plane of symmetry are used. Six measuring points were placed over the cross-section on each side of the plate, as shown in Figure 8.

The measuring holes were made in the following way: In the brass plate was milled, from the middle to the end of the plate, a 1.5 mm deep groove corresponding to each of the holes. In these grooves were placed thin steel tubes, internal diameter 1 mm, which were bent  $90^\circ$  at the middle of the plate and put through the holes in the plate. After

the tubes were placed, the grooves were soldered. The plate was then polished smooth and the projecting ends of the tube were ground level with the brass plate. A detail of the measuring hole is shown in Figure 8.

At the free end of the tube at the tunnel wall rubber tubes were joined, connecting to the manometer.

Besides the model described above another model of thickness 6.8 mm was used, made of the above mentioned plate, together with an equally thick, congruent plate without measuring holes.

The model was placed across the tunnel, supported at the tunnel walls. The model could be fixed at different heights over the tunnel bottom and at different slopes in relation to the wind. Only roofs where the slope of the two roof plates were the same were tested. The notch between the two roof plates was sealed with tape in all tests.

### **1.5 Turntable. Multi-manometer.**

Turntable. For the mounting of the house models a turntable was built into the tunnel bottom at the front of the 4th working section.

The turntable consisted of a brass plate, 6 mm thick, 21 cm in diameter. The surface of the turntable was set exactly horizontal, level with the tunnel bottom.

Around the edge of the turntable a graduated scale was engraved, so that the orientation of the models in relation to the wind direction could be read off.

In the center of the turntable was a hole, 3 cm in diameter. In this hole was fastened a steel tube, which protuded under the tunnel bottom. This tube was set in brass bearings fastened to the underside of the tunnel bottom. At the lower free end of the tube a handle was fixed, enabling the turntable to be rotated.

The house models were fastened to the turntable by means of a thin bolt, placed in the center of the steel tube and tightened by a nut at the lower end of the tube.

The rubber tubes from the models measuring points were led from inside the model out of the tunnel through the steel tube.

Figure 10 shows the mounting of a model on the turntable.

During the tests with turbulent boundary layers in the tunnel, the tunnel coating was laid up to the turntable, but not over it.

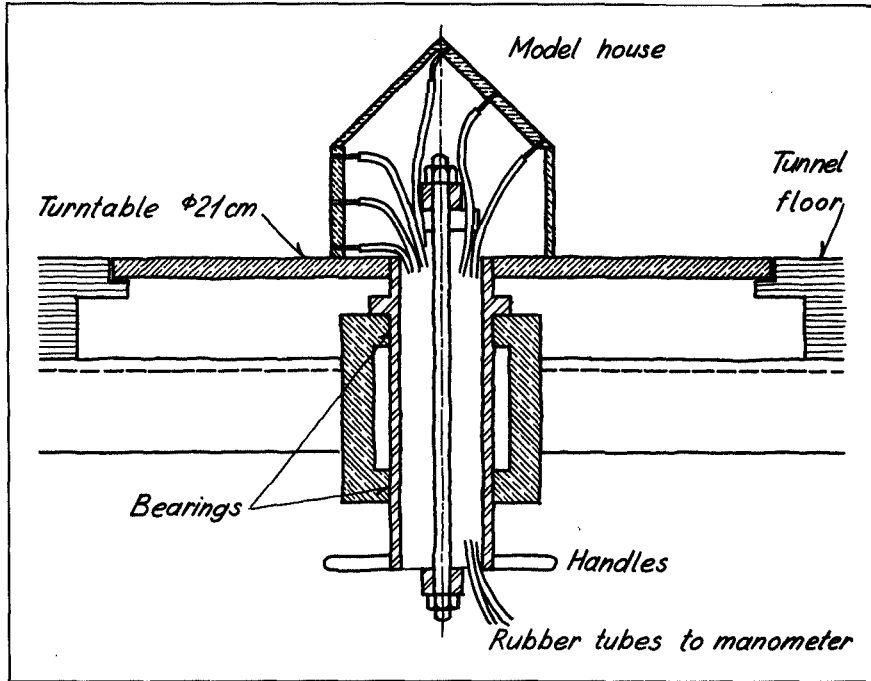


Fig. 10. Model of a house on a turntable.

The house model is fastened to the turntable. Rubber tubes are connected through the hollow turning axle to the multi-manometer shown in the next Figure.

Multi-manometer. A manometer with 15 tubes was built for simultaneous measurements at 15 different points on a model.

The multi-manometer is shown in Figure 11. The glass tubes are inclined so that the pressure is found in mm water column, when the manometer reading is multiplied by 0.4 and alcohol with specific gravity 0.8 is used as manometer liquid.

The 15 glass tubes have an internal diameter of 2.5 mm, external diameter 6.5 mm. The measuring length of the tube is 21 cm, 7 cm below and 14 cm above zero. The scale, graduated in mm, is placed under the tubes.

By placing the zero point in the bottom third of the tubes, it is possible to measure simultaneously pressure and suction at the manometer.

The reservoir of the multi-manometer has a surface area of 278 cm<sup>2</sup>, which is 380 times as large as the total

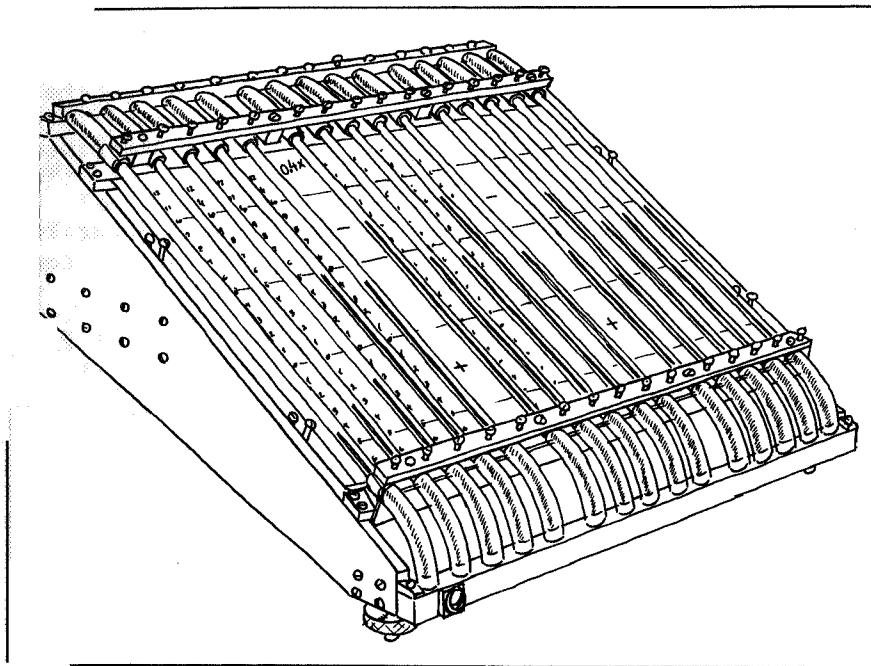


Fig. 11. Multi-manometer.

The multi-manometer has 15 glass tubes, so inclined that the enlarging factor, using alcohol, is 2.5.

There is a common reservoir for all the tubes. It is placed so that the zero point is in the bottom third of the tubes. Pressure up to 24 mm water pressure and twice as much suction can be measured.

The length of the manometer tubes is 21 cm.

cross sectional area of the tubes.

For the measurement on a house model in the tunnel, the top side of the reservoir is connected to the static pressure in the tunnel, while the upper ends of the tubes are connected to the measuring points.

## 1.6 Model arrangement and measuring procedure

The experimental technique applied for the determination of the wind load on a model of a house placed in the turbulent boundary layer in the wind tunnel is described in this section.

- 1) The turntable is mounted in the 4th section of the tunnel and a suitable coating is placed on the tunnel bottom over its whole length.
- 2) Below the tunnel roof in the 3rd section a Prandtl pitot-static tube, as described in Part I, Section 1.2, is placed over the boundary layer. With this and a FUESS manometer, Part I, Section 1.2, the velocity in the air stream over the turbulent boundary layer is measured.
- 3) The velocity profile in the 4th section is measured with the pitot-static tube for precision measurements, described in Part I, Section 1.2. The hole in the turntable is of course closed when this takes place.
- 4) The difference, usually small, between the static pressure at the Prandtl pitot tube above the boundary layer and the static pressure in the boundary layer at the position of the model is determined.
- 5) The house model is placed on the turntable and the 15 measuring holes are connected with rubber tubes to the upper end of the manometer tubes. In order to obtain a damped reading, a 60 cm long capillary tube, internal diameter 1 mm, is inserted between each measuring point and the manometer.
- 6) The static pressure from the Prandtl pitot tube is connected to the top of the reservoir of the multi-manometer.
- 7) Before the proper measuring takes place, a survey of the variation in pressure and suction at the 15 measuring points is made by observation of the manometer when the model is turned in relation to the wind direction. In this way the model positions of special interest can be found, and the general trend of the wind loading relationships can be observed.
- 8) With the model placed in the positions of special interest, measurements are taken of the loading at the 15 measuring points, possibly with several different wind directions in the tunnel.

The values of pressure and suction at the measuring points are made dimensionless by division with the velocity pressure in the turbulent boundary layer level with the ridge of the model.

In this way the shape factor  $c$  for the individual points is found.

The velocity pressure level with the roof of the model is found by multiplying the velocity pressure at the Prandtl pitot-static tube by a factor, which is the ratio between the simultaneously measured velocity pressure in the roof level without model in the tunnel and at the Prandtl pitot-static tube.

In calculating the  $c$ -values there must be a correction made for the difference that can occur between the static pressure at the Prandtl pitot-static tube and the static pressure at the model, since it is really the last mentioned, that should be applied at the top side of the reservoir of the multi-manometer.

Obviously it would have facilitated the measurements if the Prandtl pitot-static tube could simply have been placed in the boundary layer at the level of the roof of the model. The tunnel used at the Wind Laboratory is, however, too narrow for such placing of the pitot tube.

## 2. INVESTIGATION OF THE BLOCKING-EFFECT IN THE WIND TUNNEL

In this section is described the investigations seeking to clarify how large a model can be used in the wind tunnel without causing systematic errors in the measurements, due to the narrowing of the tunnel section by the model.

5 models in different scales were made of the Alberts-lund house, described in Section 1.1. The models were made of wood. The roof slope was 1:10, the length of the house was twice the width, and the height was about the same as the width.

In Table 14 data concerning the models is given. Model 1 was the smallest, model 5 the largest, linearly 4 times as large as model 1.

16 measuring points were located in the plane of symmetry as shown in Figure 6. The steel tubes inserted in the measuring points had different internal diameters, growing with the model size, see Table 14.

The models were placed in the 4th working section of the tunnel, and were tested only for wind at right angles to their longitudinal axes.

Table 14

Model No.	h	l	w	d	Roughness	$z_0$ cm	$\frac{h}{z_0}$	$\frac{A_m}{A_t}$
1	42	76	38	0.61	Sandpaper, fine	$0.7 \cdot 10^{-2}$	600	.009
2	65	117	58	0.75	Sandpaper, coarse	$1.85 \cdot 10^{-2}$	350	.021
3	84	152	75	1.00	Sandpaper, coarse	$1.85 \cdot 10^{-2}$	450	.035
4	129	235	115	1.35	Corrugated paper	$4.7 \cdot 10^{-2}$	275	.084
5	168	305	150	2.00	Corrugated paper	$4.7 \cdot 10^{-2}$	360	.142

h, l, w = height, length, width.

d = diameter of measuring holes.

Table 15

Measuring point no.	Model				
	1	2	3	4	5
1	0.58	0.58	0.57	0.57	0.56
2	0.54	0.49	0.49	0.47	0.46
3	0.63	0.59	0.58	0.54	0.54
4	0.72	0.70	0.67	0.65	0.66
5	0.46	0.41	0.45	0.43	0.40
mean	0.58	0.55	0.55	0.53	0.52
6	-0.80	-0.92	-0.90	-1.25	-1.36
7	-0.83	-0.95	-0.95	-1.28	-1.40
8	-0.78	-0.81	-0.83	-1.02	-1.26
mean	-0.80	-0.89	-0.89	-1.18	-1.34
9	-0.66	-0.70	-0.69	-0.83	-1.03
10	-0.53	-0.54	-0.54	-0.62	-0.84
11	-0.44	-0.42	-0.45	-0.48	-0.68
mean	-0.54	-0.55	-0.56	-0.64	-0.85
12	-0.31	-0.33	-0.33	-0.39	-0.59
13	-0.28	-0.31	-0.31	-0.40	-0.54
14	-0.25	-0.28	-0.29	-0.38	-0.54
15	-0.24	-0.27	-0.26	-0.36	-0.49
16	-0.27	-0.32	-0.30	-0.35	-0.49
mean	-0.27	-0.30	-0.30	-0.38	-0.53

Tunnel coatings of different roughnesses were used, as specified in Table 14, adapted so that the ratio between  $z_0$  and the model height in all cases was as far as possible the same.

The shape factors,  $c$ , are calculated as the ratio between the wind pressure on the model and the velocity pressure in the free stream in the tunnel, level with the ridge of the house.

Table 15 gives the results. It can be seen, that the windward wall has approximately the same  $c$ -values independent of model size. For the leeward wall and for the two roof sections there is good agreement between the results from models 1, 2 and 3. However, the results from models 4 and 5 differ appreciably. This deviation is due to a systematic error caused by the narrowing of the tunnel cross section. (Blocking-effect).

In Table 14 in the last column is given the relation between the front area  $A_m$  of the model and the tunnel cross

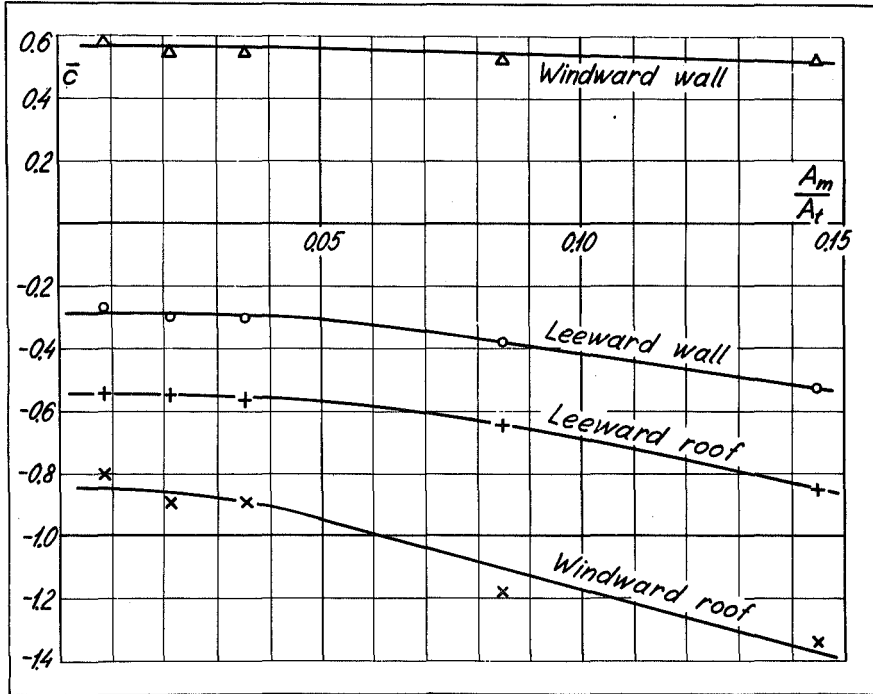


Fig. 16. The blocking-effect of the model.

The wind loading on 5 similar models of different sizes was measured.

The abscissa is the ratio between the projected area of the model house on a plane at right angles to the wind and the cross-sectional area of the tunnel. The ordinate is the mean value of the shape factor for the respective surfaces.

The roughness of the tunnel bottom was matched, according to the model law, as far as possible to the different models.

It appears, that the model should not block more than 5% of the tunnel, if errors are to be avoided.

sectional area  $A_t = 3600 \text{ cm}^2$ . This ratio can be taken as an expression for the narrowing of the tunnel cross-section.

In Figure 16  $A_m \div A_t$  is used as abscissa and the mean of the  $c$ -values for each surface in the different models is used as ordinate.

The curve trend indicates, that measurements can be taken with models having a front area of up to 5% of the cross-section, without risking appreciable systematic errors.

### 3. THE MODEL LAW

#### 3.1 Introduction

In "Model-Scale Tests", Part I, the law for model tests in the turbulent boundary layer is dealt with in relation to the phenomena dependent on the wind velocity, such as shelter effect and dispersal of smoke from chimneys.

In the present section it shall be shown, that the same model law is valid for phenomena depending on the velocity pressure.

The wind velocity in a turbulent flow over a rough surface follows the logarithmic law

$$\frac{v(z)}{v_*} = \frac{1}{\kappa} \log_e \frac{z + z_0}{z_0}$$

where  $v(z)$  is the velocity at the height  $z$ ,  $v_*$  is the friction velocity,  $\kappa = 0.4$  is Kármán's constant and  $z_0$  is the roughness parameter.

The logarithmic velocity profile is the most notable feature in a pure roughness flow. The condition of model tests is, that the velocity profile in the wind tunnel must be similar to that in nature, or, expressed more simply, that the roughness parameter for the coating of the tunnel bottom must be proportional to the roughness parameter in nature:

$$\frac{Z_0}{z_0} = \frac{D}{d},$$

where  $Z_0$  and  $z_0$  are the roughness parameter in nature and wind tunnel, respectively,  $D$  and  $d$  are a dimension of the object in nature and tunnel, respectively.

In order to show the validity of the model law in model tests with wind load on houses, measurements were first carried out for the wind load on a house in nature. Later the wind load on a model of this house placed in boundary layers of different turbulences in the wind tunnel was measured.

Some of the coatings used in the wind tunnel were smoother, others rougher than those corresponding to the terrain where the experiments in nature were carried out.

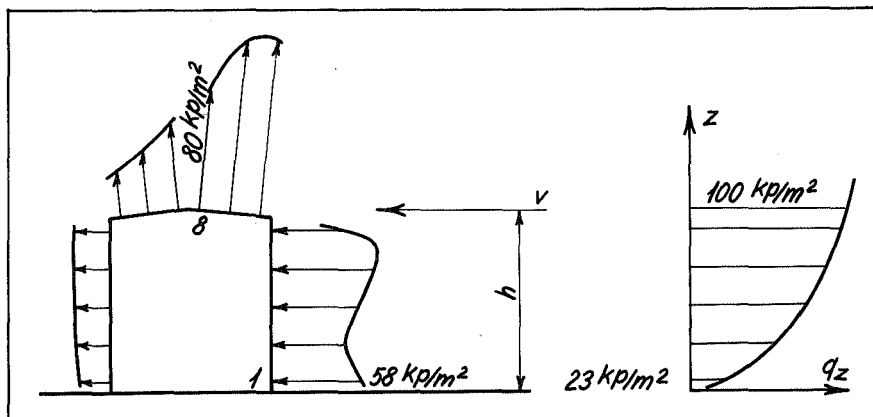


Fig. 18. See text.

### 3.2 Choice of $q_{ref}$

When the wind load on houses in nature, where the free wind increases with the height, is measured, or when model tests in a tunnel with corresponding velocity profile are carried out, the problem of which velocity pressure to refer to in calculating the shape factor arises.

In Figure 18 to the left is shown the wind load on a house. To the right is shown the variation of the velocity pressure with the height.

In principle the velocity pressure at each height together with each measured value of the load of the house can be used. With this freedom of choice practical considerations can be taken into account.

There are two simple ways: The wind load at a determined point can be made dimensionless by division with the velocity pressure in the free wind at the same height as the point. Or the velocity pressure at a determined height in the free wind can be used for all wind loads. If so it seems that the height to the ridge of the house is the most reasonable.

If the last proposal is used the measured wind loads in the Figure must be divided by  $100 \text{ kp/m}^2$ . This gives for point 1,  $c = 0.58$  (pressure), in point 8,  $c = 0.80$  (suction) etc.

If the velocity pressures at the respective heights are used, the pressure in point 1,  $58 \text{ kp/m}^2$ , must be divided with a velocity pressure of  $23 \text{ kp/m}^2$ , i.e.  $c = 2.52$ .

The free wind velocity pressure level with point 8 is  $97 \text{ kp/m}^2$ . Here  $c = 1.07$  (suction) is obtained.

For the roofs there is naturally only a small difference between the two methods, but lower down the difference is large.

The  $c$ -values corresponding to the velocity pressure level with the top of the house must be preferred. Firstly they are easier to use: For a given house all the calculations of the wind load can be made dimensionless and so only at the end multiplied with the velocity pressure. Secondly it is rather disagreeable for a physicist to work with  $c$ -values for pressure which are greater than 1 (e.g.  $c = 2.52$ ).

### 3.3 Wind load on the Albertslund house

The house described in Section 1.1 was placed in an open field at Albertslund, a farm about 20 km west of Copenhagen.

The tests referred to below were performed on the 7th May 1958. The weather was overcast with a wind of about 10 m/s at a height of 2 m above the ground. The field was at that time covered with 5 to 7 cm high wheat.

A plan of the test arrangement is shown in Figure 20. The measurements were taken with wind from the West, because the terrain in this direction was completely open and flat over a long distance.

The wheat field stretched in this direction about 100 m from the measuring place, so that it was certain there was a sufficiently thick boundary layer, formed by the roughness of the field, at the measuring place.

The velocity profile over the field was measured with four cup-anemometers, placed on a 6 m high, braced lattice mast, as described in Part I, Section 1.1. The anemometers were placed at heights 6.14 m, 3.51 m, 1.85 m and 1.02 m.

The velocity profiles measured are shown in Figure 21. The roughness parameter is  $z_0 = 0.95 \text{ cm}$ .

About 3 m from the southern gable of the house a pitot-static tube of the type described in Section 1.1. was placed, with the measuring height 1.7 m above the terrain. This measured partly the velocity pressure level with the roof of the house, partly the static pressure.

Inside the house were placed two FUESS manometers. One of these measured the velocity pressure at the pitot-static tube. The other manometer was connected at one side to the static pressure from the pitot-static tube and at the other to the pressure or suction from one of the 14 measuring

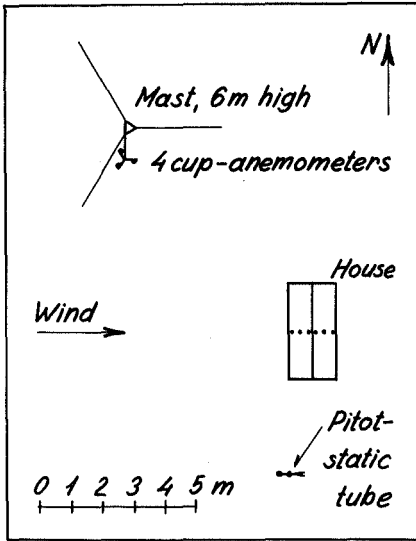


Fig. 20. Measurements of the wind load on a house in nature, the Albertslund house.

The house is shown in Figure 2. Figure 3 shows the pitot-static tube placed level with the ridge of the house. The static pressure was taken from the pitot-static tube and led to the manometer, the other side of which was connected to the measuring holes in the walls and roof of the house.

The pitot-static tube was also connected to a manometer for measuring the velocity pressure level with the ridge.

The velocity profile, shown in Figure 21, was measured on four cup-anemometers, placed on a 6 m tall mast, N.N.W. of the house.

The terrain was flat and open. From the house a field of wheat 5 to 7 cm high stretched about 100 m westward.

points in the symmetry plane of the house, see Figure 2.

Because of pulsations in the natural wind the manometers cannot be read directly. They are therefore photographed, both on the same picture.

The simultaneous reading of the two manometers were later read off the film.

A capillary tube was inserted in the total pressure tube of the pitot-static tube and in the tubes from the individual measuring points in order to damp pulsations in the manometer reading.

For each of the measuring points no. 5, 6 and 7, see Figure 2, 23 pictures in all were taken at 15 sec. intervals.

For the remainder of the measuring points about 11 pictures at 15 sec. intervals were taken of each point.

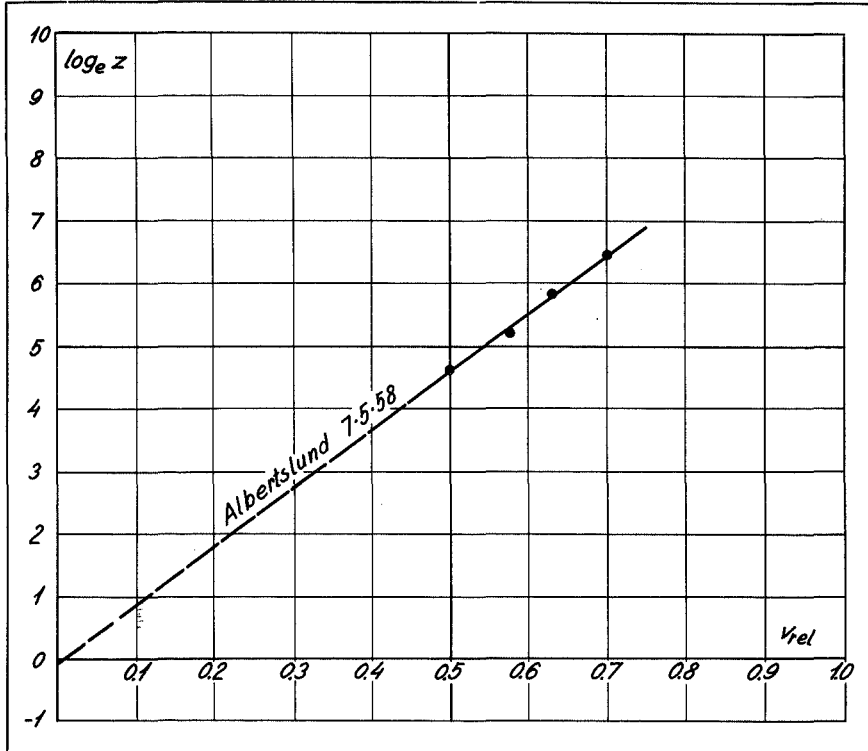


Fig. 21. Velocity profile at the Albertslund house.

The abscissa is the wind velocity relative to the velocity at 100 m height. The ordinate is the logarithm of the height above the ground. The roughness parameter is 0.95 cm.

The terrain is a field of wheat about 5 to 7 cm high.

In addition, points no. 4, 7 and 13 were measured with undamped manometer, in order to compare the effect of the manometer damped and undamped. For the undamped manometer 36 pictures at 10 sec. intervals were taken for each of the 3 points.

In Table 23 are given the results from point 4 with manometer damped as an example of the test results and their handling.

The shape factor  $c$  for the measuring point is found as the ratio between the simultaneous measured values of pressure at the point and the velocity pressure at the pitot-static tube.

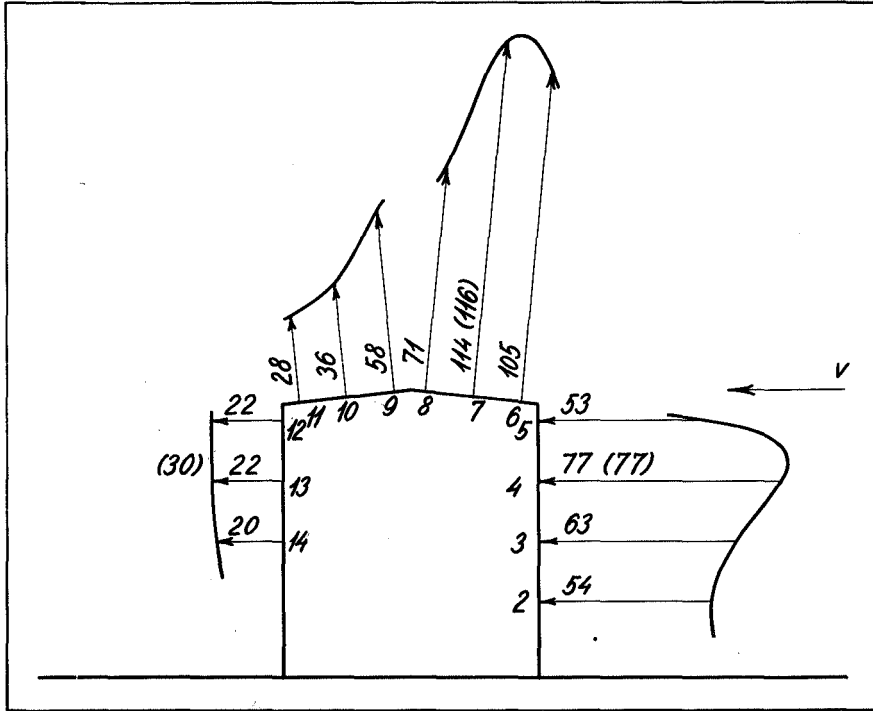


Fig. 22. The wind load on a house in nature, the Albertslund house. The wind load is noted as a percentage of the velocity pressure level with the ridge.

The measurements are carried out with damped manometers. The measuring points 4, 7 and 13 were also tested with undamped manometer. The results are noted in the parenthesis.

For the damped manometer the mean value of the shape-factor is  $\bar{c} = 0.77$  (pressure).

For the undamped manometer a mean value of  $\bar{c} = 0.77$ , based on 36 pictures, was also found.

The complete result of the measurements on the house in Albertslund is shown in Figure 22. The shape factors given are calculated as the mean of all the observations for each measuring point, and are relative to the velocity pressure in the free wind at the roof level.

The arrows in the Figure give the loading direction; pressure towards the surface, suction away from it.

Table 23

photo No.	Q mm H <sub>2</sub> O	P mm H <sub>2</sub> O	$c = \frac{P}{Q}$
1	8.03	4.8	0.60
2	7.68	5.8	0.76
3	7.83	6.3	0.80
4	9.33	7.2	0.77
5	4.83	4.15	0.86
6	4.88	3.5	0.72
7	5.03	3.6	0.71
8	5.23	4.65	0.89
9	7.83	7.05	0.90
10	10.33	7.3	0.70
11	10.33	7.3	0.71

$$\bar{c} = 0.77$$

Q: velocity pressure at the pitot-static tube.

P: pressure at the measuring point.

### 3.4 Wind load on the model of the Albertslund house

A wooden model of the Albertslund house was built to the scale 1:20, see Figure 6. In the plane of symmetry measuring points corresponding to the measuring points on the Albertslund house were placed, except in the model there were 5 measuring points in each facade.

The model was placed on the tunnel bottom in the 4th section with the longitudinal axis at right angles to the wind direction. The wind load on the plane of symmetry of the model was determined at 7 different turbulent boundary layers in the tunnel.

In Table 24 the tunnel coatings used, their roughness parameters  $z_0$  and the relation between model height and  $z_0$  are given.

In addition to the seven tests mentioned, where the model was placed in a turbulent boundary layer, there was also carried out a test with the model placed on a thin plate, suspended horizontally in the middle of the tunnel

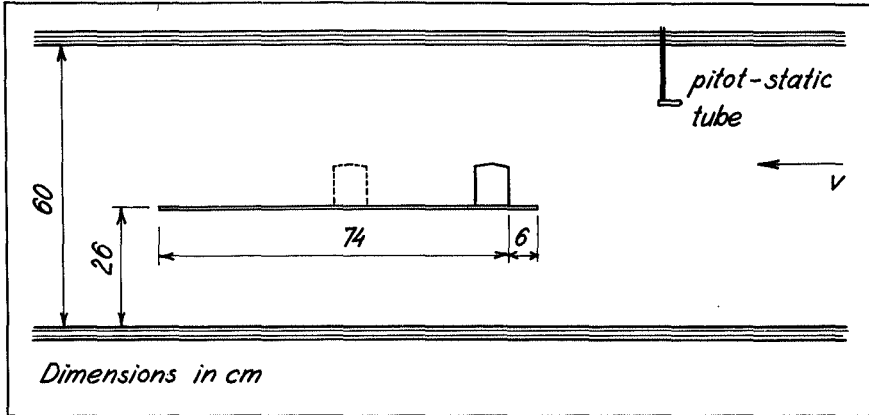


Fig. 24. Model of the Albertslund house placed on a plate freely suspended in the wind tunnel.

Tests with the model placed 6 cm and 36 cm from the leading edge of the plate were carried out.

Such a model arrangement is often used, in spite of the incorrect results it causes.

Table 24

Tunnel coatings	$z_0$ cm	$h/z_0$
Masonite	$1.8 \cdot 10^{-3}$	4600
Sandpaper, coarse	$1.85 \cdot 10^{-2}$	450
Corrugated paper	0.047	180
Broken stones	0.21	40
1.1 cm lists	0.21	40
2.5.2 cm lists	0.61	14
7.3 cm lists	2.3	3.6

in the free air stream, see Figure 24.

This model arrangement is well known through its wide spread use in numerous experiments, and it is therefore interesting to see, how the wind load in such an arrangement differs from the load on the model placed in a turbulent boundary layer as is the case in nature.

The plate used in the tests was 6 mm thick. It was placed horizontally across the first section of the tunnel. The model was placed with its windward wall 6 cm from the leading edge of the plate in one test, 36 cm in another test.

In this position the model is exposed to an airstream, the velocity of which is independent of the height above the "ground", especially in the first test. It can therefore be said that the roughness parameter is infinitesimally small, i.e. the ratio  $h/z_0 = \infty$ .

The results are shown in Figures 26 and 27. The wind load on the model is given as a percentage of the velocity pressure level with the ridge of the roof. The arrows indicate the direction of the load.

The results from the tests with the model placed on the suspended plate are shown in Figure 26 at the top to the left.

The  $c$ -values noted and the full-line curves correspond to the model placed 6 cm from the leading edge of the plate. The broken-line curves give the results for the model placed 36 cm from the leading edge. In the other cases in Figures 26 and 27 the model is fully submerged in the turbulent boundary layer.

The results from a model test with  $h/z_0 = 180$ , corresponding to the measurements in nature,<sup>0</sup> are shown in Figure 26 at the bottom to the right.

The results from two tests carried out with the same value of  $z_0$ , but with tunnel coatings of quite different types, namely broken stones and lists, are shown in Figure 27 at the top.

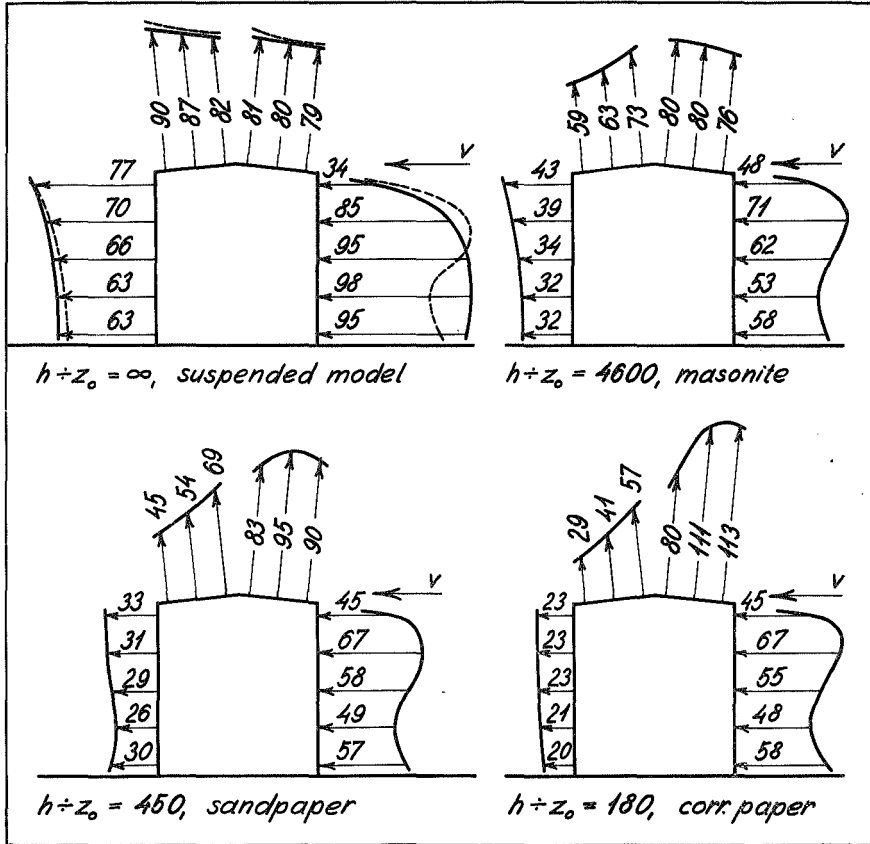


Fig. 26. Model of the Albertslund house in boundary layers of different roughnesses.

The wind load is given as a percentage of the velocity pressure level with the ridge.

At the top to the left are given the results from the arrangement shown in Figure 24. The  $c$ -values noted and the full line curve correspond to the results when the model is placed 6 cm from the leading edge of the plate. The results when the model is placed 36 cm from the leading edge are shown in the broken line curve.

In the other cases the model is fully submerged in the turbulent boundary layer.

At the bottom to the right are given the results for a model test with  $h/z_0 = 180$ , i.e. corresponding to the conditions of the measurements in nature.

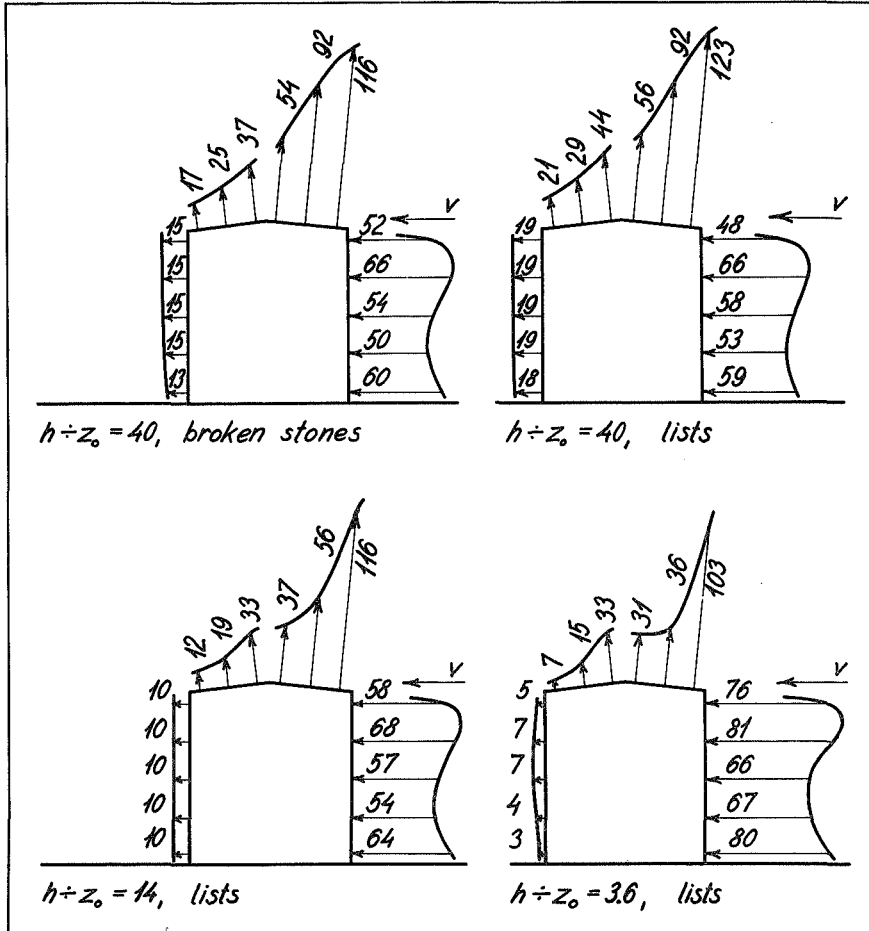


Fig. 27. Model of the Albertslund house in boundary layers of different roughnesses.

The wind load is given as a percentage of the velocity pressure level with the ridge.

At the top are shown the results from two tests, carried out with the same value of  $z_0$ , but with tunnel coatings of quite different types, namely broken stones and lists.

### 3.5 Conclusion

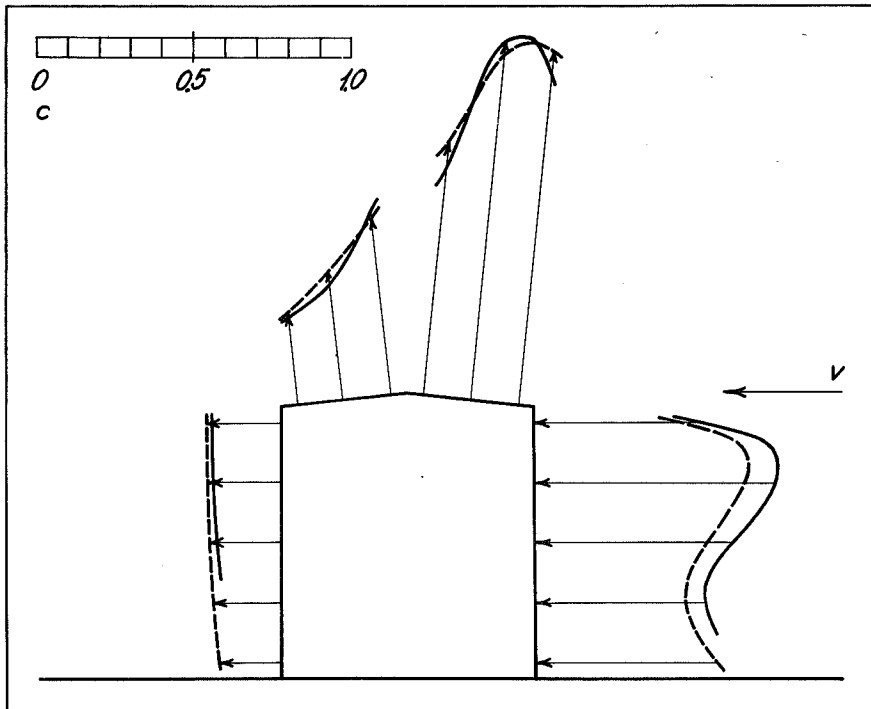


Fig. 28. The wind load on the Albertslund house and a model of this house in corresponding roughness conditions.

The measurements in nature are shown with a full line. The results of the model tests are shown with a broken line.

At the leeward wall and over the whole roof the model test is in complete agreement with the conditions in nature. At the windward wall there is a small difference.

In Figure 28 the wind load on the Albertslund house is shown with a full line. The ratio between the height of the house and the roughness parameter of the field was 180. In Figure 28 the result of a model test, in which  $h+z_0$  was also 180, i.e. a test in agreement with the model law, is shown with a broken line.

Taking into consideration that the measurements in nature involve a mean error of 0.03 in the  $c$ -values, it will be seen that the agreement is complete at the leeward wall and the windward and leeward roof surfaces, whilst there is some deviation at the windward wall.

Now it will be useful to consider, which values of  $h+z_0$  occur in practice. It depends partly on the variation in height of the house, and partly on the variation in roughness of the terrain.

For the roughness of the terrain the following four types are used:

- T 1,  $z_0 = 1$  cm, extremely smooth, open terrain.  
 T 2,  $z_0 = 10$  cm, agricultural land with hedgerows and buildings.  
 T 3,  $z_0 = 1$  m, an area of houses of one storey with gardens.  
 T 4,  $z_0 = 10$  m, a densely built-up area of houses of five to six stories.

The houses are divided into the following four types:

- H 1,  $h = 4$  m, one story  
 H 2,  $h = 10$  m, three stories  
 H 3,  $h = 30$  m, ten stories  
 H 4,  $h = 90$  m, thirty stories.

The following values of  $h+z_0$  are obtained combining the four types of terrain with the four types of houses:

	h	T 1	T 2	T 3	T 4
		$z_0 = 1$ cm	10 cm	1 m	10 m
H 1	4 m	400	40		
H 2	10 m	1000	100	10	
H 3	30 m		300	30	
H 4	90 m		900	90	9

When no value is noted in the Table for some of the combinations it is because these combinations are of no practical importance.

For instance, H 1 / T 3 means that a one story house is situated among similar houses. Under such circumstances of course the wind load is small. Moreover, the wind load cannot be calculated on the basis of the shape factors normally used, but shape factors derived from model tests in which the close environs are correctly reproduced must be used.

Furthermore H 3 / T 1 means that a 30 m high house is situated in a boundary layer of an extremely smooth open terrain. Only an airport can offer such a terrain of suf-

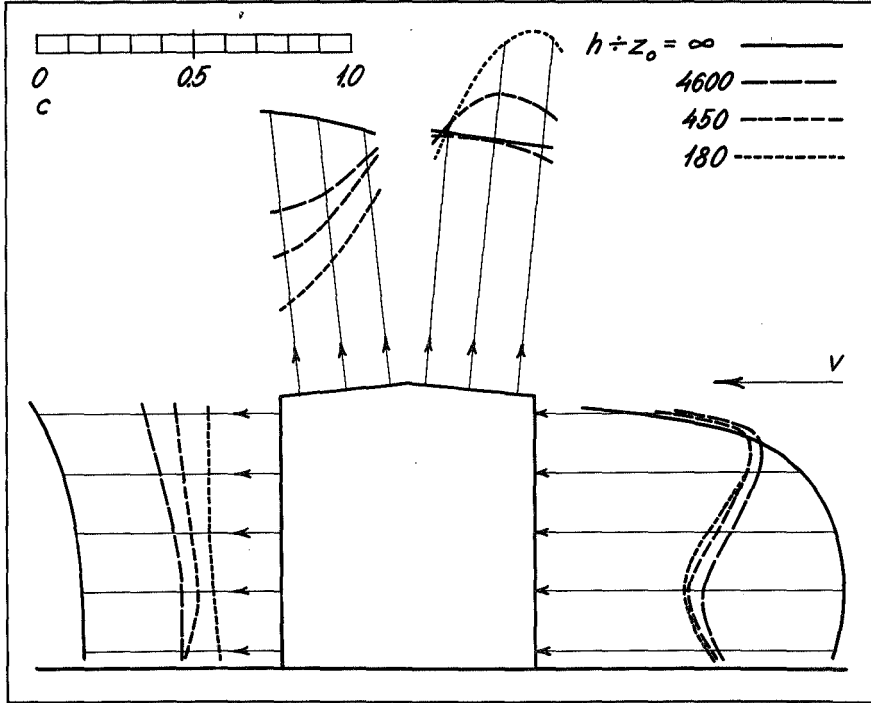


Fig. 30. The wind load on a model of the Albertslund house in different roughness conditions.

$h \div z_0 = \infty$  indicates a suspended model.

In practice  $h \div z_0$  will be between 10 and 1000 with median value 200.

The Figure shows the smoothest cases.

ficient extent, and in its close proximity a 30 m high house cannot be built.

So the range of practical importance will be covered by the interval  $10 < h \div z_0 < 1000$ , the median value of which will be of an order of 200.

In Figure 30 the tests over the smoothest surfaces are shown. The test with the house on the suspended plate in the tunnel is indicated with  $h \div z_0 = \infty$ .

When this test is compared with the results from the tests with  $h \div z_0 = 180$ , it will be seen that the deviations are substantial.

The suspended model gives more than twice the pressure expected on a real house in nature at the bottom of the

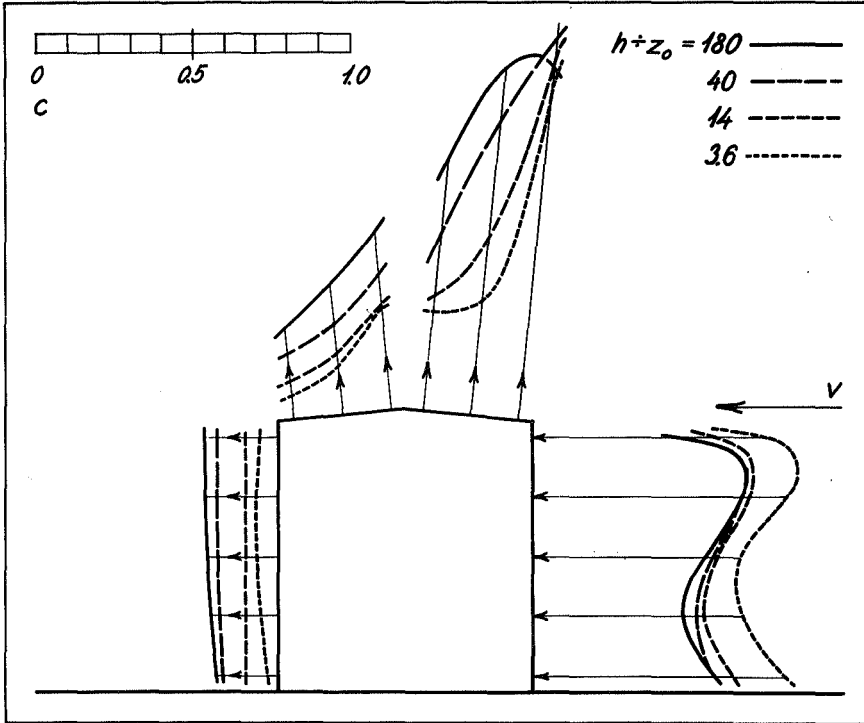


Fig. 31. The wind load on a model of the Albertslund house in different roughness conditions.

In practice  $h/z_0$  will be between 10 and 1000 with median value 200.

The Figure shows the roughest cases.

windward wall, and more than three times the suction expected on the leeward wall.

At the foremost part of the windward roof surface the suspended model gives suctions 30 per cent smaller than occur in actual practice.

In Part I, page 38, an explanation of why the conditions are so different for a suspended model and a model placed on the bottom of the tunnel is given.

In the course of time a great deal of measurements on a house model, suspended in a tunnel on a plate of moderate extent, have been performed, and such tests are still being carried out.

It is evident from the above mentioned that such experiments are absolutely misleading about what happens in reality.

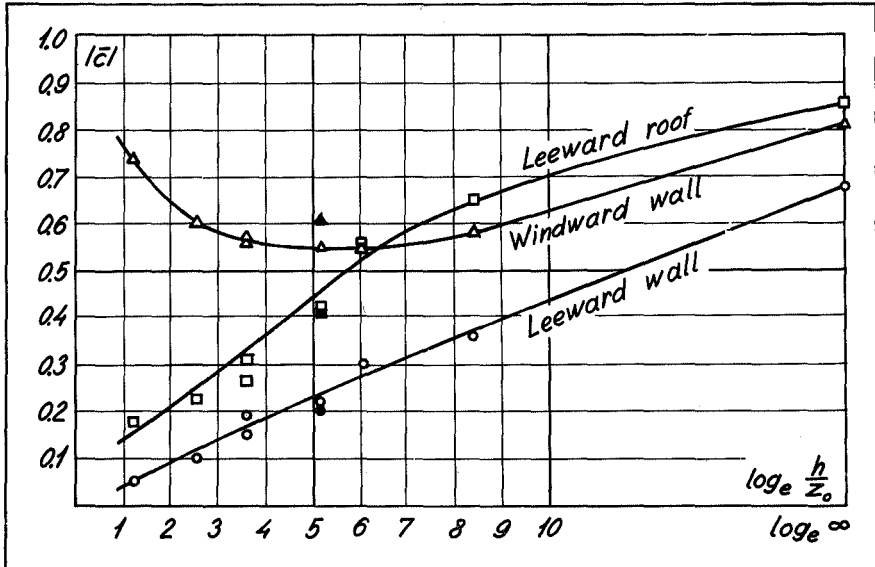


Fig. 32. Wind load on the Albertslund house.

The abscissa is the logarithm of the ratio between the height of the house and the roughness parameter.

The ordinate is the mean value of the shape factor for the surface concerned.

Open signs indicate the model tests, filled signs the measurements in nature.

It appears from Figure 30 that, except for the suspended model, the pressure on the windward wall only depends a little on the turbulence of the boundary layer.

At the foremost part of the windward roof surface, the suction increases with the roughness. At the leeward roof surface and the leeward wall the suction decreases with increasing roughness.

In Figure 31 are shown the tests carried out over the roughest surfaces. The result from the test with  $h/z_0 = 180$  is repeated.

Here also the pressure on the windward wall, except for the roughest case, only varies a little with the roughness.

The suction on the leeward roof surface and the leeward wall decreases with increasing roughness. The same is the case for the suction on the windward roof surface, apart from the front border.

The suction on the leeward wall, in all cases is

rather constant over the height of the wall. In Figure 32 the mean value is shown as ordinate, the abscissa being the logarithm of  $h/z_0$ . It appears that the suction on the leeward wall increases evenly from 0.05 in the roughest case to 0.68 in the smoothest case, viz. the suspended model. The solid point represents measurements in nature.

The suction on the leeward roof section varies somewhat from the ridge to the edge of the roof; if we consider the mean value we obtain the curve as per Figure 32 which shows that the value increases from 0.18 in the roughest case to 0.86 in the smoothest case. The measurement in nature is shown by the solid point.

It will be noticed from Figure 32 that the mean pressure on the windward wall has the value of 0.74 in the roughest case; the pressure decreases with increasing smoothness to 0.53, and subsequently increases again to the value of 0.81 for the suspended model.

On the windward roof surface the suction varies a great deal for the medium and large roughnesses. Figure 34 shows how the suction in the centre of the roof surface depends upon the roughness. There is a distinct maximum at  $h/z_0 = 120$ . In the very rough case the suction factor is 0.36, and in the very smooth case it is 0.80.

Figure 32 enables a quantitative judgement to be made of the importance of the model test being carried out with a correct value of the roughness parameter.

We may first consider the subject with a view to obtaining in a model test a reasonably correct mean value of the wind load on a surface. In Figure 32 the highest value of the differential coefficient is

$$\frac{d \bar{c}}{d \log_e \frac{h}{z_0}} = 0.09.$$

If in a model test it is desired to ensure that  $c$  is loaded maximally with an error of 0.05 caused by an incorrect turbulence, the  $\log_e h/z_0$  should thus deviate max. 0.55, which again means that  $h/z_0$  must not exceed an error of 1.7 times. Consequently a coating for the tunnel bottom must be used which has a roughness between 0.6 and 1.7 times the correct one according to scale.

As mentioned the values of  $h/z_0$  between 10 and 1000 have most interest in practice. The interval corresponds to  $\log_e h/z_0$  between 2 and 7.

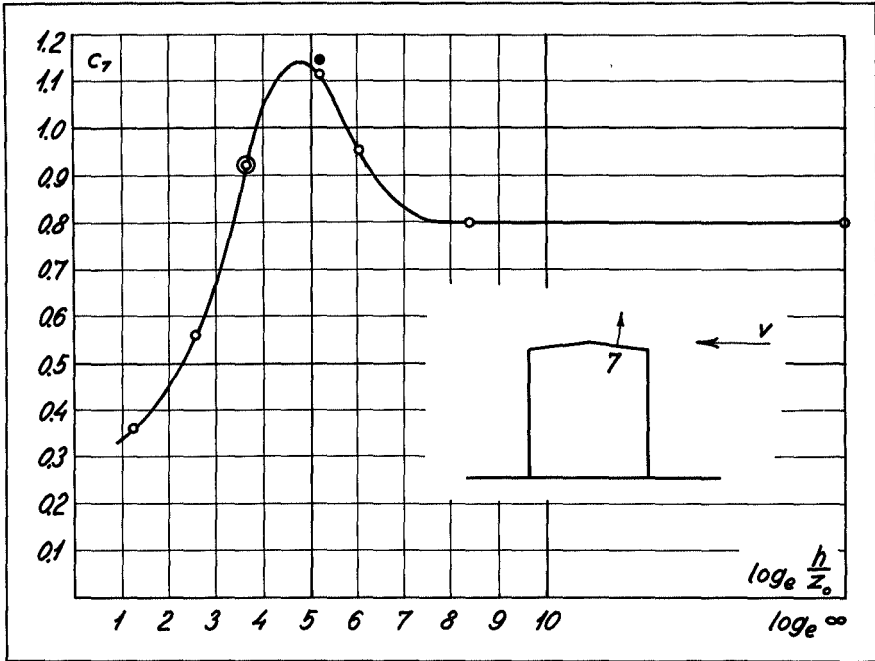


Fig. 34. Wind load on the Albertslund house.

The abscissa is the logarithm of the ratio between the height of the house and the roughness parameter.

The ordinate is the shape factor for the suction at the centre of the windward roof surface.

Inside this range the maximum  $c$ -value can occur in the smoothest case. This applies to the suction on the leeward wall and the leeward roof surface.

But the maximum  $c$ -values can also occur in the roughest case. This applies to the pressure at the windward wall.

Finally the maximum  $c$ -value of the suction at the center of the windward roof is found neither in the roughest nor in the smoothest case, but in a case between these two.

The consequence of this is that model tests normally must be carried out with different roughnesses.

## 4. STREAM FLOW ABOUT A HOUSE

### 4.1 Introduction.

In "Wind-pressure on Buildings, Second Series", Nøkkentved has dealt with the problem concerning stream flow about buildings.

Despite the fact that his experiments were carried out over very smooth surfaces, they are of interest as a basis for an understanding of the results in the previous section.

Figure 36a shows the steady state flow over a house with  $45^\circ$  roof slope. The picture originates from a test in a water tank.

The model, placed on a relatively large base plate, was moved through the water. Aluminium powder was sprinkled on the surface of the water. By taking time exposure photographs a picture was obtained where every aluminium particle formed a line, of length proportional to the velocity of the flow at that place.

It appears from the picture that there are two rather distinct zones: A irrotational motion to the left of and over the house limited below by a surface of discontinuity. Under this surface there is a sheltered zone in which the velocities are small.

The surface of discontinuity passes in a concave upwards curve from a point on the ground at some distance windward of the house up to the edge of the roof, and then in a convex upwards curve from the ridge to leeward of the house.

The surface of discontinuity is a vortex-sheet and can be regarded as a row of small eddies on which the free air stream rolls over the shelter zone in front of and behind the house.

In Figure 36b the situation is shown schematically. The line of discontinuity is drawn from Figure 36a, from which the velocities are also determined. By means of Bernoulli's equation it can be calculated, that the pressure to windward of the house corresponds to  $c = 0.75$ , the pressure at the roof to  $c = 0.50$ , and the suction to leeward to  $c = 0.50$ .

To the right in Figure 36b is shown the shape factor from a test in the wind tunnel.



Fig. 37a. See text.

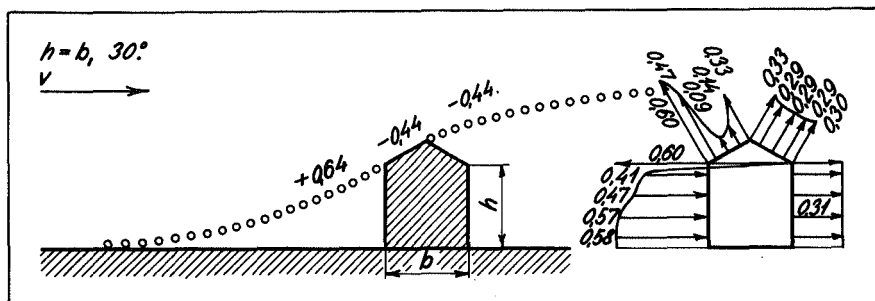
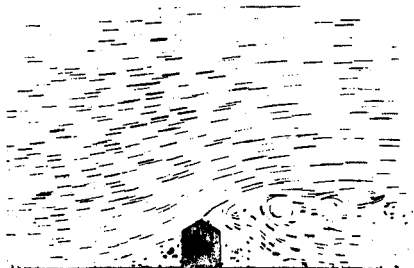


Fig. 37b. See text.

vortex-sheet to windward of the house only changes a little, when  $h \div z_0$  is changed.

The conditions at the other surfaces of the house are quite different. Here the suctions change greatly when  $h \div z_0$  is altered. At the leeward roof surface and the leeward wall the suctions always decrease when the turbulence is increased.

At the windward roof surface the conditions are more complicated as the suctions are both rising and falling with increasing turbulence, see Figure 34.

A better understanding of these phenomena can be obtained by studying the shape of the surface of discontinuity, stretching to leeward of the house.

At the Wind Laboratory measurements of the shape of the surface of discontinuity were begun.

They were terminated because of the demolition of the Wind Laboratory and are only little more than orientative, but the method used seems to be promising and it is to be hoped that others will take it up.

## 4.2 Experimental arrangement and technique

The wooden models of the type described in Section 1.4 were used.

One of the models had a saddle roof with a slope of 1:10; the height to the ridge was 84 mm, the length and width were 152 mm and 75 mm, respectively.

The other model had a saddle roof with a slope 15°; the height to the ridge was 79 mm, the length and width were 140 mm and 70 mm, respectively.

The models were placed at right angles to the wind direction in the 4th section of the tunnel.

The determination of the position of the vortex-sheet was made only in the symmetry plane of the model, where the flow is two-dimensional.

In the tests three different types of turbulence were used: Small turbulence,  $z_0 = 1.8 \cdot 10^{-3}$  cm, produced by smooth masonite plates, medium turbulence,  $z_0 = 0.047$  cm, from corrugated paper, and large turbulence,  $z_0 = 0.40$  cm, from 2.5·2 cm lists.

The position of the vortex-sheet was determined by means of the hot-wire anemometer, described in Part I, Section 1.3.

The hot-wire anemometer reacts differently when placed in the disturbed, eddy-filled zone below the vortex-sheet, than when placed in the irrotational flow above the vortex-sheet. Thus it is possible to fix the position of the vortex-sheet.

The hot-wire itself is very sensitive to the turbulence in the air flow passing the wire.

The cooling and so the resistance, of the wire placed in an airflow with small turbulence, is rather constant, with only small oscillations about a mean value. Corresponding to this, the disturbances in the current in the Wheatstone bridge are only small, so that the pointer in the ammeter of the bridge only makes small oscillations.

Conversely, if the hot-wire is placed in a very turbulent airflow, the turbulence involves large variations in the cooling, and therefore the pointer in the ammeter makes correspondingly large oscillations about a mean position.

This property of the hot-wire together with the difference in turbulence above and below the vortex-sheet makes a quantitative determination of the position of the vortex sheet possible.

The hot-wire was placed so that it could be moved in the vertical symmetry plane of the tunnel, this being also

the symmetry plane for the model; the arrangement allowed an exact determination of the co-ordinates of the wire.

The hot-wire was 3 mm long and placed horizontally at right angles to the wind.

To determine, for example, the position of the vortex-sheet above the ridge of the house with slope 1:10, the hot-wire is first placed in the undisturbed airflow, vertically above the ridge.

A constant wind velocity in the tunnel is maintained during the experiment. The oscillations of the pointer in the ammeter of the Wheatstone bridge are used as a measure for the turbulence of the airflow undisturbed by the model. Of course these oscillations are greater when the experiment is carried out in the boundary layer produced by 2.5·2 cm lists, than in that produced by smooth masonite plates.

The hot-wire is then slowly moved down towards the roof of the model. When it arrives at or under the vortex-sheet, that is, in a more turbulent zone, oscillations will occur on the ammeter of quite another order of magnitude than those occurring when the wire was above the vortex-sheet.

The position of the vortex-sheet can be determined most exactly near its windward starting point. To leeward of the model the transition between the irrotational airflow and the eddy zone is less distinct.

### 4.3 Test results

Figures 40 and 41 show cross sections in the symmetry planes of the two houses with the surfaces of discontinuity drawn. The shape factors for the wind load measured in the same arrangement are also given.

At roof slope 1:10 the surface of discontinuity starts from the windward edge. In the smooth case the inclination here is smallest; so is the curvature and corresponding to this the suction at the windward edge of the roof.

In the roughest case the surface of discontinuity at the windward edge of the roof is steep and has a pronounced curvature, corresponding to the strong suction. But at the centre of the windward roof section the curvature is very reduced, and over the leeward roof edge the surface of discontinuity is quite flat. The suctions on the roof and the leeward wall are in accordance with this.

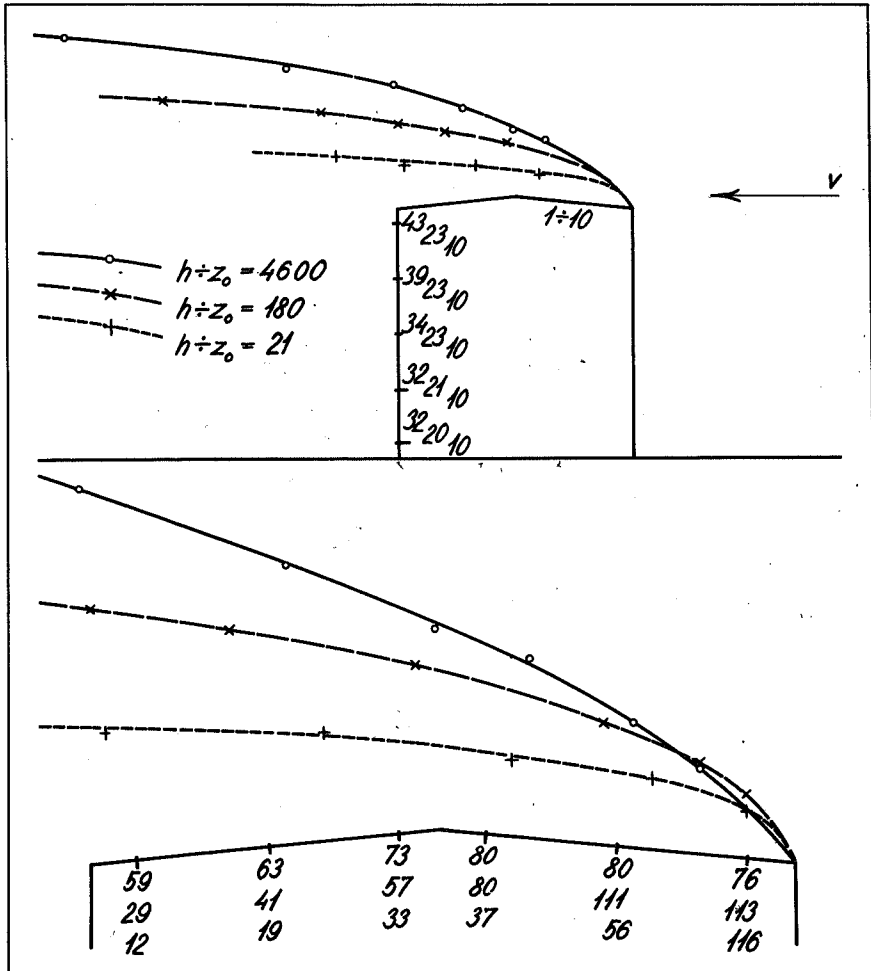
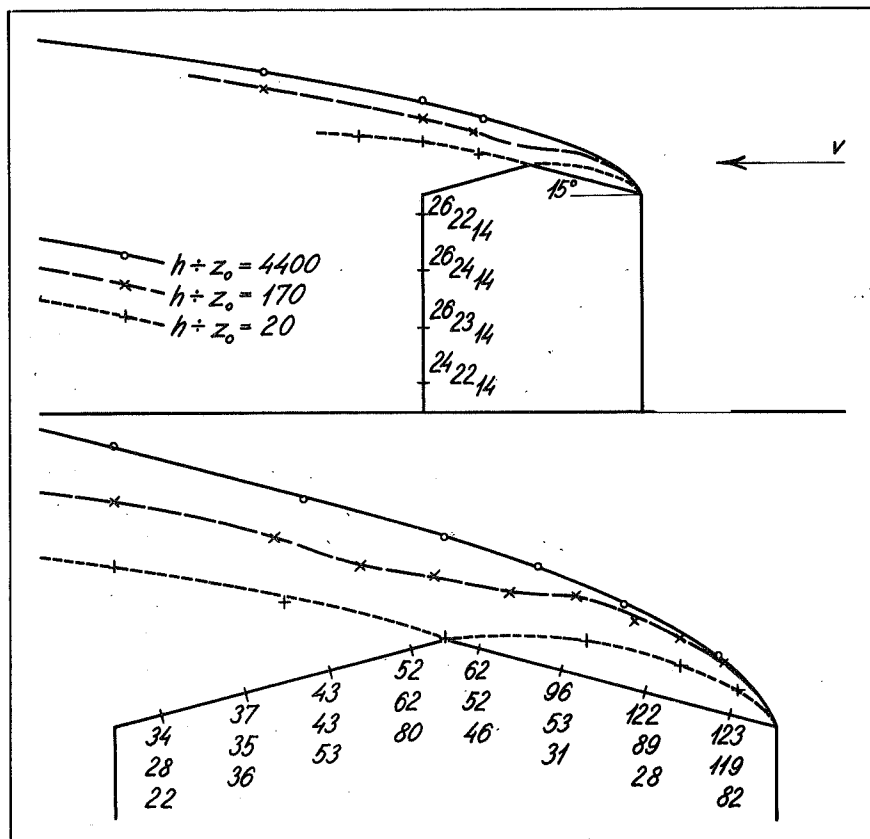


Figure 41 shows the conditions at a roof with  $15^\circ$  roof slope. In the smoothest case they are similar to those in the previous Figure. But the roughest case shows something quite different. Here the surface of discontinuity curves from the windward roof edge to the ridge, and from the ridge to leeward of the house. So it limits two separate zones. For medium turbulence there is a marked lowering of the surface of discontinuity over the ridge.



Figs. 40 and 41. Surface of discontinuity over a saddle roof.

Fig. 40: slope of roof 1:10,

Fig. 41: " " " 15°.

The full-line curves show the surface of discontinuity, when the model is placed on a very smooth tunnel bottom.

The short-broken-line curves correspond to a very rough case.

At the windward edge of the roof the surface of discontinuity is determined with an error of 0.7% of the height of the house. To the leeward of the house the error is 4% of the height.

At the roof and the leeward wall the factors for suction in percentages are noted. The uppermost numbers correspond to the smoothest case, the lowest to the roughest case.

It will be seen that there is a qualitative agreement between the suctions and the curvature of the surface of discontinuity.

## 5. EXTERIOR WALLS

### 5.1 Key to the models

The different model tests are given in the following key signs:

$$h \div l \div w, x, \alpha, \frac{H}{z_0}$$

$h \div l \div w$  are numbers proportional to the height to the edge of the roof, the length and the width.

For  $x$  is given either  $s$  = saddle roof,  $d$  = desk roof,  $h$  = hip roof or nothing = horizontal roof.

$\alpha$  is the roof slope in degrees.

$\frac{H}{z_0}$  is the ratio between the height to the uppermost line in the roof and the roughness parameter.

Table 42

$h \div l \div w$	$\alpha$	Turbulence	Figure on page
2.4÷1÷1	0°	s	48
		l	49
5÷5÷1	0°	s	50 and 51
		l	52 and 53
1÷2÷1	0°	s	54
		l	55
	s 45°	s	56 and 57
		l	58
0.5÷2÷1	s 45°	s	59
	0°	s	60
	0° *)	s	61

\*) with eaves      s = small turbulence  
                               l = large turbulence

## 5.2 Scope of the tests

Seven different types of houses are investigated in the model tests with wind load on exterior walls.

In Figures 44, 45a and 45b the types are shown and the placing of the measuring holes is given.

The models were made of brass, see Section 1.4. They were placed on the turntable in the 4th section of the tunnel and the measurements were carried out as described in Section 1.6.

Two types of turbulence were used, namely small turbulence,  $z_0 = 1.8 \cdot 10^{-3}$  cm, produced by smooth masonite plates, and large turbulence,  $z_0 = 0.45$  cm, from 2.5·2 cm lists.

The turbulence used for the different models is given in Table 42.

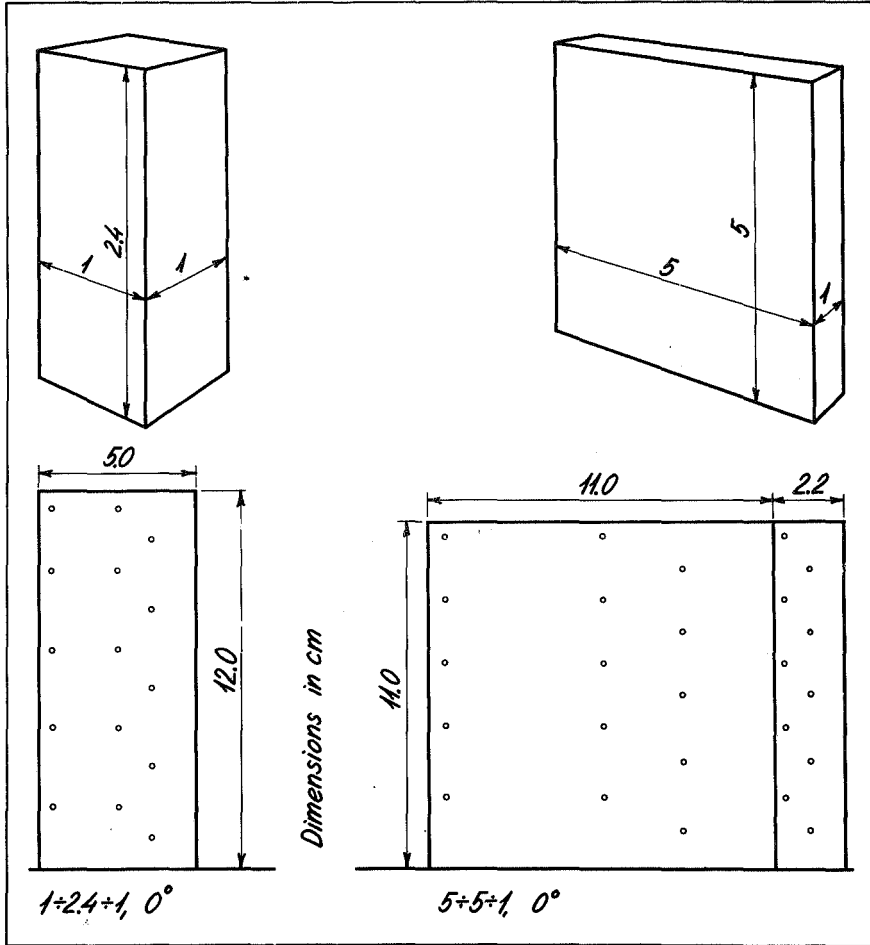
## 5.3 Test results

The shape factors for the exterior walls derived from the tests are given in Figures 48 to 61.

The shape factor is  $c = p/q$ , where  $p$  is the pressure or suction at the point concerned and  $q$  is the velocity pressure measured level with the highest line in the roof.

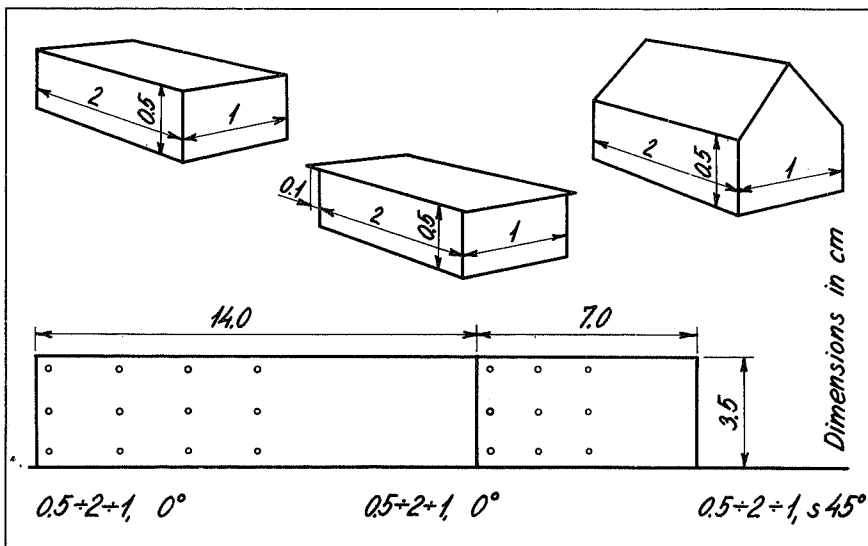
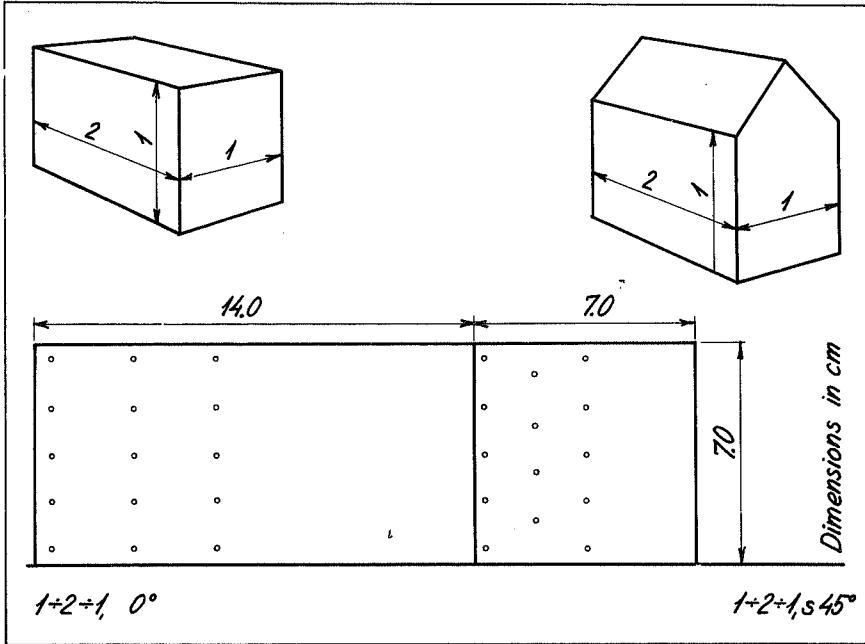
Curves through points with identical  $c$ -values are drawn, and the extreme point values are given.

For each of the models the shape factors are given for the model positions having the most interesting loading conditions.



Figs. 44, 45a and 45b. House models for investigations of the wind load on exterior walls.

The small circles indicate the measuring holes.



## 5.4 Conclusions

From the test results given in Figures 48 to 61 the following deductions, among others, about wind load on exterior walls can be made:

The maximum overturning moment on a house occurs when the wind is at right angles to the exterior walls.

Both the pressure at the windward wall and the suction at the leeward wall are greater in small turbulence than in large turbulence. So the greatest overturning moment occurs in a flow of small turbulence.

Large suction values occur at the windward edge of a wall, when the wind is blowing approximately parallel to the wall. Here suction values corresponding to  $c = 1.2$  are encountered locally. If measuring holes had been placed even closer to the edge, even greater suction values would probably have been measured.

A wall section with an area  $a$  can receive a greater mean wind load the smaller  $a$  is in relation to the whole area  $A$  of the wall. This applies both to suction and pressure.

In preparation of general rules for wind loads on exterior walls it would be useful to introduce this fact. So in the Danish Standard Code of Practice the pressure on a windward wall is given by

$$c = 1.0 - 0.3 \frac{a}{A}.$$

A paradox should be mentioned here. A house with a height of 50 m and a similar house, 5 m high, are placed in an open terrain with  $z_0 = 10$  cm, in such a way that their mutual influence is insignificant.

The wind velocity at 10 m height is presumed to be 40 m/s. Then in a height of 50 m it is 54 m/s and  $q = 182$  kp/m<sup>2</sup>. In a height of 5 m it is 34 m/s and  $q = 72$  kp/m<sup>2</sup>.

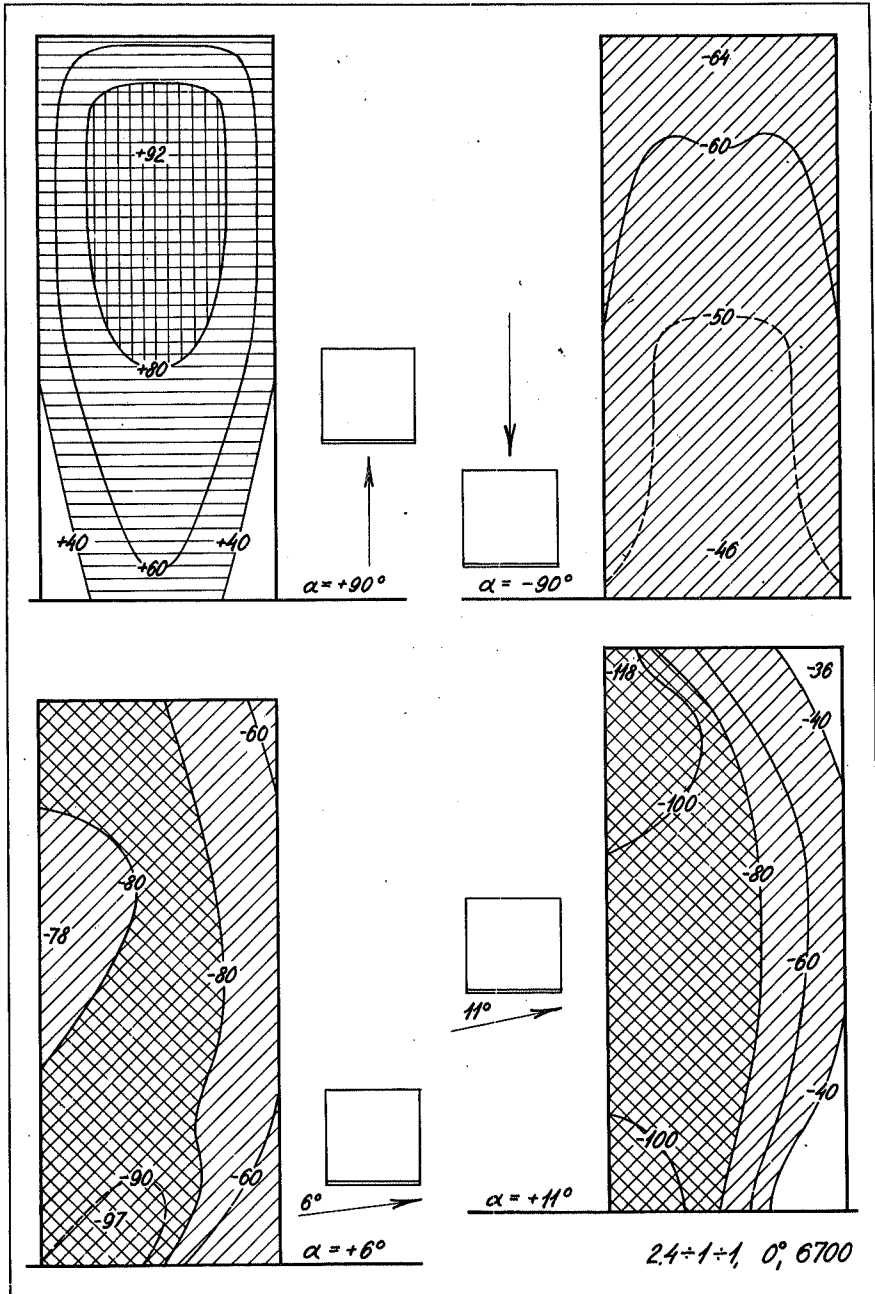
We will compare the wind load on the windward facade in the two houses at a height of 2.5 m above the ground, when the wind is blowing at right angles to the facade.

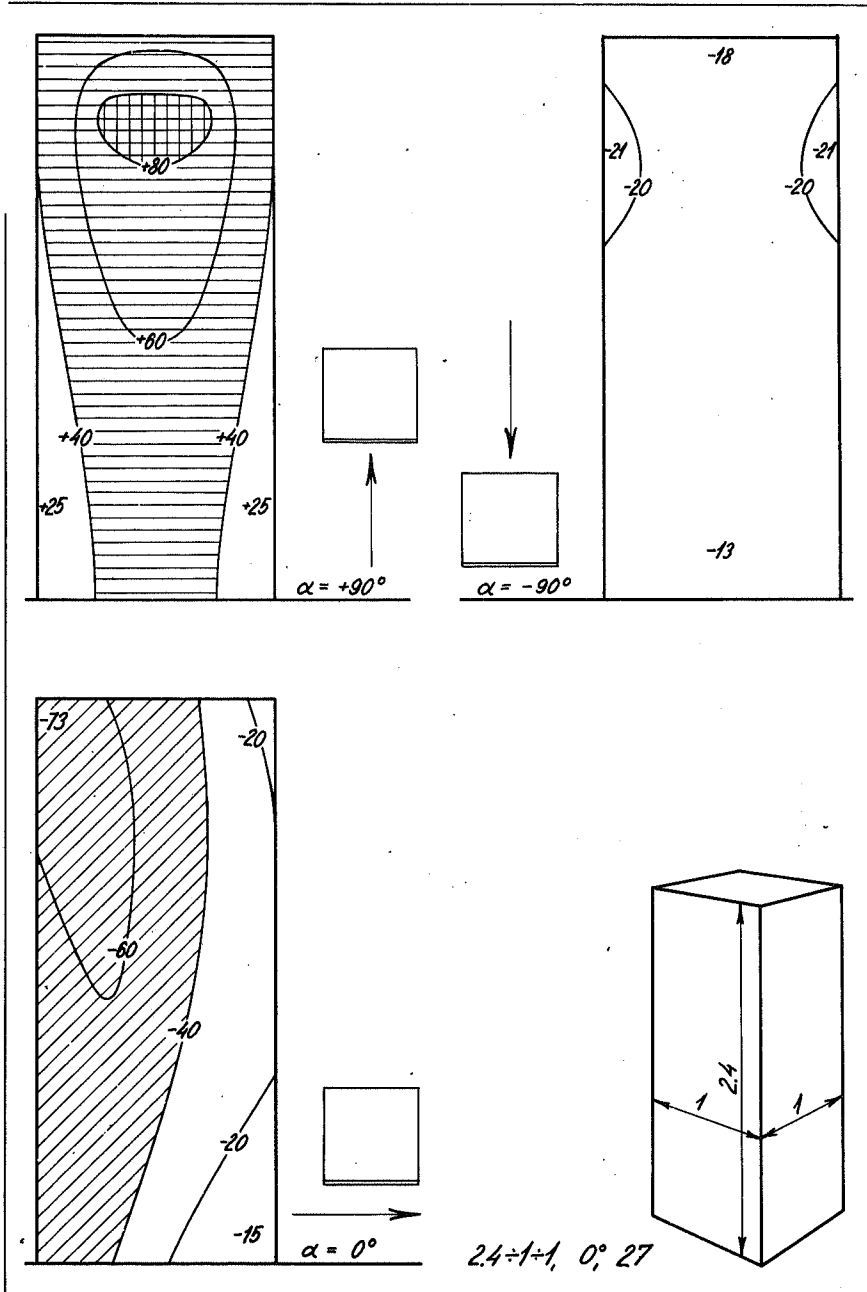
2.5 m corresponds to half the height of the small house, but for the tall house it is relatively almost at base level.

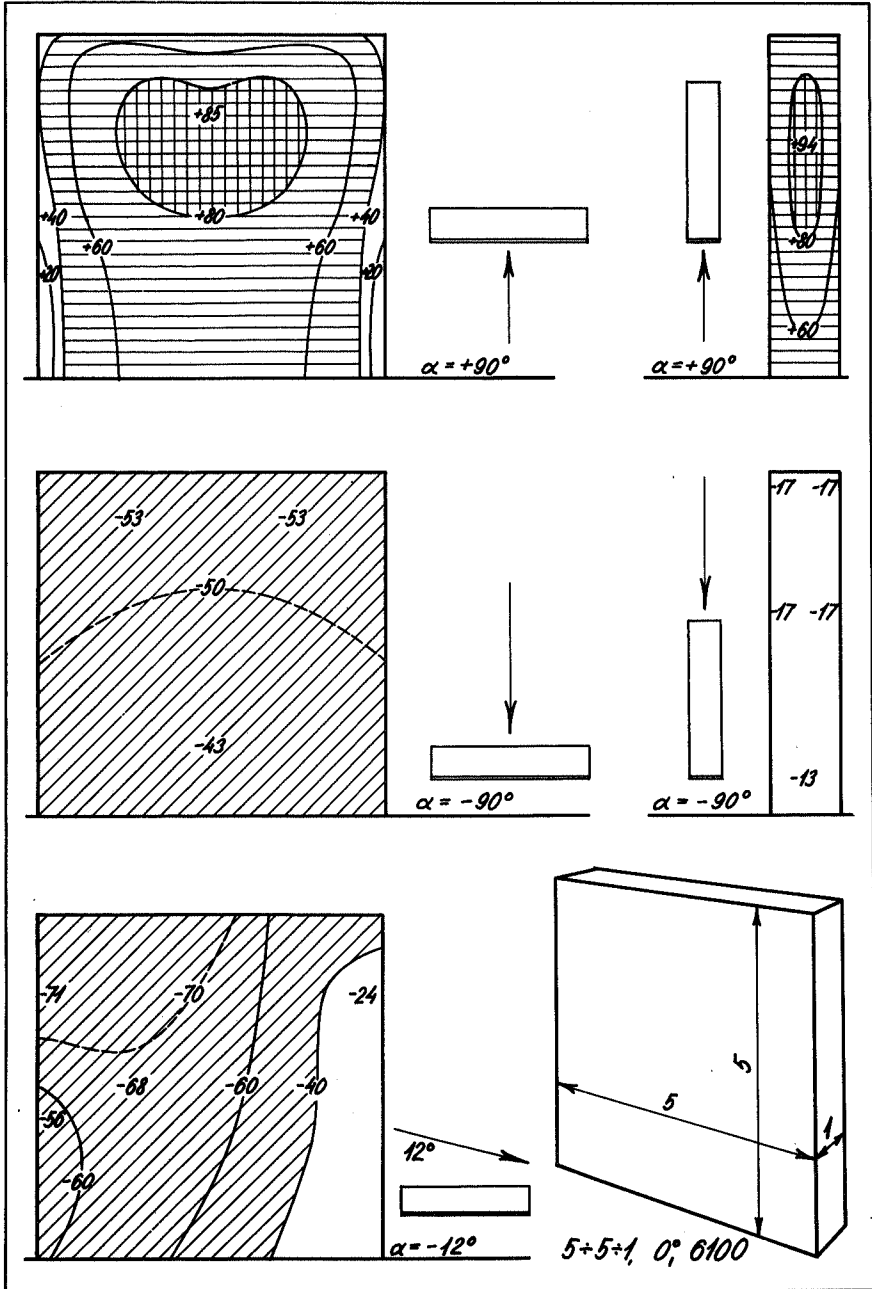
It appears from the Figures given in this Section, that the shape factors in these two levels, for a rough terrain and for a smooth terrain respectively, only differ a little

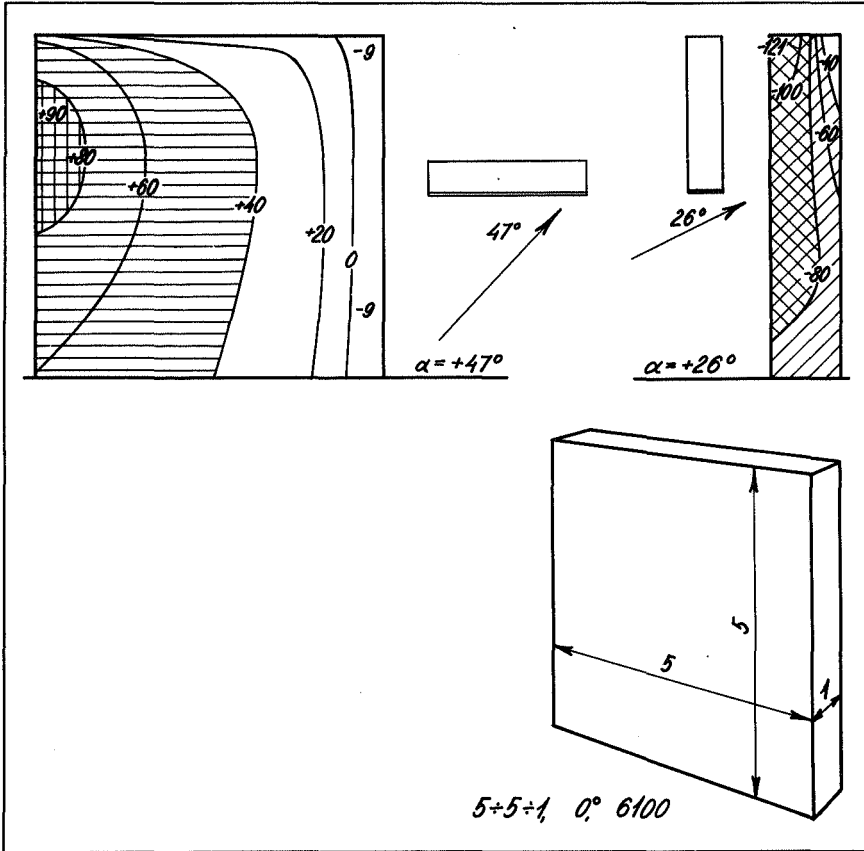
From this it follows that the wind load at a level of 2.5 m above the ground on the tall house is more than twice as great as on the small house.









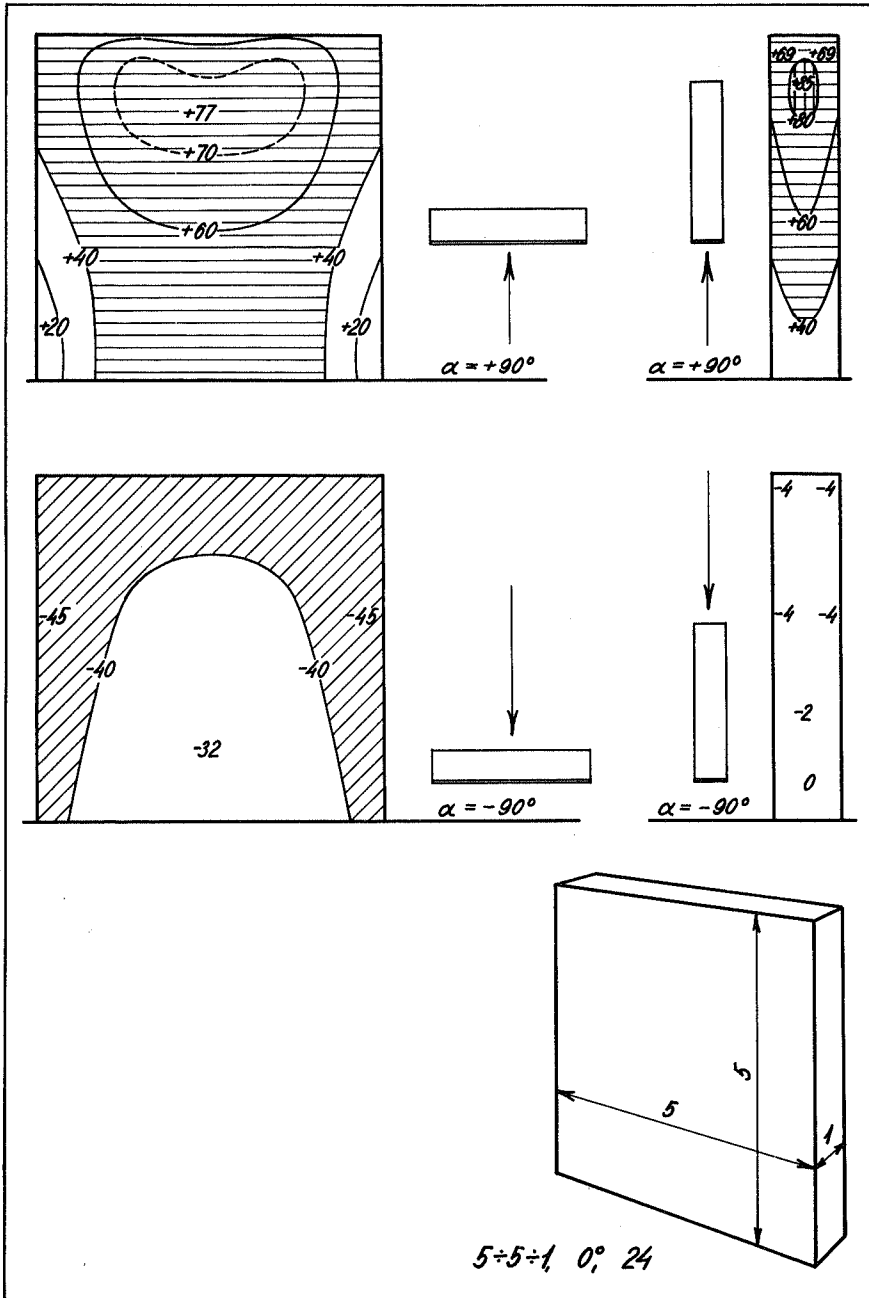


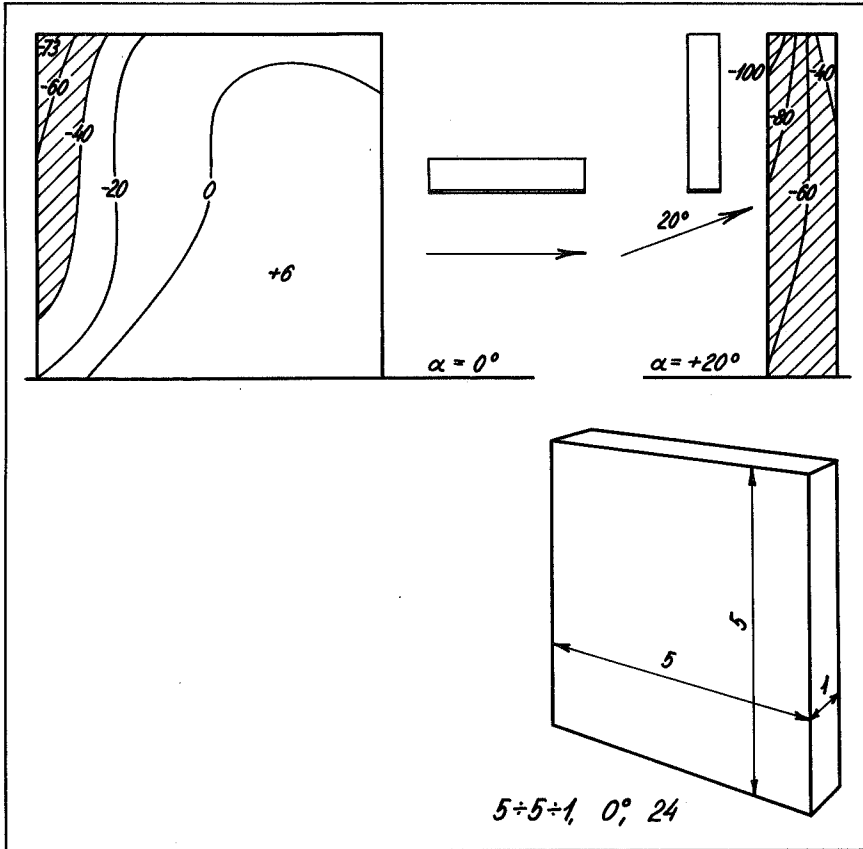
Figs. 48 to 61. Wind load on exterior walls.

The shape factors are given as a percentage. Pressure is indicated by + and by horizontal and vertical hatching.

Suction is indicated by - and by oblique hatching.

Areas where the shape factors are between 40 and 80 per cent are single hatched. Areas where the shape factors are more than 80 per cent are double hatched.



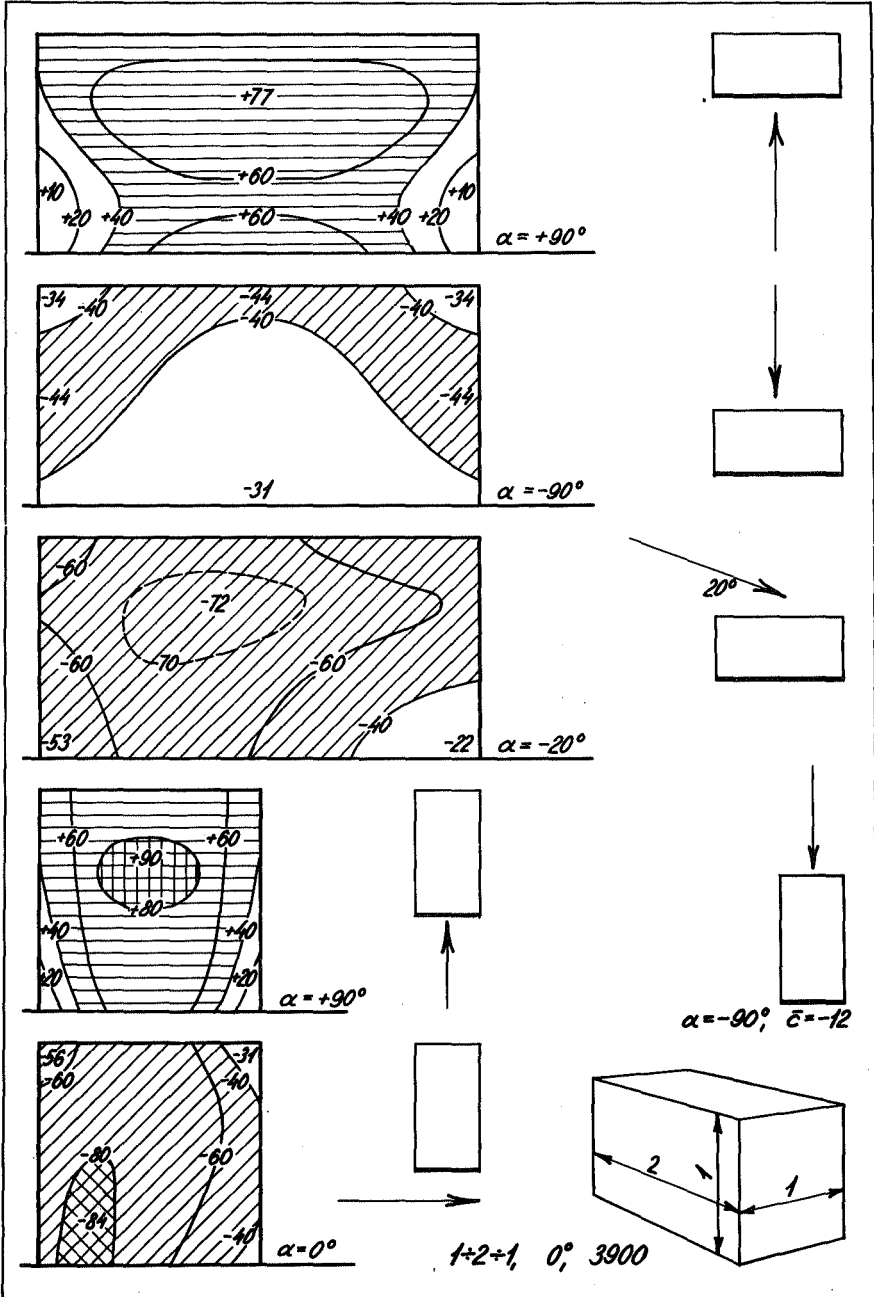


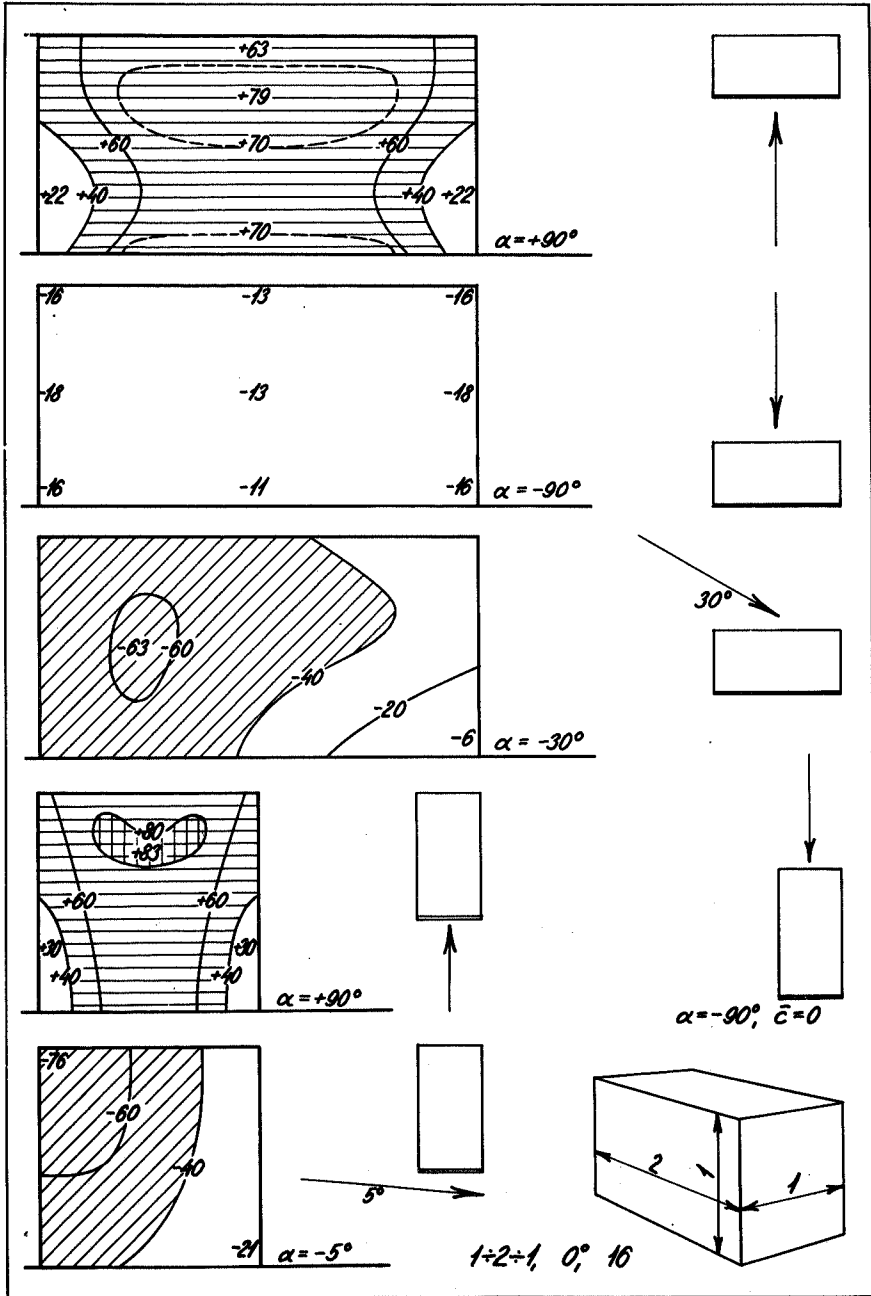
Figs. 48 to 61. Wind load on exterior walls.

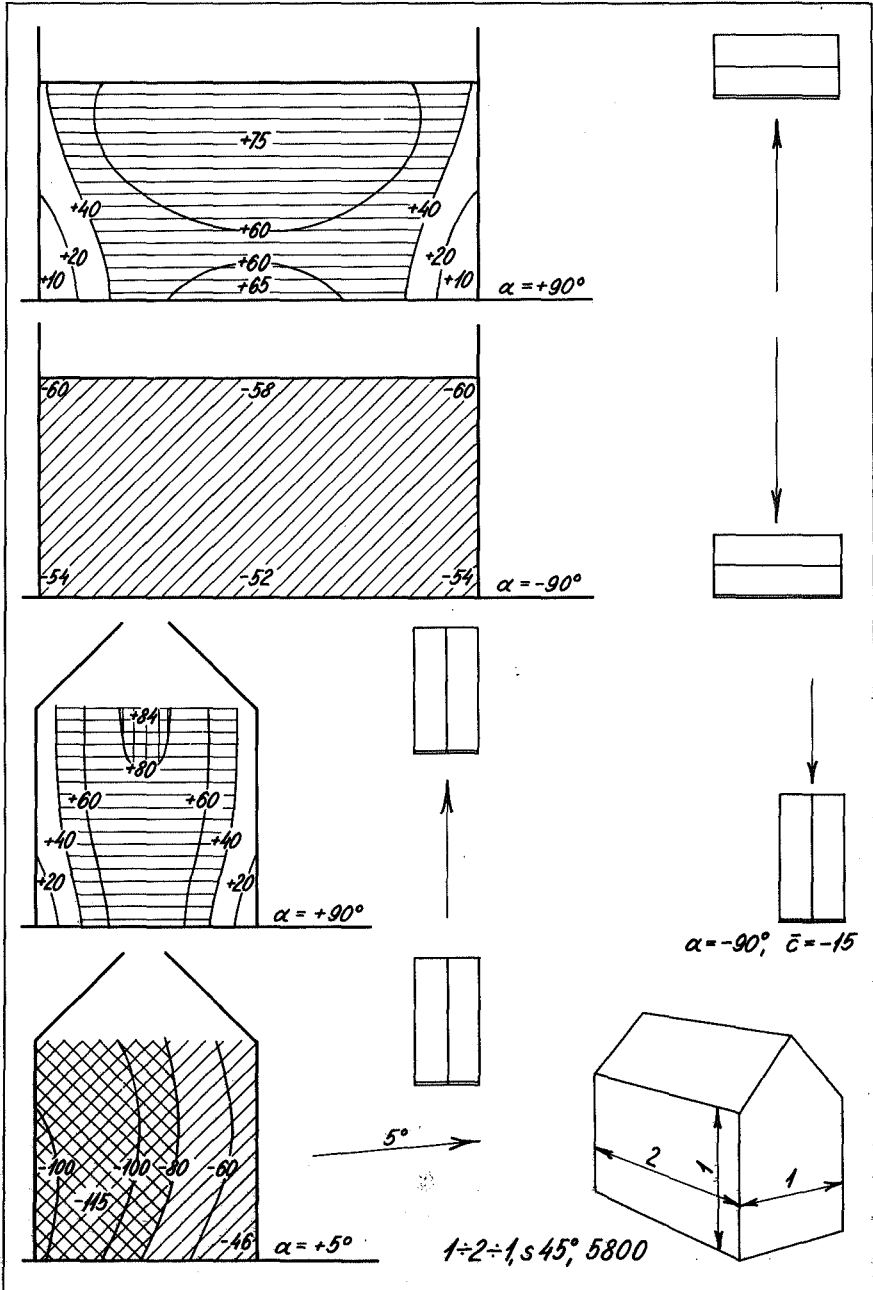
The shape factors are given as a percentage. Pressure is indicated by + and by horizontal and vertical hatching.

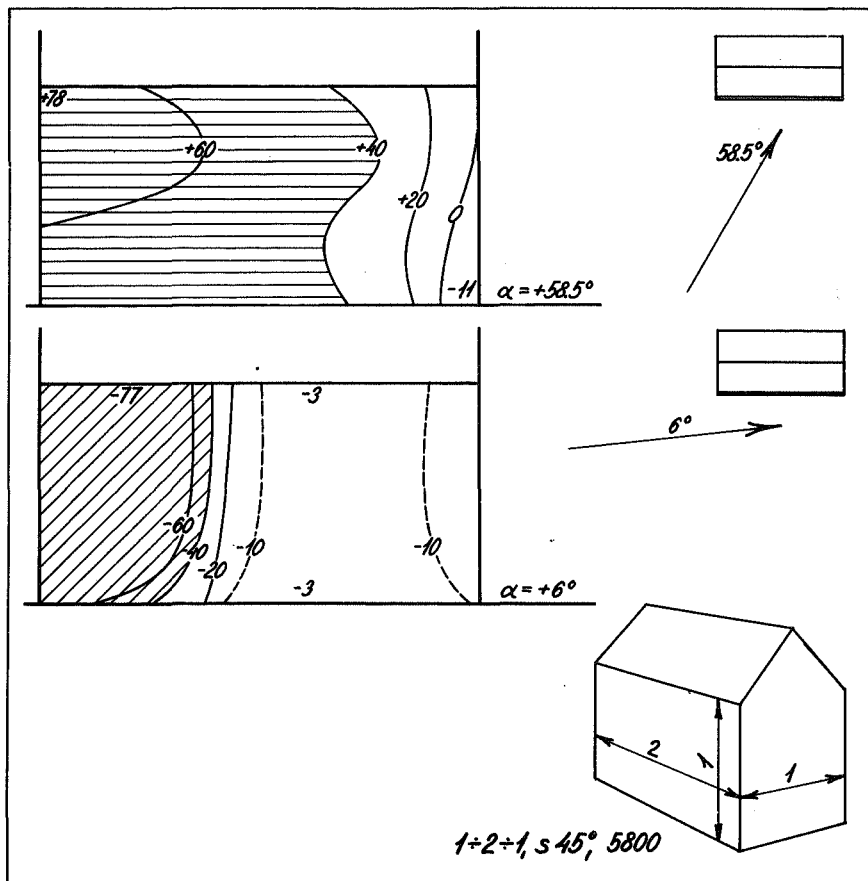
Suction is indicated by - and by oblique hatching.

Areas where the shape factors are between 40 and 80 per cent are single hatched. Areas where the shape factors are more than 80 per cent are double hatched.







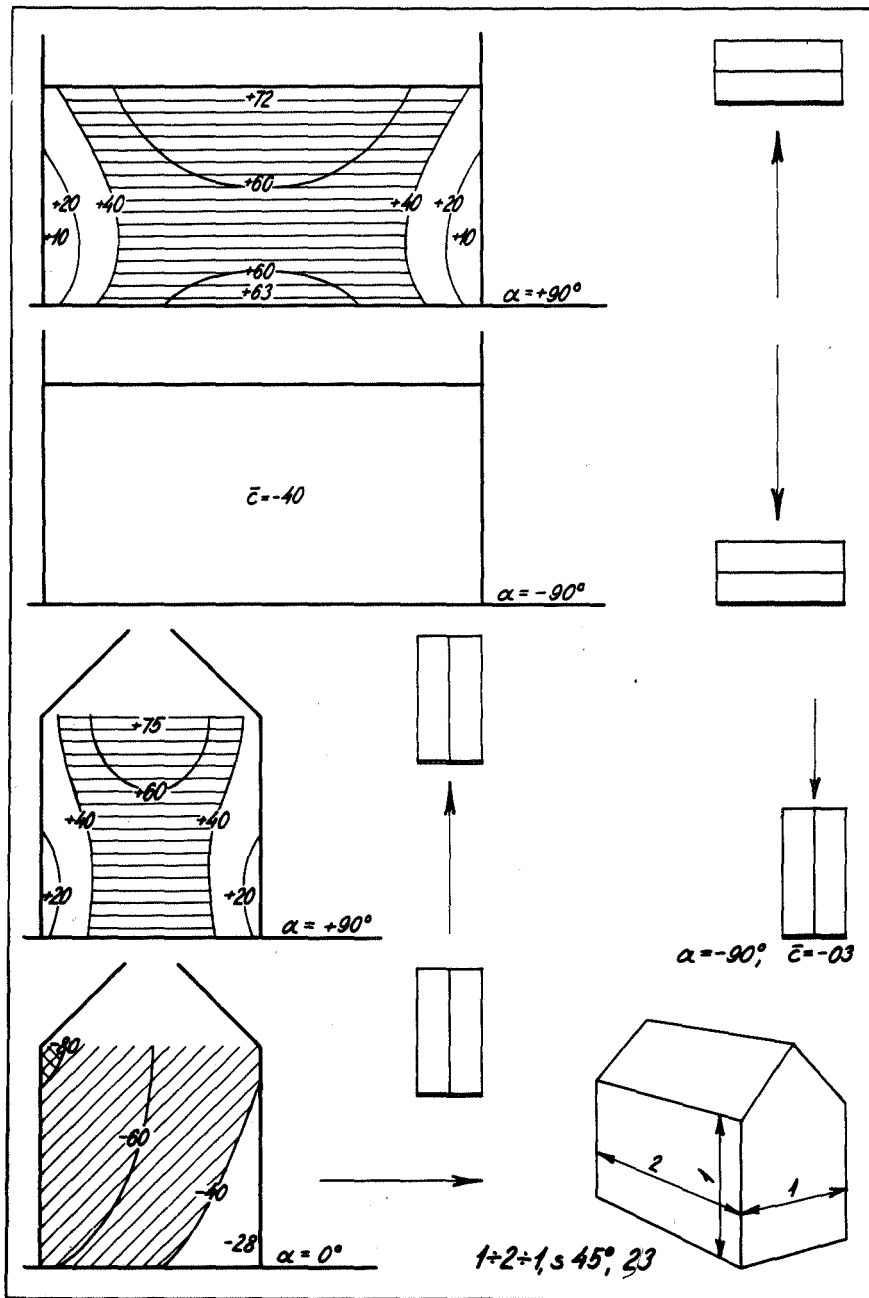


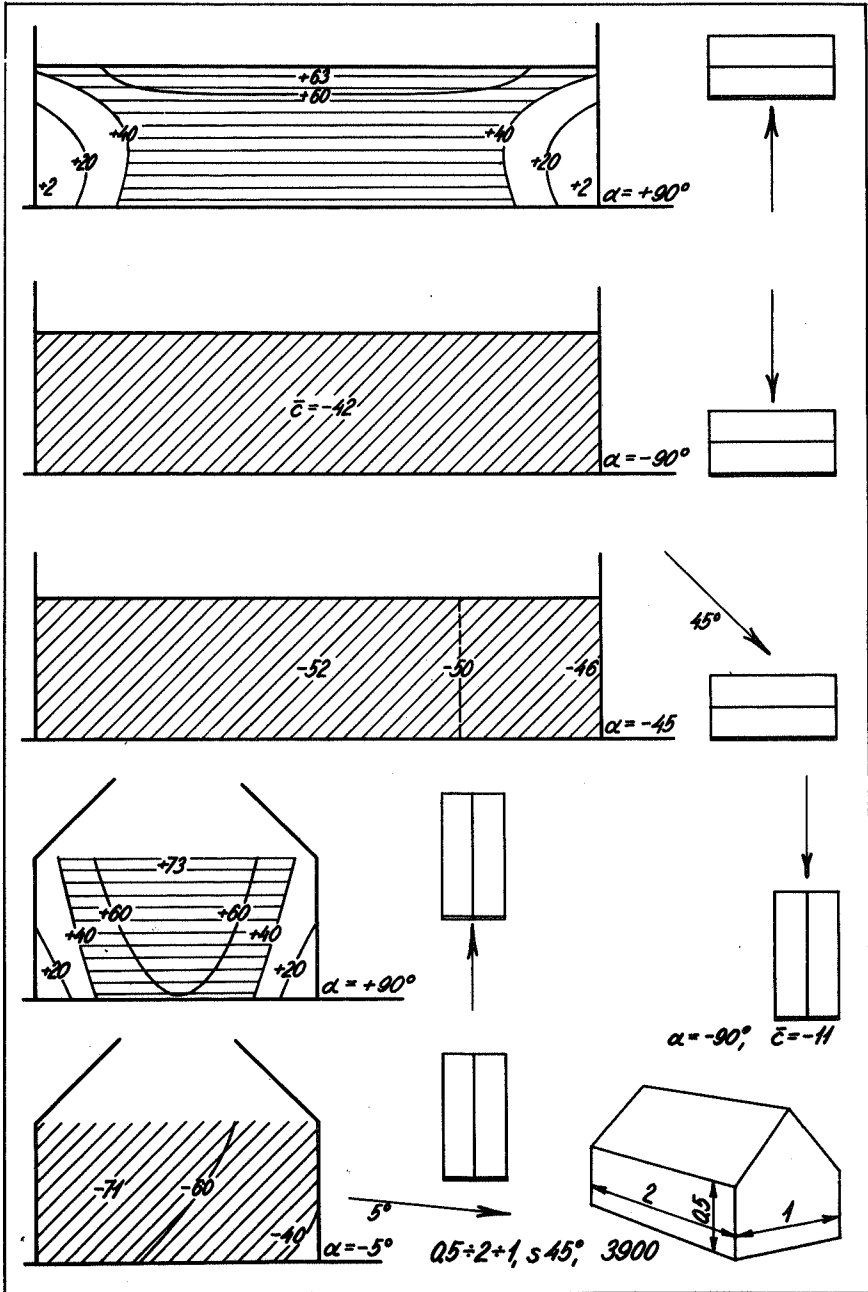
Figs. 48 to 61. Wind load on exterior walls.

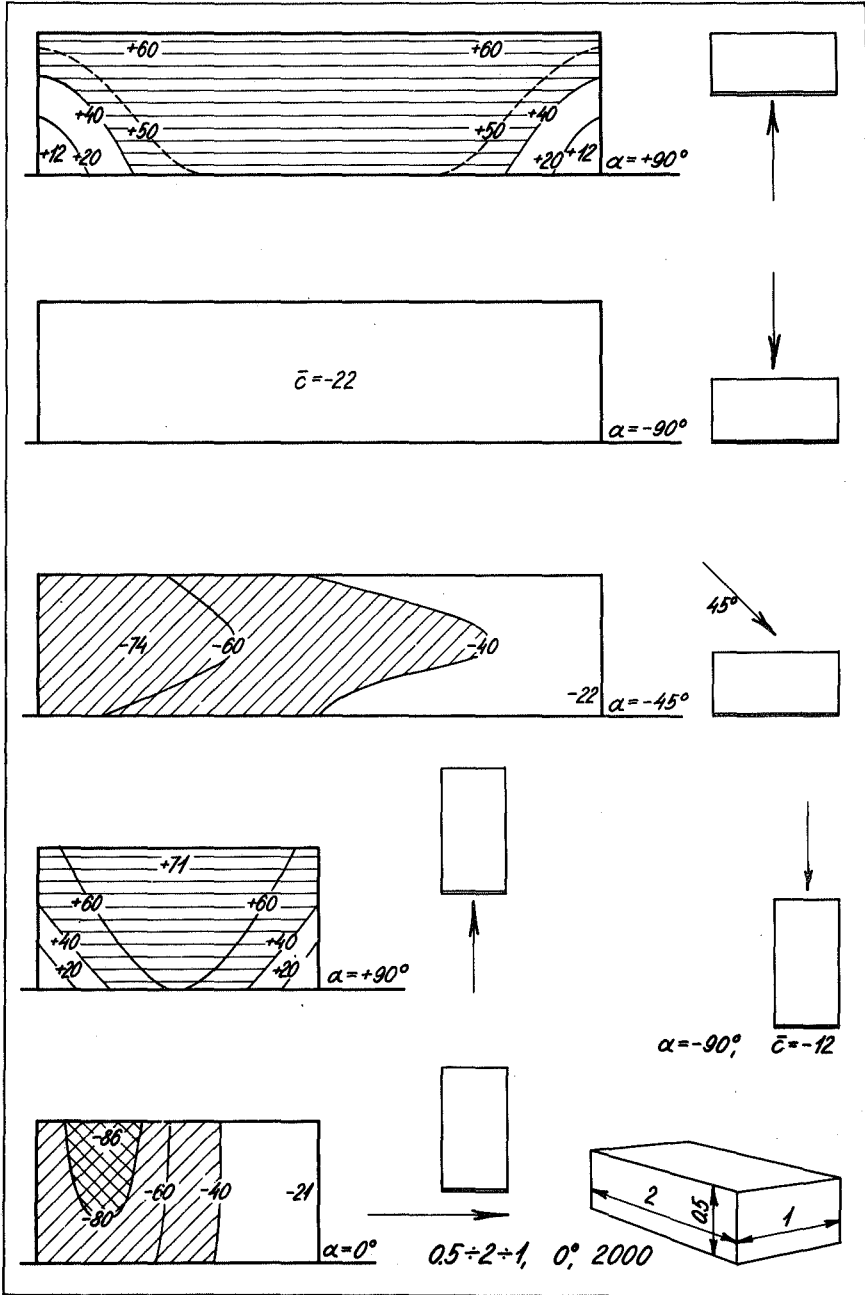
The shape factors are given as a percentage. Pressure is indicated by + and by horizontal and vertical hatching.

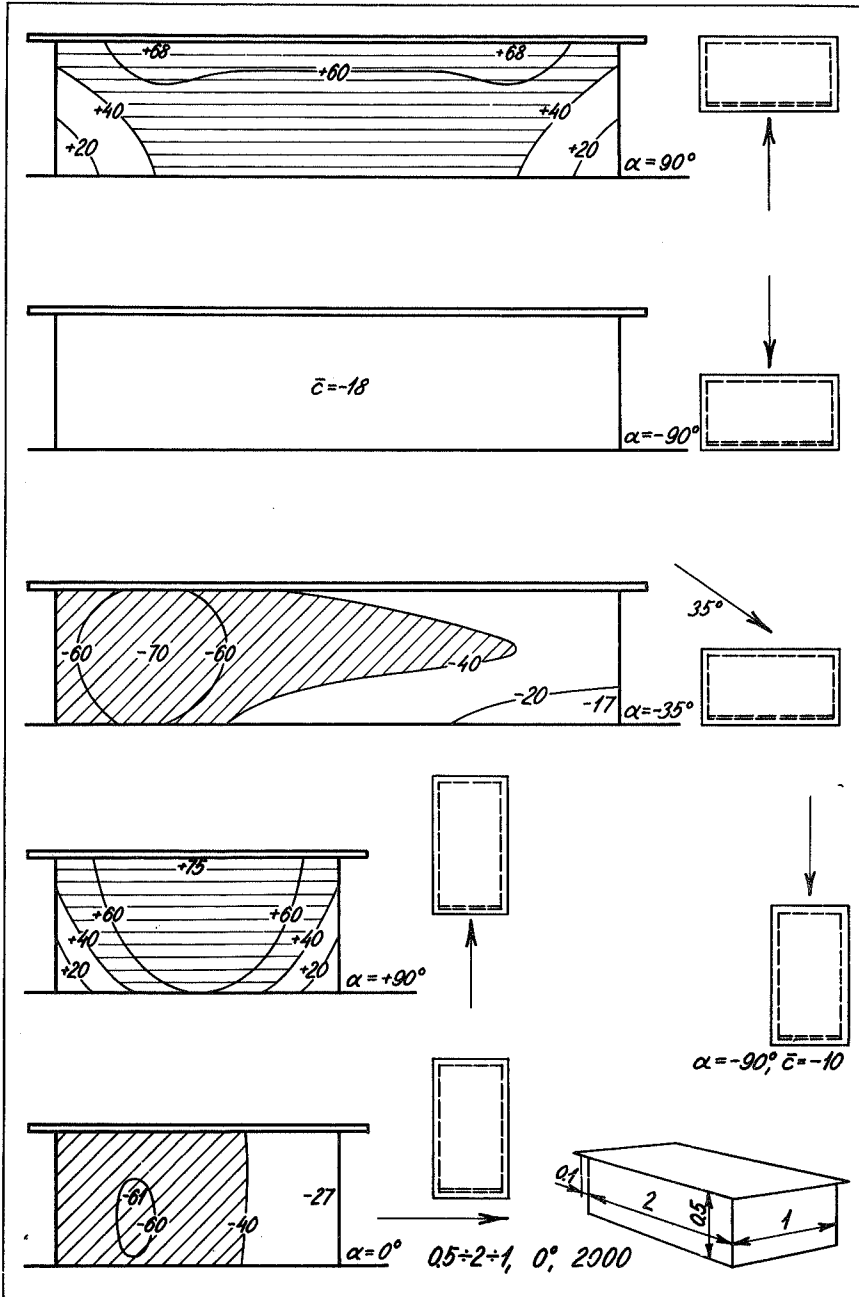
Suction is indicated by - and by oblique hatching.

Areas where the shape factors are between 40 and 80 per cent are single hatched. Areas where the shape factors are more than 80 per cent are double hatched.









## 6. HORIZONTAL ROOFS ON HOUSES

### 6.1 Scope of the tests

For the model tests with wind load on horizontal roofs three different types of houses were investigated. In Figure 64 the house types are shown and the placing of the measuring holes is given.

The models were of brass, see Section 1.4. They were placed on the turntable in the 4th section of the tunnel, and the measurements were performed as described in Section 1.6.

Three types of turbulent boundary layers were used, namely small turbulence,  $z_0 = 1.8 \cdot 10^{-3}$  cm, produced by smooth masonite plates, medium turbulence,  $z_0 = 0.047$  cm, from corrugated paper and large turbulence,  $z_0 = 0.45$  cm, from 2.5·2 cm lists. The Table gives a summary of the tests with horizontal roofs.

h÷l÷w	$\alpha$	Turbulence	Figure on page
2.4÷1÷1	0°	s	65
		l	65
1÷2÷1	0°	s	66
		m	67
		l	68
0.5÷2÷1	0°	s	69

s = small turbulence  
m = medium turbulence  
l = large turbulence.

### 6.2 Test results

In Figures 65 to 69 the shape factors derived from the tests are given.

The shape factor is  $c = p/q$ , where  $p$  is the suction at the point concerned and  $q$  is the velocity pressure level with the roof.

Curves are drawn through points with equal  $c$ -values, and extreme point values are given.

For each model the shape factors are given for the model positions with the most interesting loading conditions.

### 6.3 Conclusions

It can be seen from Figures 65 to 69 that there is almost always suction all over the horizontal roof.

This suction is greatest either right at the windward edge of the roof or quite close behind; from here the suction decreases with increasing distance from the windward edge.

A comparison between similar house types in different roughness conditions shows that when the wind blows at right angles to the facade or the gable the suction in the smooth case will be more uniformly distributed over the roof than in the rough case, in which the suction values decrease rapidly from the windward edge of the roof. The mean value of the suction over the whole roof or a large part of the roof is greatest in the smooth case. But the maximum values are greatest in the rough case.

When the wind blows skew to the house there is suction over the whole surface in all cases. This suction is greatest at the edge of the roof in the vicinity of the windward corner, but not at the corner. The suction decreases with increasing distance from the windward edge of the roof.

The smooth tests show for skew wind the greatest suction both for maximum values and for mean values over large or small areas of the roof.

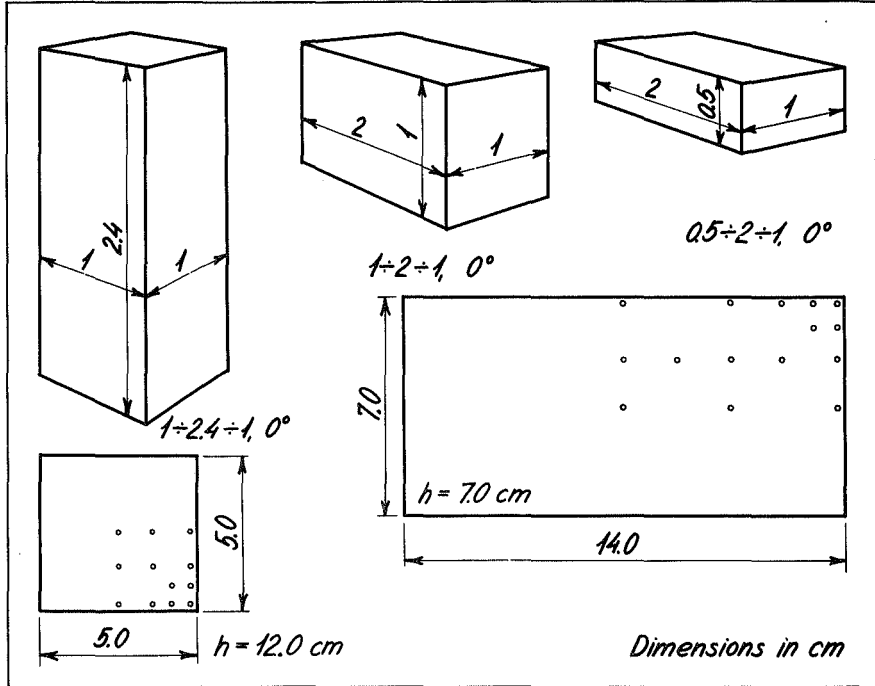


Fig. 64. House models for investigation of the wind load on horizontal roofs on houses.

The small circles indicate measuring holes.

Figs. 65 to 69. The wind load on horizontal roofs on houses.

The wind direction is given by the angle between the wind and the longitudinal axis of the house.

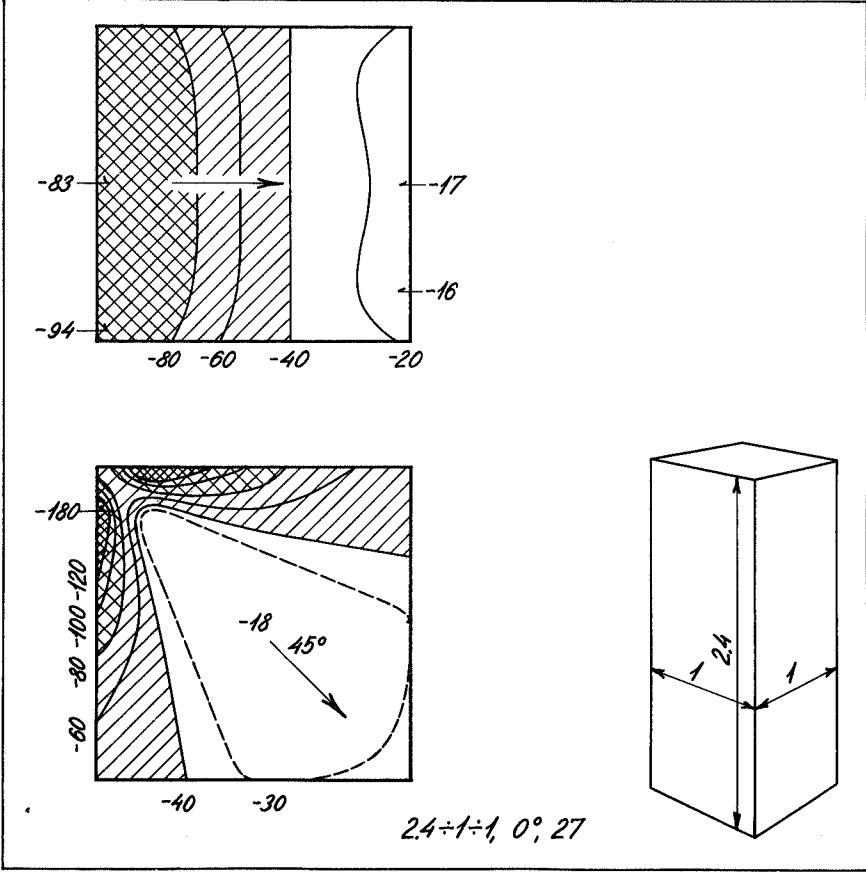
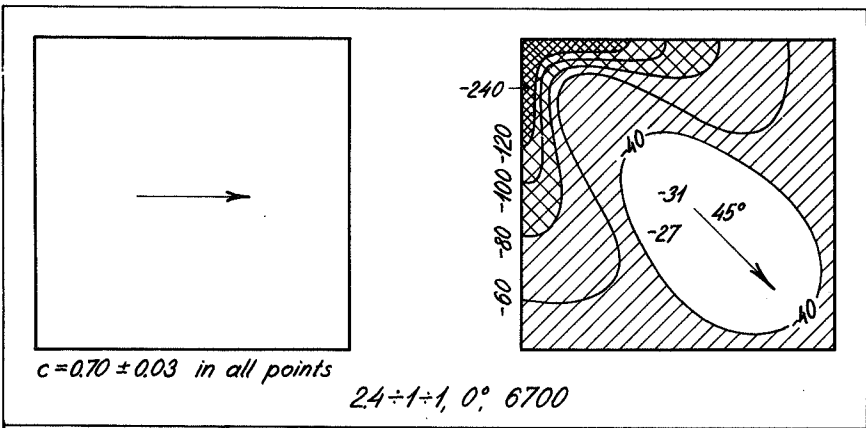
The shape factors are given as a percentage. Suction is indicated by a negative sign and oblique hatching, pressure by a positive sign and horizontal-vertical hatching.

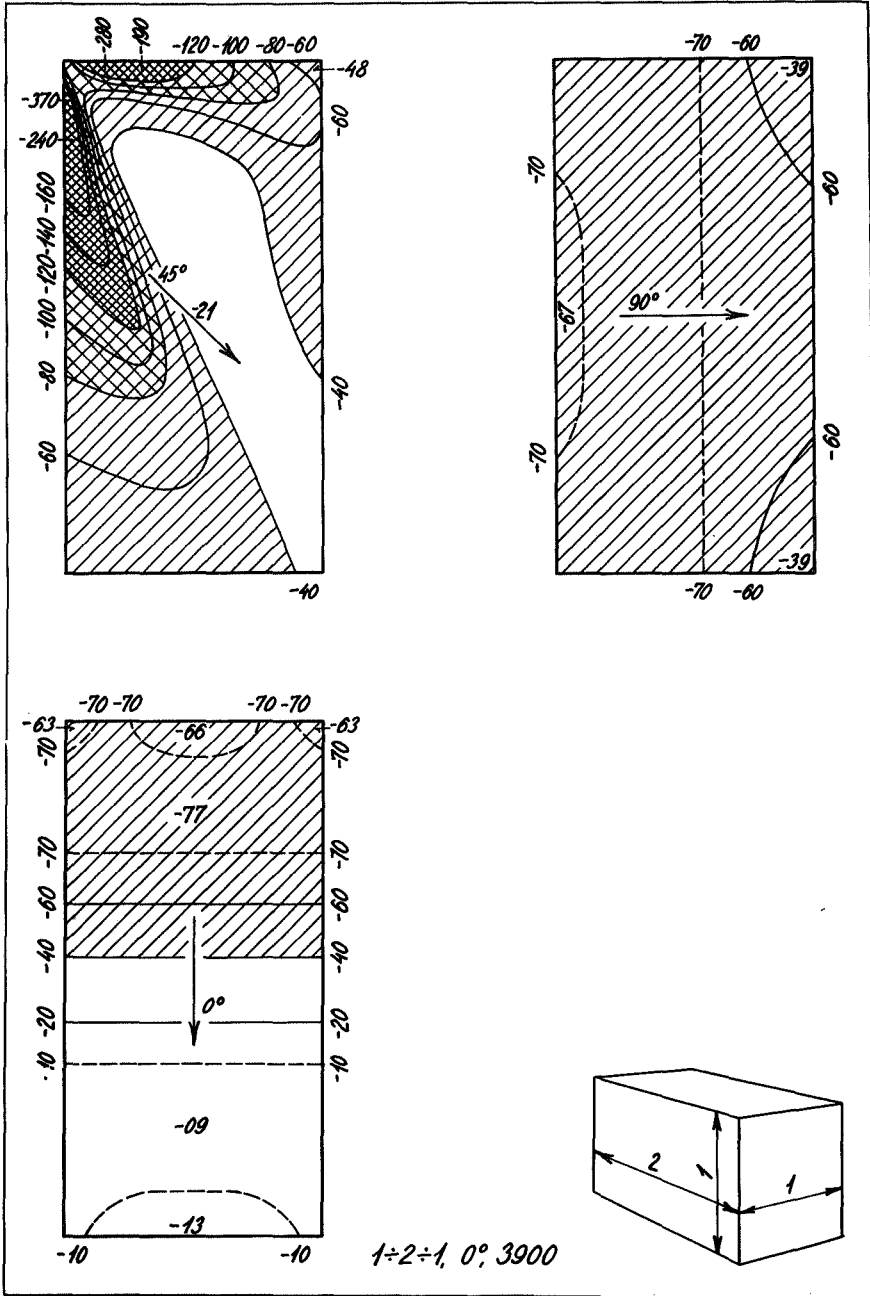
Contour lines are drawn for the wind load at  $c = 20$   $40$   $60$  per cent etc.

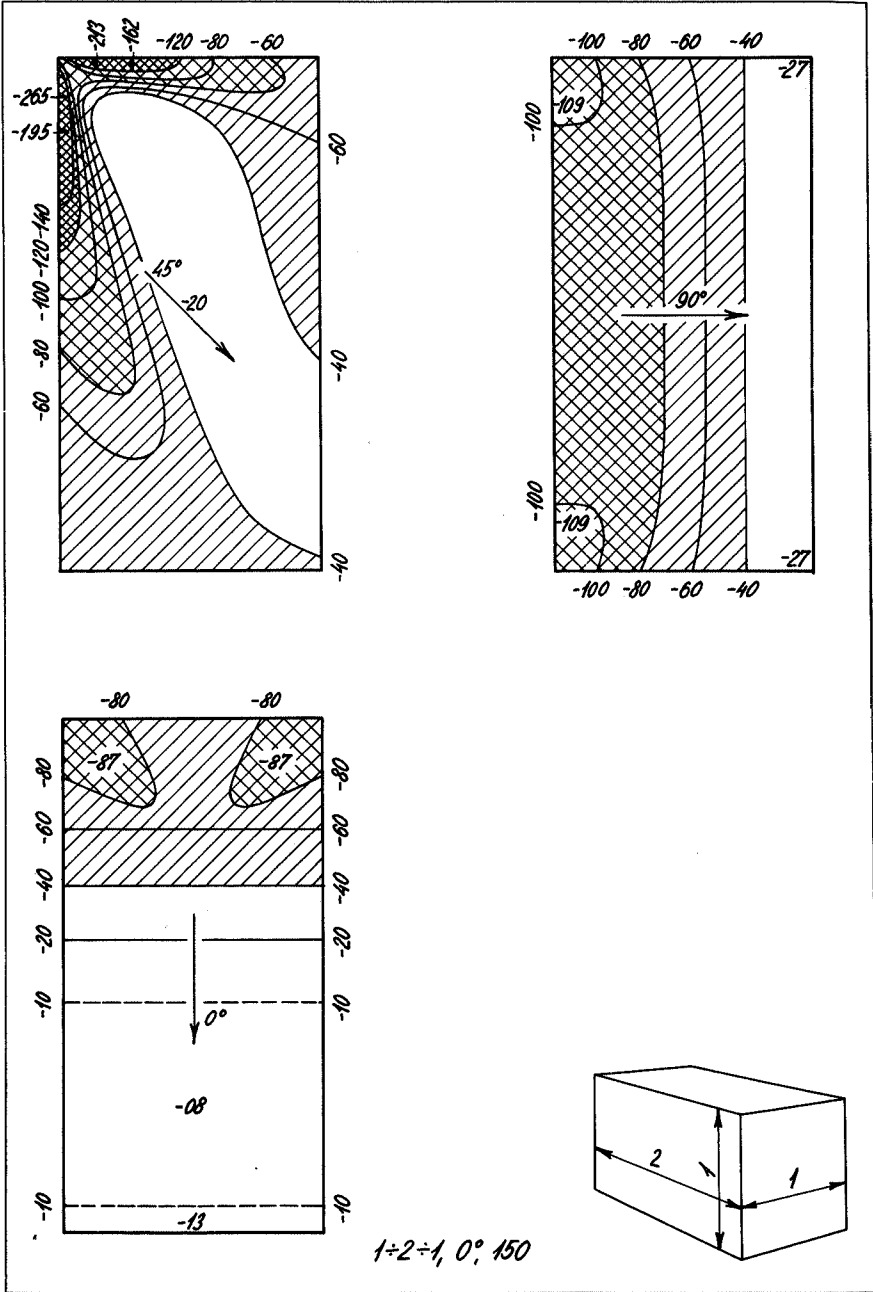
In some cases intermediate contours, for example  $c = 30$  or  $c = 50$  per cent, are shown as broken lines.

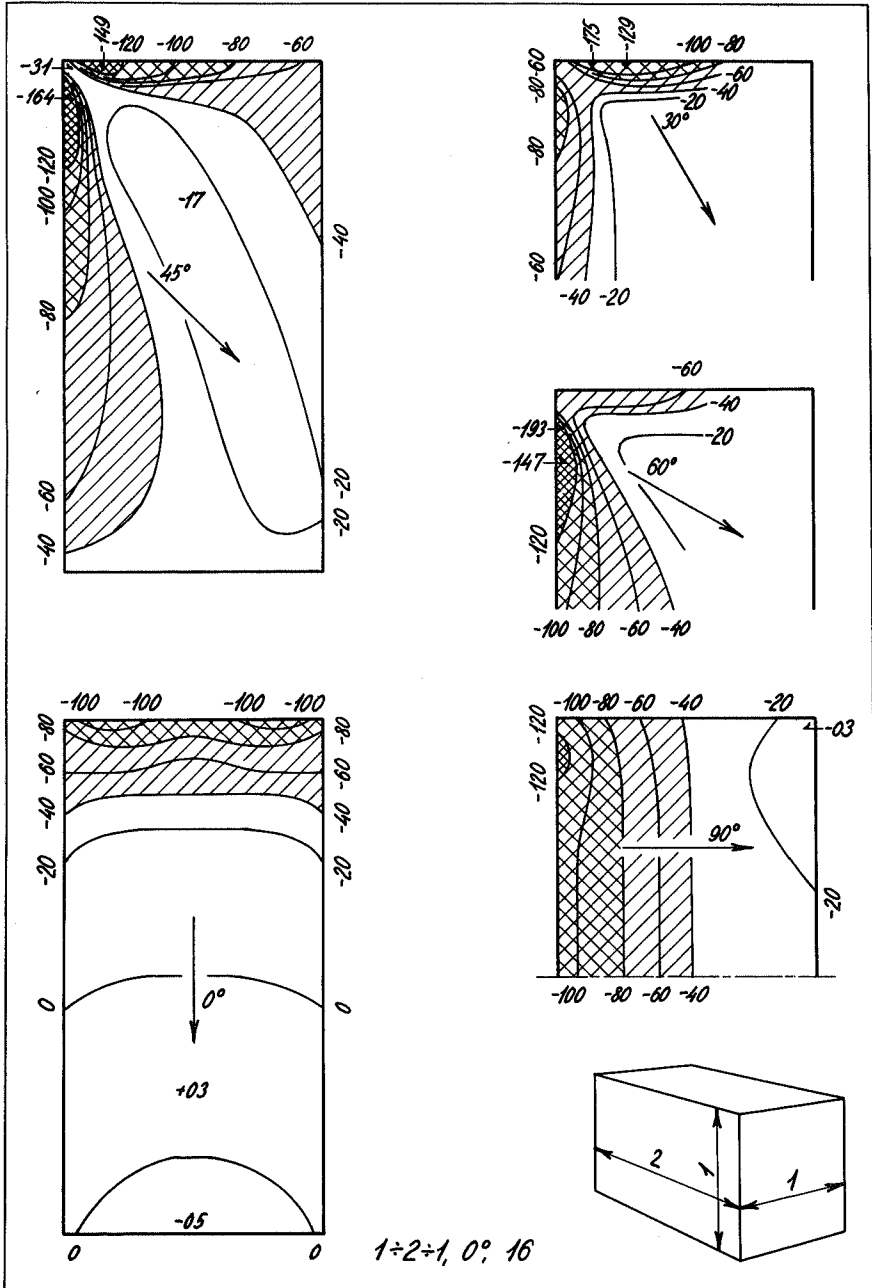
Areas in which the shape factor is between 40 and 80 per cent are single hatched, areas between 80 and 120 per cent are double hatched and areas of more than 120 per cent are densely double hatched.

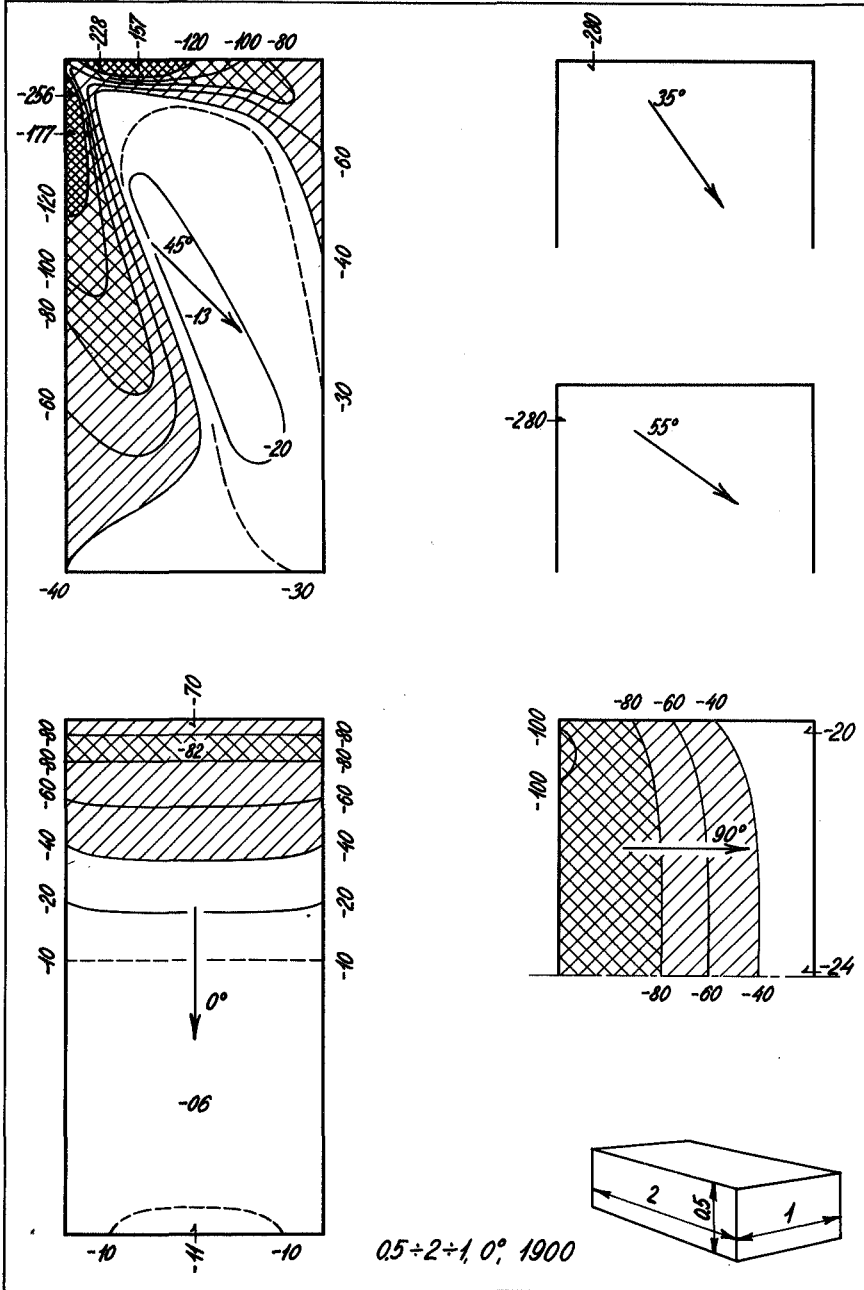
The extreme values of the shape factors are noted.











## 7. DESK ROOFS ON HOUSES

### 7.1 Scope of the tests

For the model tests with wind load on desk roofs nine different types of houses were investigated. In Figure 71 and 72 the house types are shown and the placing of the measuring holes is given.

The models were of brass, see Section 1.4. They were placed on the turntable in the 4th section of the tunnel, and the measurements were performed as described in Section 1.6.

Two types of turbulent boundary layers were used, namely small turbulence,  $z_0 = 1.8 \cdot 10^{-3}$  cm, from smooth masonite plates and large turbulence,  $z_0 = 0.45$  cm, from 2.5·2 cm lists.

The Table gives a summary of the tests with the desk roofs.

$h+1:w$	$\alpha$	Turbulence	Figure on page
2+4+1	d 5.7°	s	74 and 75
		l	76 and 77
1+2+1	d 6°	s	78 and 79
		l	80 and 81
	d 10°	s	82 and 83
		l	84 and 85
	d 15°	s	86 and 87
l		88 and 89	
d 25°	s	90 and 91	
	l	92 and 93	
0.5+2+1	d 6°	s	94 and 95
	d 10°	s	96 and 97
	d 15°	s	98 and 99

s = small turbulence

l = large turbulence

## 7.2 Test results

In Figure 74 to 99 the shape factors derived from the tests are given.

The shape factor is  $c = p/q$ , where  $p$  is the suction at the point concerned and  $q$  is the velocity pressure level with the highest line in the roof.

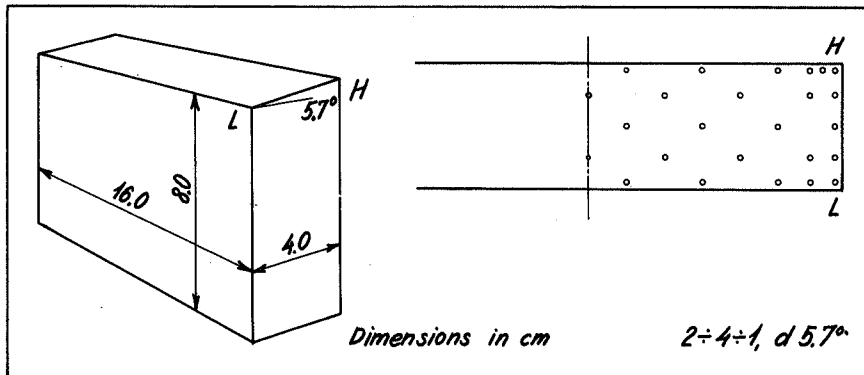
Curves are drawn through points with equal  $c$ -values, and extreme point values are given.

For each model the shape factors are given for the model positions with the most interesting loading conditions.

For some of the model arrangements only the load on a part of the roof is given, namely when the load here has an extreme value and the load on the remaining part of the roof is of less interest.

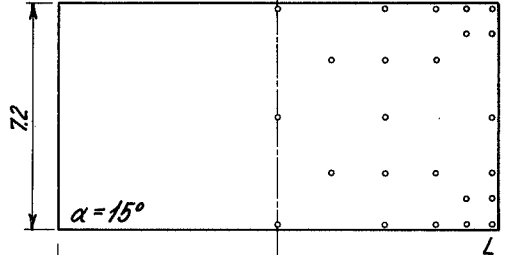
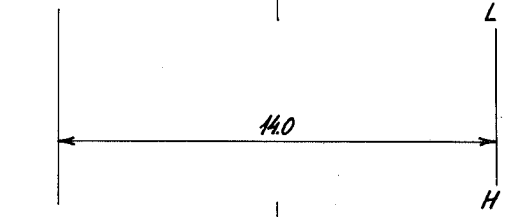
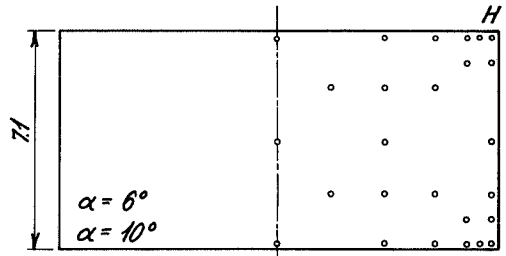
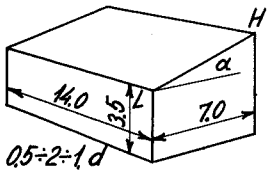
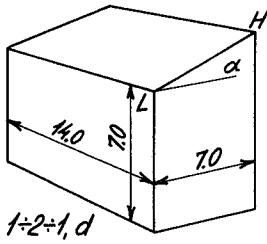
For some of the very large suction values, which were measured locally at the corners of the roof, a slight dependence on the wind velocity was found, so that the suction increased a little when the wind velocity increased.

Concerning these points the shape factors were determined by measurements taken with the greatest possible wind velocity in the tunnel.



Figs. 71 and 72. House models for investigation of the wind load on desk roofs on houses.

The small circles indicate measuring holes.



Dimensions in cm

### 7.3 Conclusions

The investigations dealt with desk roofs up to  $15^\circ$  slope. In the smooth tunnel tests there will in all cases be suction all over the roof. In the rough tunnel tests pressure occurs on the roof, but of small magnitude and extent.

When the wind is blowing parallel to the house the conditions of course are nearly as if the roof was horizontal, that is they are almost independent of the roof slope.

In the rough cases the suction is greater at the windward roof edge than in the smooth cases. But in the rough cases the decrease in suction with the distance from the windward edge is greater, so that there will be smaller areas with suction values of more than for instance  $c = 0.40$  in the rough cases than in the smooth.

When the wind blows at right angles to the house, with the lower edge leading, the greatest suction values will occur in the smooth cases.

But in the rough cases greater suction will usually occur when the high edge is leading rather than the lower.

The worst conditions occur when the wind blows skew to the house. Then very great suction occurs near the windward corner of the roof. These suction values are particularly great when the high corner is leading or, if the roof slope is  $6^\circ$  or  $10^\circ$ , when the lower corner is leading.

The greatest suction measured corresponds to  $c = 4.20$ . It is found in a smooth airflow at the high corner of the roof. In the rough airflow the greatest suction measured corresponds to  $c = 3.54$ .

Figs. 74 to 99. The wind load on desk roofs on houses.

The wind direction is given by the angle between the wind and the longitudinal axis of the house.

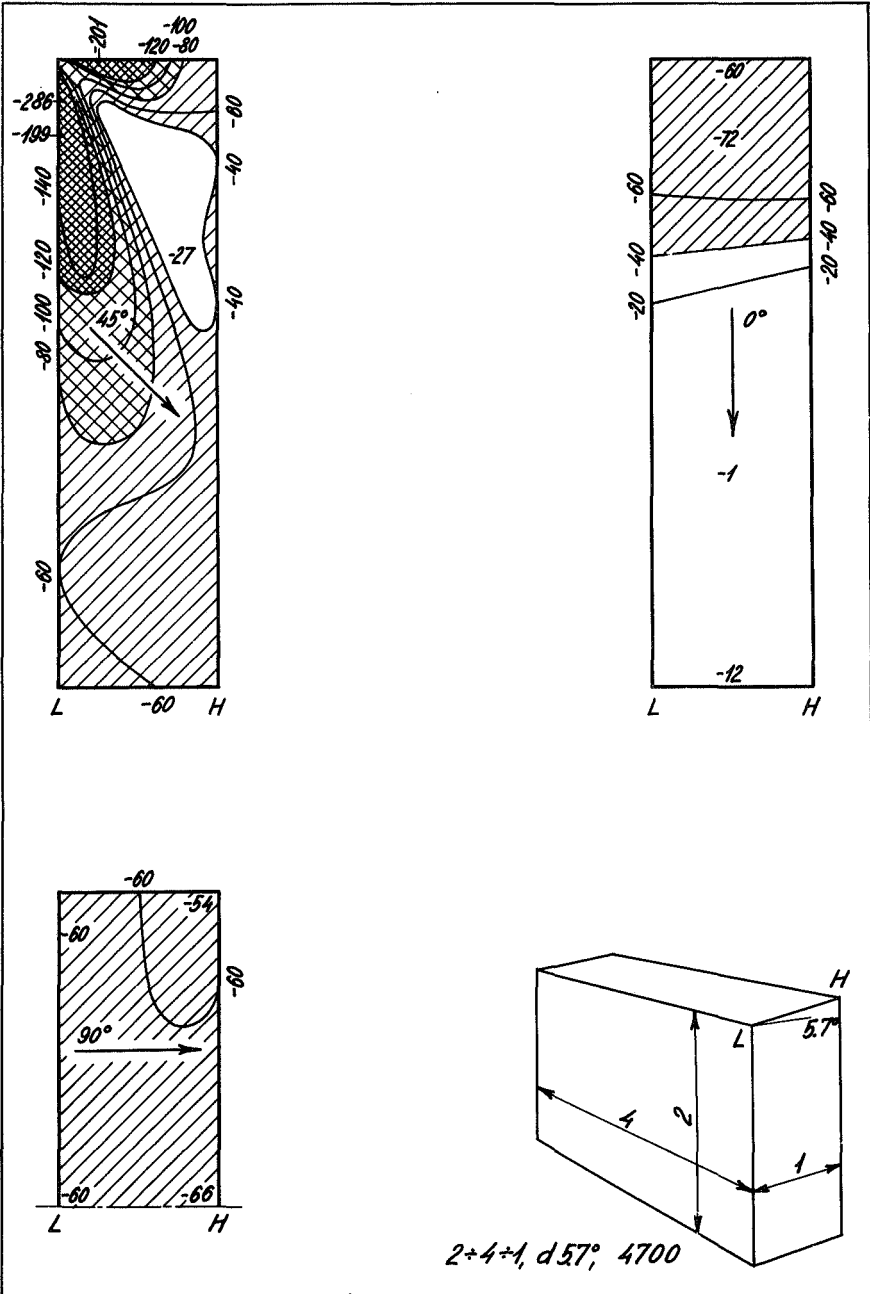
The shape factors are given as a percentage. Suction is indicated by a negative sign and oblique hatching, pressure by a positive sign and horizontal-vertical hatching.

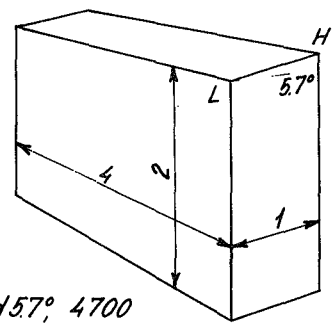
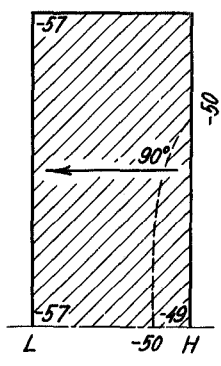
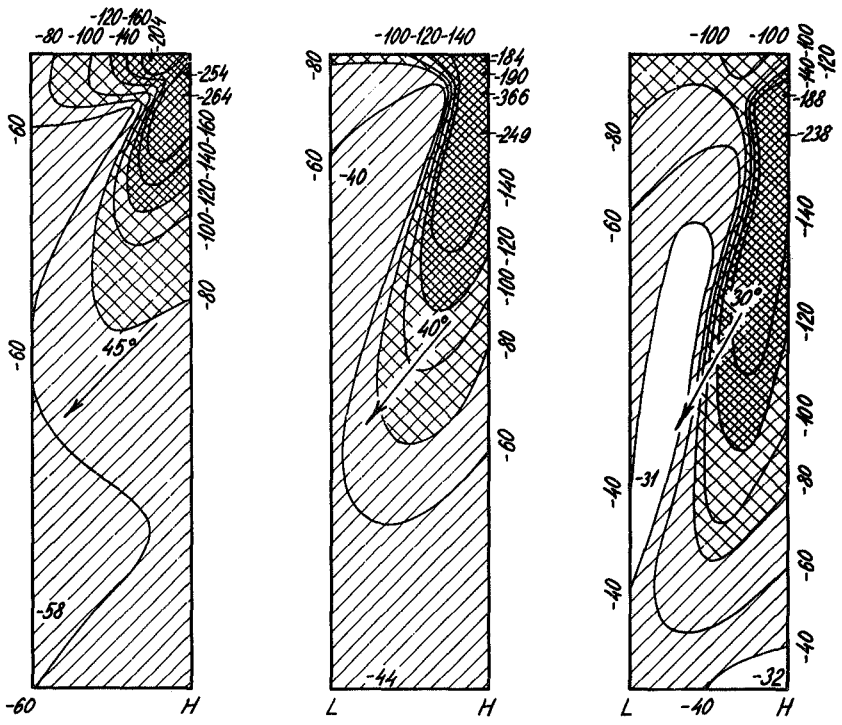
Contour lines are drawn for the wind load at  $c = 20$  40 60 per cent etc.

In some case intermediate contours, for example  $c = 30$  or  $c = 50$  per cent, are shown as broken lines.

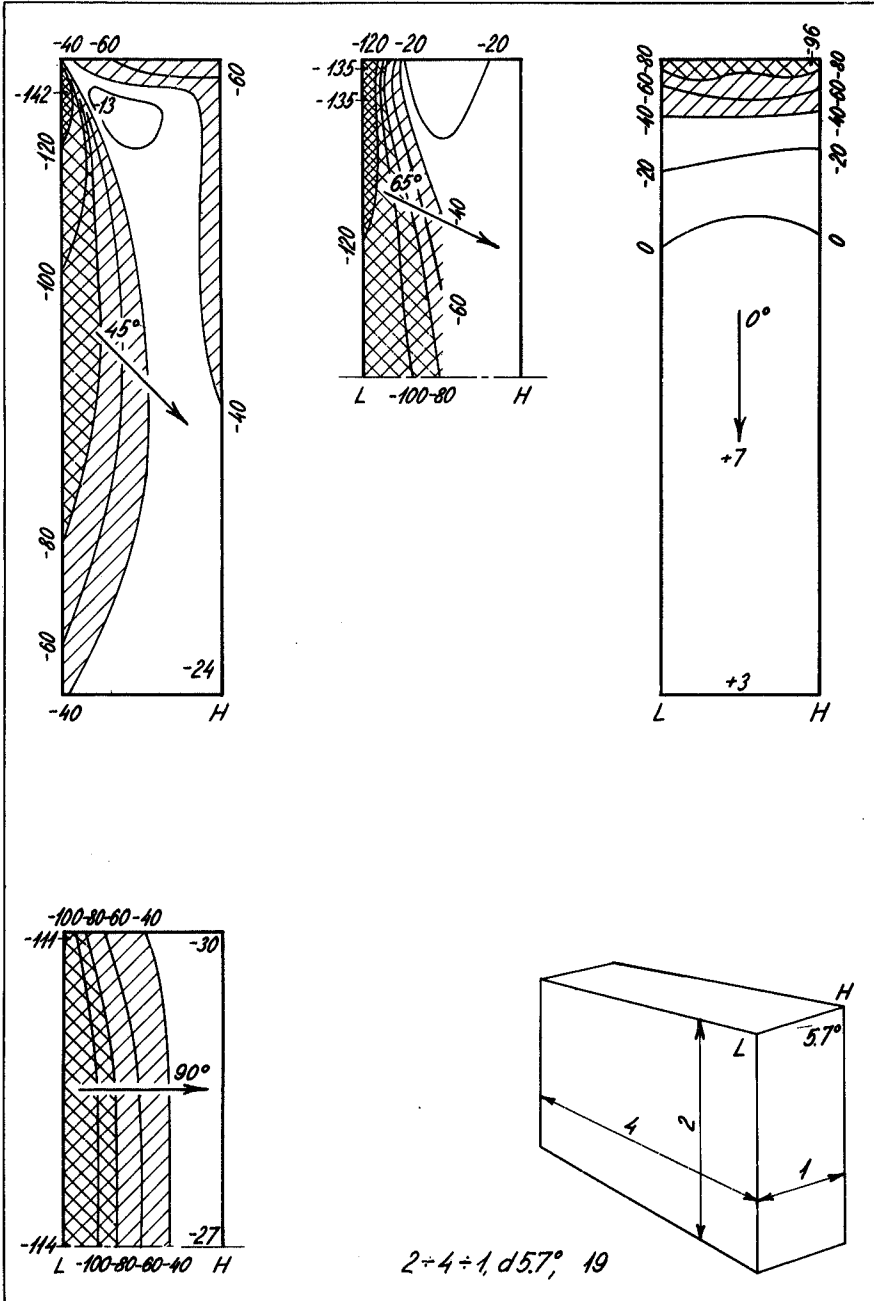
Areas in which the shape factor is between 40 and 80 per cent are single hatched, areas between 80 and 120 per cent are double hatched and areas of more than 120 per cent are densely double hatched.

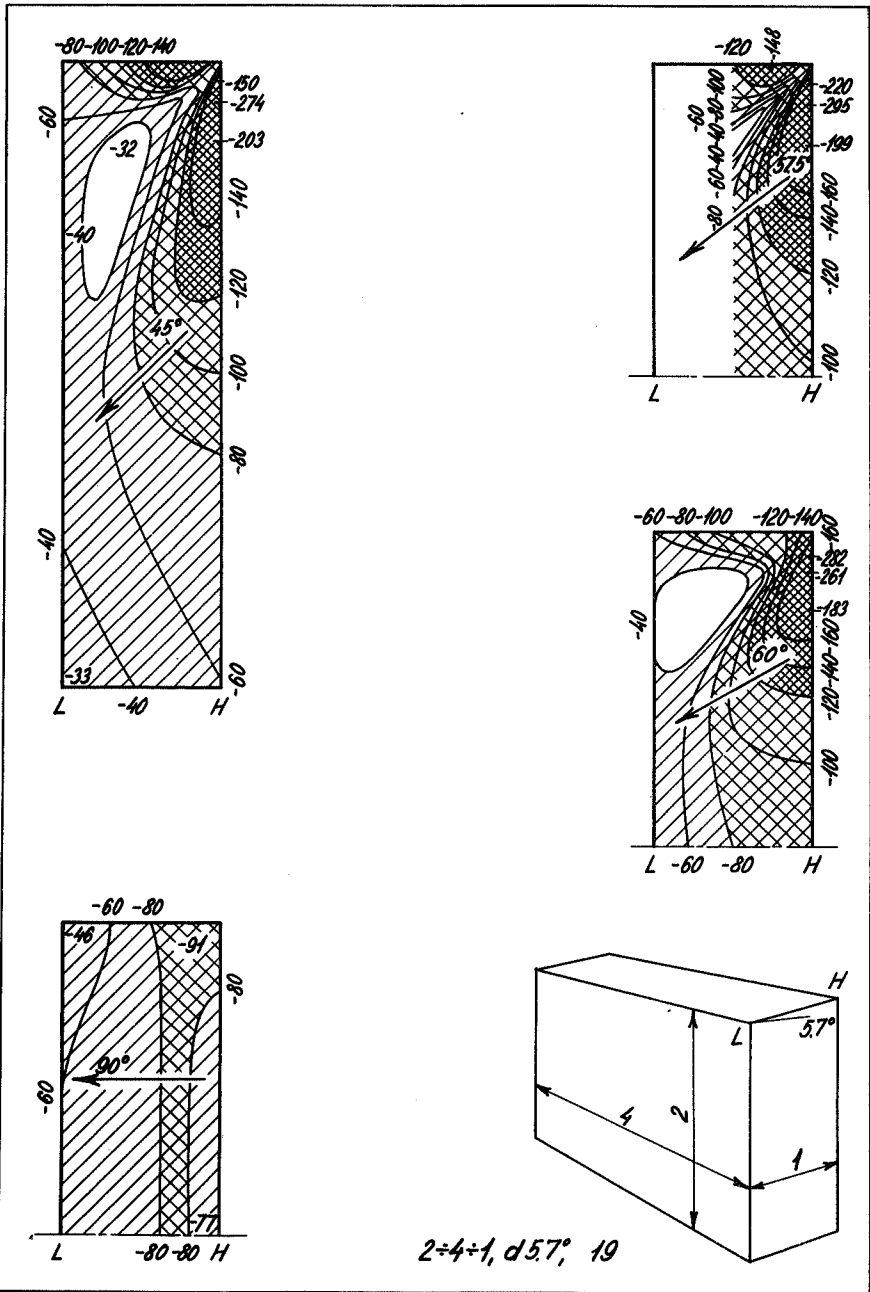
The extreme values of the shape factors are noted.

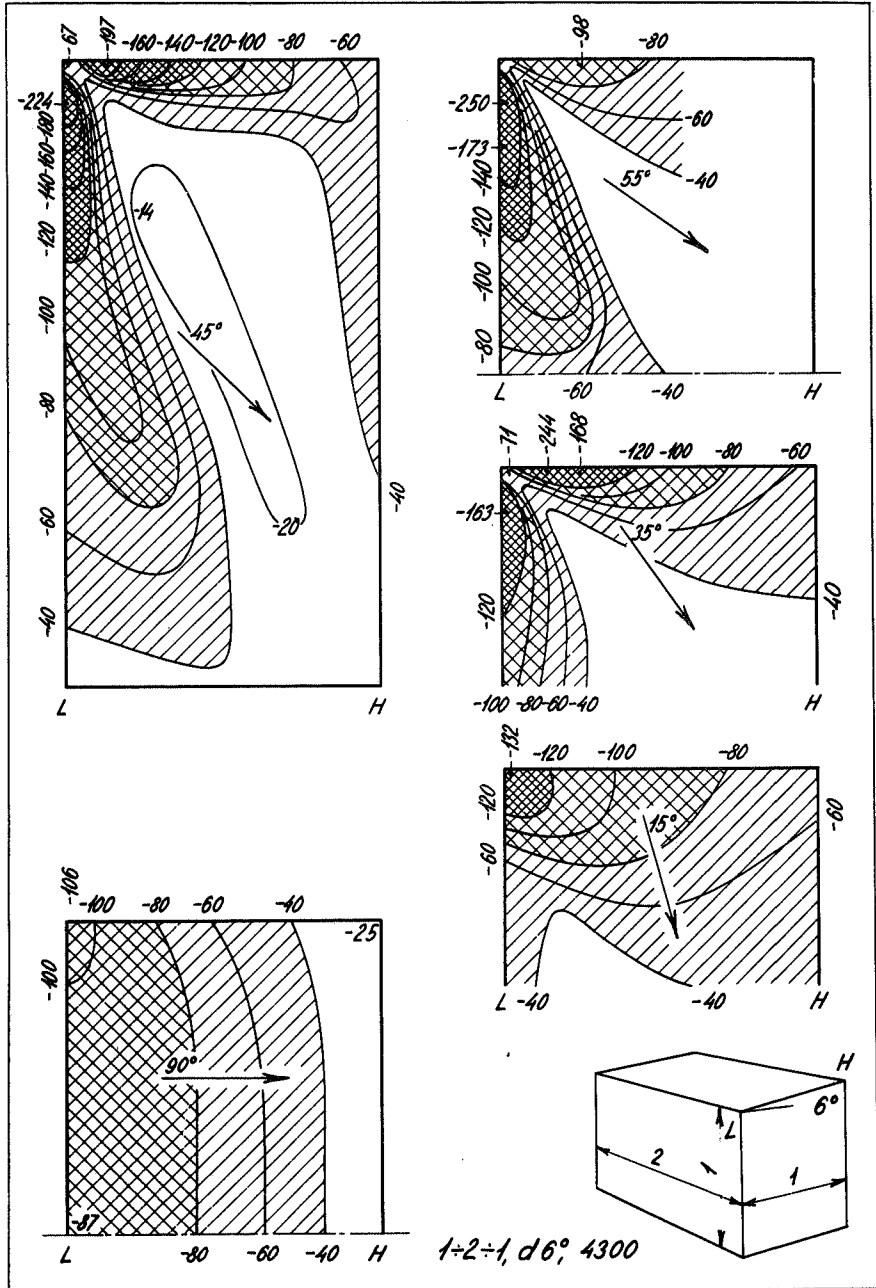


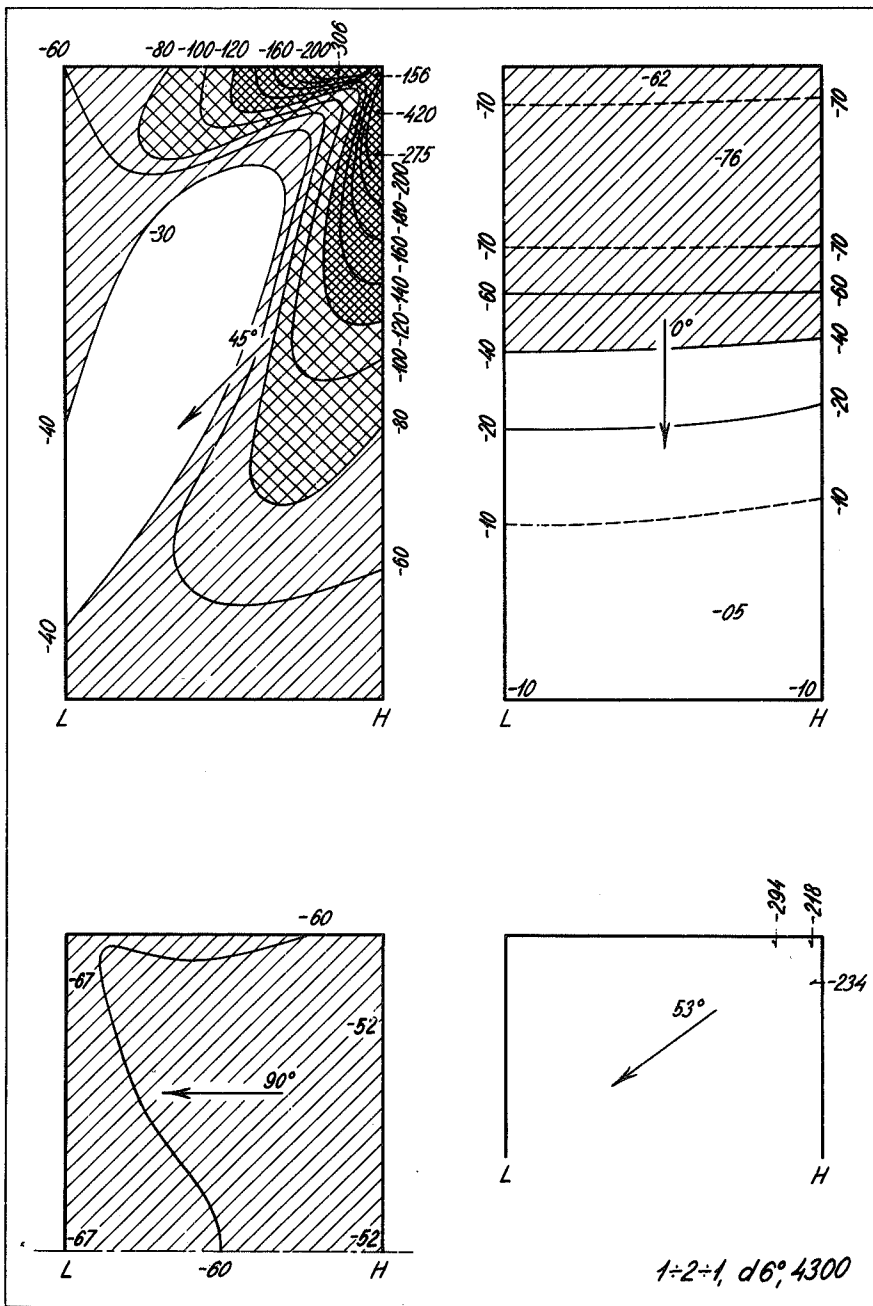


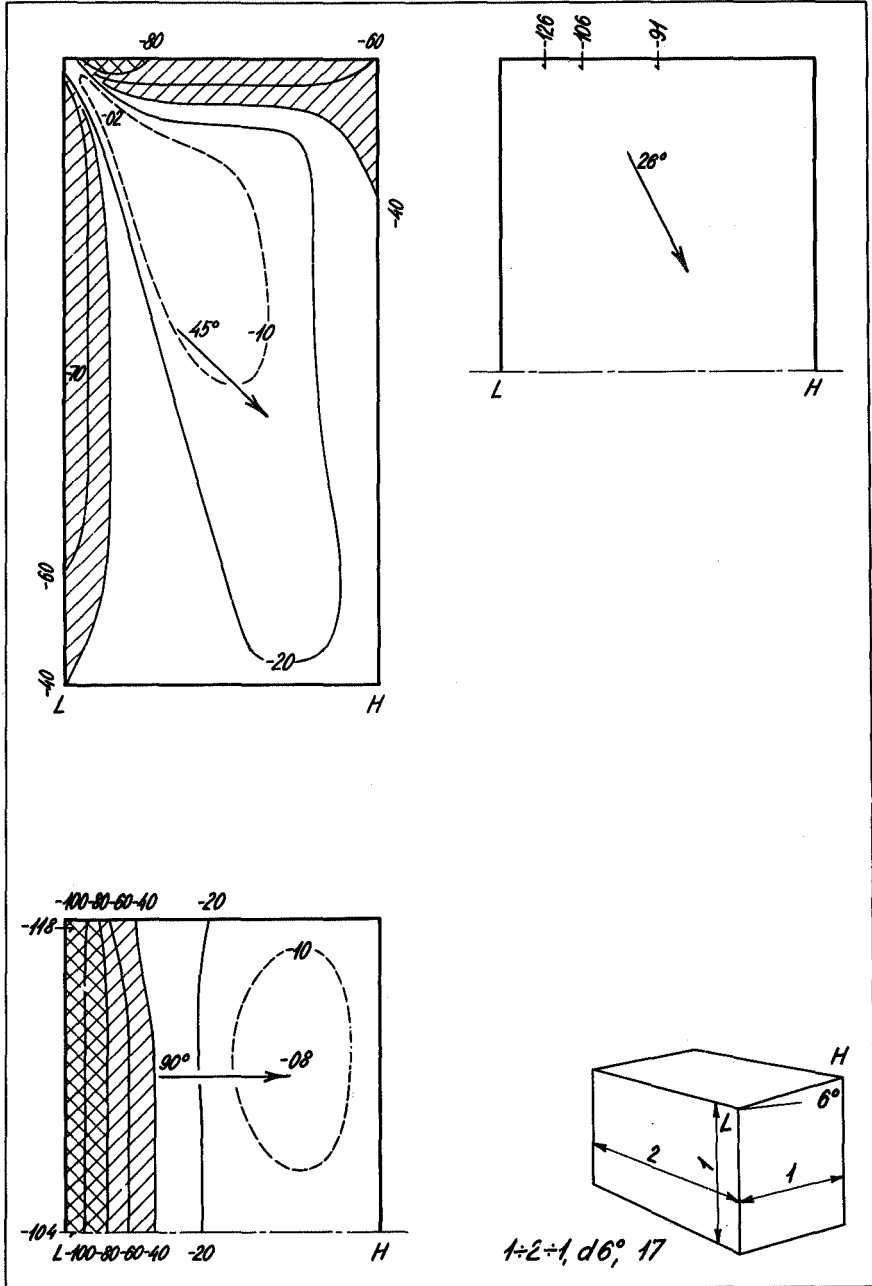
$2+4+1, d 5.7^\circ, 4700$

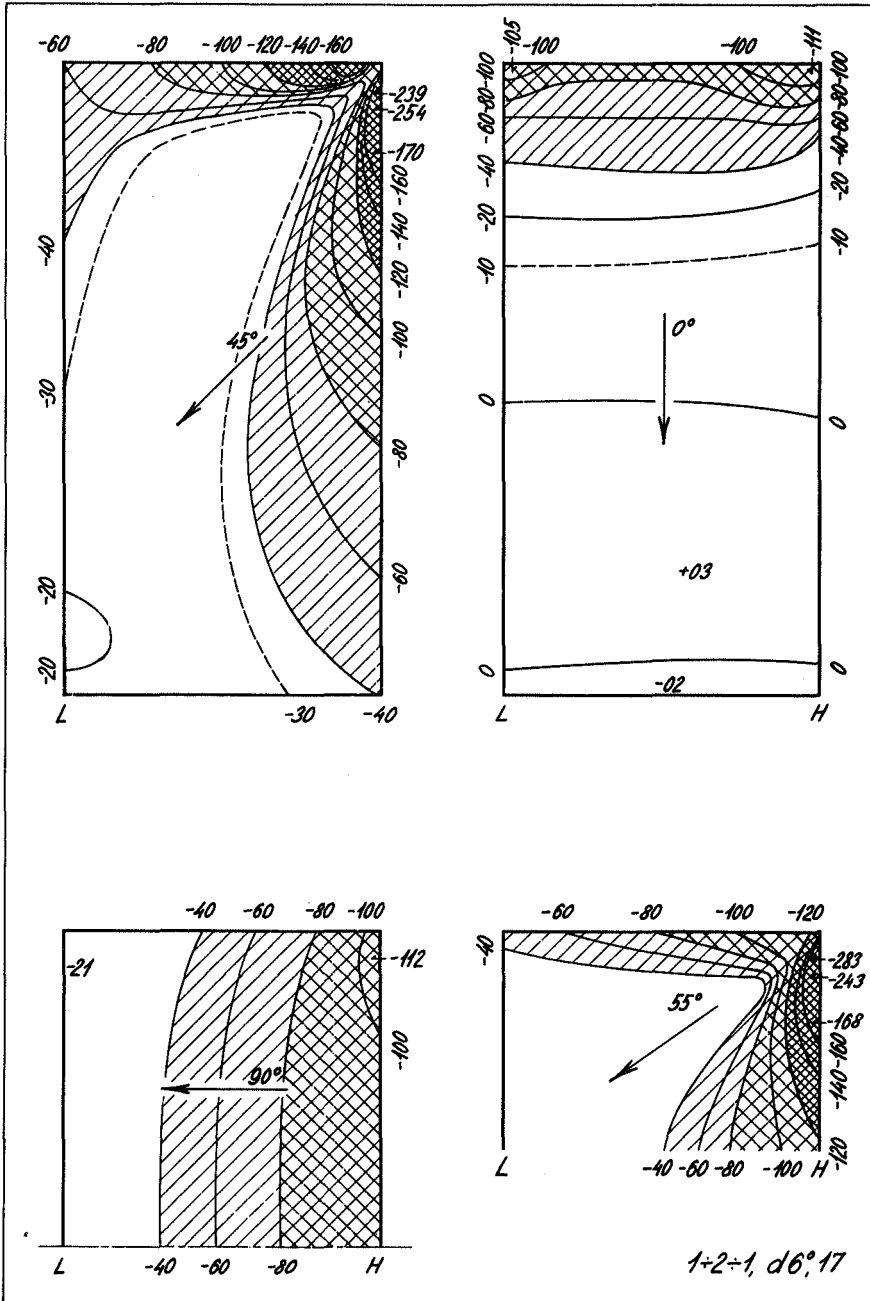


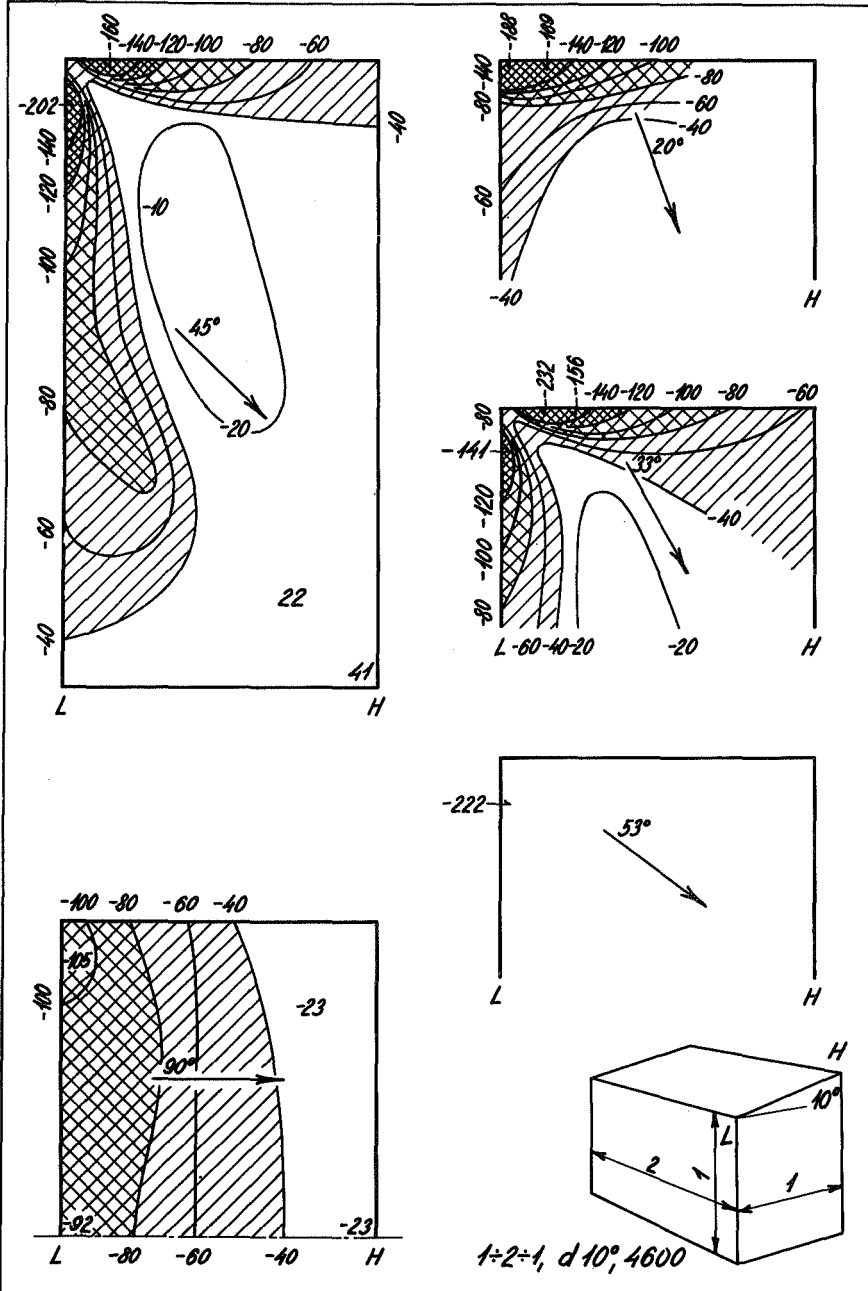


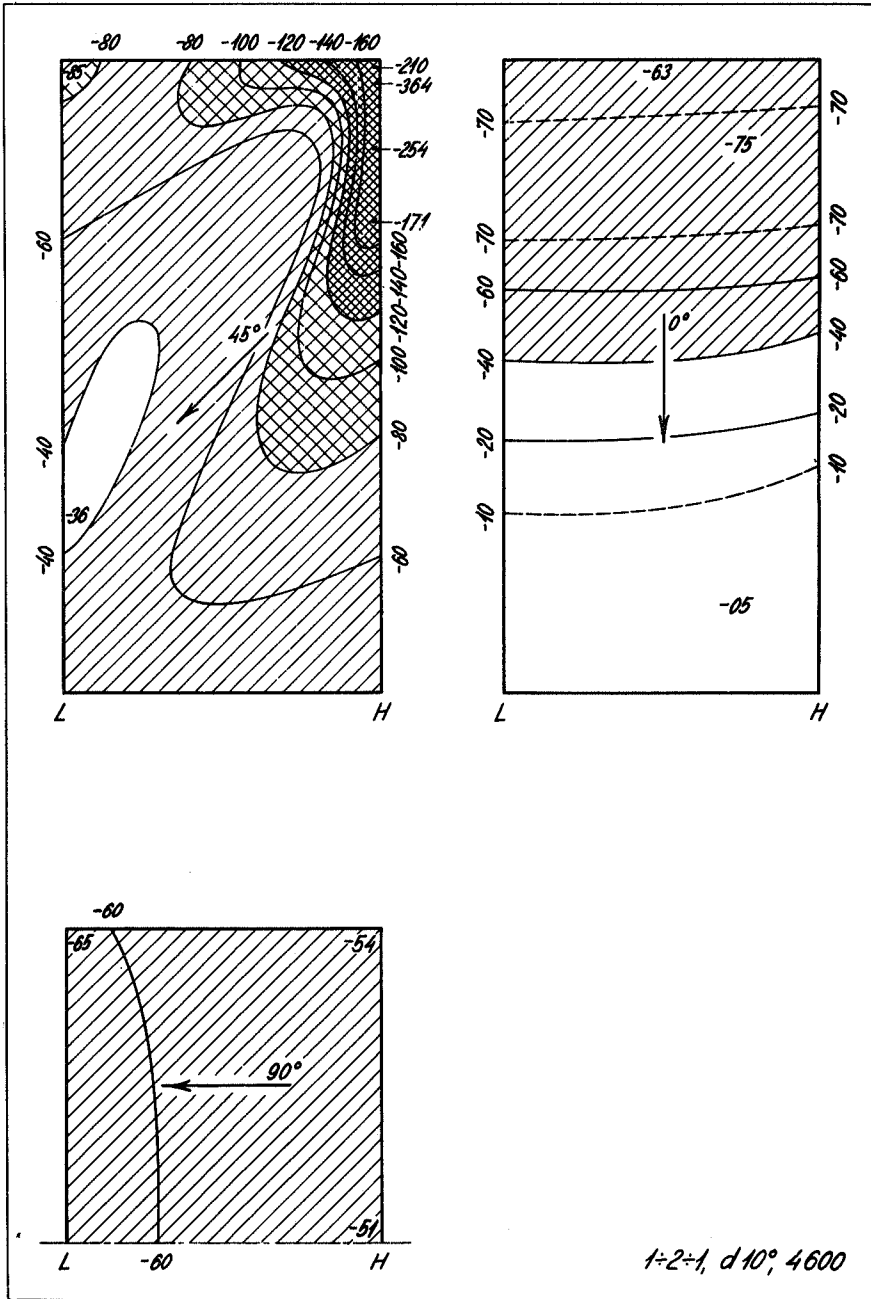


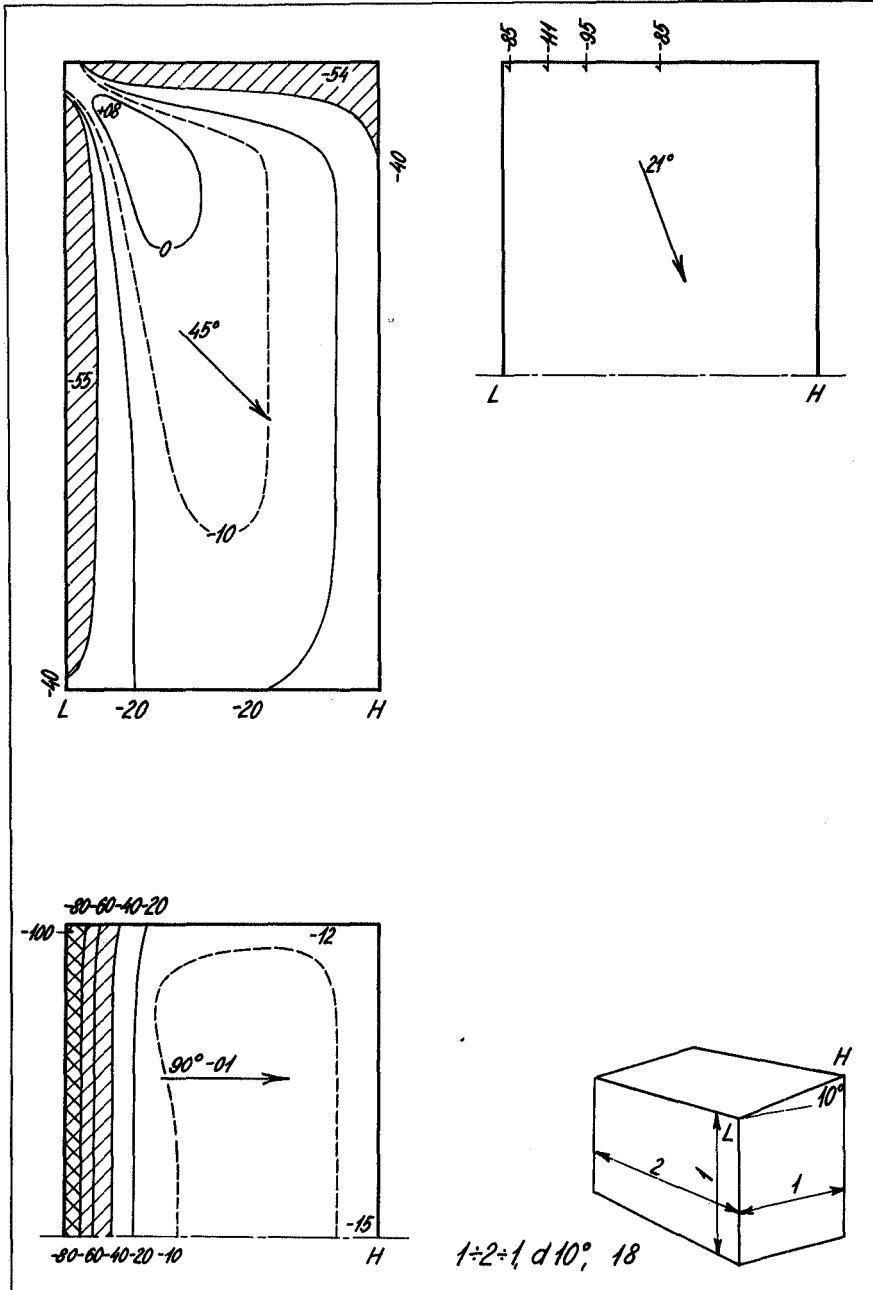


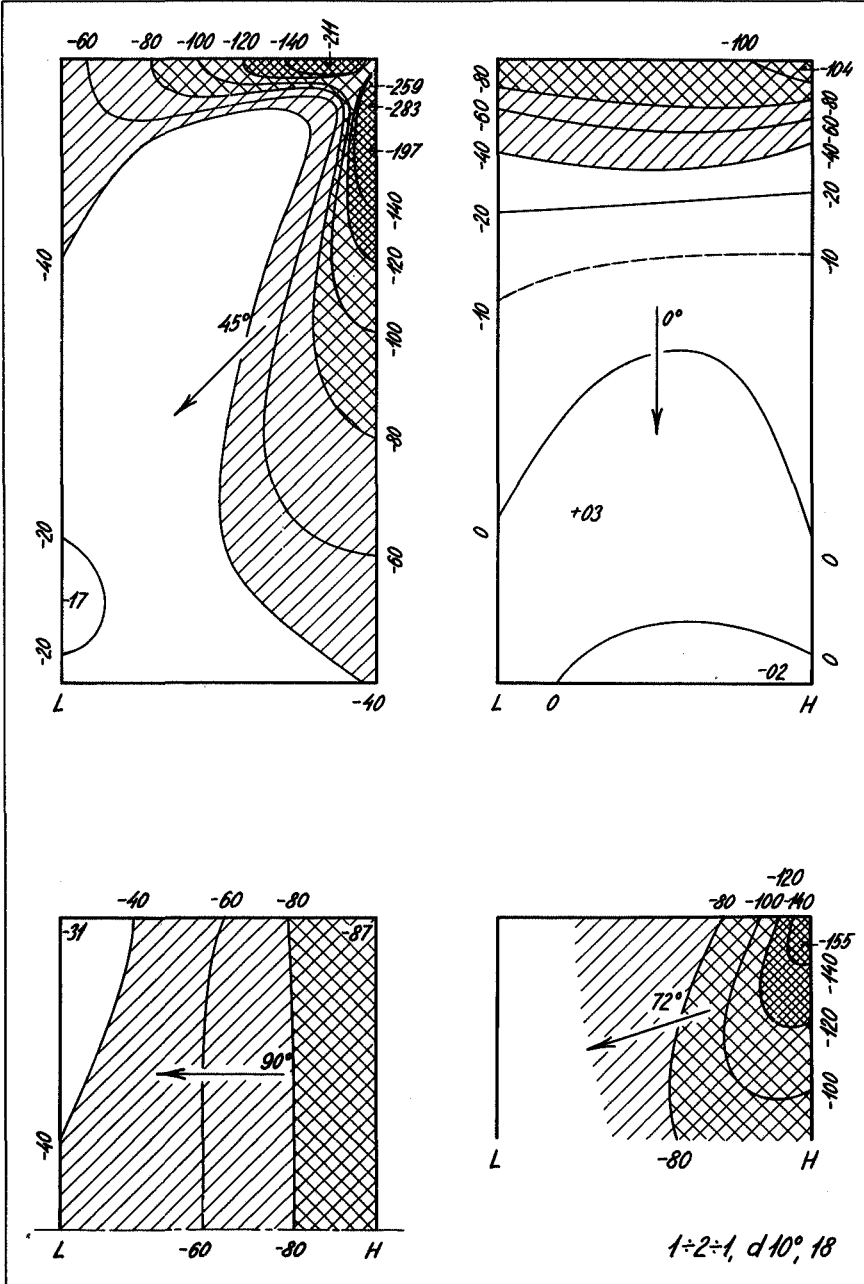


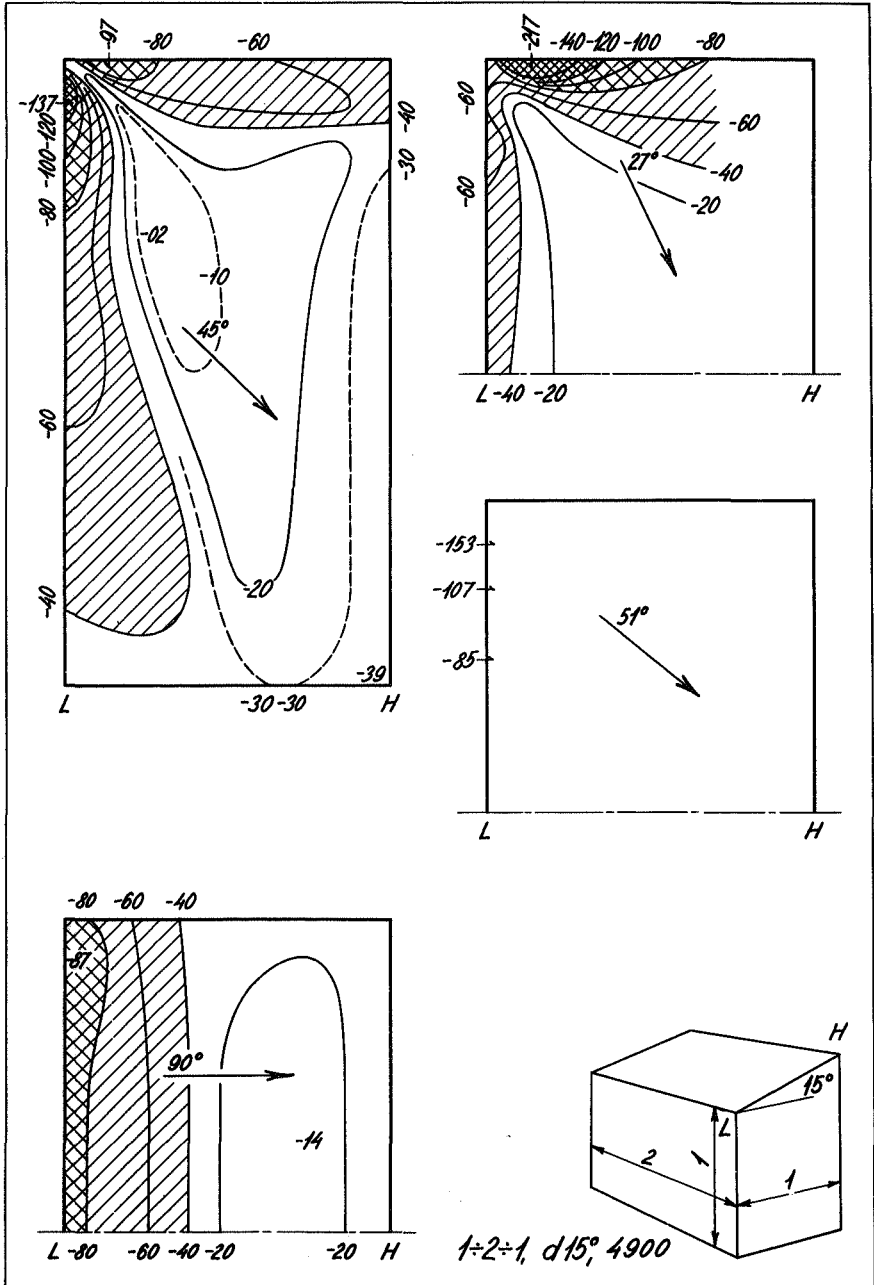


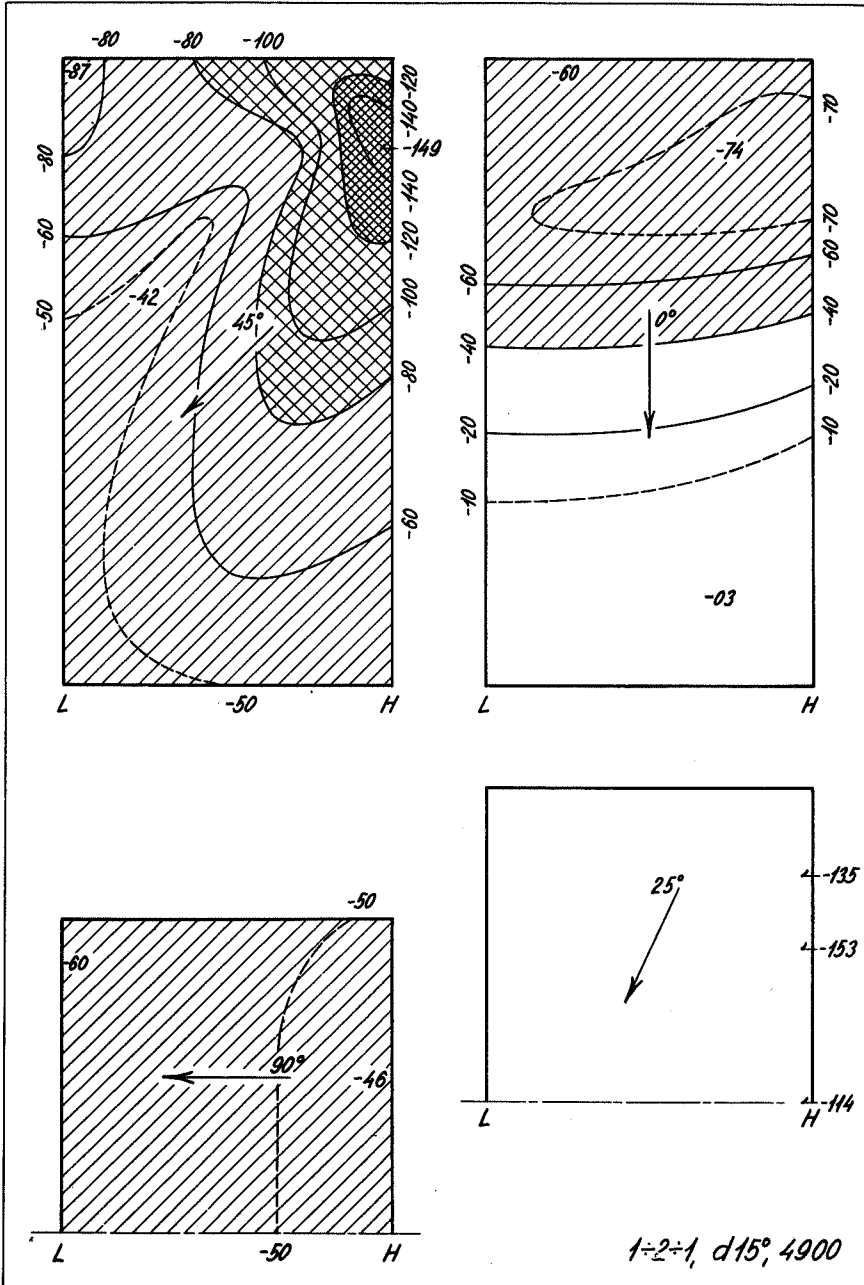


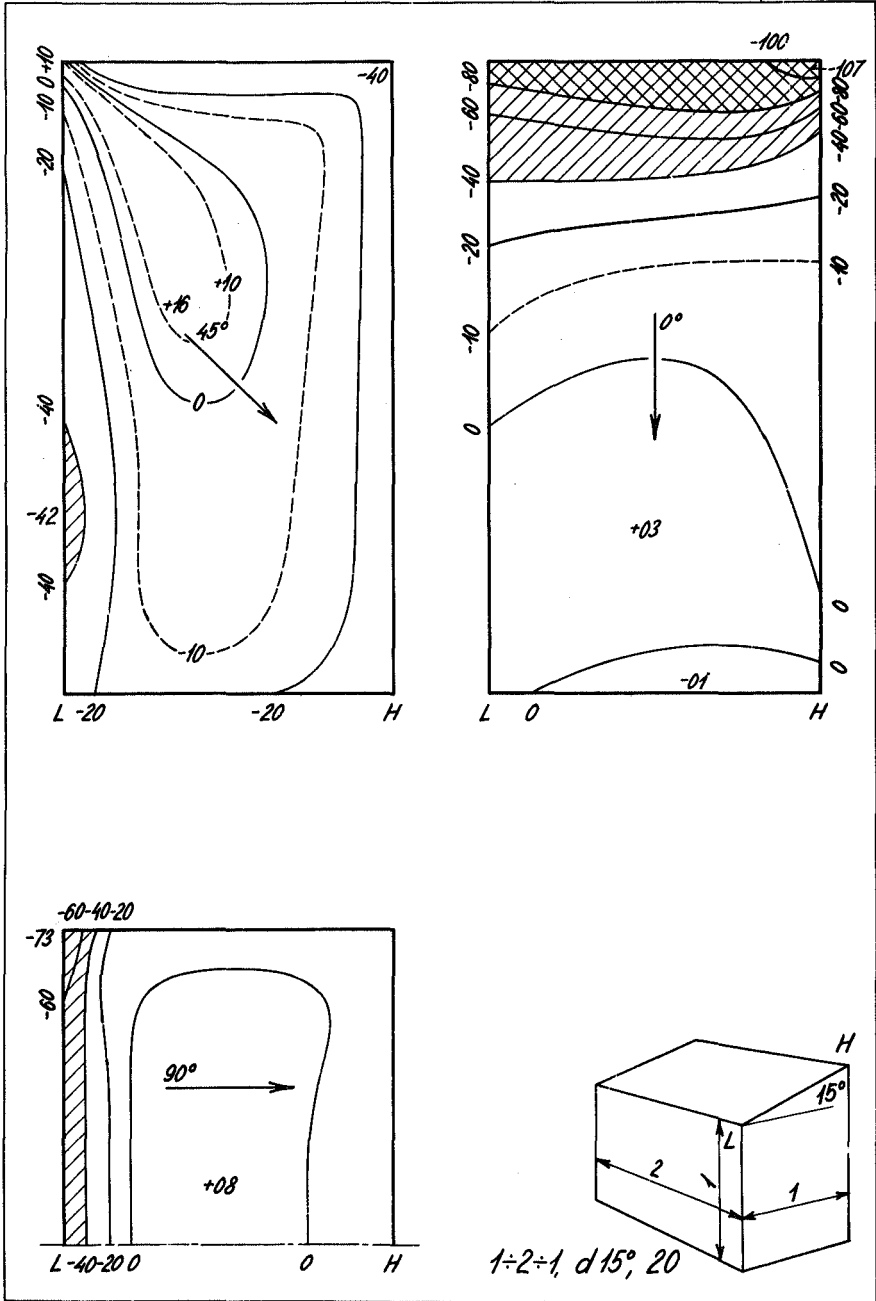


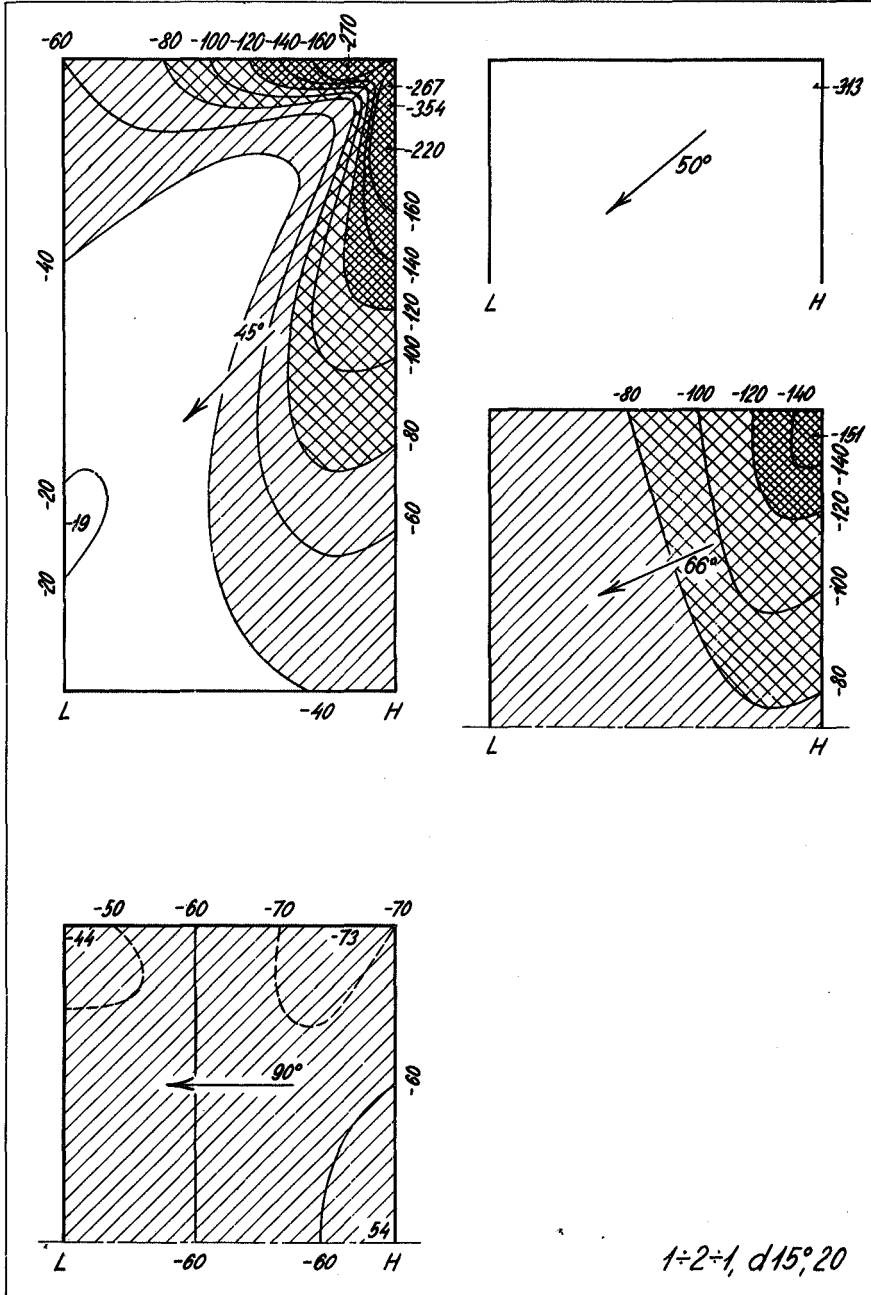




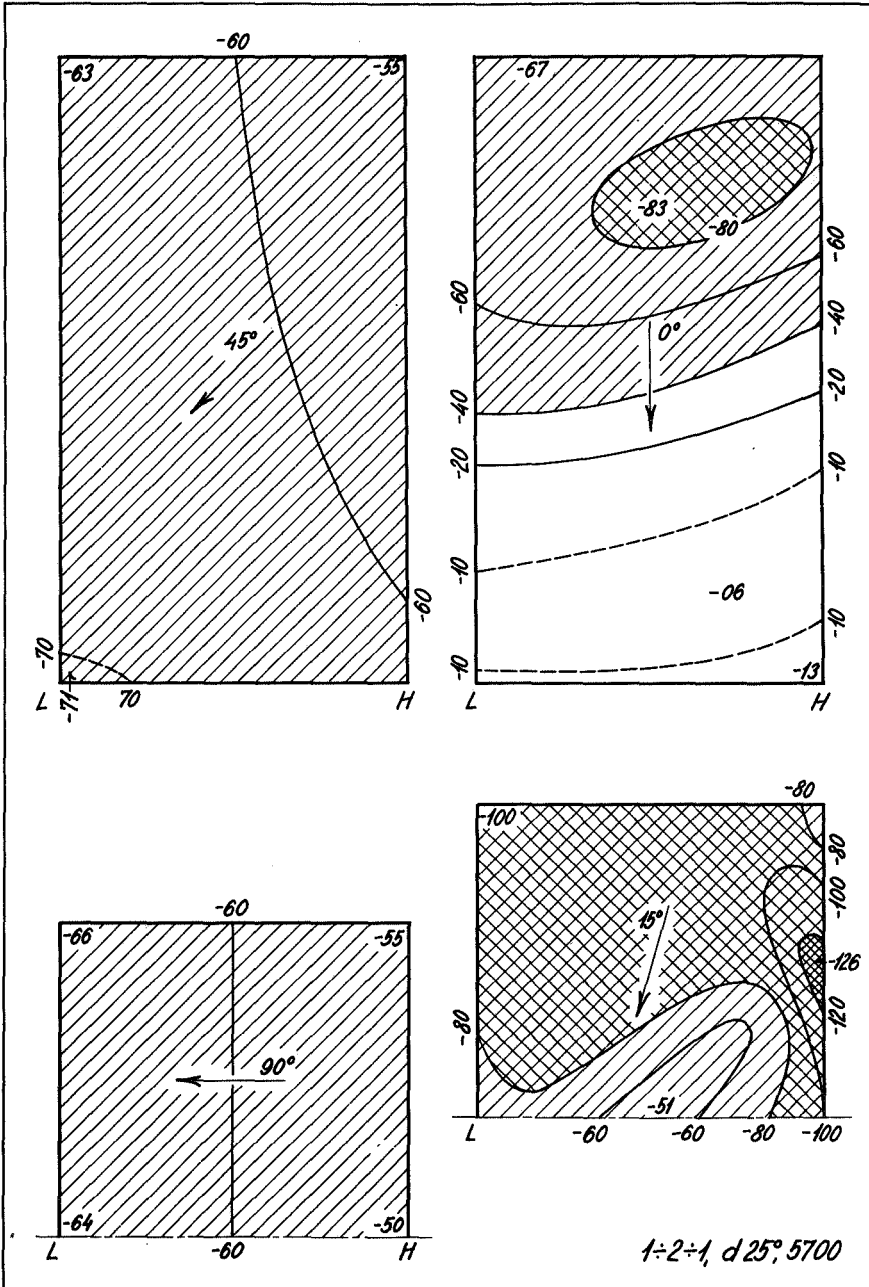


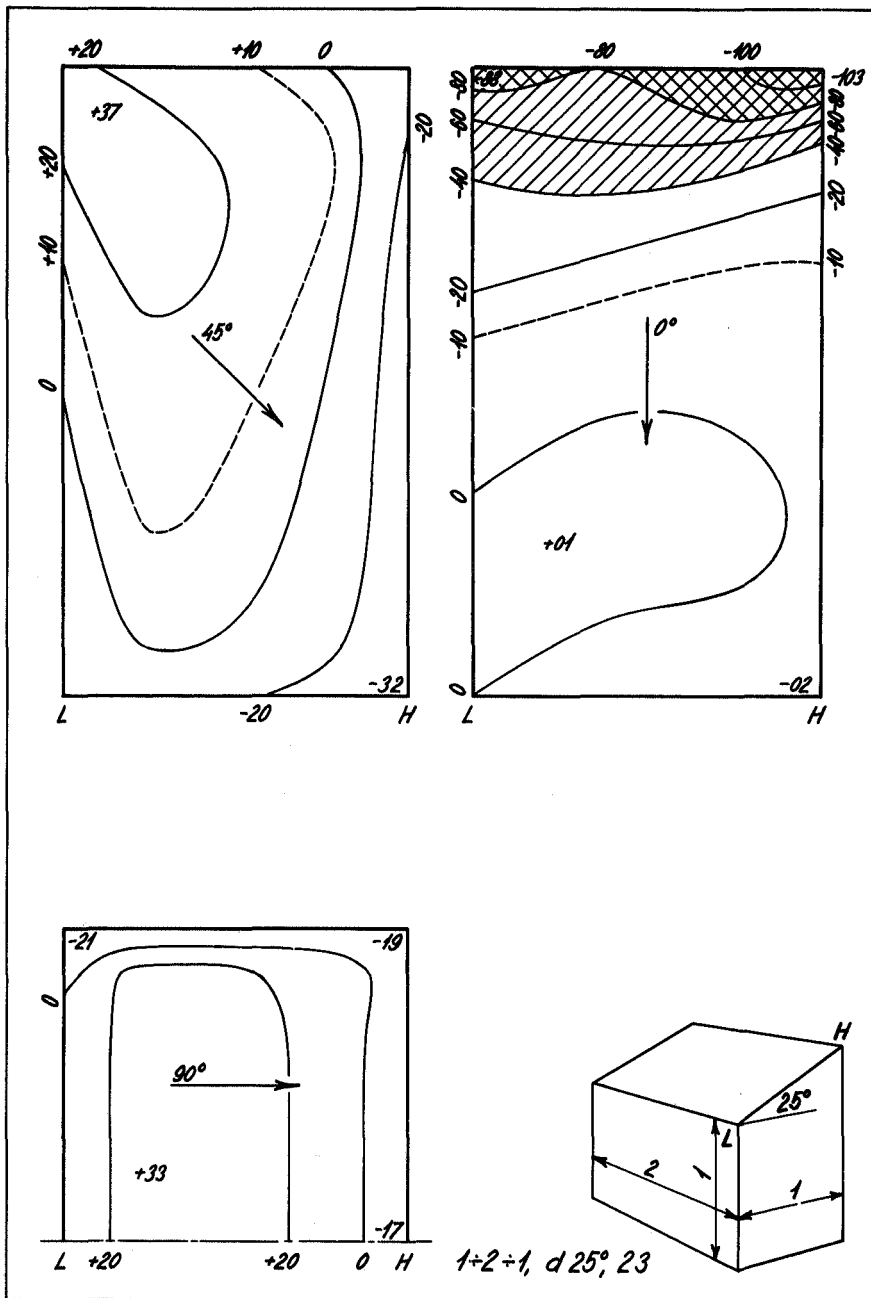


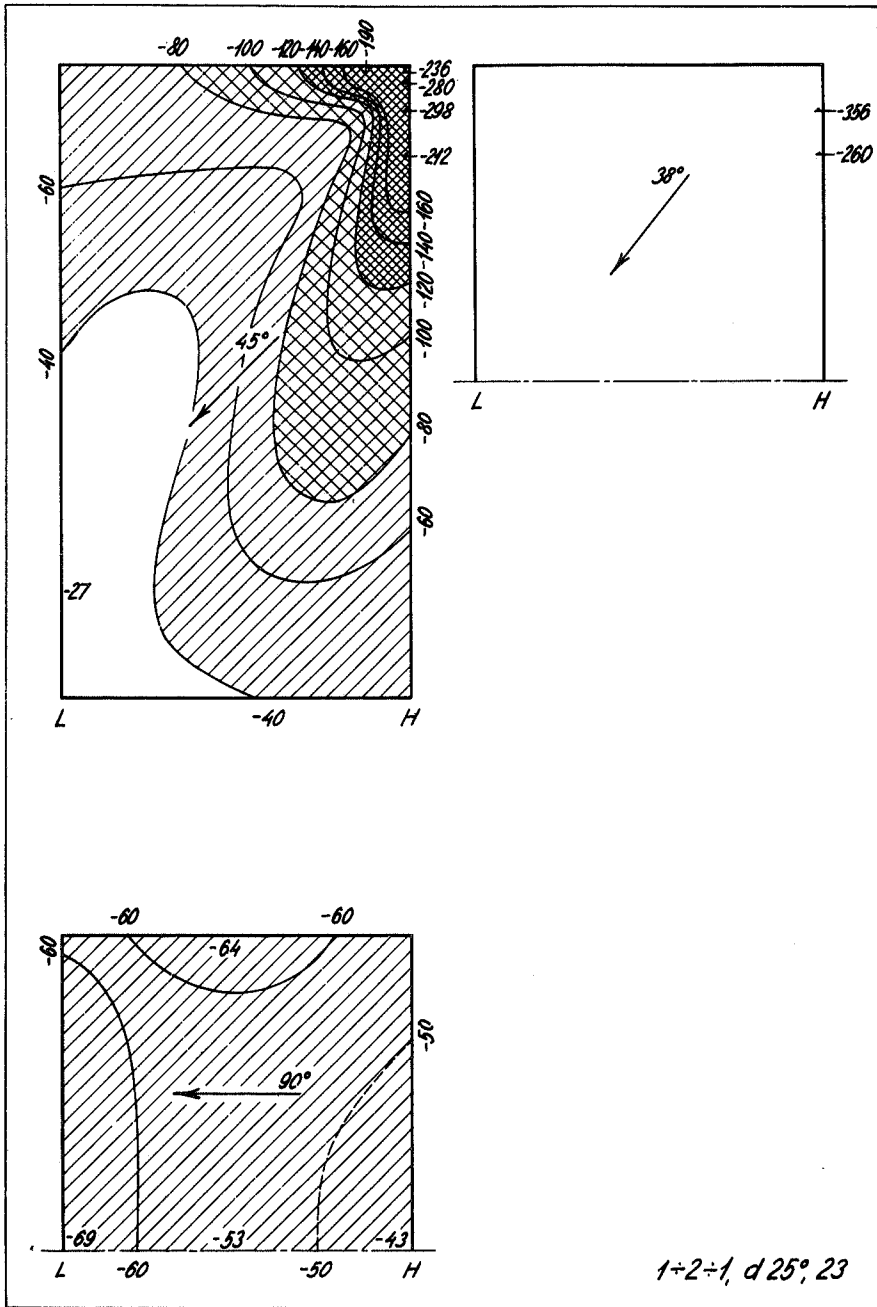


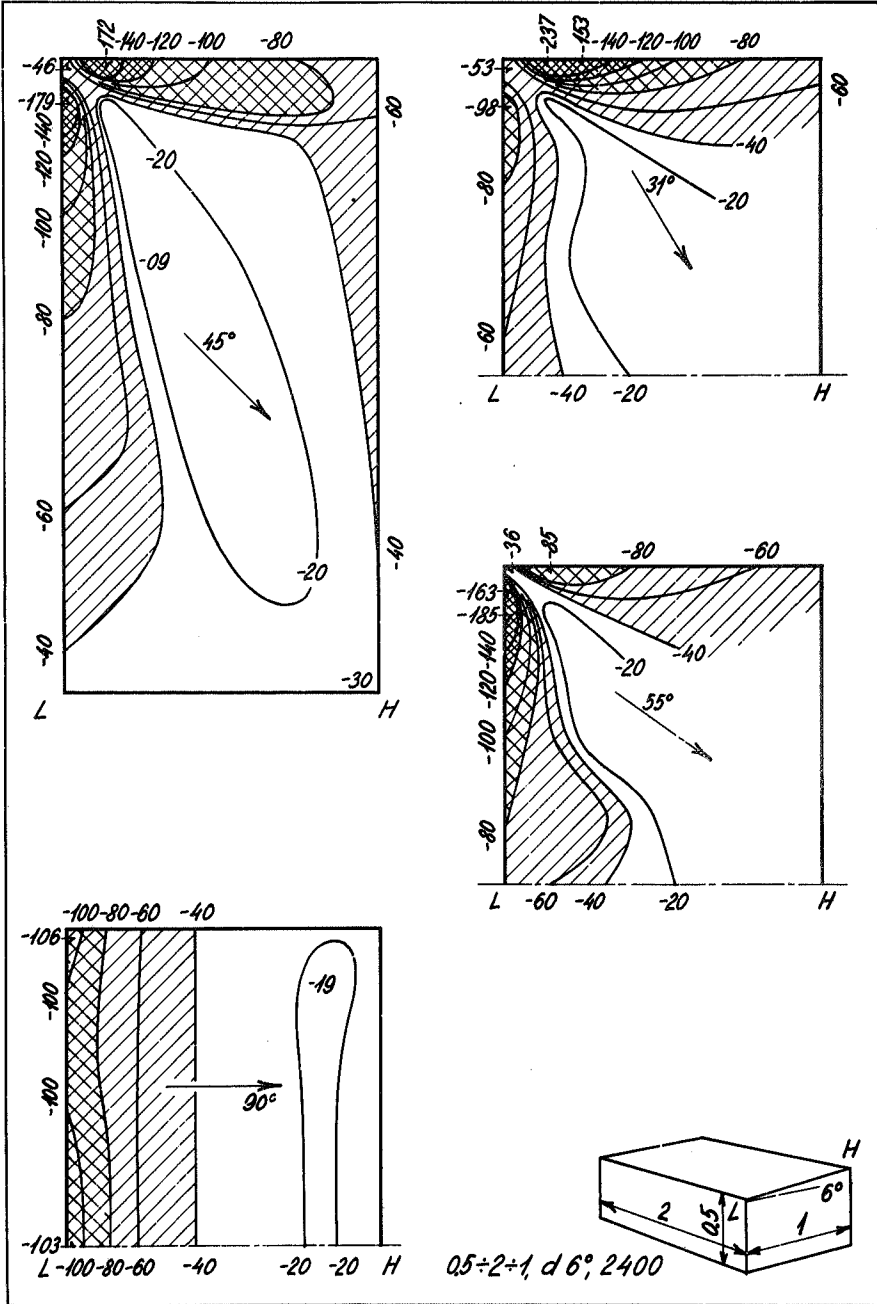




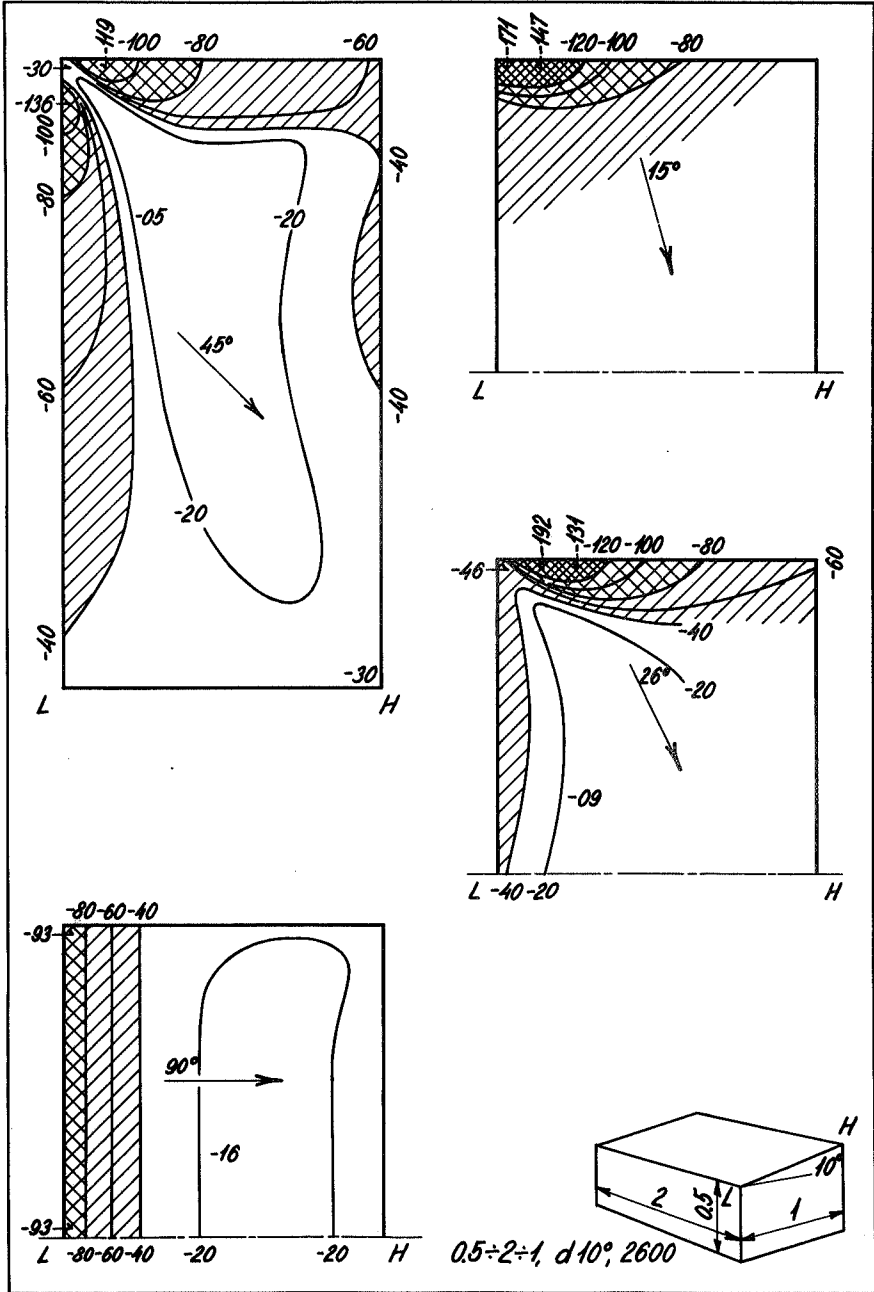


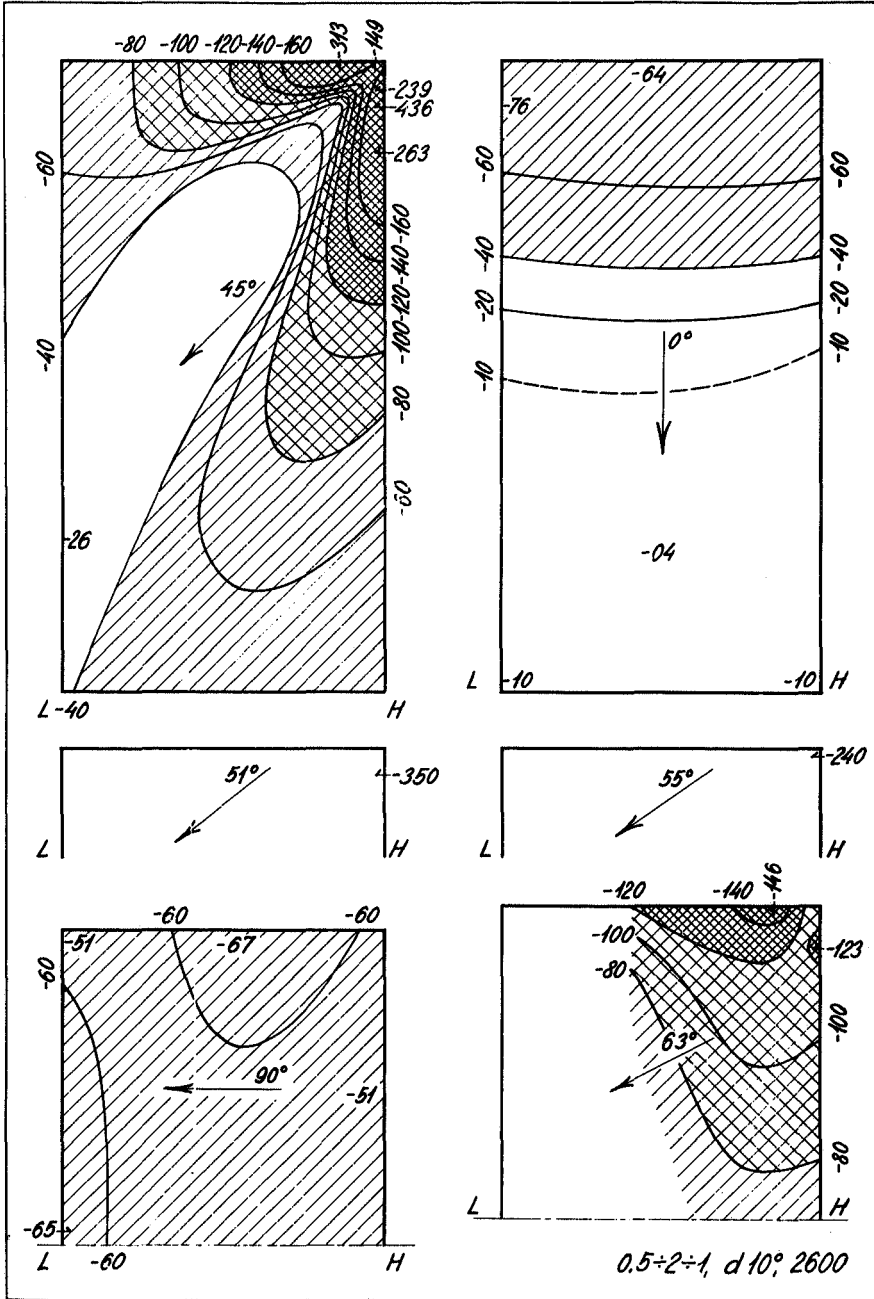


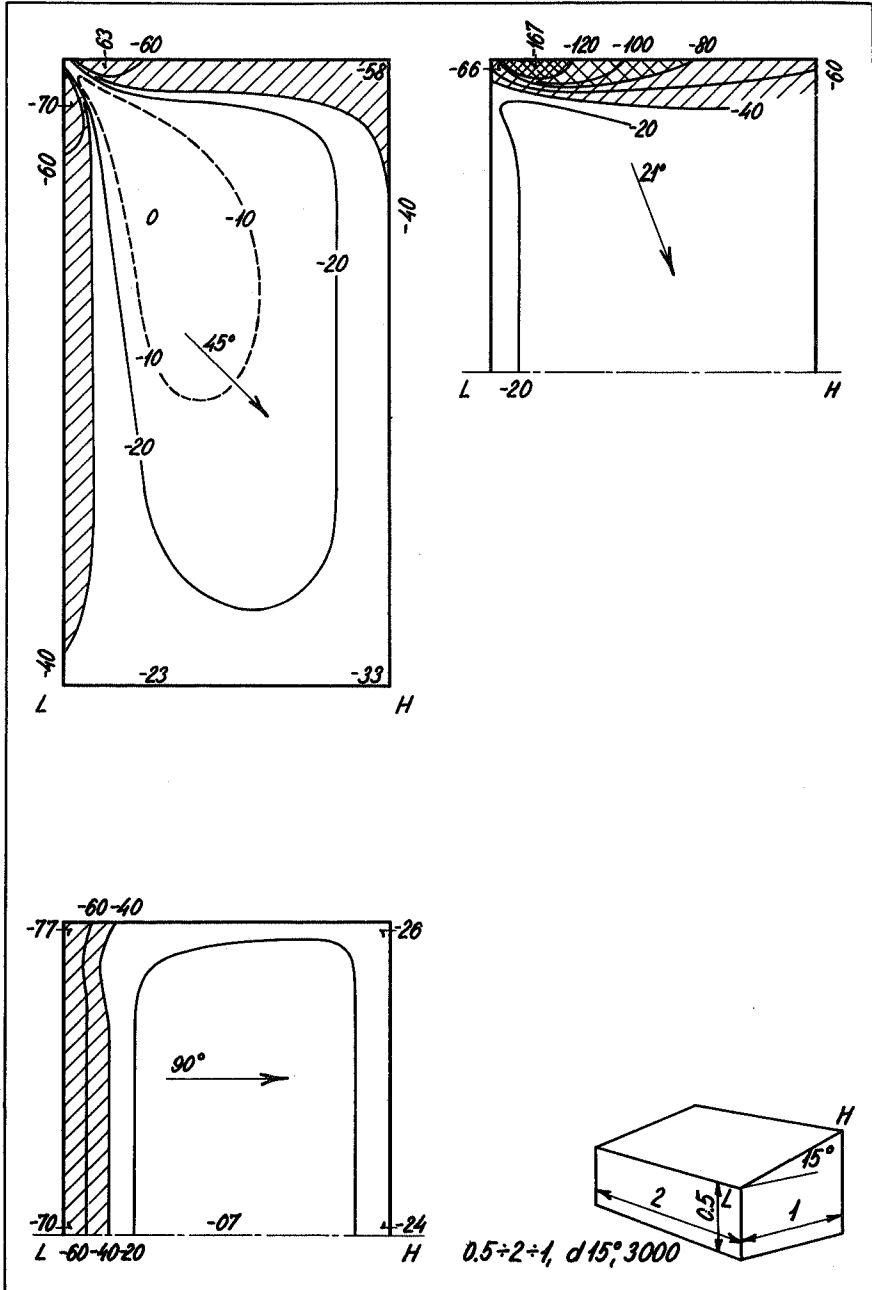


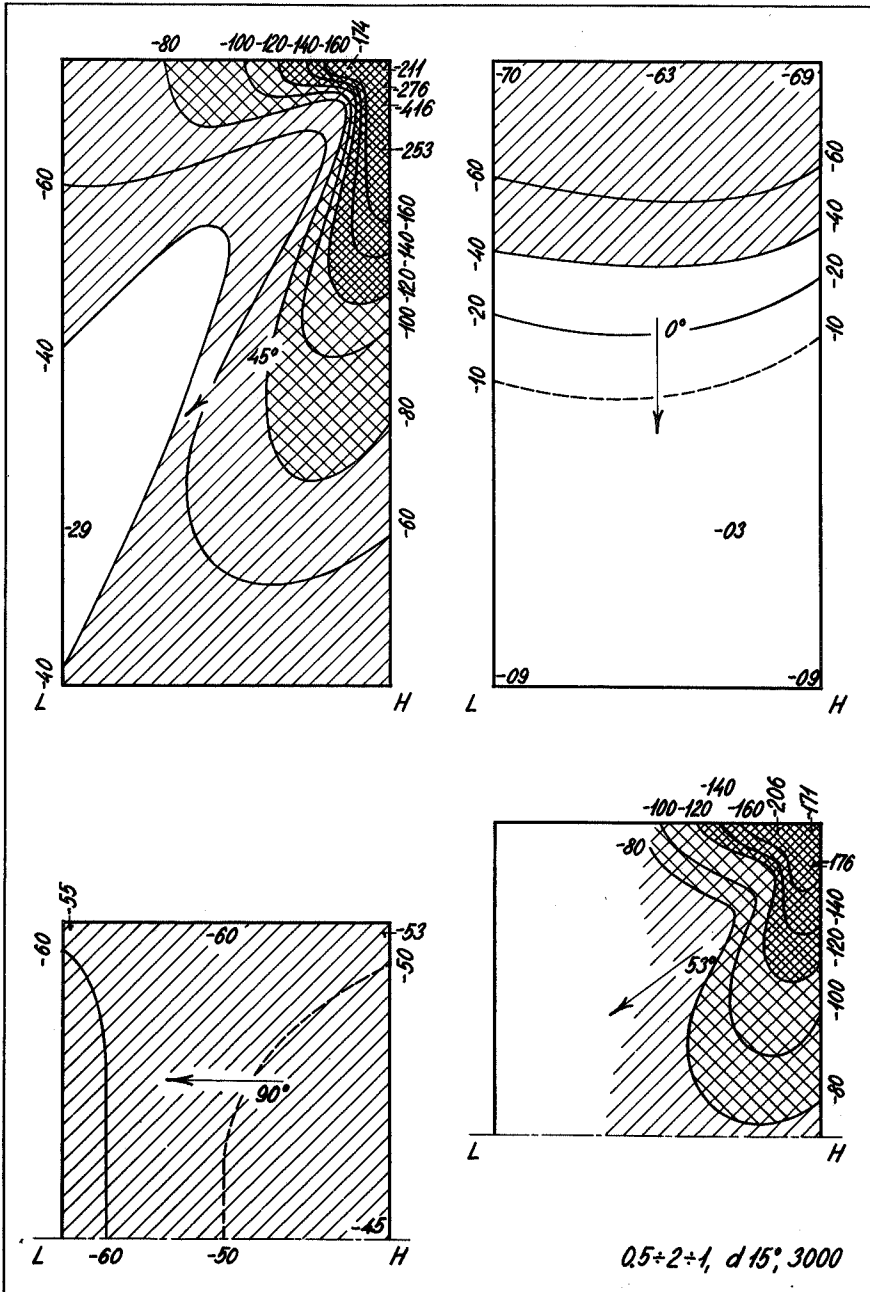












## 8. SADDLE ROOFS ON HOUSES

### 8.1 Scope of the tests

In the model tests with wind load on saddle roofs 16 different house types are investigated. In Figures 102 to 105 the types are shown and the placing of the measuring holes are given.

The models were of brass, see Section 1.4. They were placed on the turntable in the 4th section and the measurements were carried out as described in Section 1.6.

Three types of turbulent boundary layers were used, namely small turbulence,  $z_0 = 1.8 \cdot 10^{-3}$  cm, produced by smooth masonite plates, medium turbulence,  $z_0 = 0.047$  cm, from corrugated paper and large turbulence,  $z_0 = 0.45$  cm, from 2.5·2 cm lists.

Three of the models were built with hip roofs, the four roof sections having identical slopes.

Table 101 gives a summary of the tests with saddle roofs on houses.

### 8.2 Test results

In Figures 108 to 137 the shape factors derived from the tests are given.

The shape factor is  $c = p/q$ , where  $p$  is the load at the point concerned and  $q$  is the velocity pressure level with the highest line in the roof.

Curves are drawn through points with equal  $c$ -values and extreme point values are given.

For each model the shape factors are given for the model positions with the most interesting loading conditions.

For some of the model arrangements only the load on a part of the roof is given, namely when the load here has an extreme value and the load on the remaining part of the roof is of less interest.

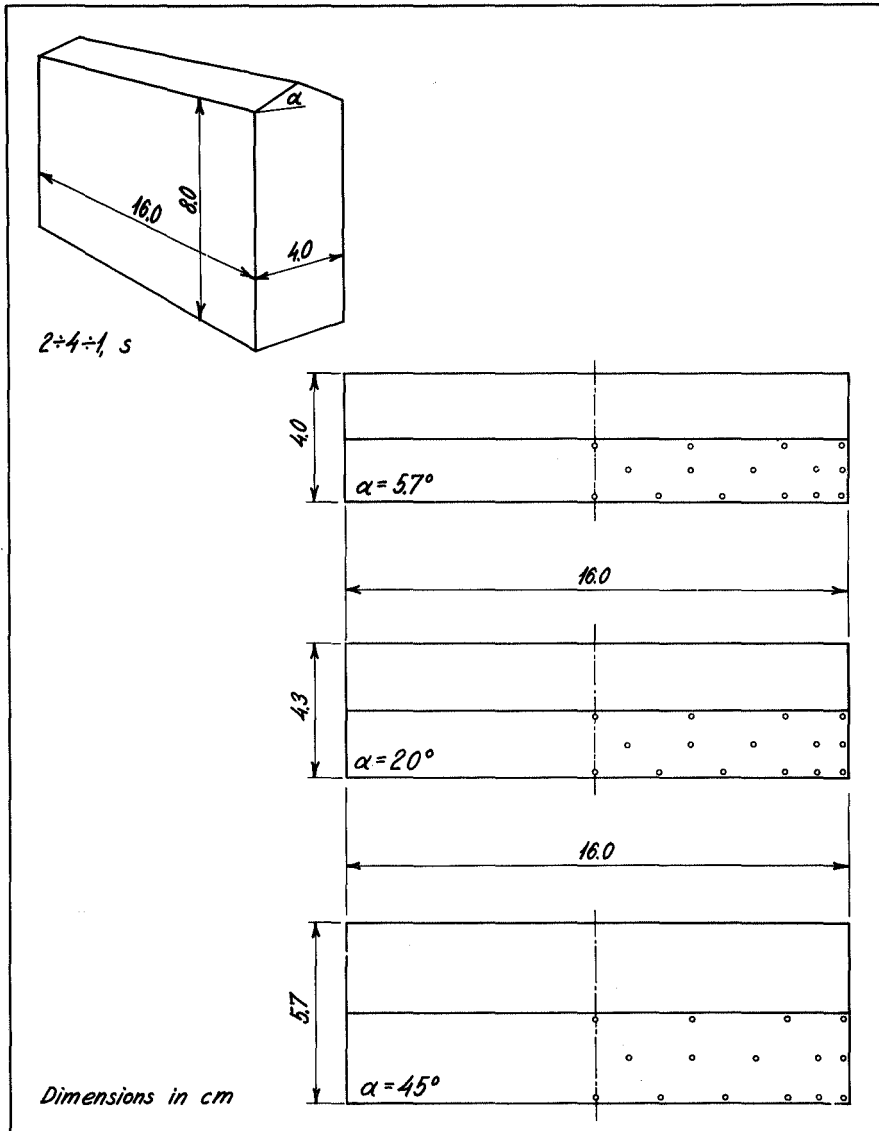
For some of the very large suction values, which were measured locally at the corners of the roof, a slight dependence on the wind velocity was found, so that the suction increased a little when the wind velocity increased.

Concerning these points the shape factors were determined by measurements taken with the greatest possible wind velocity in the tunnel.

Table 101

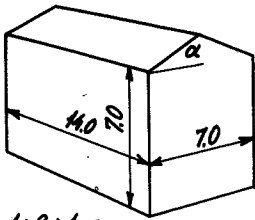
h÷l÷w	$\alpha$	Turbulence	Figure on page
2÷4÷1	s 5.7°	s	108
		l	109
	s 20°	s	110
		l	111
	s 45°	s	112
		l	113
1÷2÷1	s 5.7°	s	114
		m	115
	h 5.7°	s	116
	h 10°	s	118
		m	119
	s 20°	s	120
		m	121
		l	122
	s 30°	s	123
		m	124
		l	125
	s 45°	s	126
		m	127
		l	128
	0.5÷2÷1	s 5.7°	s
h 10°		s	130
s 20°		s	131
s 30°		s	132
s 45°		s	133
1÷4÷1	s 5.7°	s	134 and 135
	s 20°	s	136 and 137

s = small turbulence  
m = medium turbulence  
l = large turbulence  
h. = hip roof.

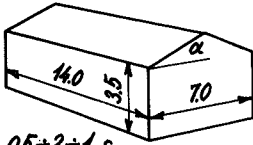


Figs. 102. to 105. House models for investigation of the wind load on saddle roofs on houses.

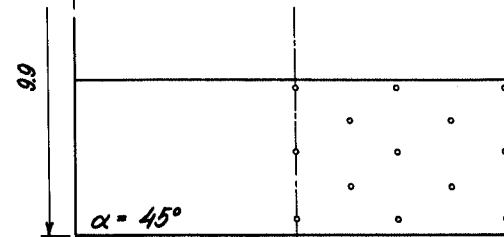
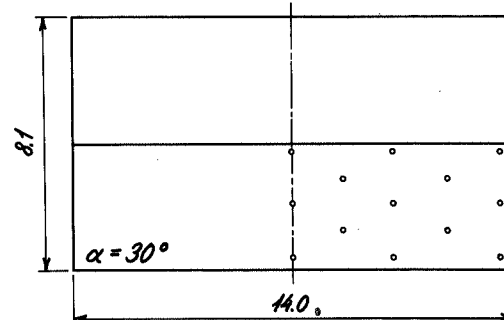
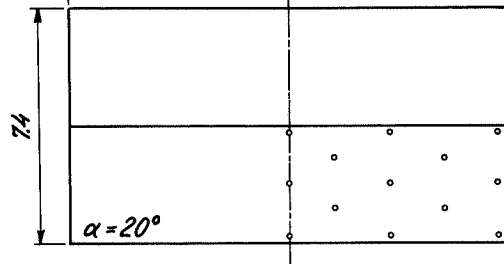
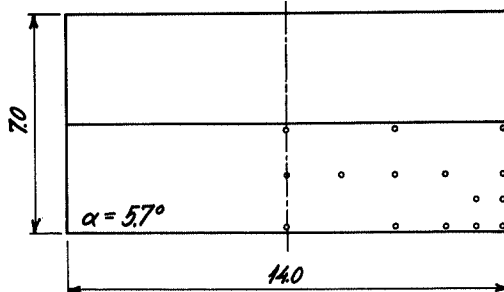
The small circles indicate measuring holes.



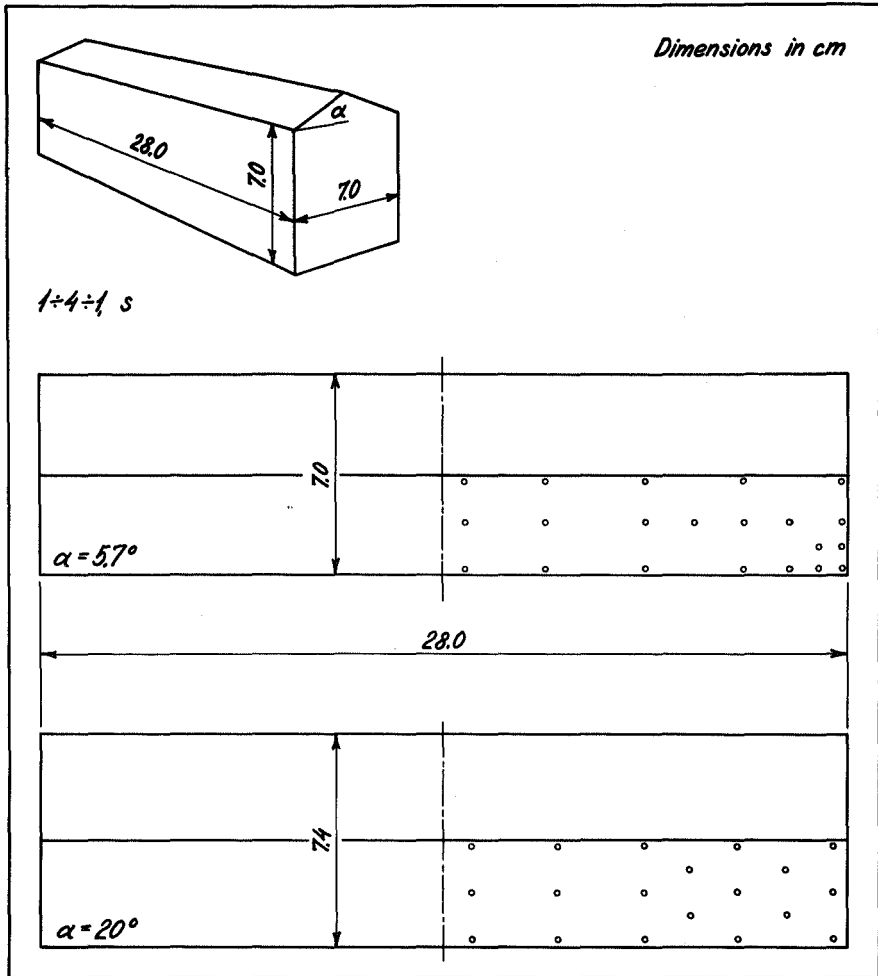
$1+2+1$  s



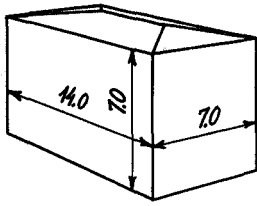
$0.5+2+1$  s



Dimensions in cm

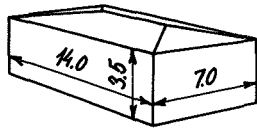


Figs. 102 to 105. House models for investigation of the wind load on saddle roofs on houses.  
The small circles indicate measuring holes.

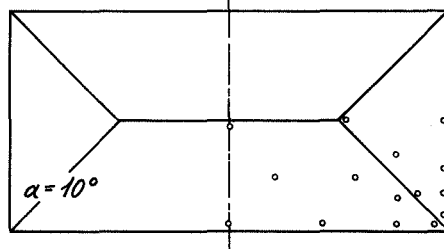
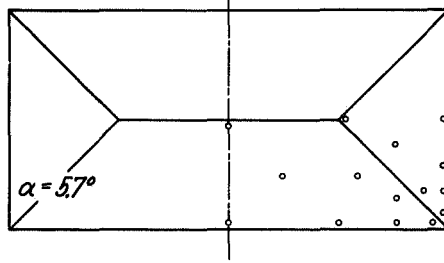


$$1 \div 2 \div 1, h$$

*Dimensions in cm*



$$0.5 \div 2 \div 1, h$$



### 8.3 Conclusions

When the wind blows parallel to the house the conditions naturally are nearly independent of the roof slope. At the windward gable rather great suction occurs. The suction decreases with increasing distance from the gable to a value near zero or perhaps to a small pressure. In large turbulence the suction decreases more rapidly with increasing distance from the gable than in small turbulence.

When the roof slope is  $5.7^\circ$  and the wind blows against a corner there is a very great suction in the vicinity of the corner, especially in small turbulence. For the low house,  $0.5 \div 2 \div 1$ , the largest value measured corresponds to  $c = 2.52$ . For the other houses the greatest suction measured are between 3.0 and 3.4. The hip roof with  $5.7^\circ$  slope does not give anything particularly new.

At  $20^\circ$  roof slope in smooth airflow large suction occurs in the vicinity of the windward corner when the wind blows skew to the house;  $c = 1.10$  is the maximum value for the low house,  $0.5 \div 2 \div 1$ . For the others the maximum values are between 1.5 and 1.85, greatest for the high house.

At  $20^\circ$  roof slope large suction also occurs at the leeward roof section on the part nearest to the wind. Here  $c = 1.93$  was measured for the low house,  $0.5 \div 2 \div 1$ , and  $c = 2.15$  for the long house,  $1 \div 4 \div 1$ . These suction are found both in small and in large turbulence.

At  $30^\circ$  roof slope pressure occurs on the roof, but only in large turbulence, and the maximum value is only 0.22. For this roof slope the maximum value of the suction is moderate, the greatest measured is  $c = 1.1$ .

For wind at right angles to the ridge and for skew wind, roofs with  $45^\circ$  slopes have pressure at the windward lower edge and the windward corner, respectively. The pressures are greatest in large turbulence. The maximum value is  $c = 0.60$ . The suction are moderate with maximum values between 0.90 and 1.13; these values occurring both in large and small turbulences.

Figs. 108 to 137. The wind load on saddle roofs on houses.

The wind direction is given by the angle between the wind and the longitudinal axis of the house.

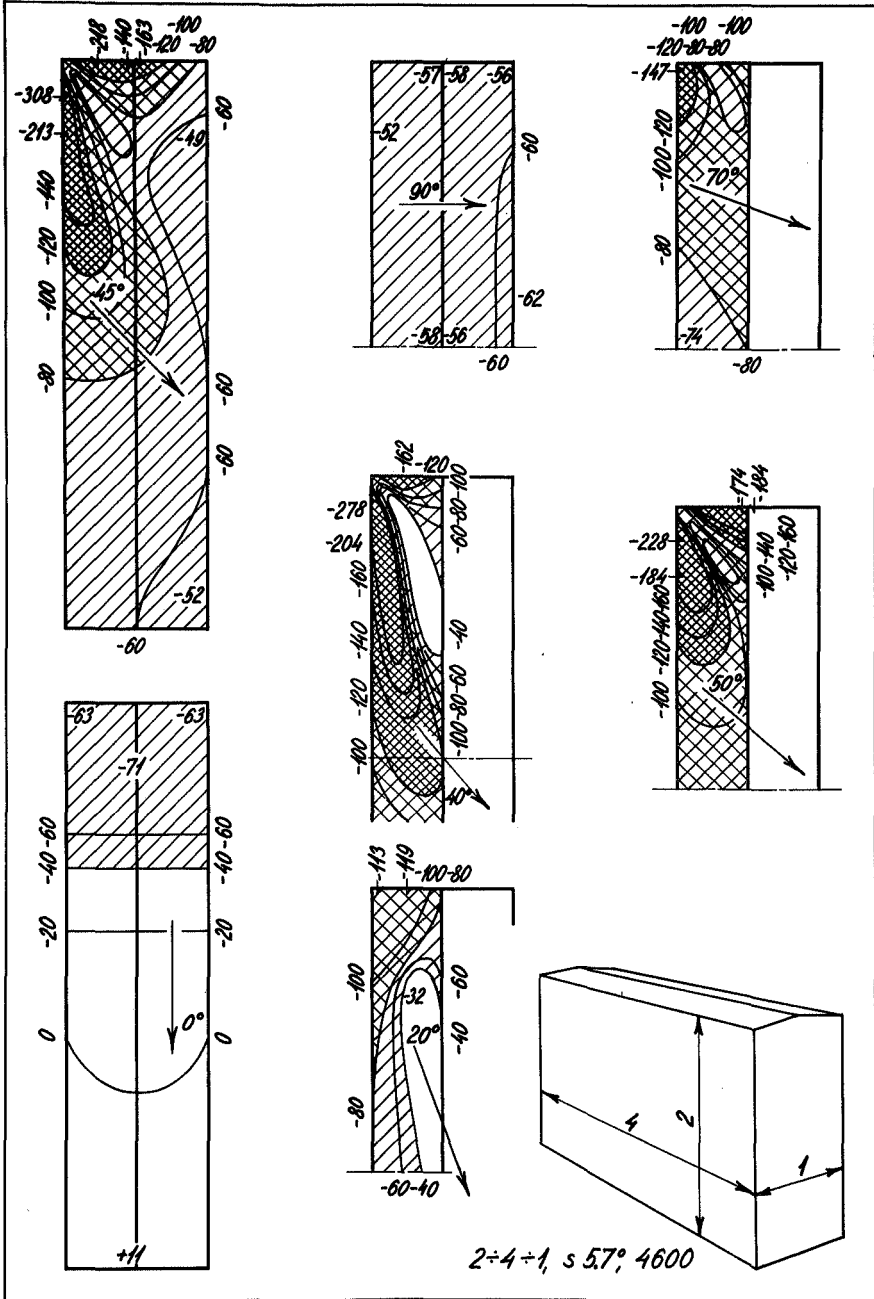
The shape factors are given as a percentage. Suction is indicated by a negative sign and oblique hatching, pressure by a positive sign and horizontal-vertical hatching.

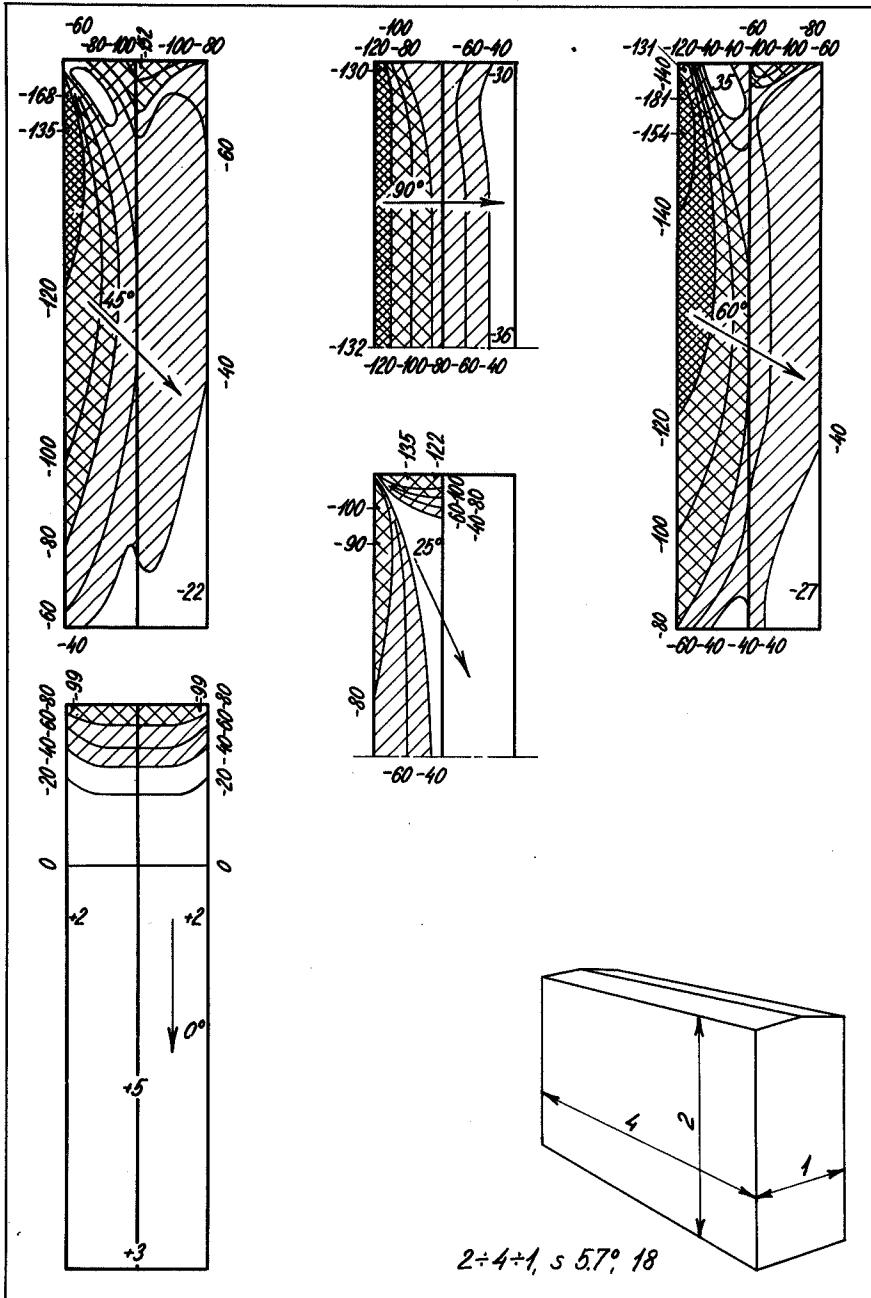
Contour lines are drawn for the wind load at  $c = 20$   $40$   $60$  per cent etc.

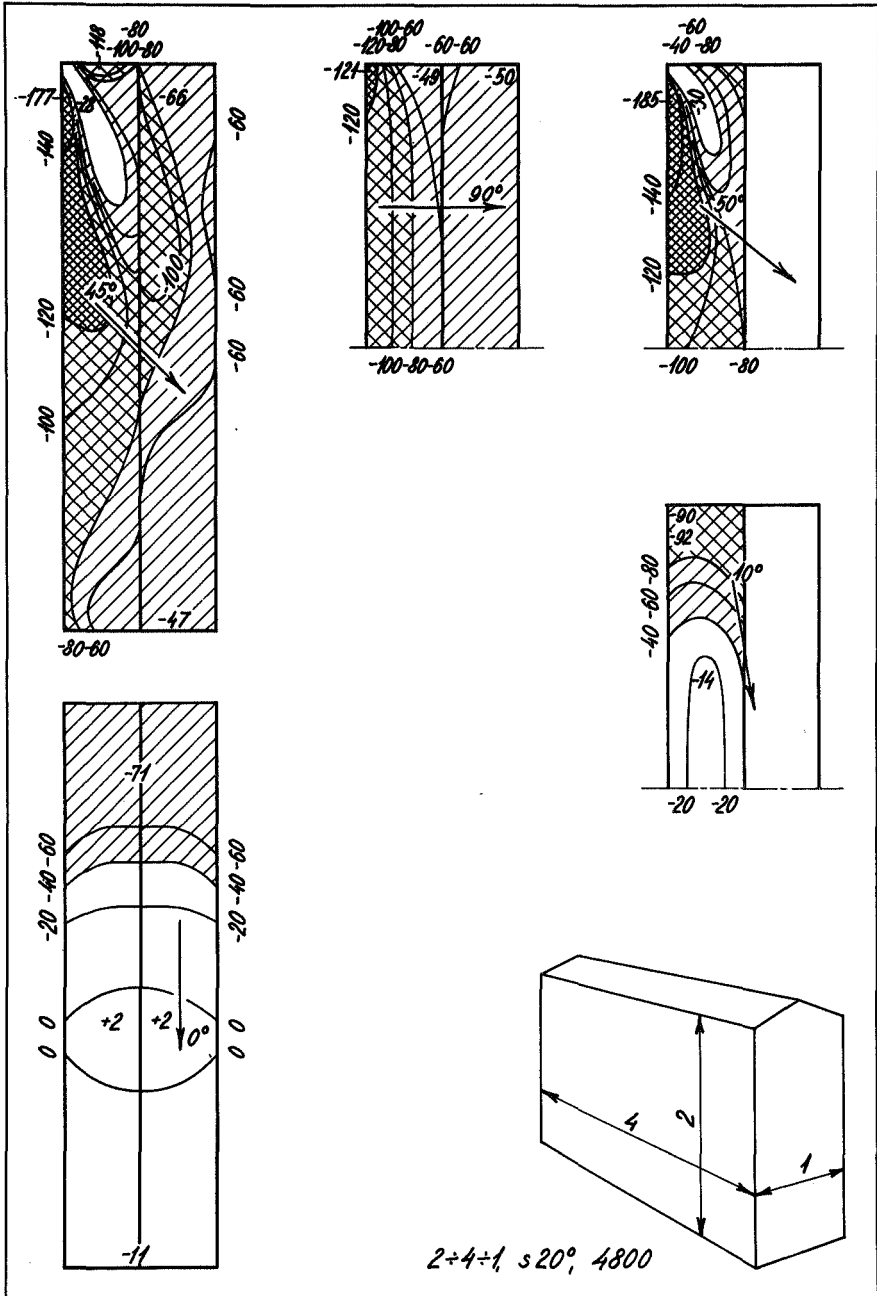
In some cases intermediate contours, for example  $c = 30$  or  $c = 50$  per cent, are shown as broken lines.

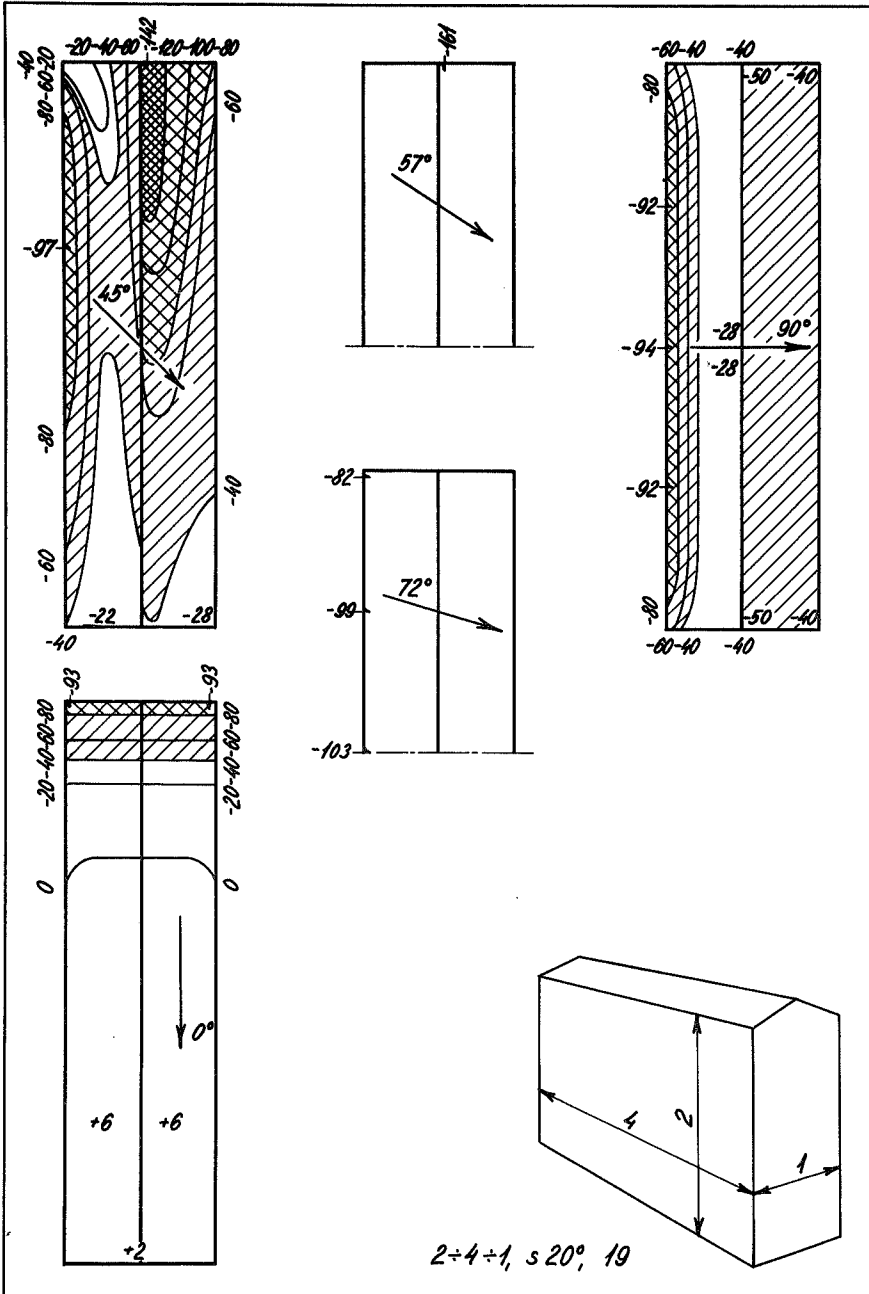
Areas in which the shape factor is between 40 and 80 per cent are single hatched, areas between 80 and 120 per cent are double hatched and areas of more than 120 per cent are densely double hatched.

The extreme values of the shape factors are noted.

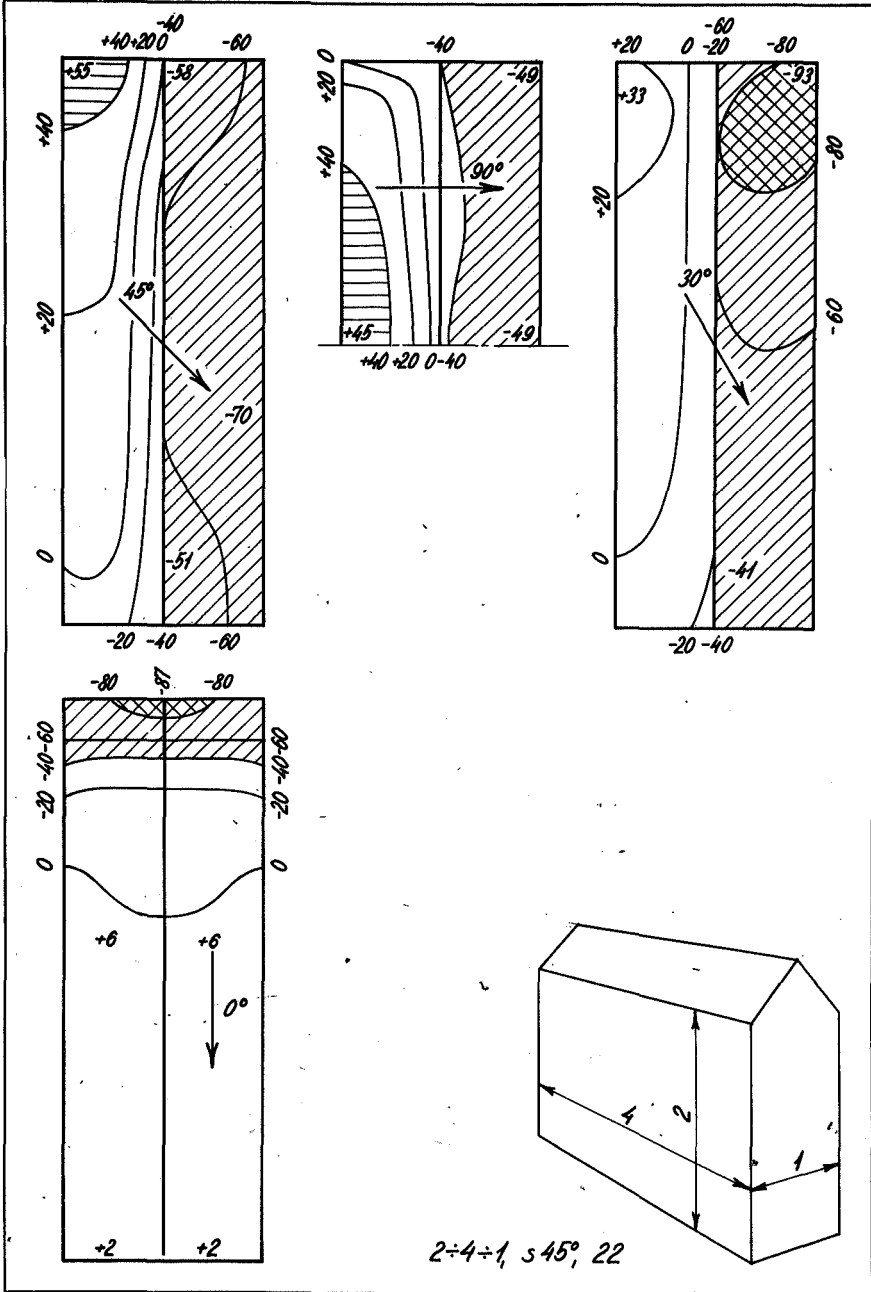


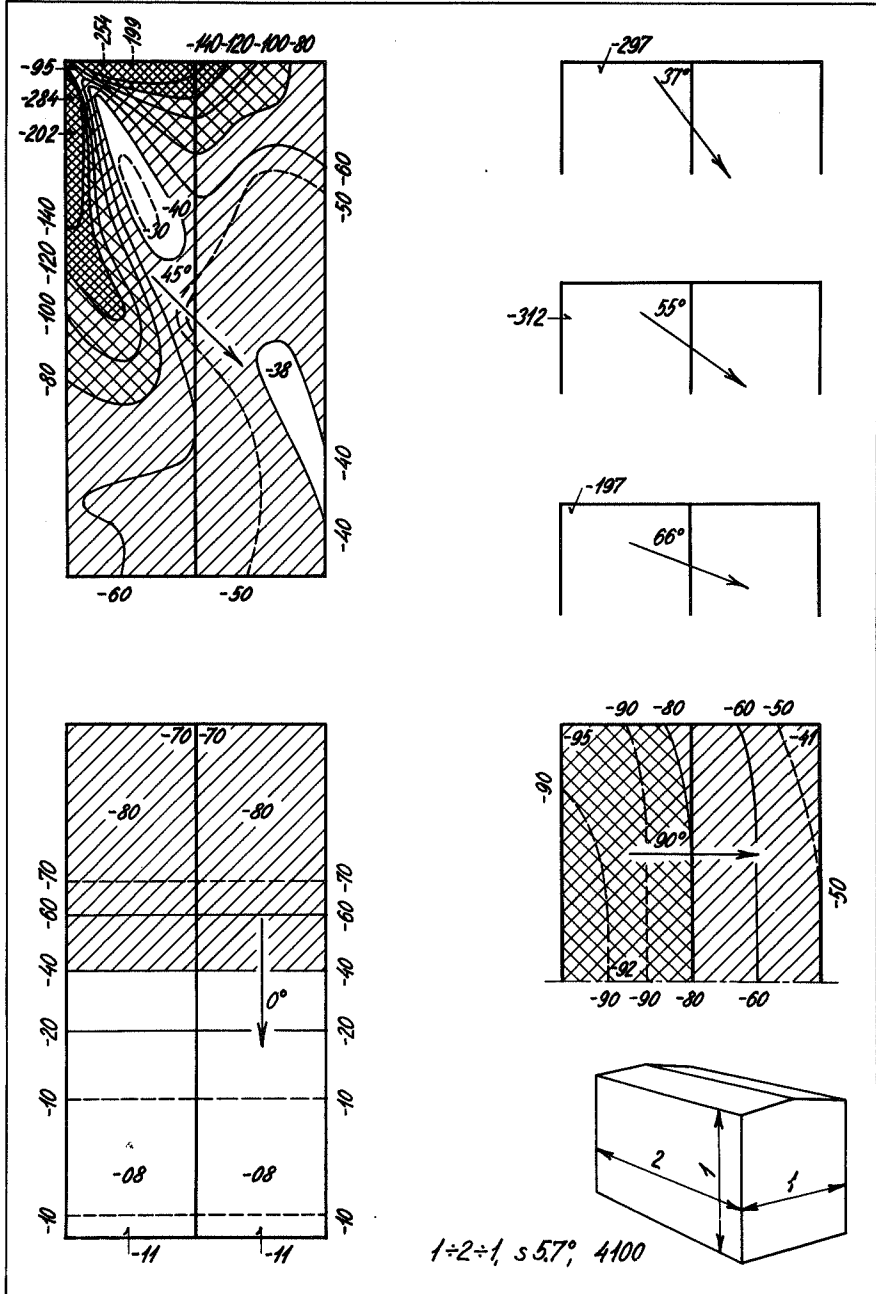


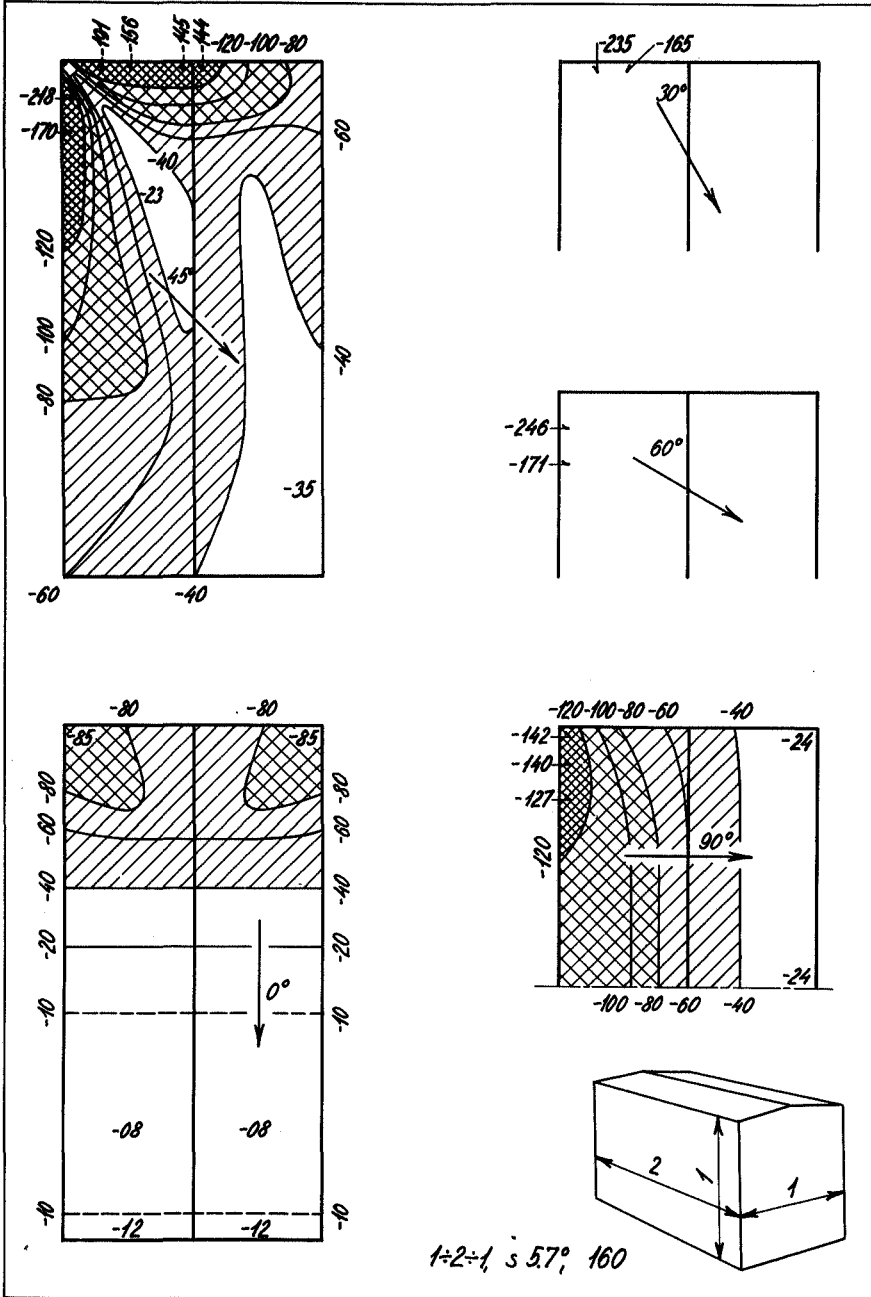


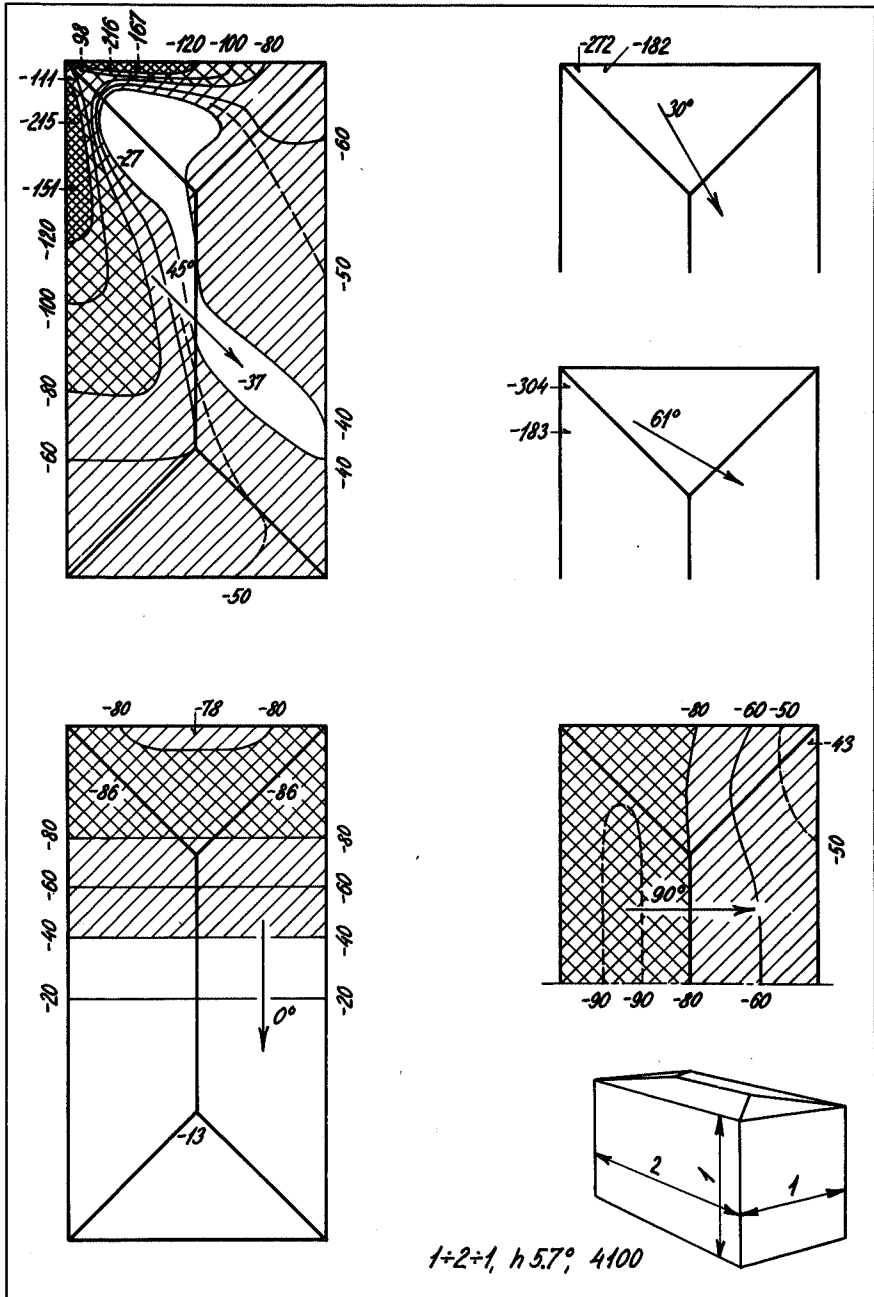












Figs. 108 to 137. The wind load on saddle roofs on houses.

The wind direction is given by the angle between the wind and the longitudinal axis of the house.

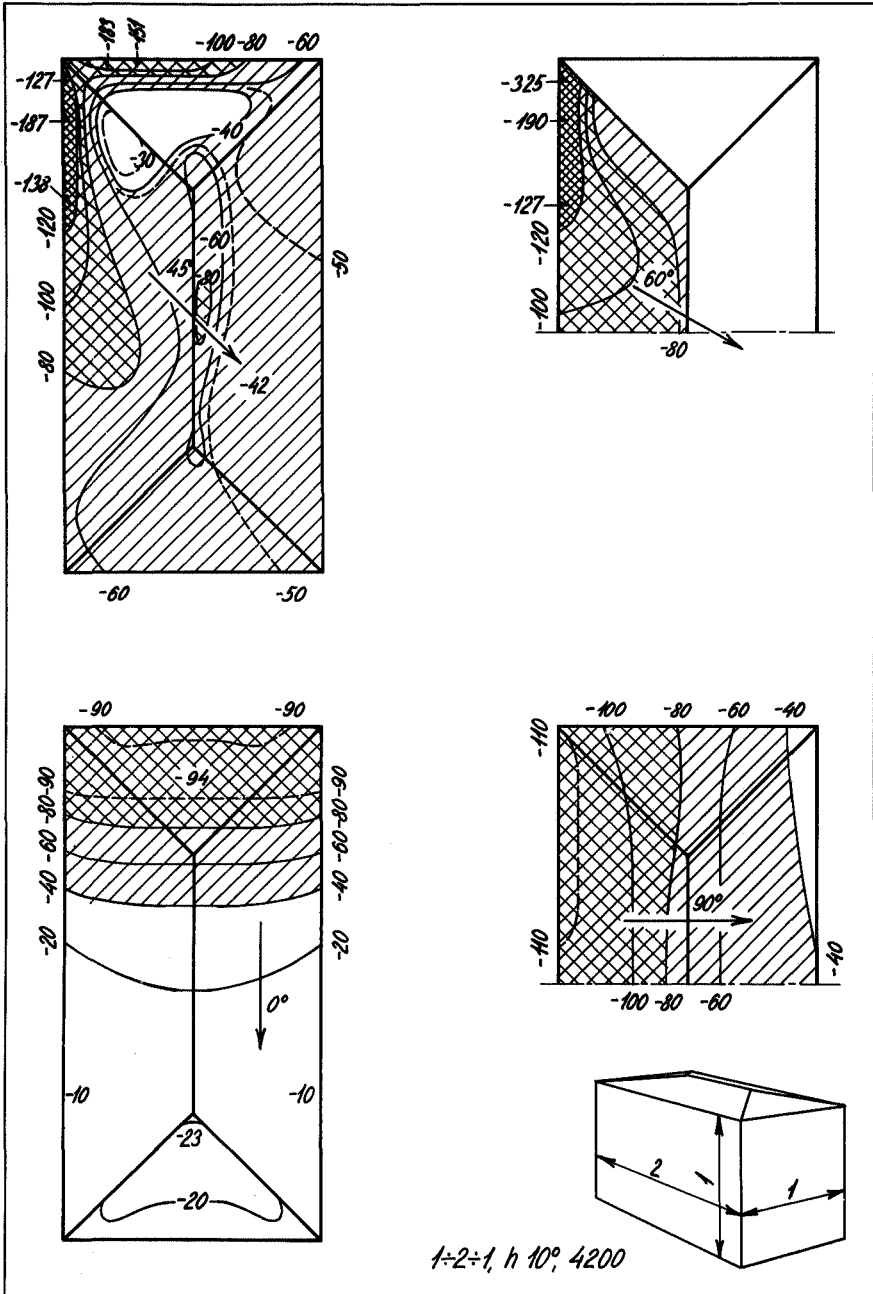
The shape factors are given as a percentage. Suction is indicated by a negative sign and oblique hatching, pressure by a positive sign and horizontal-vertical hatching.

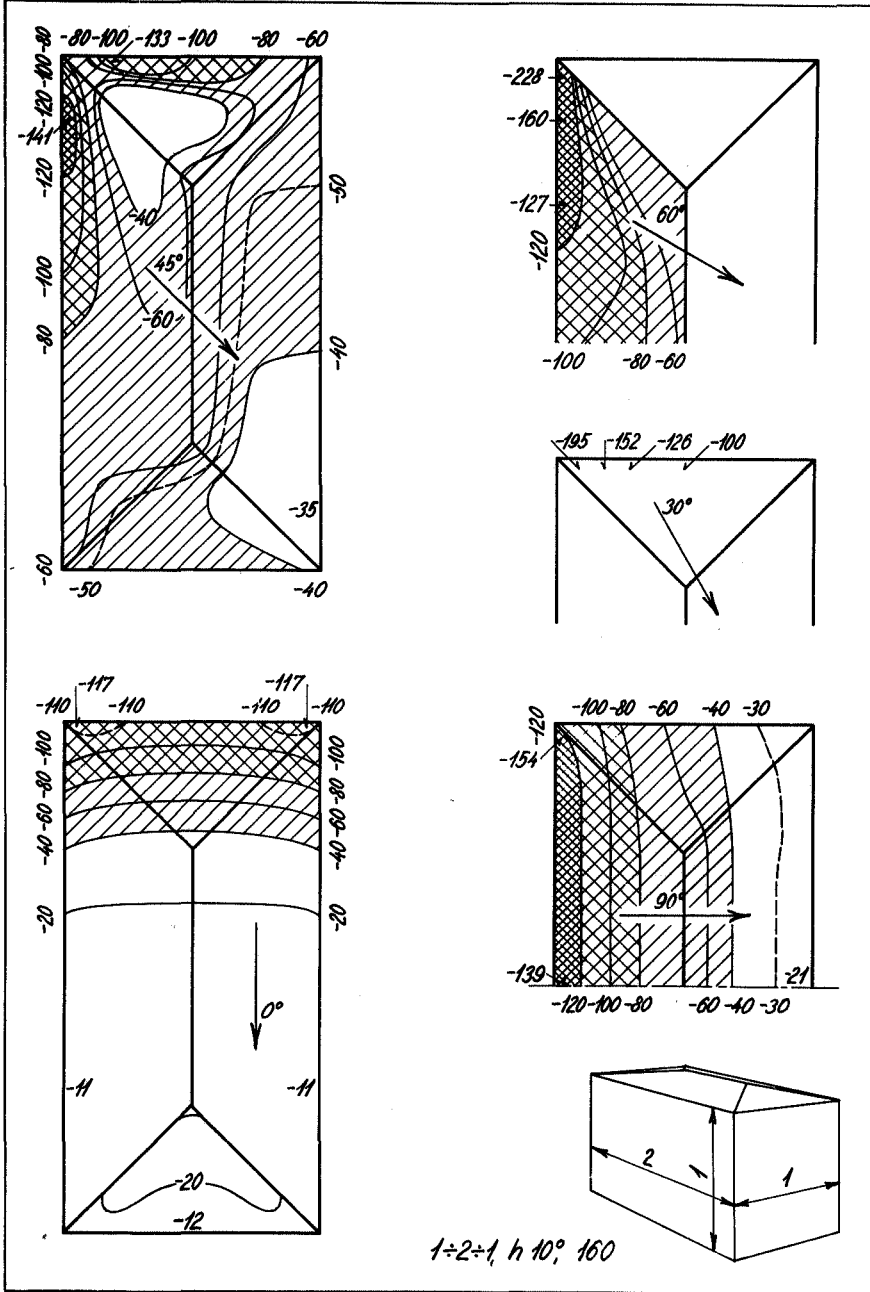
Contour lines are drawn for the wind load at  $c = 20$   $40$   $60$  per cent etc.

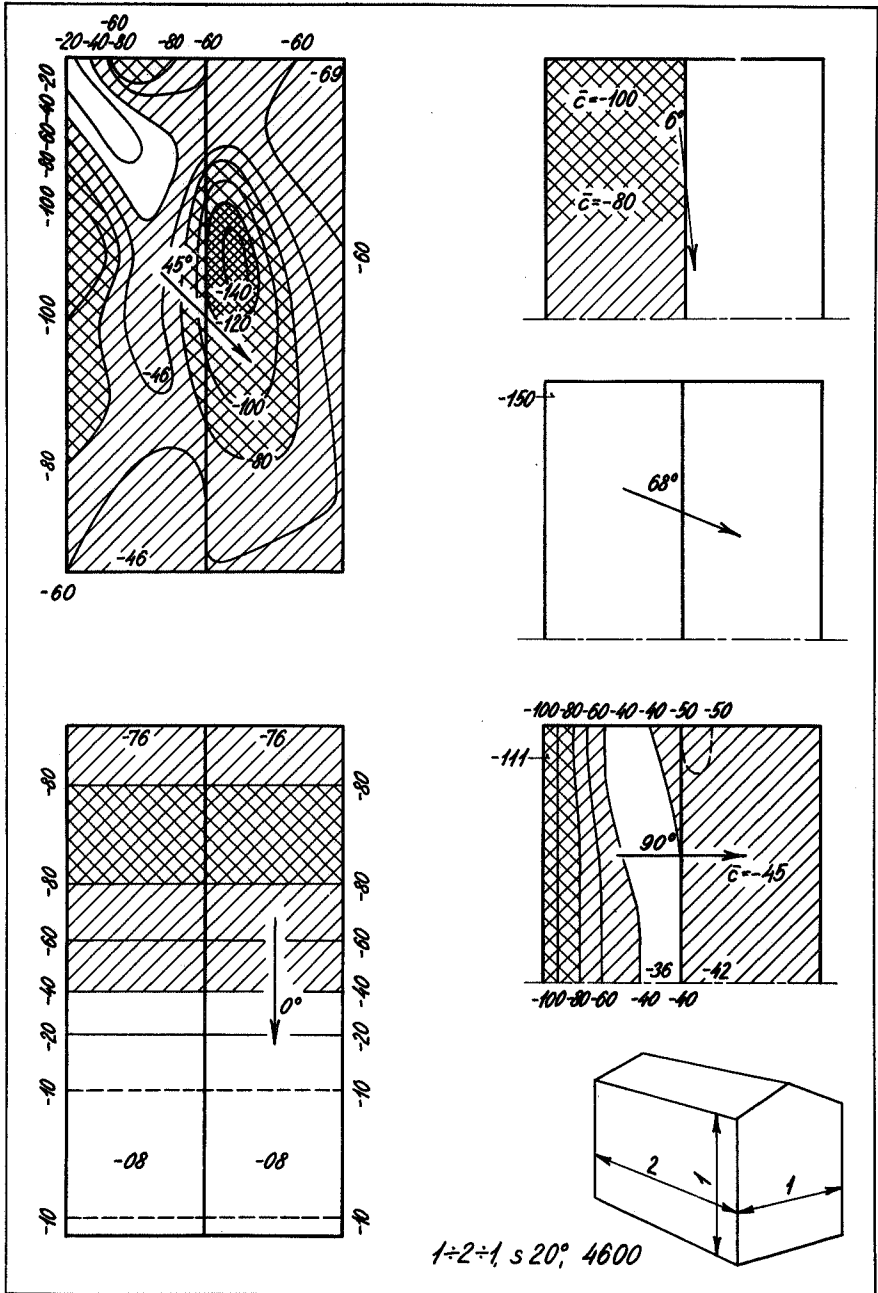
In some cases intermediate contours, for example  $c = 30$  or  $c = 50$  per cent, are shown as broken lines.

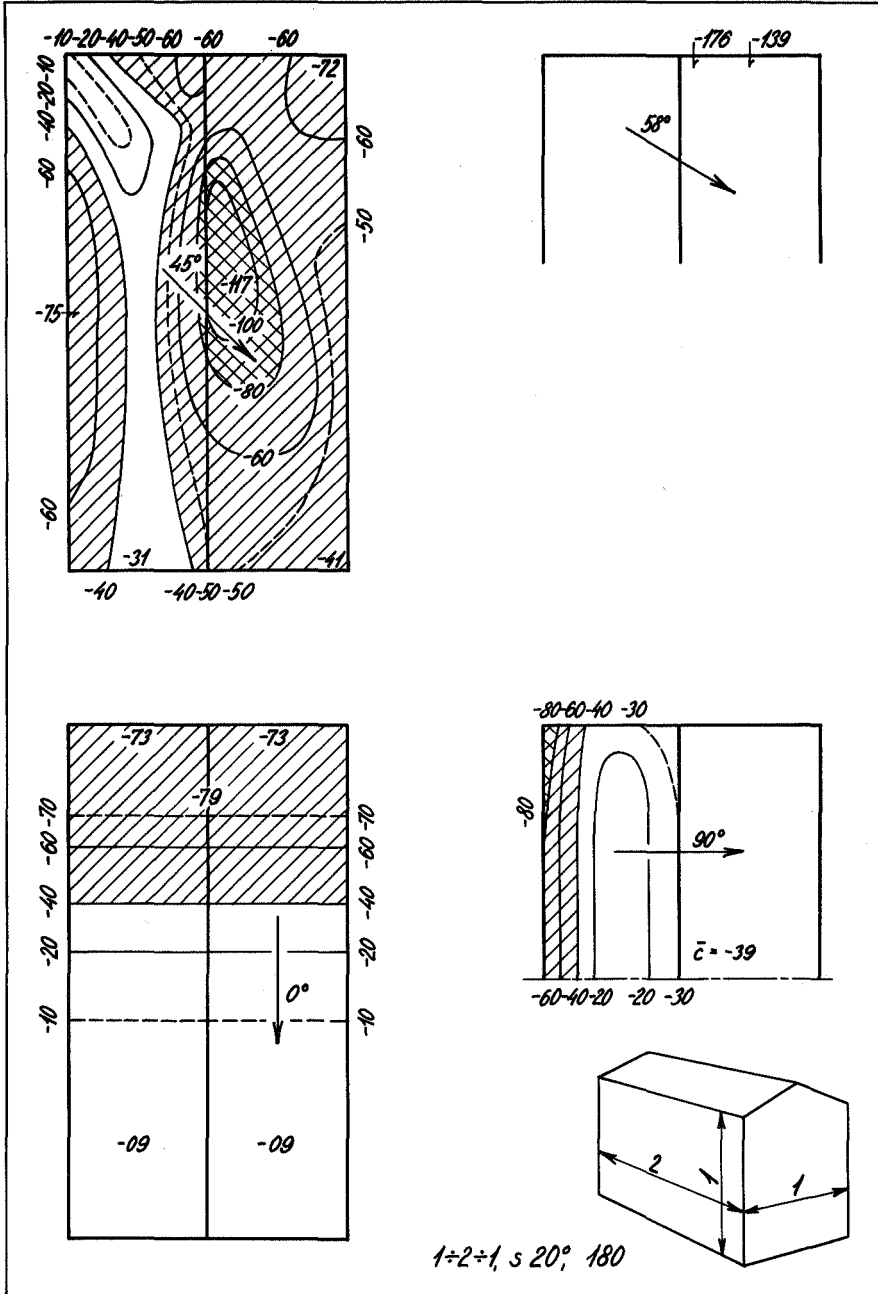
Areas in which the shape factor is between 40 and 80 per cent are single hatched, areas between 80 and 120 per cent are double hatched, and areas of more than 120 per cent are densely double hatched.

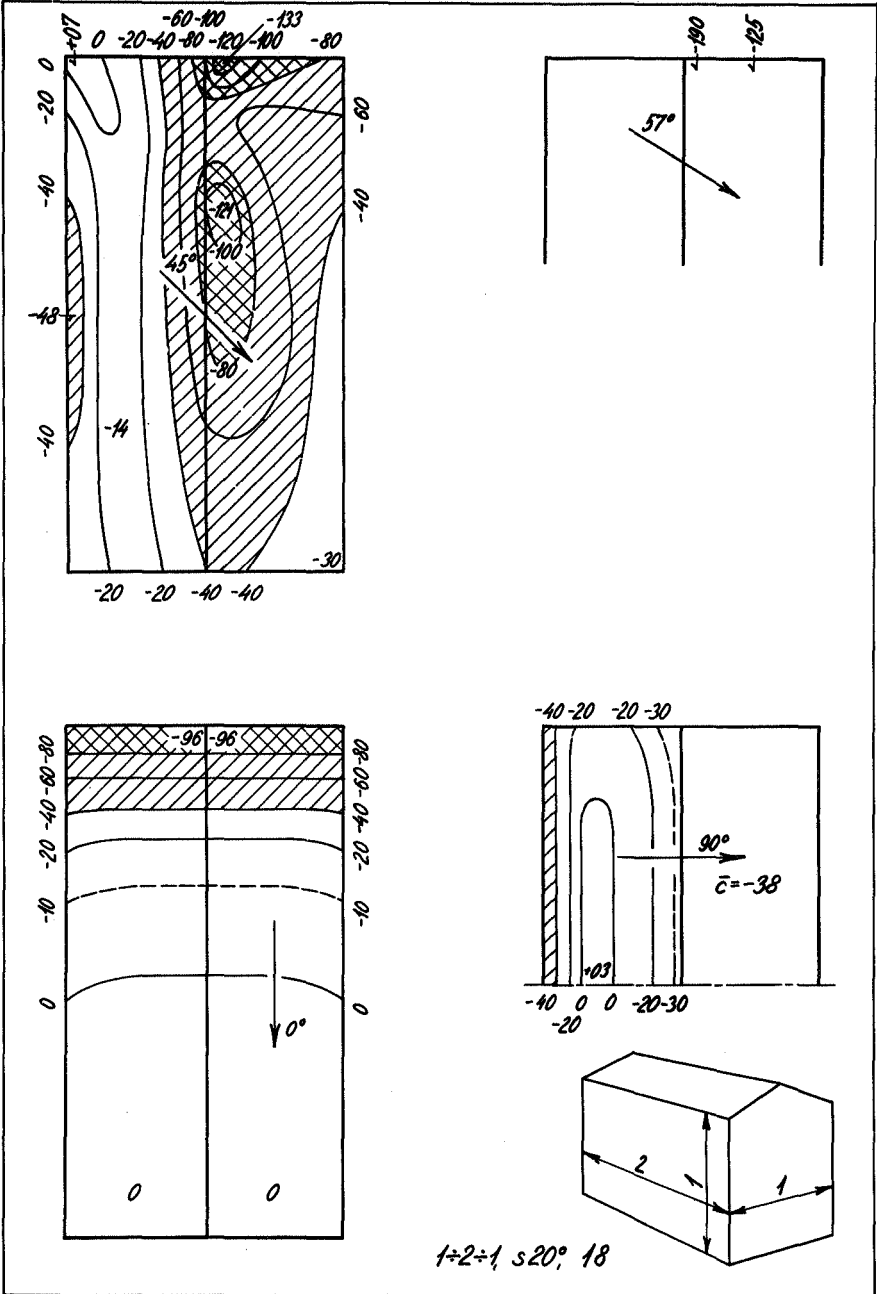
The extreme values of the shape factors are noted.

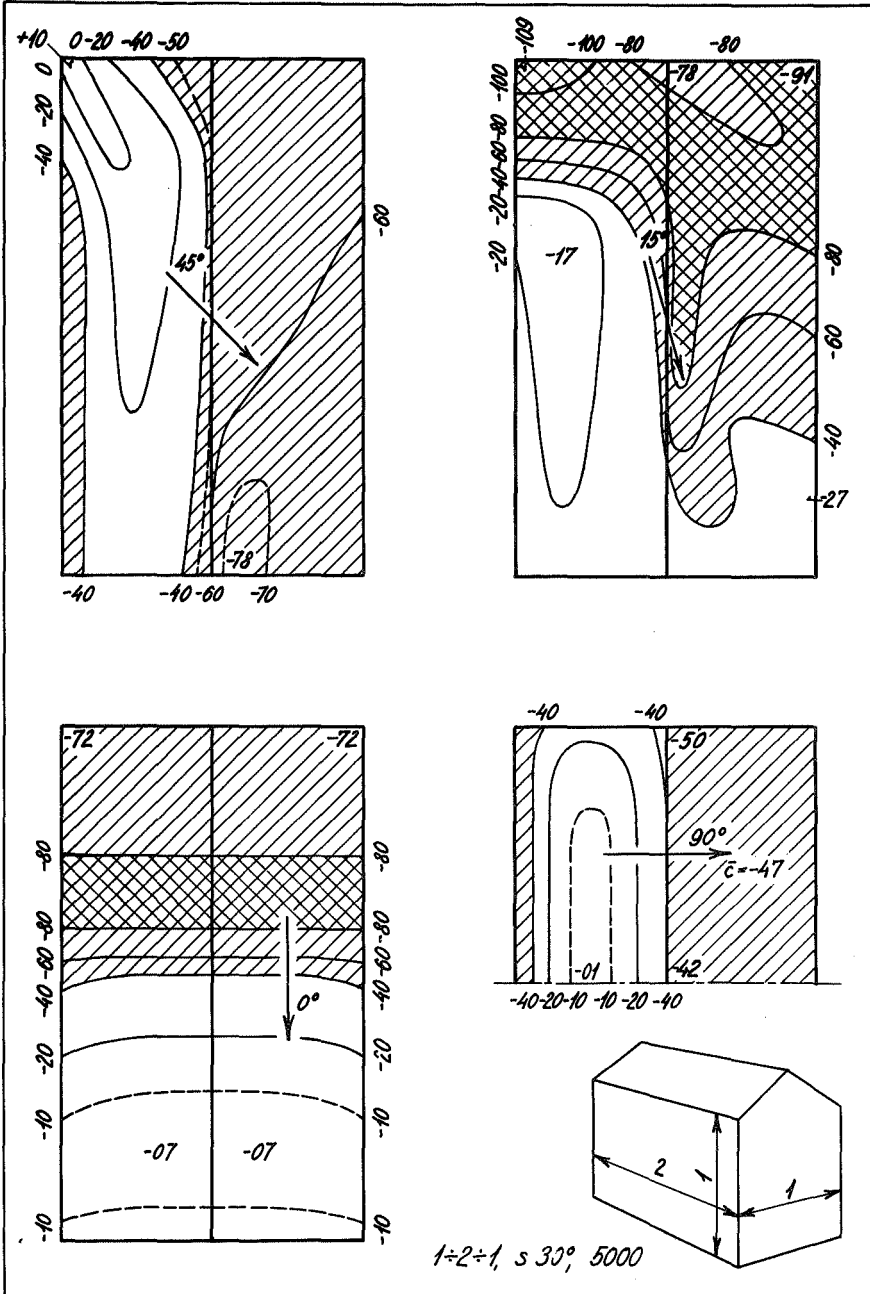


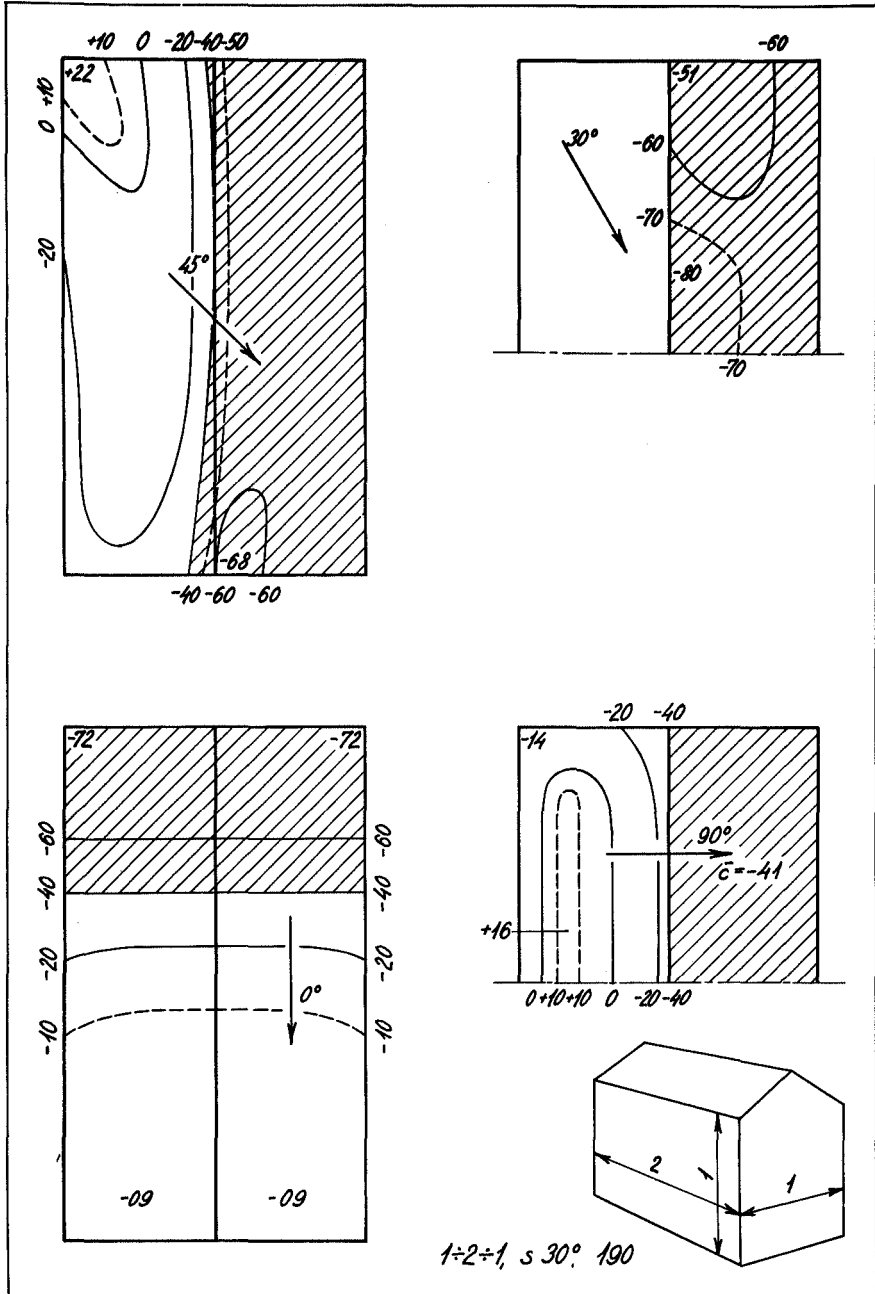


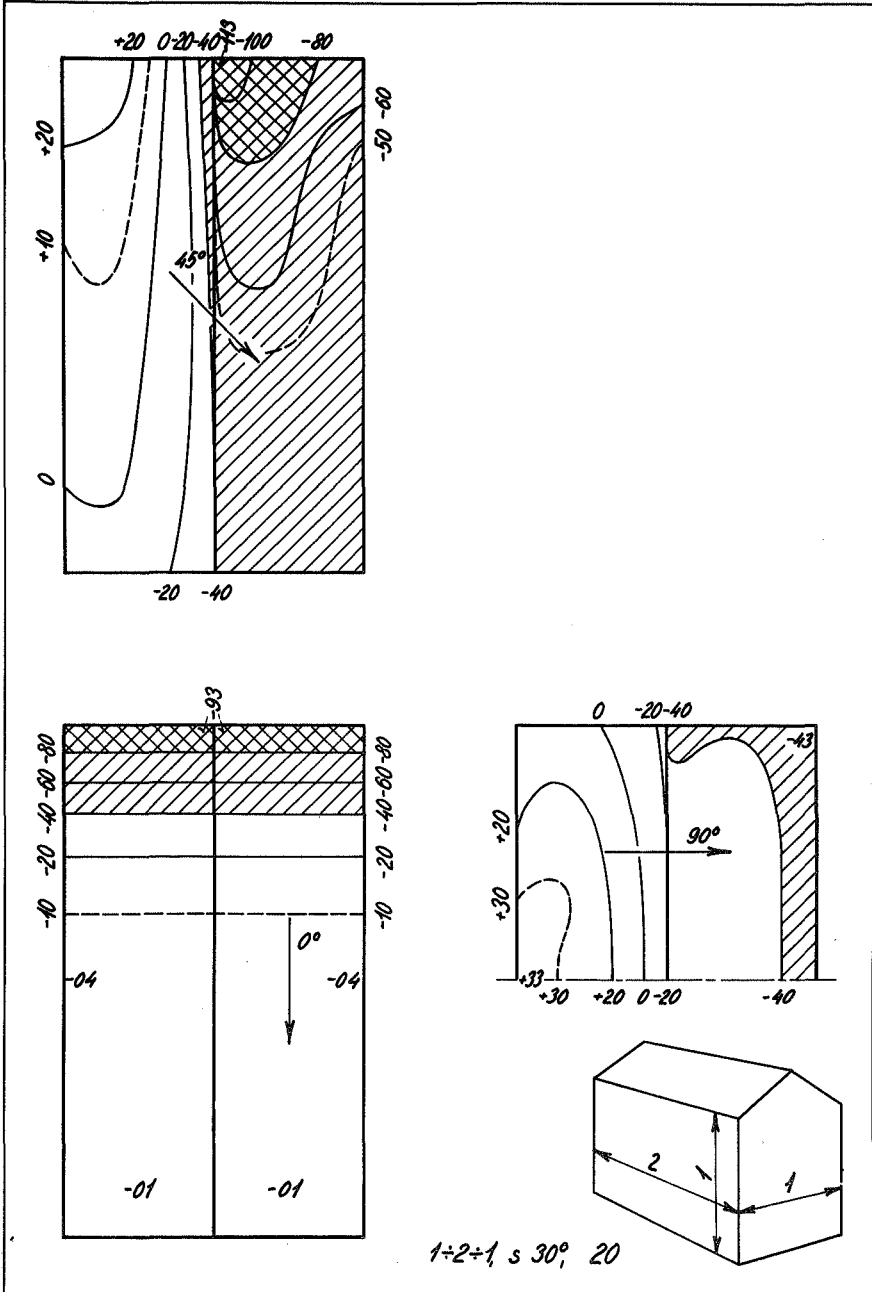


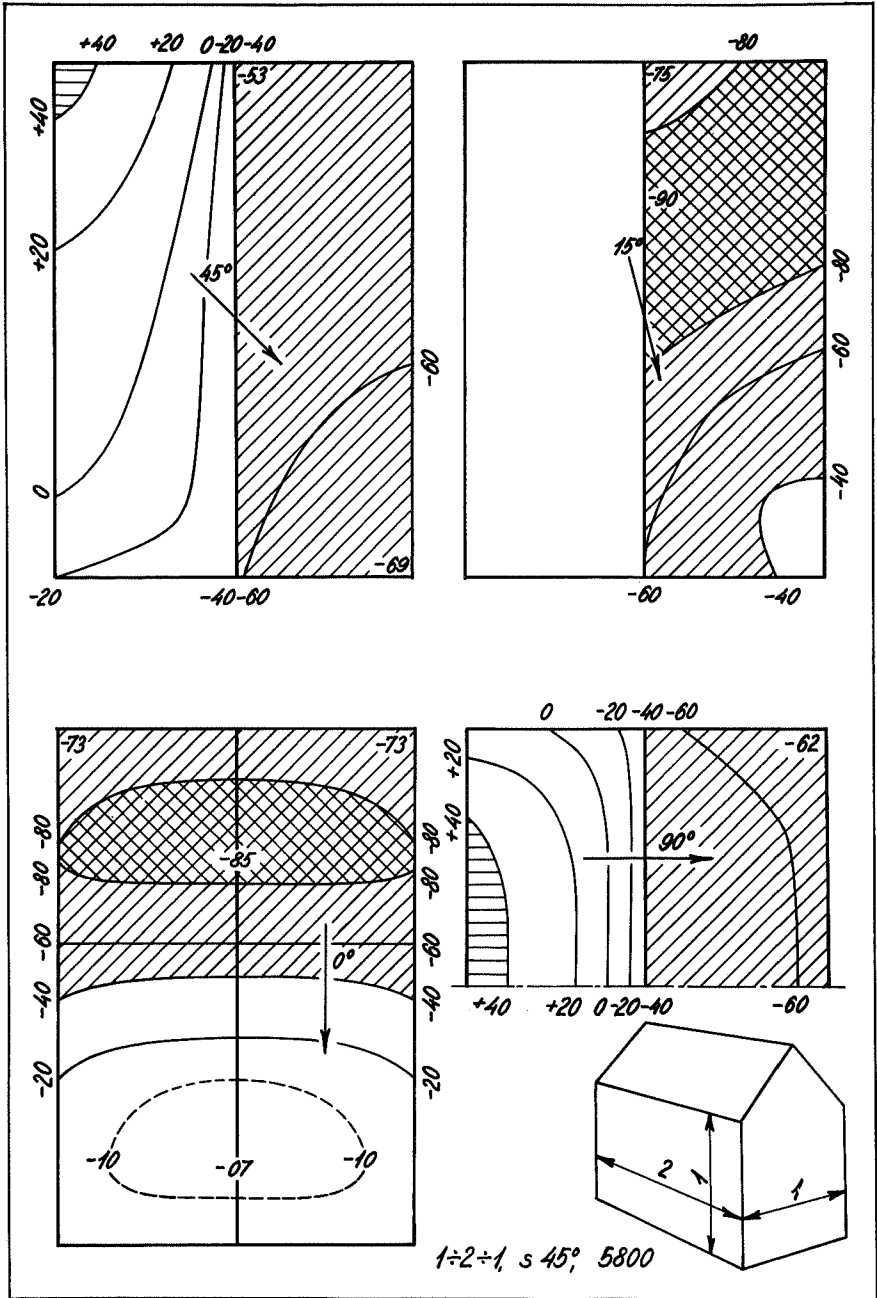


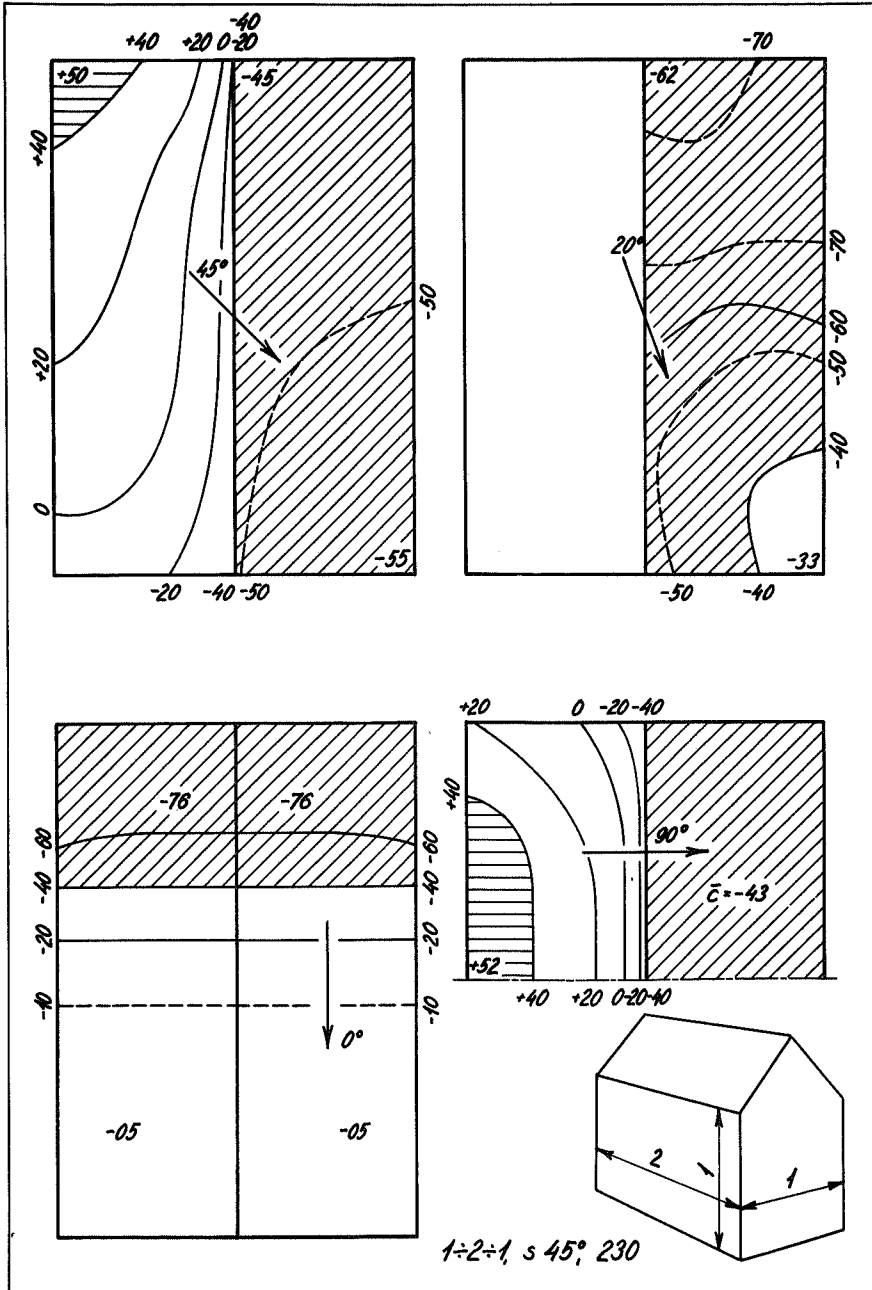


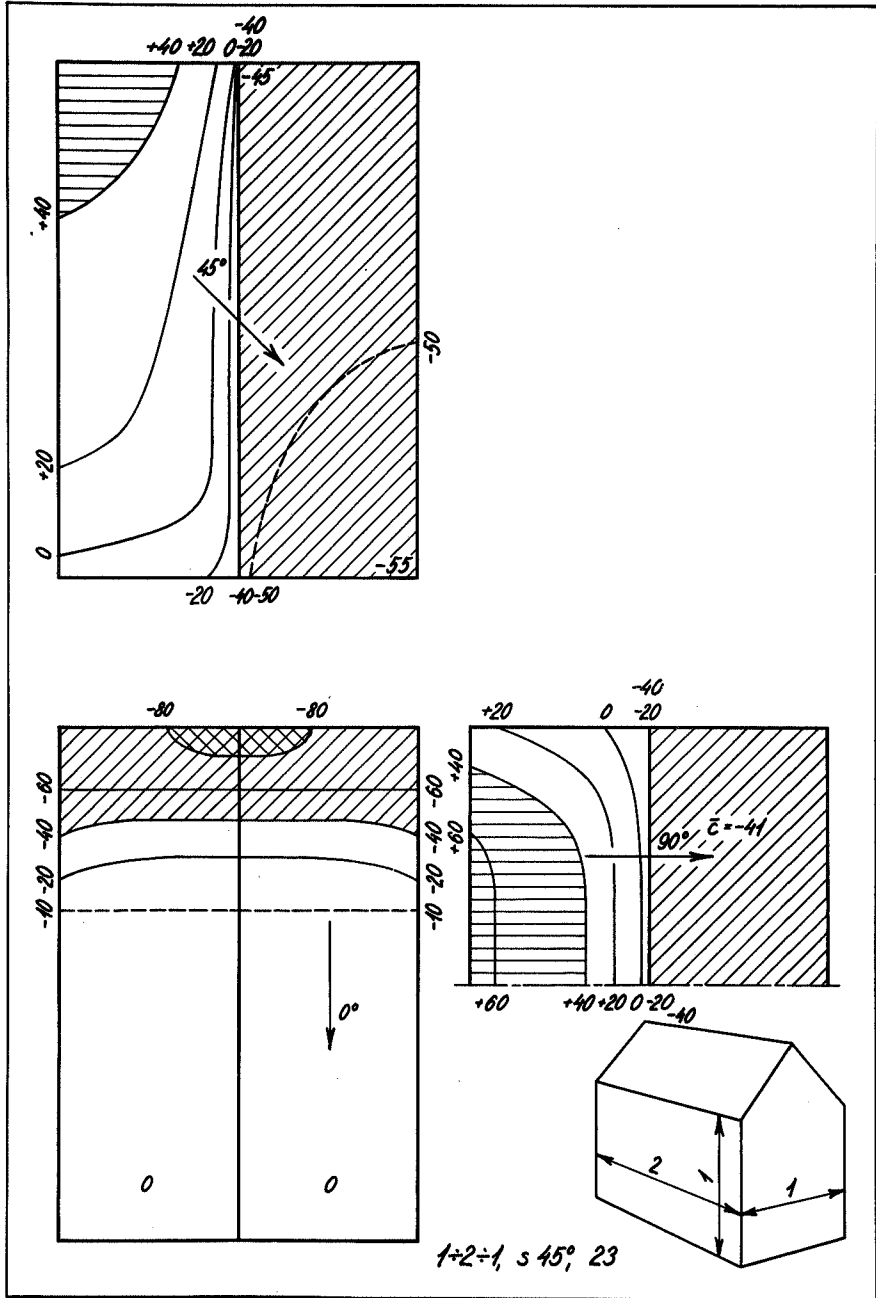




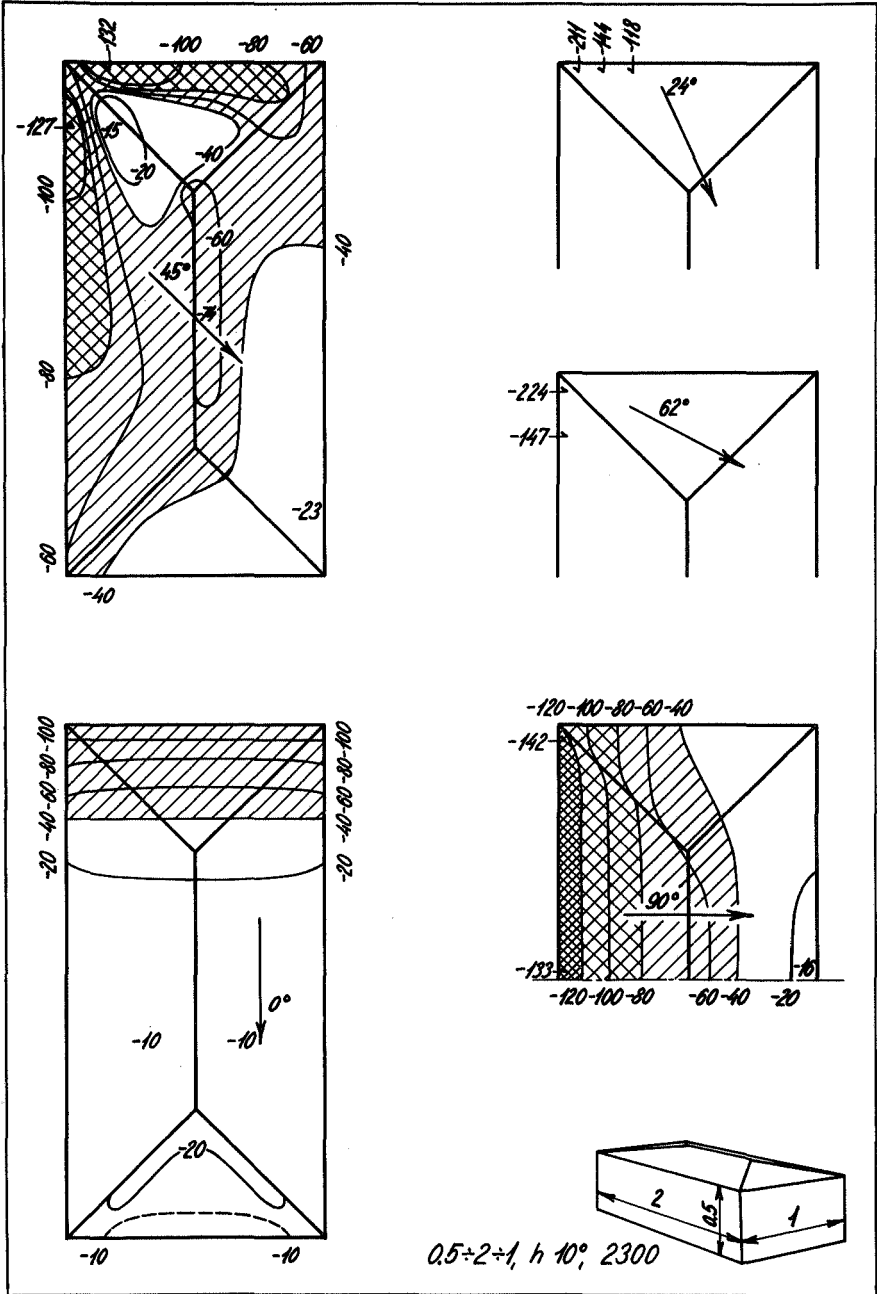


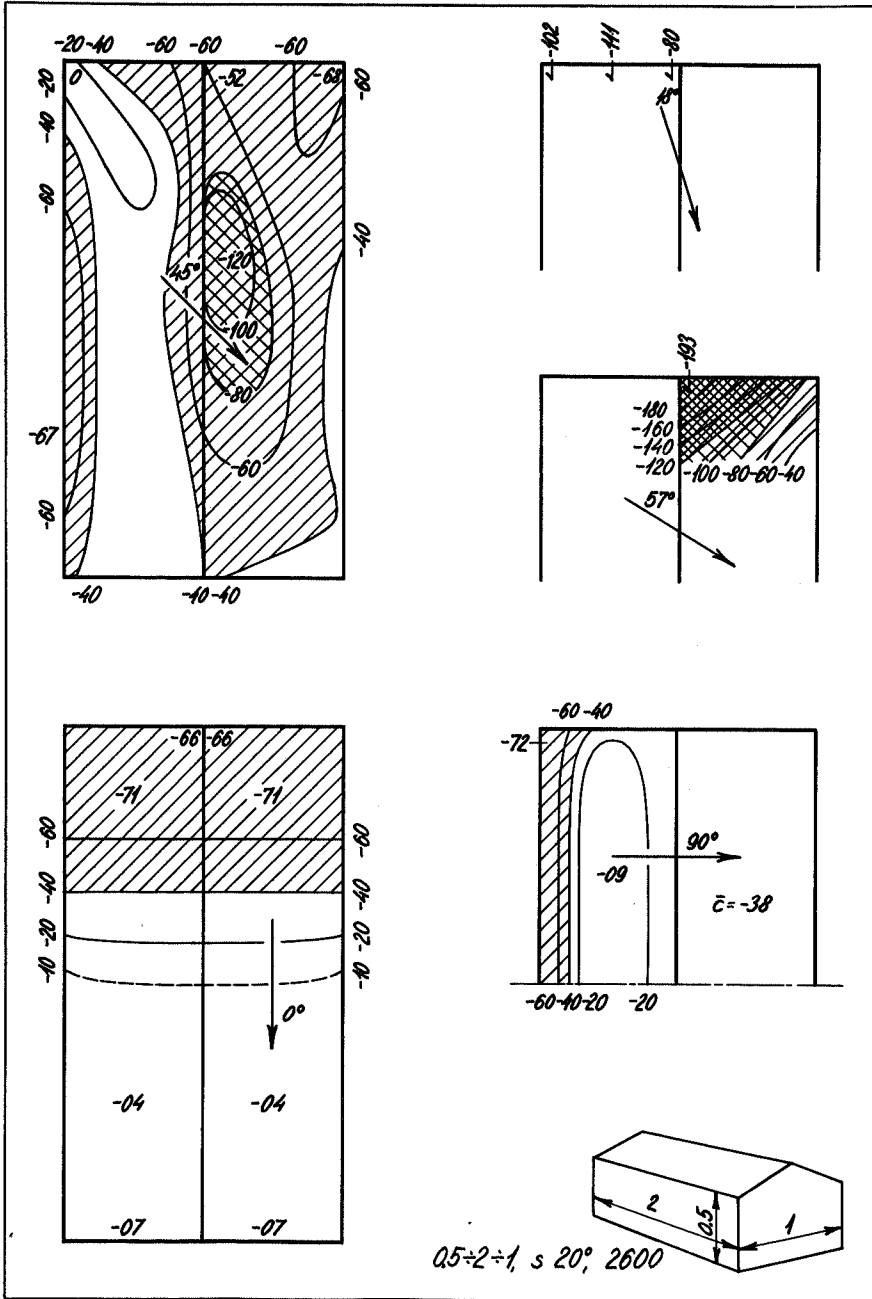


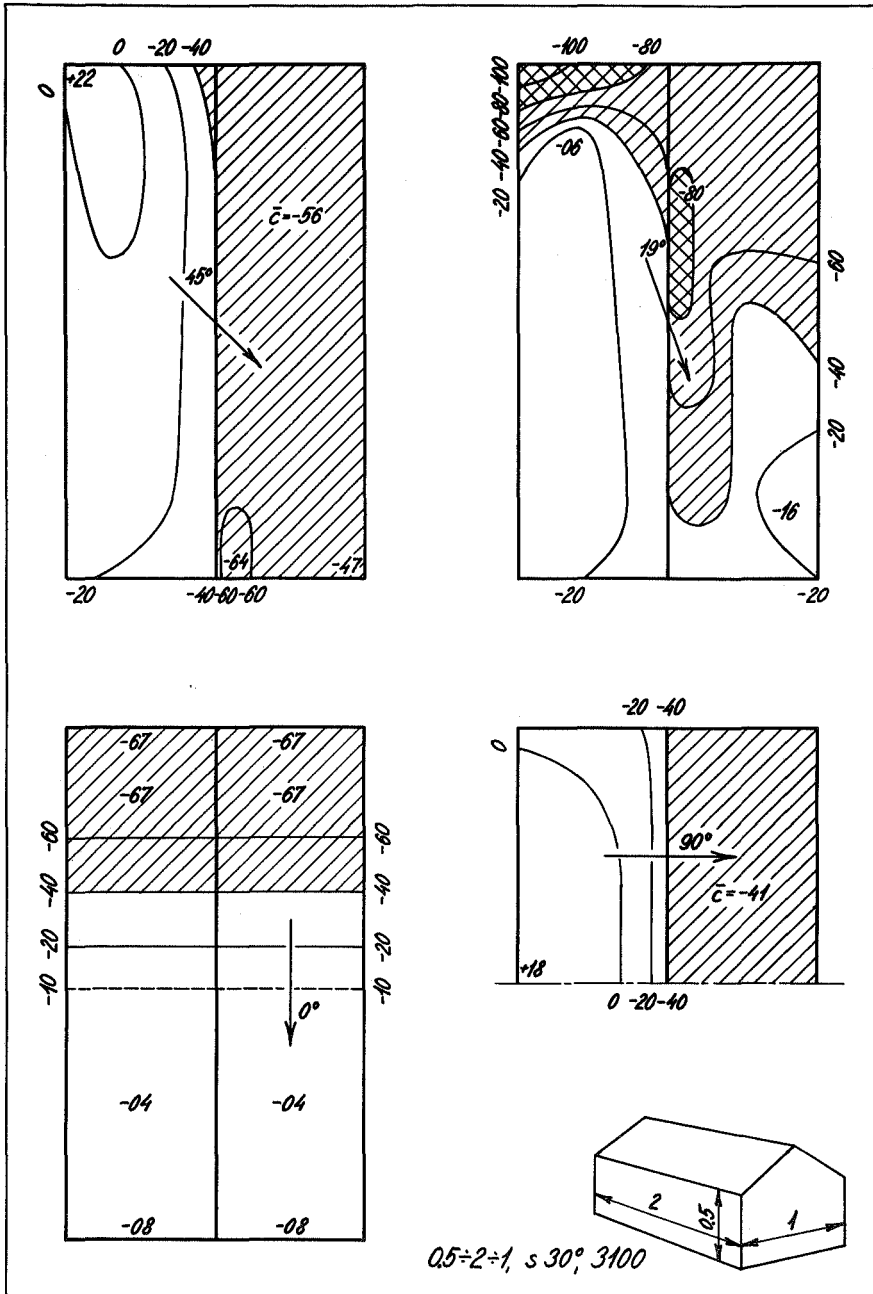


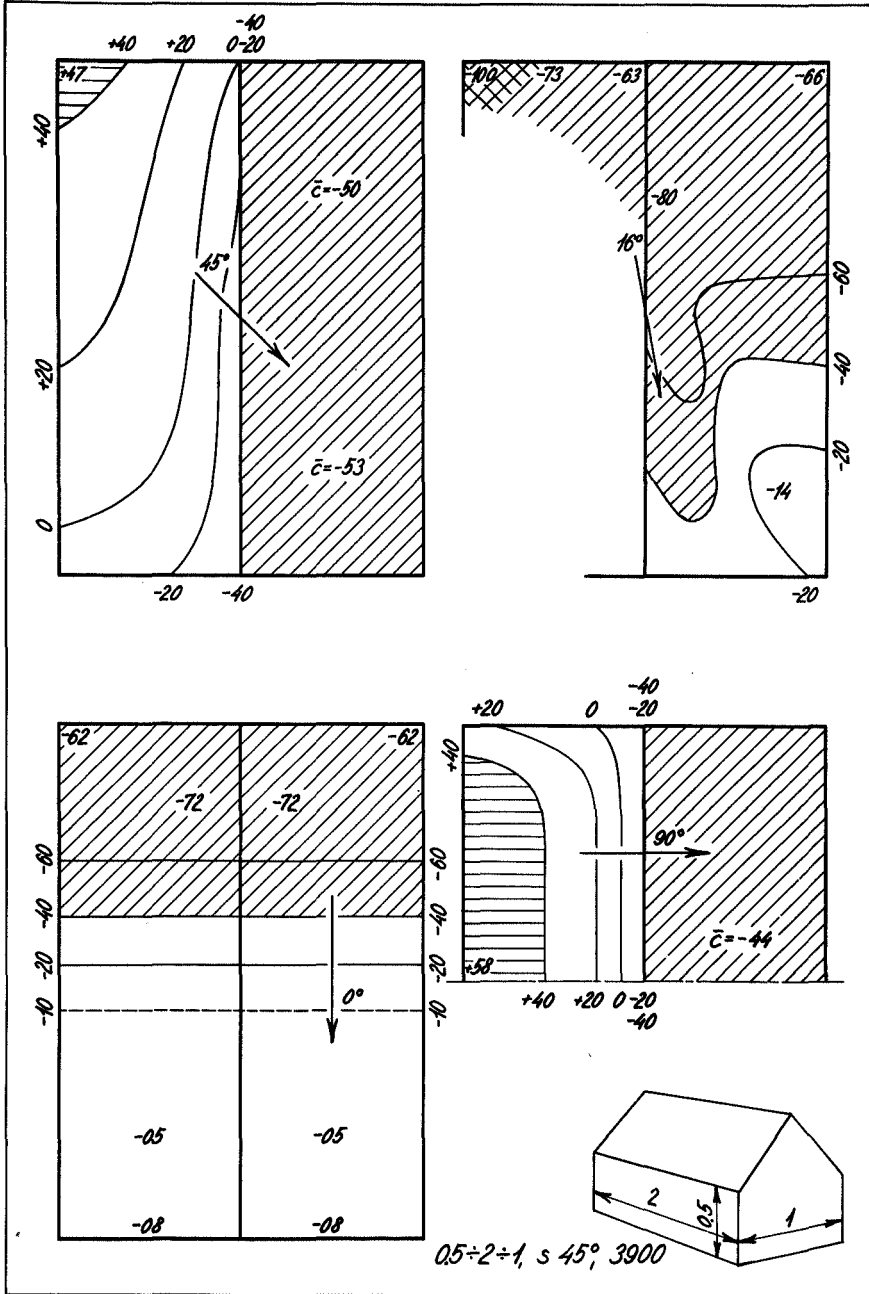




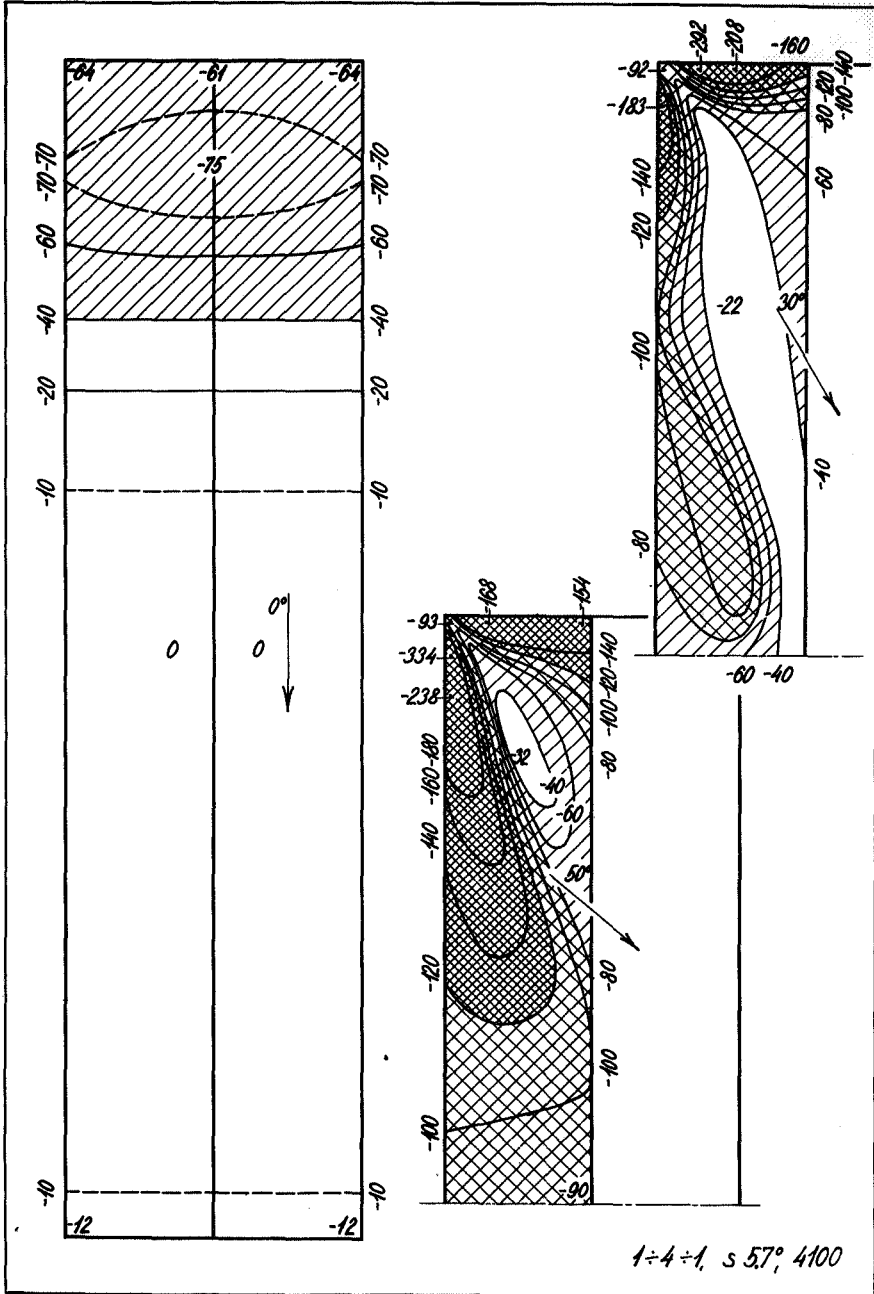




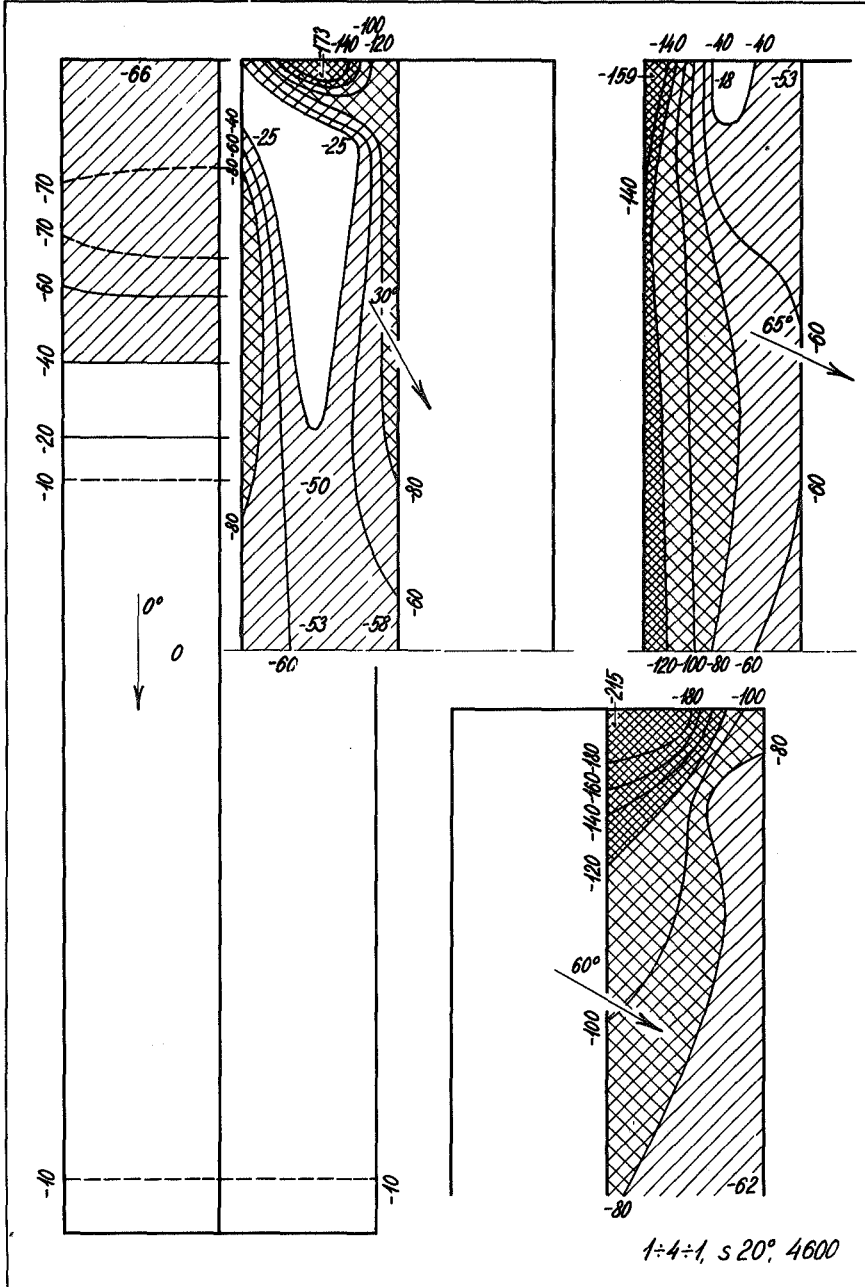












## 9. FREE DESK ROOFS

### 9.1 Scope of the tests

All the model tests with free desk roofs were two-dimensional.

The model described in Section 1.4 was used. It was placed across the 4th section of the tunnel as described in 1.4.

The distribution of the wind load in the symmetry plane of the model was investigated for the roof placed at different heights over the tunnel bottom and at different inclinations.

In the tests with free desk roofs the height is the distance from the tunnel bottom to the centre of the roof.

The width of the roof is called  $b$ . The following height positions were investigated:

$$H = 1.5 b, 1.0 b, 0.75 b \text{ and } 0.5 b.$$

The roof slope  $\alpha$  is given a sign, positive when the windward roof edge is higher than the leeward. The roof slope was varied between  $+30^\circ$  and  $-30^\circ$ .

Three types of turbulent boundary layers were used, namely small turbulence,  $z_0 = 1.8 \cdot 10^{-3}$  cm, from smooth masonite, medium turbulence,  $z_0 = 0.037$  cm, from corrugated paper and large turbulence,  $z_0 = 0.77$  cm, from 2.5·2 cm lists.

Table 139 gives a summary of the tests with free desk roofs.

Table 138

Thickness of the roof 0.068  $b$

$\alpha$	$\frac{H}{b}$	Turbulence	Figure on page
$\pm 30^\circ$	1.0	s	149
$+4^\circ$	1.0	s	149
$-4.3^\circ$	1.0	s	149

Table 139

Thickness of the roof 0.035 b

$\alpha$	$\frac{H}{b}$	Turbulence	Figure on page
$\pm 30^\circ$	1.5	s	141
		l	141
	1.0	s	142
		m	142
		l	142
0.75	s	143	
0.5	s	143	
	l	143	
$\pm 20^\circ$	1.0	s	144
		m	144
		l	144
$\pm 15^\circ$	1.0	s	145
$\pm 10^\circ$	1.5	s	145
		l	145
	1.0	s	146
		m	146
		l	146
0.5	s	147	
l	147		
$\pm 7^\circ$	1.0	s	147
$+3.8^\circ$	1.0	s	148
		l	148
$-4.1^\circ$	1.0	s	148
$-3.8^\circ$	1.0	l	148

s = small turbulence  
m = medium turbulence  
l = large turbulence.

In the experiments mentioned above the thickness of the roof is  $0.035 b$ , where  $b$  is the width of the roof. In addition a few experiments with a roof twice as thick,  $0.068 b$ , were made. The scope of these tests is given in Table 138.

## 9.2 Test results

In Figures 141 to 148 the shape factors derived from the tests are given. The shape factor is  $c = p/q$ , where  $p$  is the wind load at the point concerned and  $q$  is the velocity pressure level with the mean height of the roof.

The tests are designated by the following key:

$\frac{H}{b}$ ,  $\alpha$ , turbulence,

where  $H$  is the height to the center of the roof,  $b$  is the width of the roof and  $\alpha$  is the roof slope. The turbulence is  $s =$  small,  $m =$  medium or  $l =$  large.

The shape factors are given in magnitude and direction both for the top side and the under side of the roof. The loading curves and arrows corresponding to the upper side of the roof are drawn in full lines. Those corresponding to the under side are drawn in broken lines.

The total load is equal in magnitude and direction to the distance from the broken line curve to the full line curve.

In the Figures the factors  $C$  for the resulting wind load and the distance from the leading edge are also given.

Figs. 141 to 148. Free desk roofs.

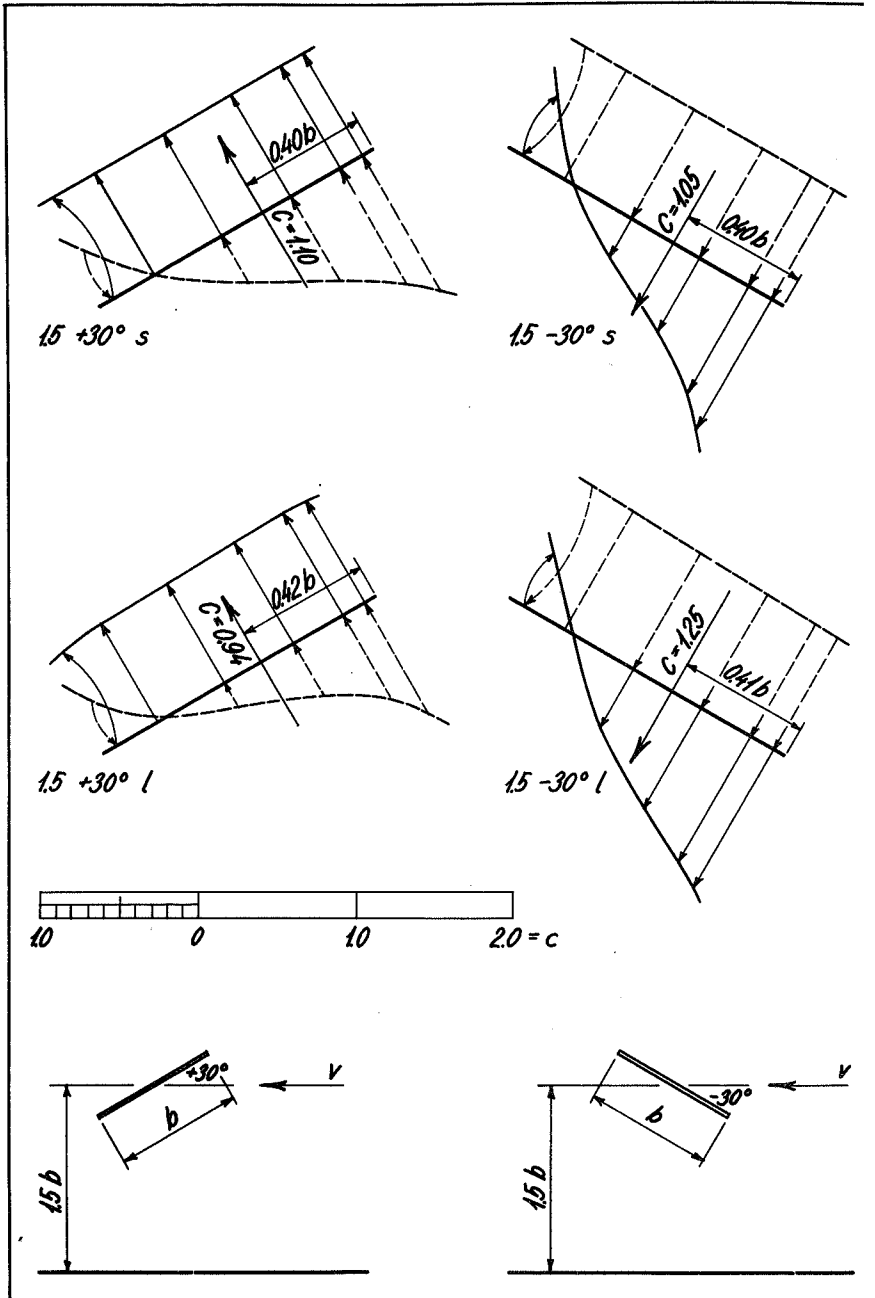
The key is  $H/b$ ,  $\alpha$  and turbulence.  $H$  is the height to the centre of the roof,  $b$  is the width of the roof and  $\alpha$  is the roof slope, positive when the high edge is leading. The turbulence is  $s =$  small ( $z_0 = 1.8 \cdot 10^{-3}$  cm),  $m =$  medium ( $z_0 = 0.037$  cm) or  $l =$  large ( $z_0 = 0.77$  cm).

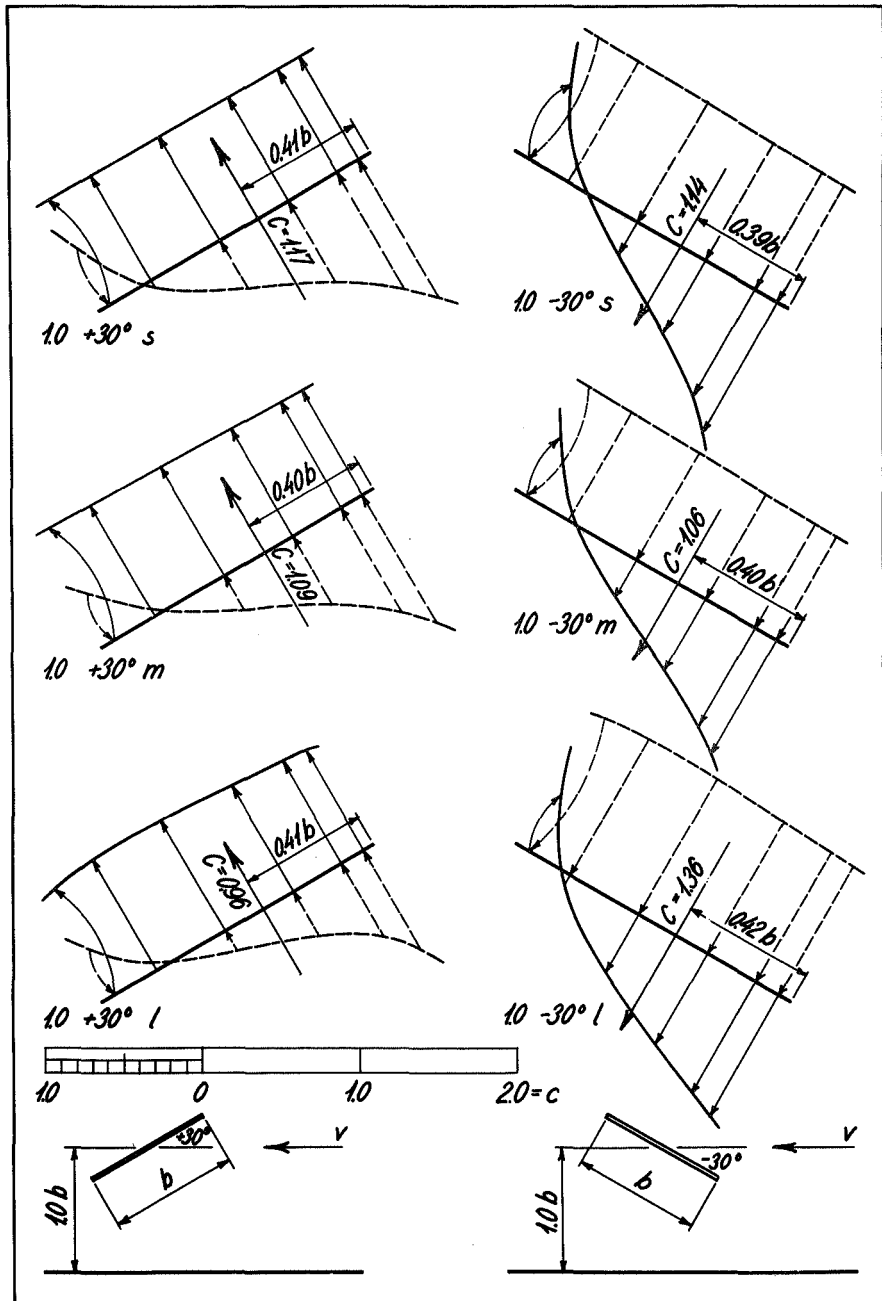
Full line curves and arrows correspond to the upper side of the roof. The arrows go from the roof surface to the curve. Broken line curves and arrows correspond to the under side of the roof. The arrows go from the curve to the roof surface.

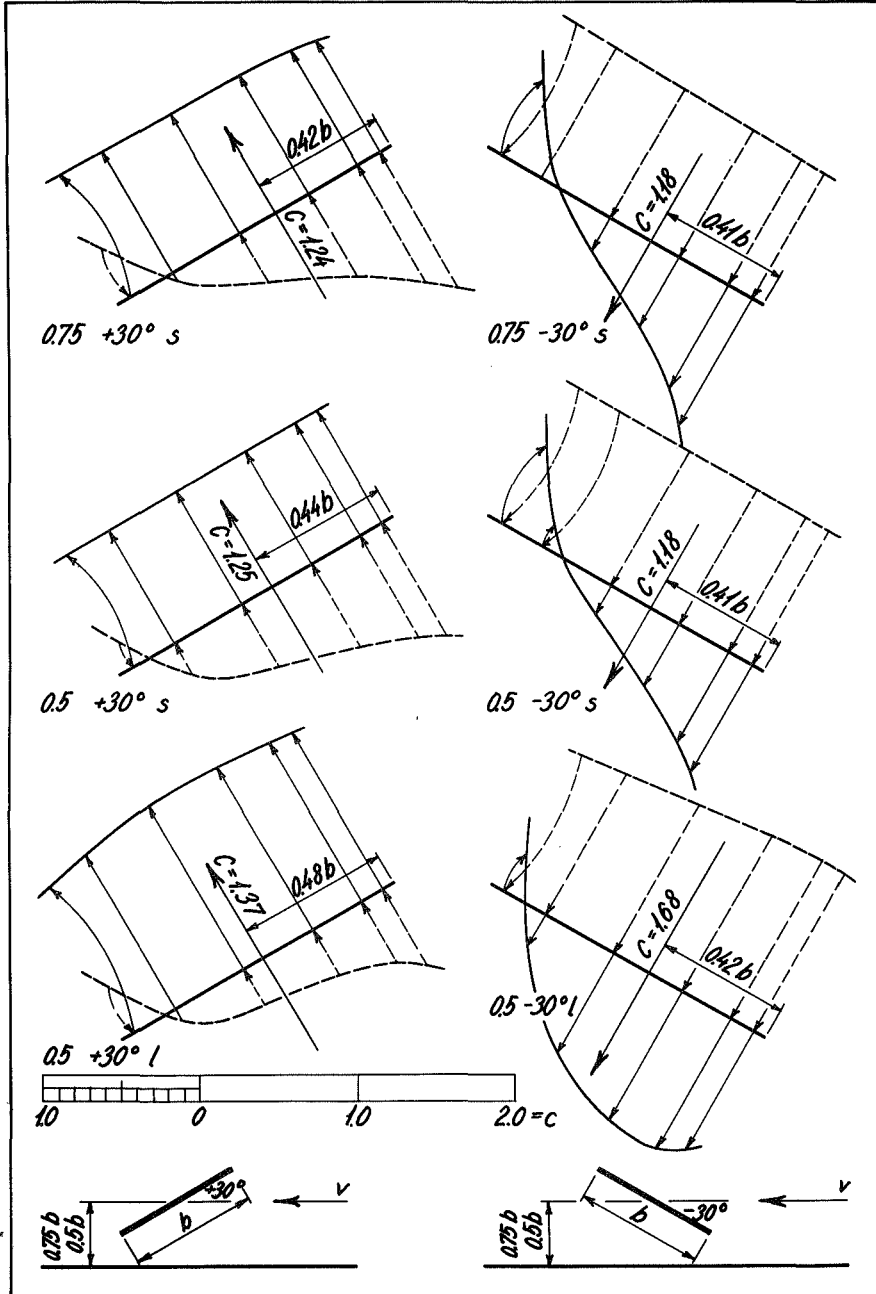
The total load is in magnitude and direction equal to the distance from the broken line curve to the full line curve.

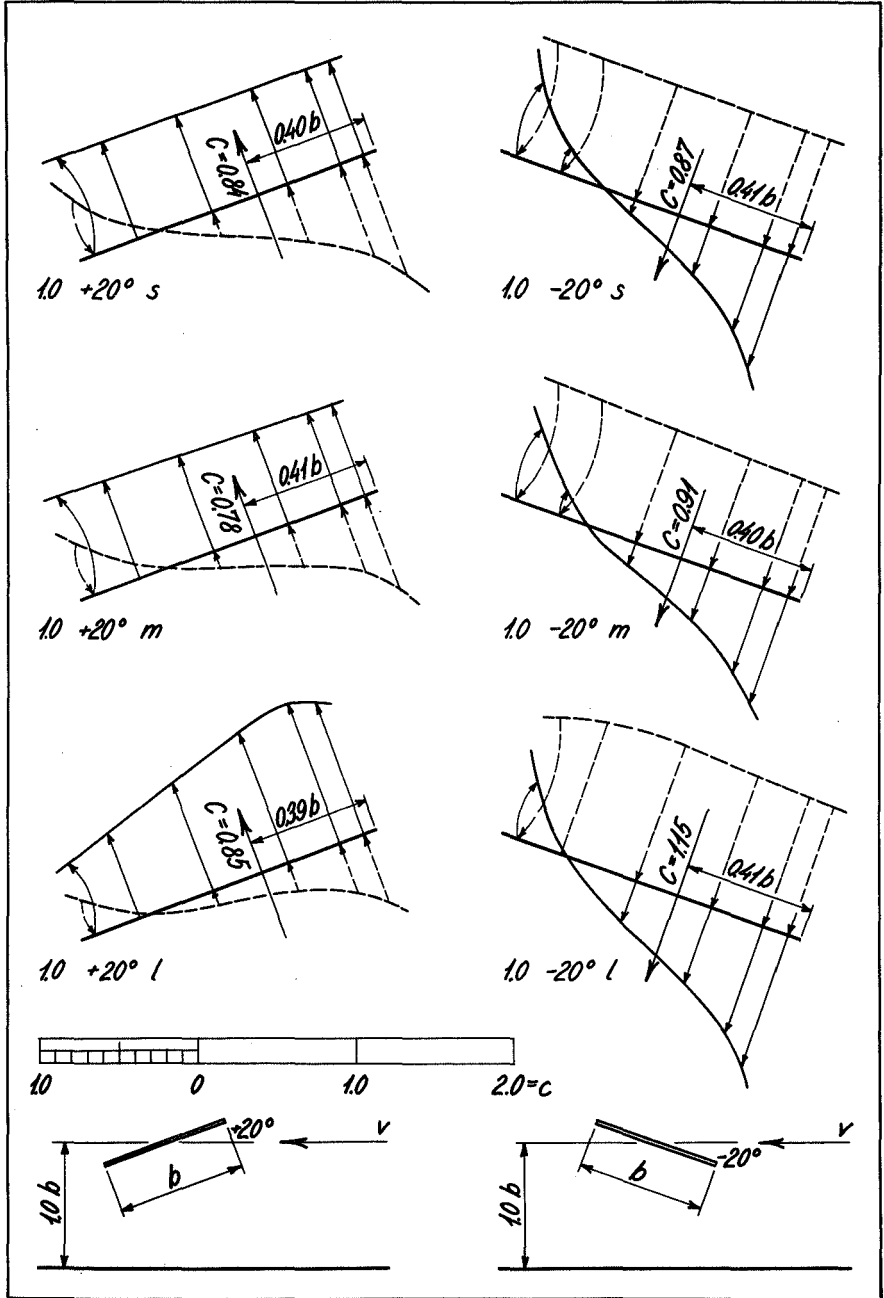
When the loads on the two sides of the roof are in opposite directions the arrows are curved for clarity.

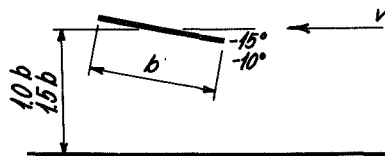
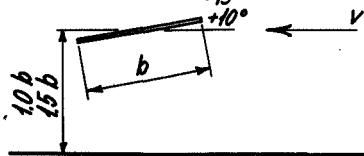
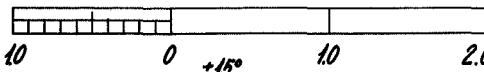
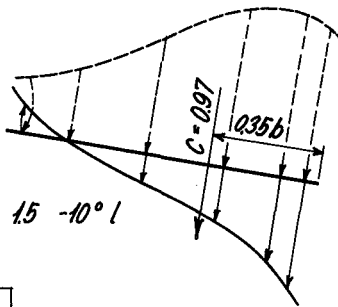
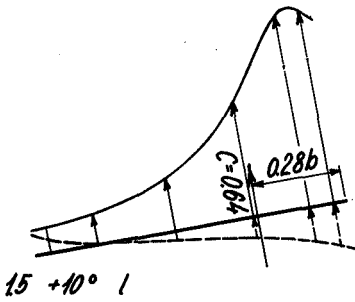
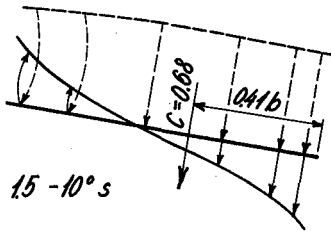
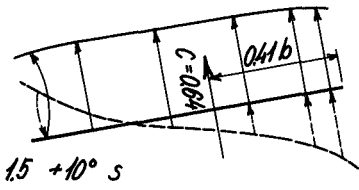
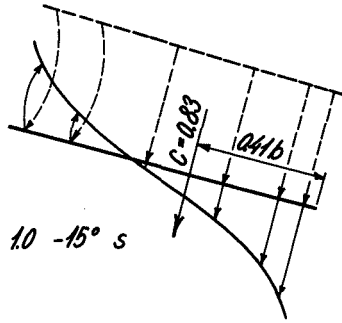
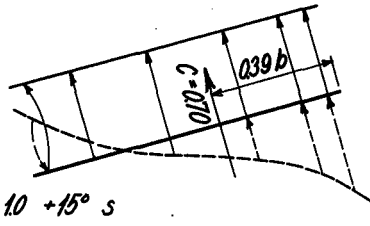
$C$  is the factor for the resulting wind load on the roof, and  $e$  gives its distance from the leading edge.

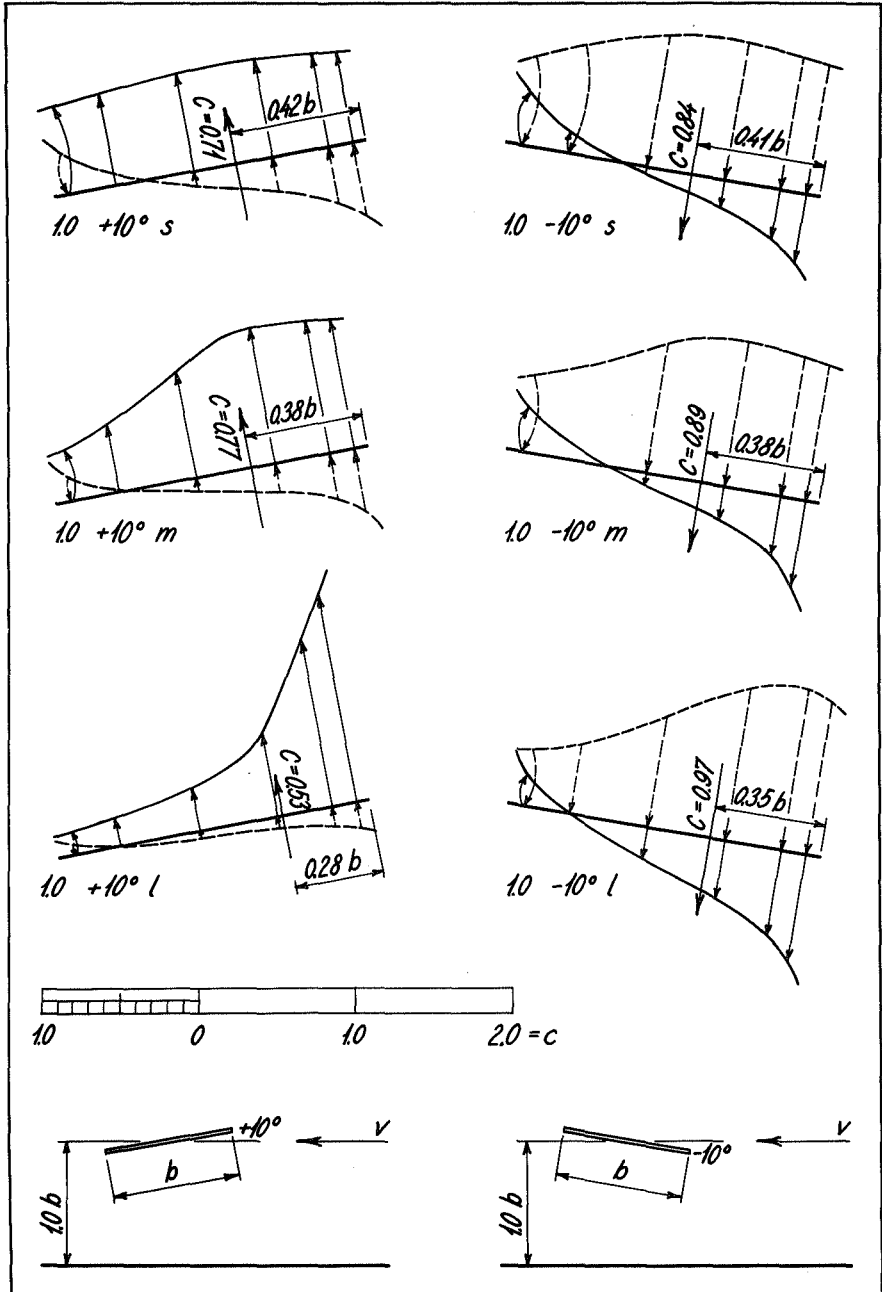


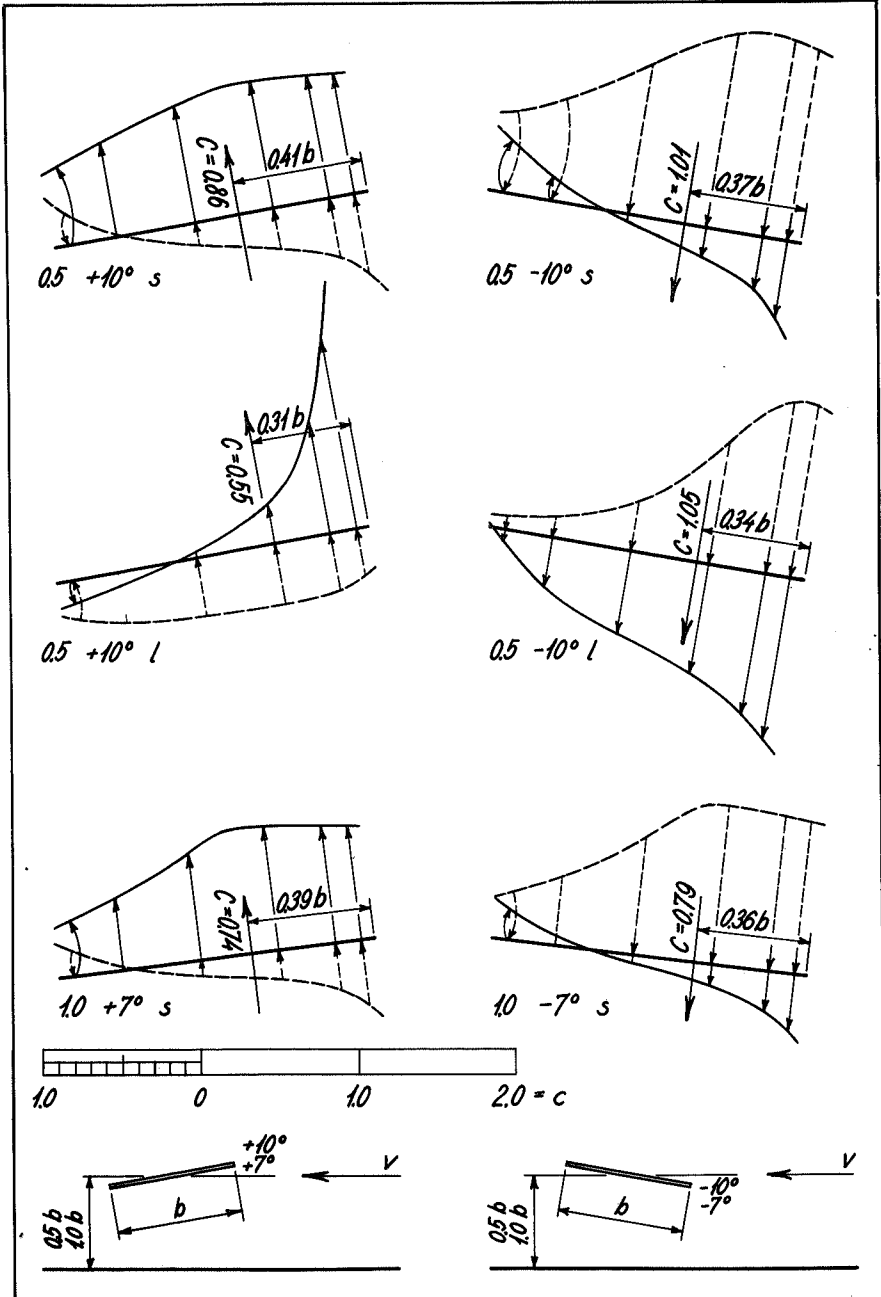




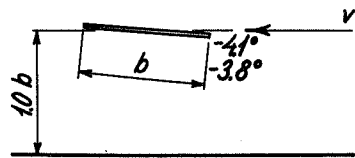
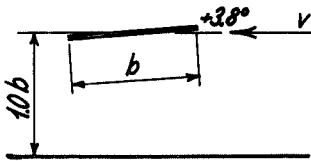
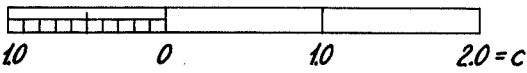
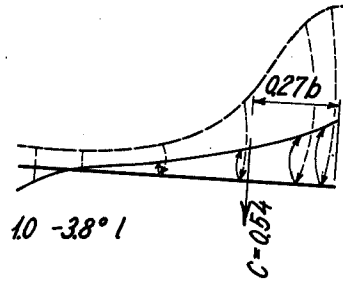
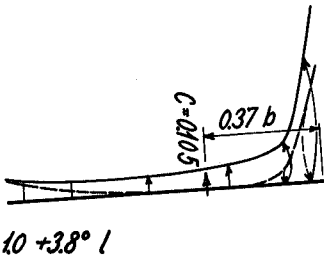
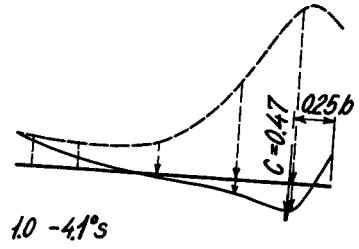
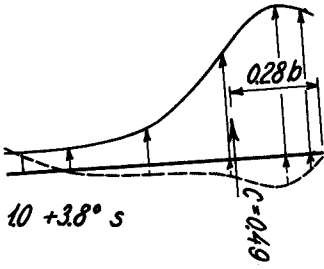








Unstable



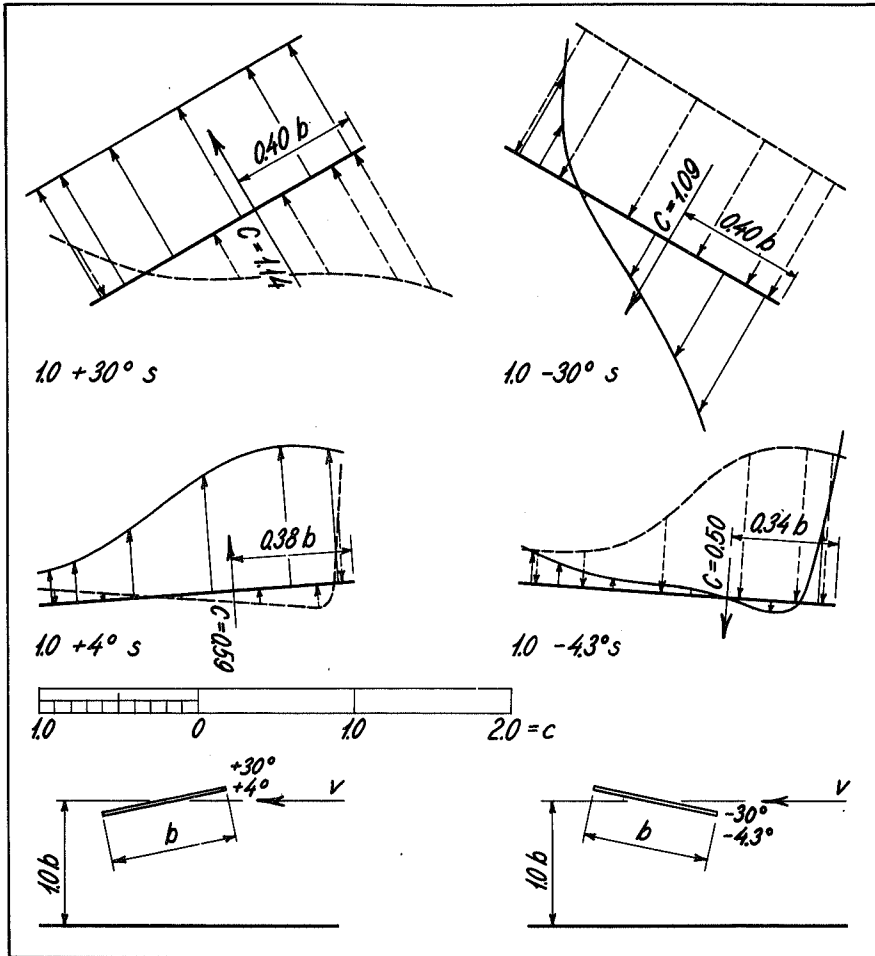


Fig. 149. Free desk roofs.

In Figures 141 to 148 the thickness of the roof is  $0.035b$ . In Figure 149 the thickness is  $0.068b$ .

For further information see legend on page 140.

### 9.3 Conclusions

In Figure 151 the results from the tests with  $h \div b = 1$  are shown. The abscissa is the roof slope. The ordinate is both the factor  $C$  for the resulting wind load, corresponding to the thick line curves and filled points, and the distance,  $e$ , of the resulting wind load from the leading edge of the roof made dimensionless by division with  $b$ , corresponding to the thin line curves and open points.

The results of the tests over the smooth tunnel bottom are shown with circular points and full line curves. The tests with large turbulence are shown with triangular points and broken line curves. The tests with medium turbulence are shown with square points.

It appears that  $C$ , when  $\alpha$  is positive, is almost always greatest in small turbulence, but, when  $\alpha$  is negative, it is greatest in large turbulence.

In large turbulence  $C$  increases with increasing roof slope, but in small turbulence there is a drop in the  $C$  value in the range from  $10^\circ$  to  $15^\circ$  roof slope both for positive and negative  $\alpha$ .

The point of attack for the wind load lies in most cases at a distance of  $0.3 b$  to  $0.4 b$  from the windward edge of the roof.

In Figure 152 the curves for  $H \div b = 1$  and small turbulence are shown. Abscissa and ordinate are the same as used in Figure 151. Also the results from the tests with  $H \div b = 1.5$ ,  $0.75$  and  $0.5$  are shown with points.

It appears that  $C$  is greatest when  $H \div b$  is small. But at steep roof slopes there is only a small difference in the  $C$  values for the high roofs and for the low roofs. The position of the point of attack is rather independent of  $H \div b$ .

Figure 153 shows the conditions at large turbulence. Here  $C$  is almost always greatest for the low roofs. But in contrast with the smooth cases it is at the steep roof slopes particularly that  $C$  varies greatly with  $H \div b$ .

In Figure 154 the curves from Figure 152 are repeated, i.e.  $H \div b = 1$  and small turbulence. These curves correspond to a roof thickness  $0.035 b$ . Also the resulting  $C$  values for a roof of double thickness, namely  $0.068 b$  are shown with points.

It appears that the roof thickness for the range investigated is of little significance both for  $C$  and for the position of the point of attack.

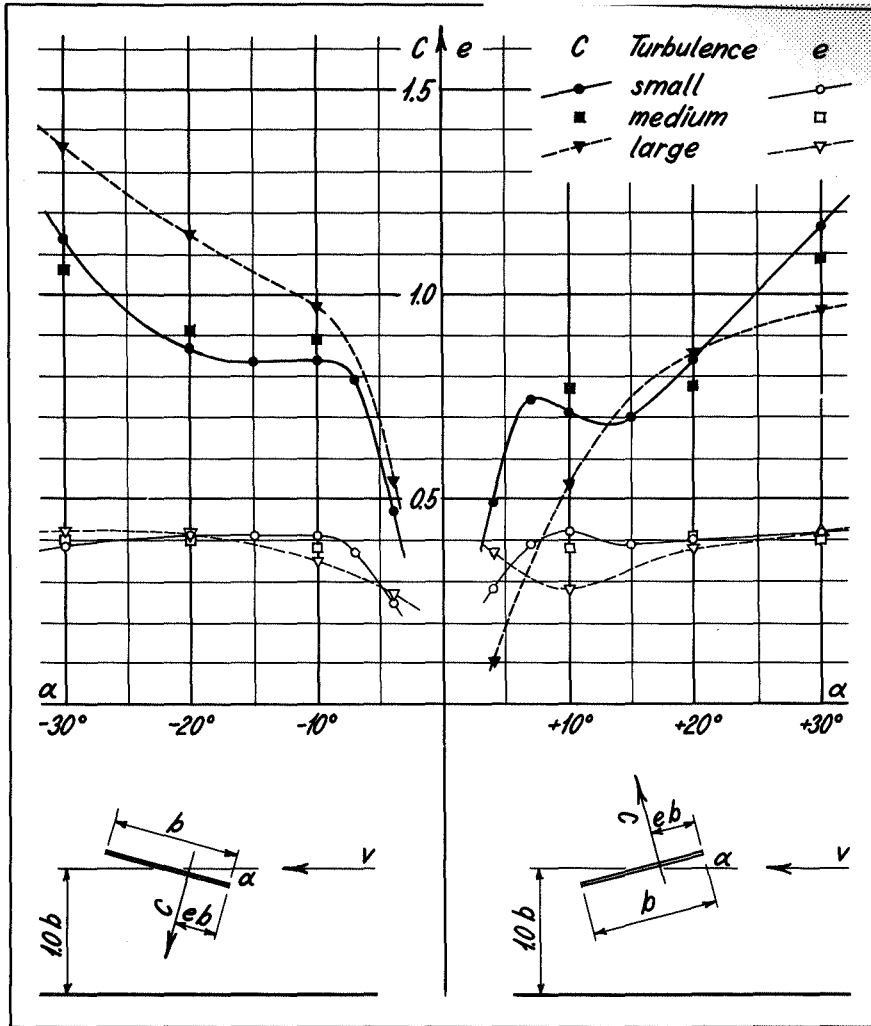


Fig. 151. Free desk roofs. Influence of turbulence.

The abscissa is the roof slope in degrees. The ordinate is both the factor for the resulting wind load, corresponding to the thick line curves and filled points, and the factor  $e$  for the point of attack of the resulting wind load, corresponding to the thin line curves and open points.

Full line curves and circular points are for the tests in small turbulence. Square points are for the tests in medium turbulence. Broken line curves and triangular points are for the tests in large turbulence.

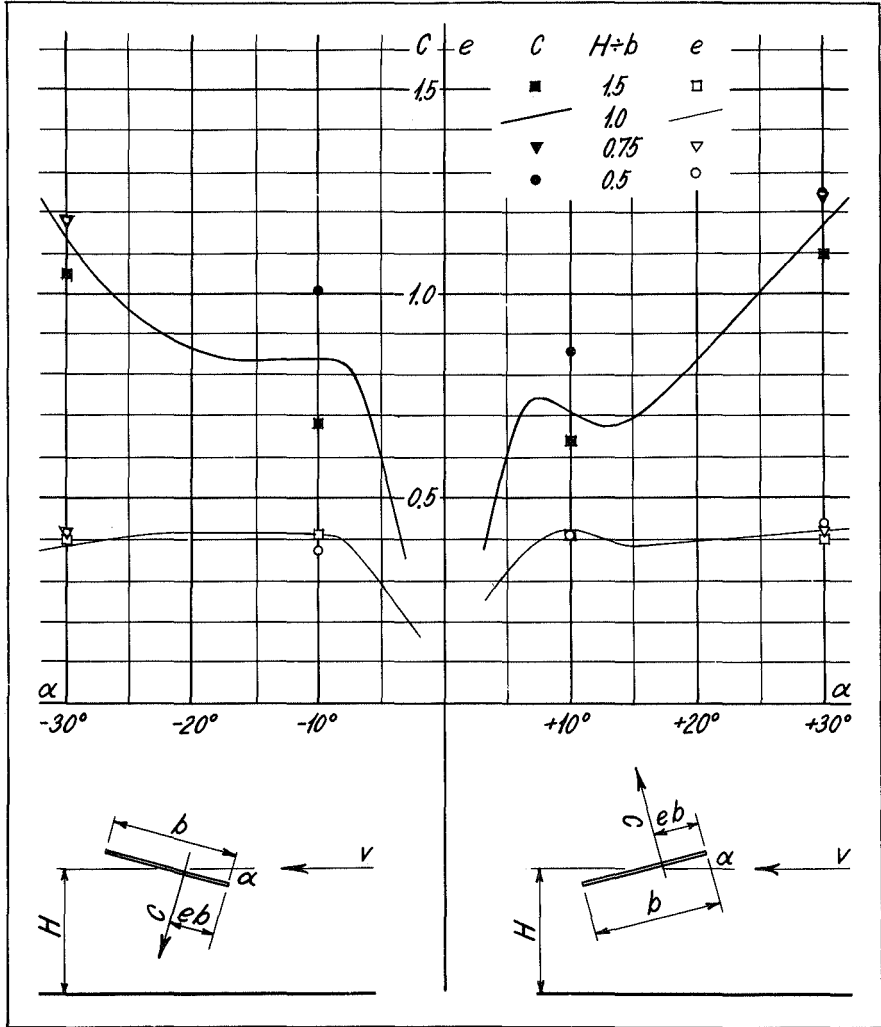


Fig. 152. Free desk roofs. Small turbulence. Influence of the height. The abscissa is the roof slope in degrees. The ordinate is both the factor  $C$  for the resulting wind load, corresponding to the thick line curves and filled points, and the factor  $e$  for the point of attack of the resulting wind load corresponding to the thin line curves and open points. The curves show the conditions at the roof with  $H/b = 1$ . The points show the results for values of  $H/b = 1.5$  0.75 and 0.5.

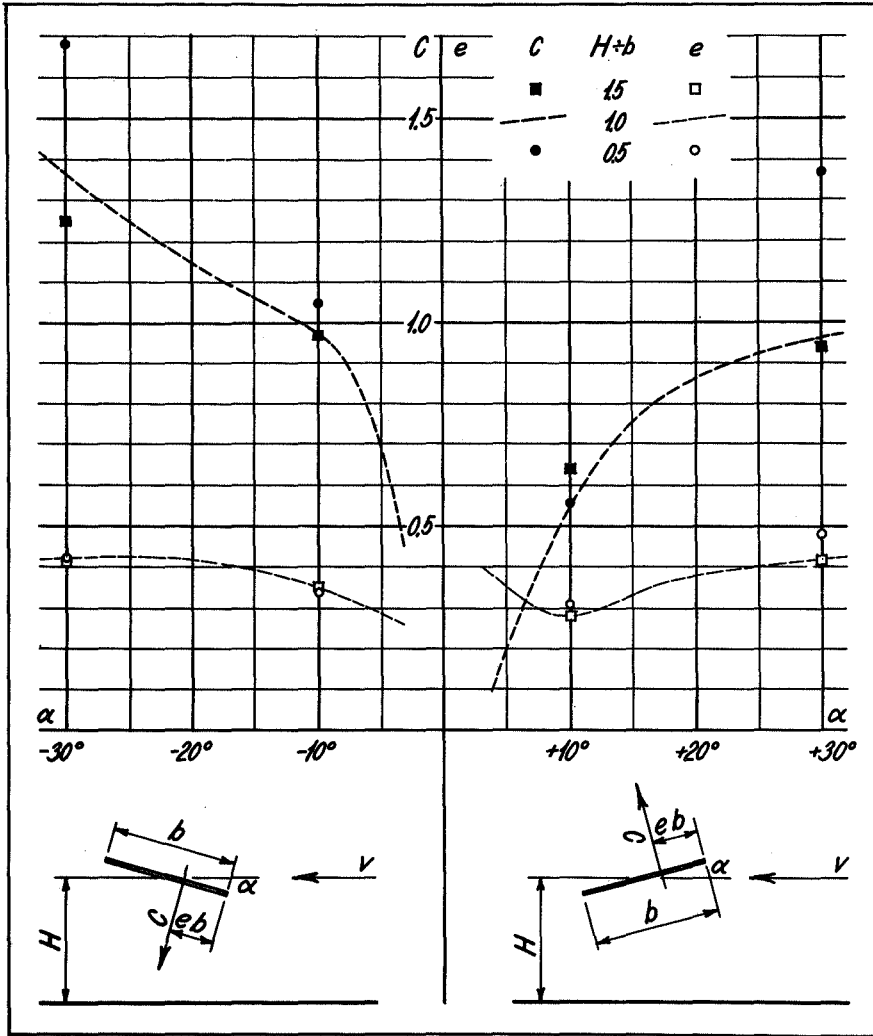


Fig. 153. Free desk roofs. Large turbulence. Influence of the height. The abscissa is the roof slope in degrees. The ordinate is both the factor  $C$  for the resulting wind load, corresponding to the thick line curves and filled points, and the factor  $e$  for the point of attack of the resulting wind load corresponding to the thin line curves and open points. The curves show the condition at the roof with  $H/b = 1$ . The points show the results for values of  $H/b = 1.5$  0.75 and 0.5.

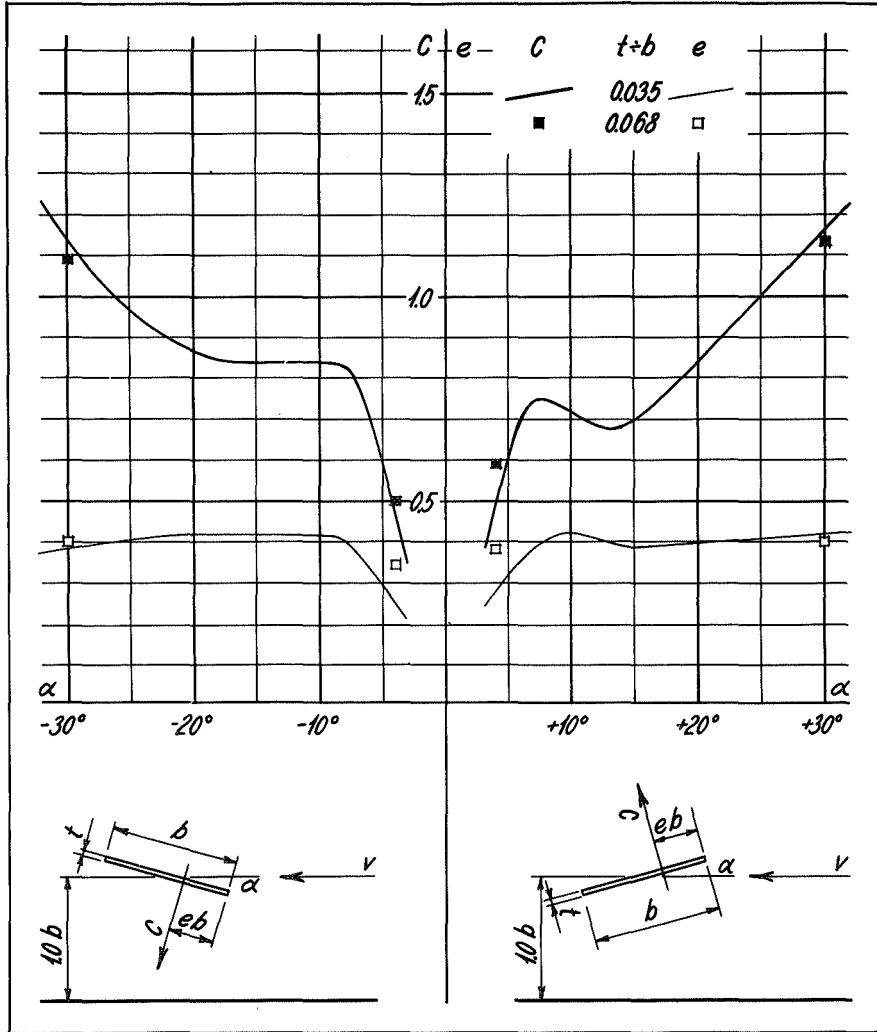


Fig. 154. Free desk roofs. Influence of the thickness.

The abscissa is the roof slope in degrees. The ordinate is both the factor  $C$  for the resulting wind load, corresponding to the thick line curves and filled points, and the factor  $e$  for the point of attack of the resulting wind load corresponding to the thin line curves and open points.

The curves show the conditions at the roof with  $t:b = 0.035$ . The points show the results for values of  $t:b = 0.068$ .

## 10. FREE TROUGH AND SADDLE ROOFS

### 10.1 Scope of the tests

All model tests with free trough roofs and saddle roofs were two-dimensional.

The model described in Section 1.4 was used. It was placed across the 4th section of the tunnel as described in 1.4.

The distribution of the wind load in the symmetry plane of the model was investigated with the roof placed at different heights above the tunnel bottom and at different inclinations.

The two sections of the roof have identical width,  $b$ , and are always placed at the same slope. The mean height of the roof is called  $H$ . The following height positions were investigated:

$H = 1.5 b, 1.0 b$  and  $0.5 b$ .

The roof slope  $\alpha$  is denoted positive for trough roofs and negative for pitched roofs. It was varied between  $+30^\circ$  and  $-30^\circ$ .

All the tests with free trough and saddle roofs were carried out in small turbulence, viz.  $z_0 = 1.8 \cdot 10^{-3}$  cm.

Table 156 gives a survey of the tests with free trough and saddle roofs.

### 10.2 Test results

In Figures 157 to 166 the shape factors derived from the tests are given. The shape factor is  $C = p/q$ , where  $p$  is the wind load at the point concerned and  $q$  is the velocity pressure level with the mean height of the roof.

The tests are designated by the following key:

$\frac{H}{b}, \alpha, s.$

$H$  is the mean height of the roof,  $b$  is the width of one part of the roof,  $\alpha$  is the roof slope.  $s$  indicates that the turbulence, as mentioned above, is small.

The shape factors are given in magnitude and direction both for the top side and the under side of the roof.

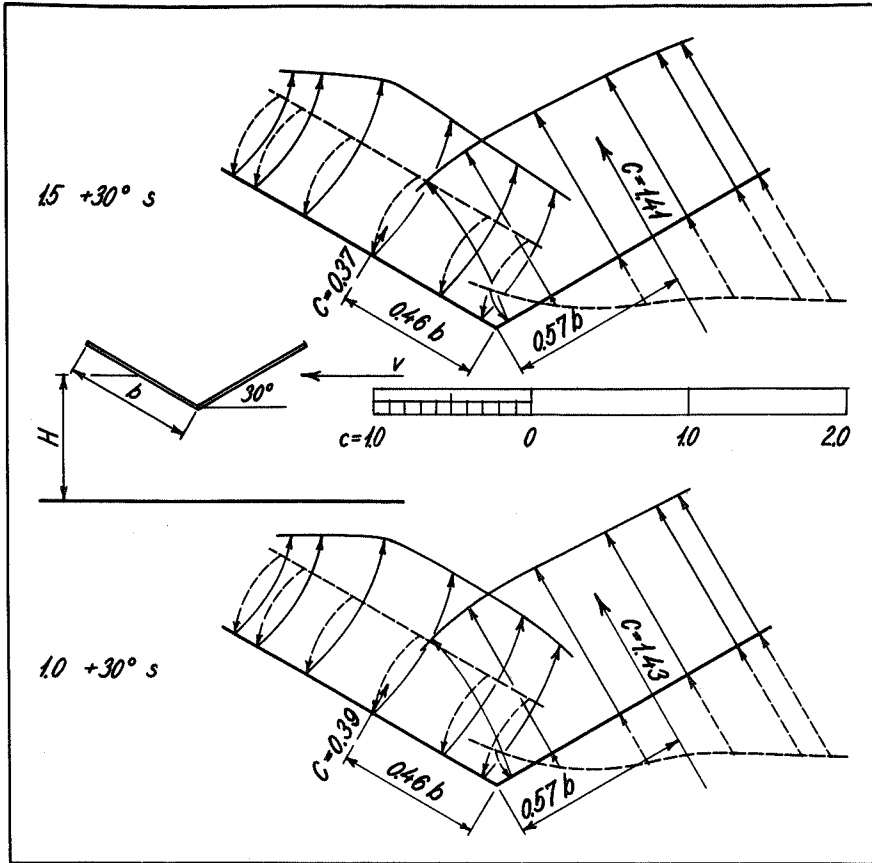
Table 156

	$\alpha$	$\frac{H}{b}$	Figure on page
Trough roofs	+30°	1.5	157
		1.0	157
	+20°	1.5	158
		1.0	158
		0.5	158
	+15°	1.5	159
		0.5	159
	+10°	1.5	160
		1.0	160
		0.5	160
	+4.8°	1.5	161
		0.5	161
Saddle roofs	-5°	1.5	162
		0.5	162
	-10°	1.5	163
		1.0	163
		0.5	163
	-15°	1.5	164
		0.5	164
	-20°	1.5	165
		1.0	165
		0.5	165
	-30°	1.5	166
		1.0	166

The loading curves and arrows corresponding to the upper side of the roof are drawn in full lines. Those corresponding to the under side are drawn in broken lines.

The total load is in magnitude and direction equal to the distance from the broken line curve to the full line curve.

In the Figures the factors C for the resulting wind load on each of the two roof sections and their distances from the centre line of the roof are also given.



Figs. 157 to 166. Free trough and pitched roofs.

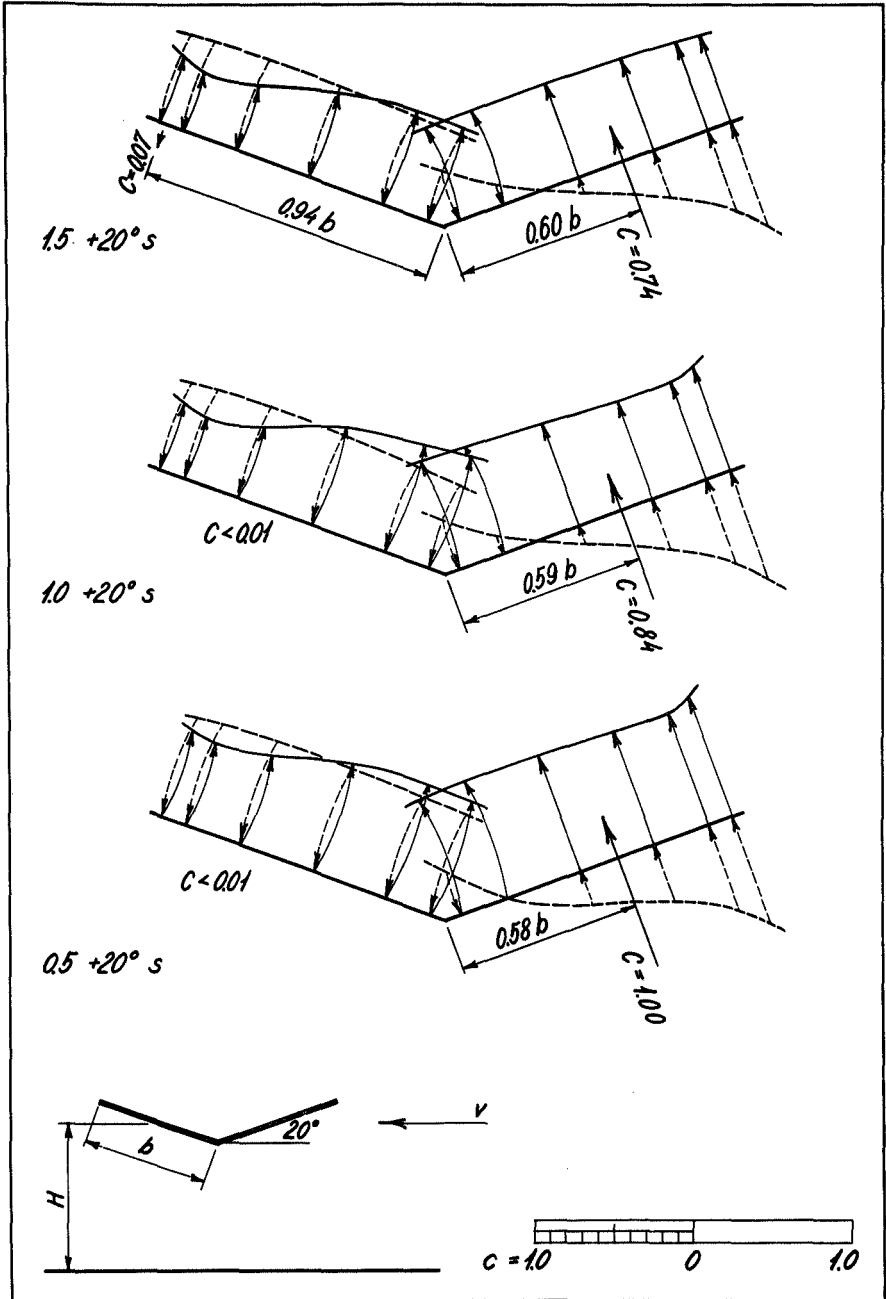
The key is  $H/b$ ,  $\alpha$ , turbulence.  $H$  is the mean height of the roof,  $b$  is the width of one part of the roof,  $\alpha$  is the roof slope, positive for trough roofs and negative for pitched roofs. The turbulence is in all cases small =  $s$  ( $z_0 = 1.8 \cdot 10^{-3}$  cm).

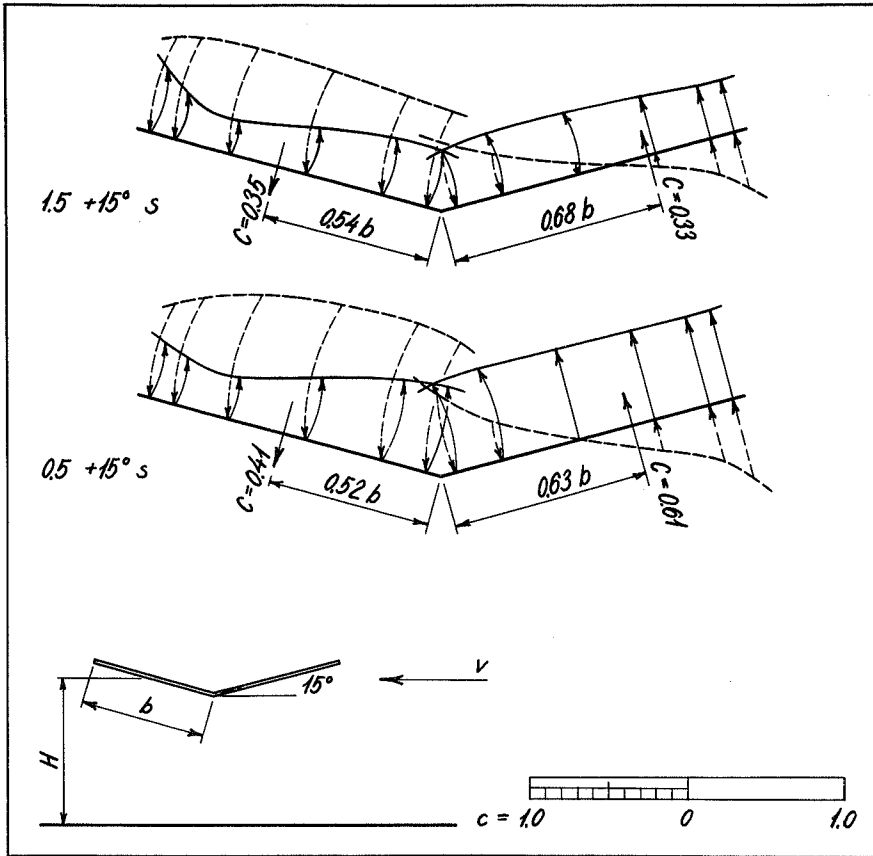
Full line curves and arrows correspond to the upper side of the roof. The arrows go from the roof surface to the curve. Broken line curves and arrows correspond to the under side of the roof. The arrows go from the curve to the roof surface.

The total load is equal in magnitude and direction to the distance from the broken line curve to the full line curve.

When the loads on the two sides of the roof are in opposite directions the arrows are curved for clarity.

$C$  is the factor for the resulting wind load on the roof, and  $e$  gives its distance from the centre line of the roof.





Figs. 157 to 166. Free trough and pitched roofs.

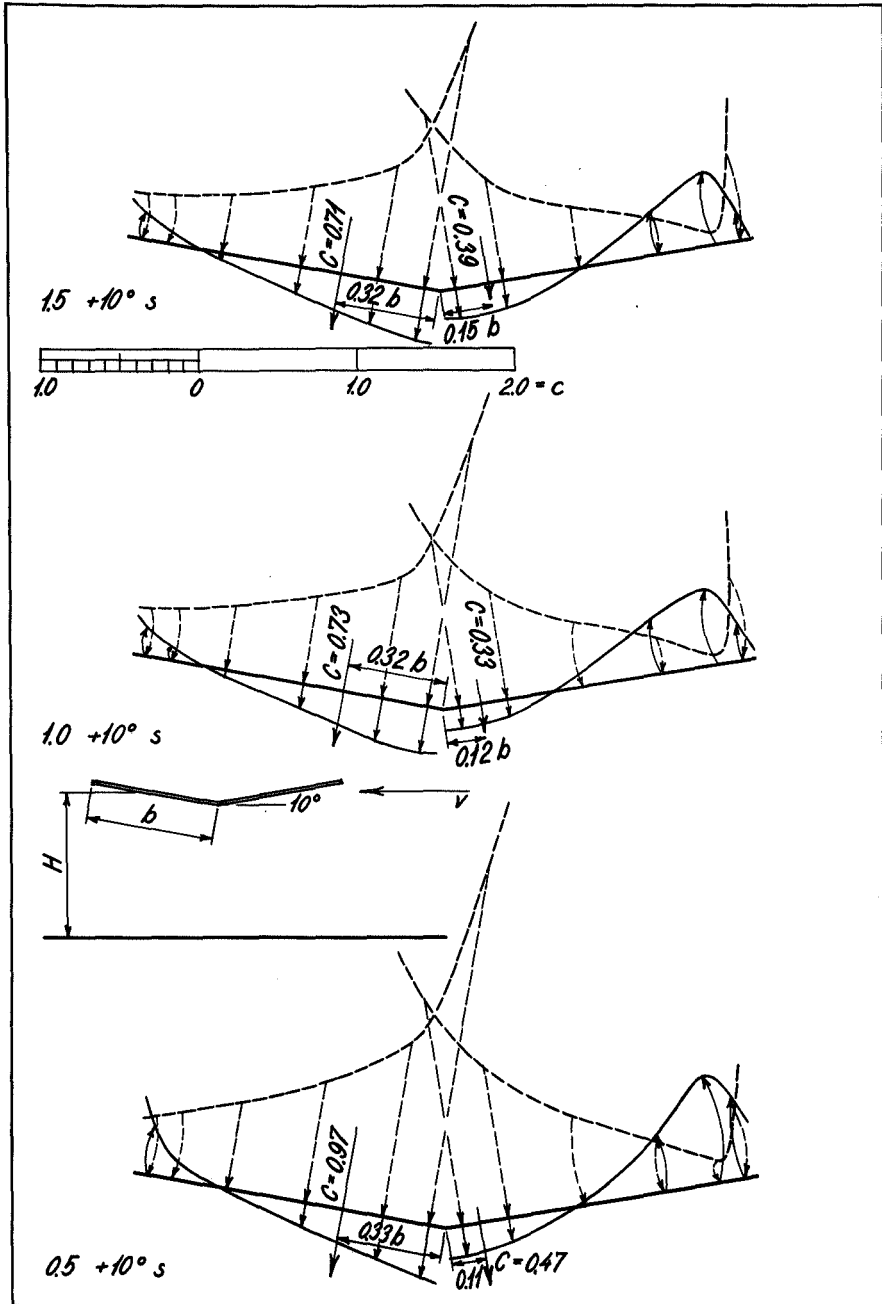
The key is  $H/b$ ,  $\alpha$ , turbulence.  $H$  is the mean height of the roof,  $b$  is the width of one part of the roof,  $\alpha$  is the roof slope, positive for trough roofs and negative for pitched roofs. The turbulence is in all cases small =  $s$  ( $z_0 = 1.8 \cdot 10^{-3}$  cm).

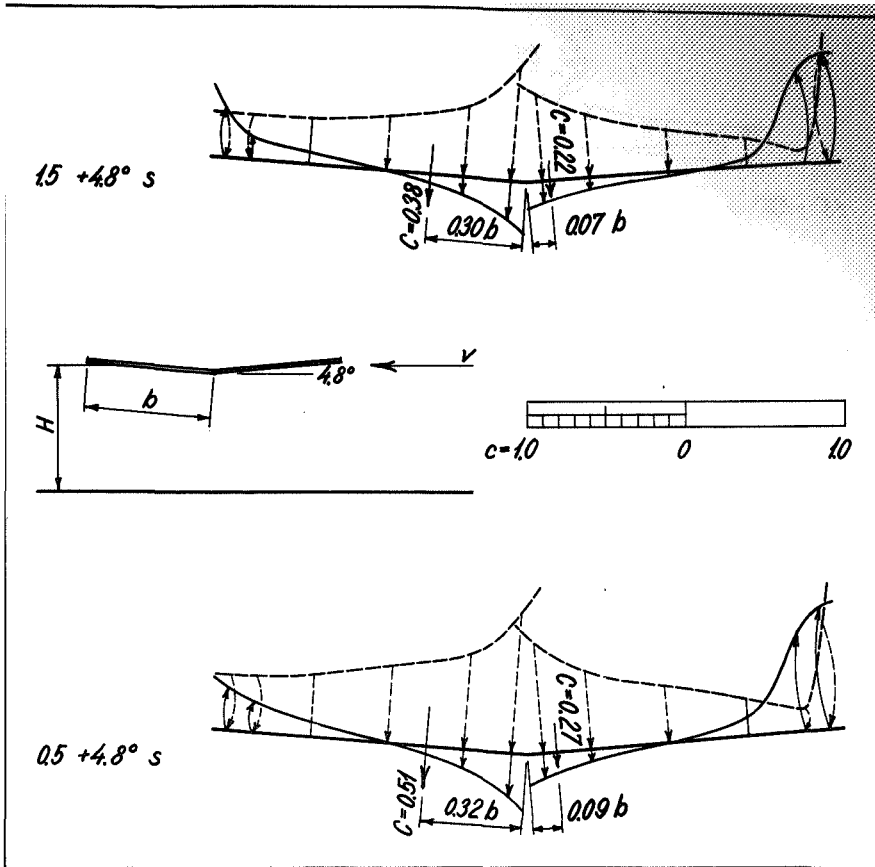
Full line curves and arrows correspond to the upper side of the roof. The arrows go from the roof surface to the curve. Broken line curves and arrows correspond to the under side of the roof. The arrows go from the curve to the roof surface.

The total load is equal in magnitude and direction to the distance from the broken line curve to the full line curve.

When the loads on the two sides of the roof are in opposite directions the arrows are curved for clarity.

$C$  is the factor for the resulting wind load on the roof, and  $e$  gives its distance from the centre line of the roof.





Figs. 157 to 166. Free trough and pitched roofs.

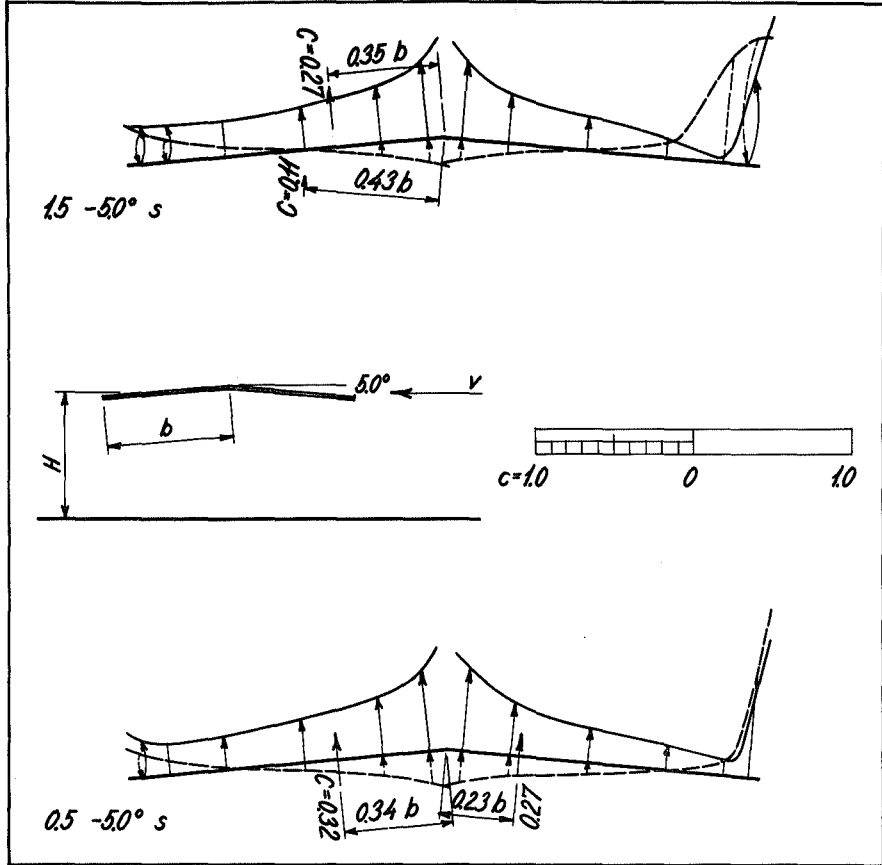
The key is  $H/b$ ,  $\alpha$ , turbulence.  $H$  is the mean height of the roof,  $b$  is the width of one part of the roof,  $\alpha$  is the roof slope, positive for trough roofs and negative for pitched roofs. The turbulence is in all cases small =  $s$  ( $z_0 = 1.8 \cdot 10^{-3}$  cm).

Full line curves and arrows correspond to the upper side of the roof. The arrows go from the roof surface to the curve. Broken line curves and arrows correspond to the under side of the roof. The arrows go from the curve to the roof surface.

The total load is equal in magnitude and direction to the distance from the broken line curve to the full line curve.

When the loads on the two sides of the roof are in opposite directions the arrows are curved for clarity.

$C$  is the factor for the resulting wind load on the roof, and  $e$  gives its distance from the centre line of the roof.



Figs. 157 to 166. Free trough and pitched roofs.

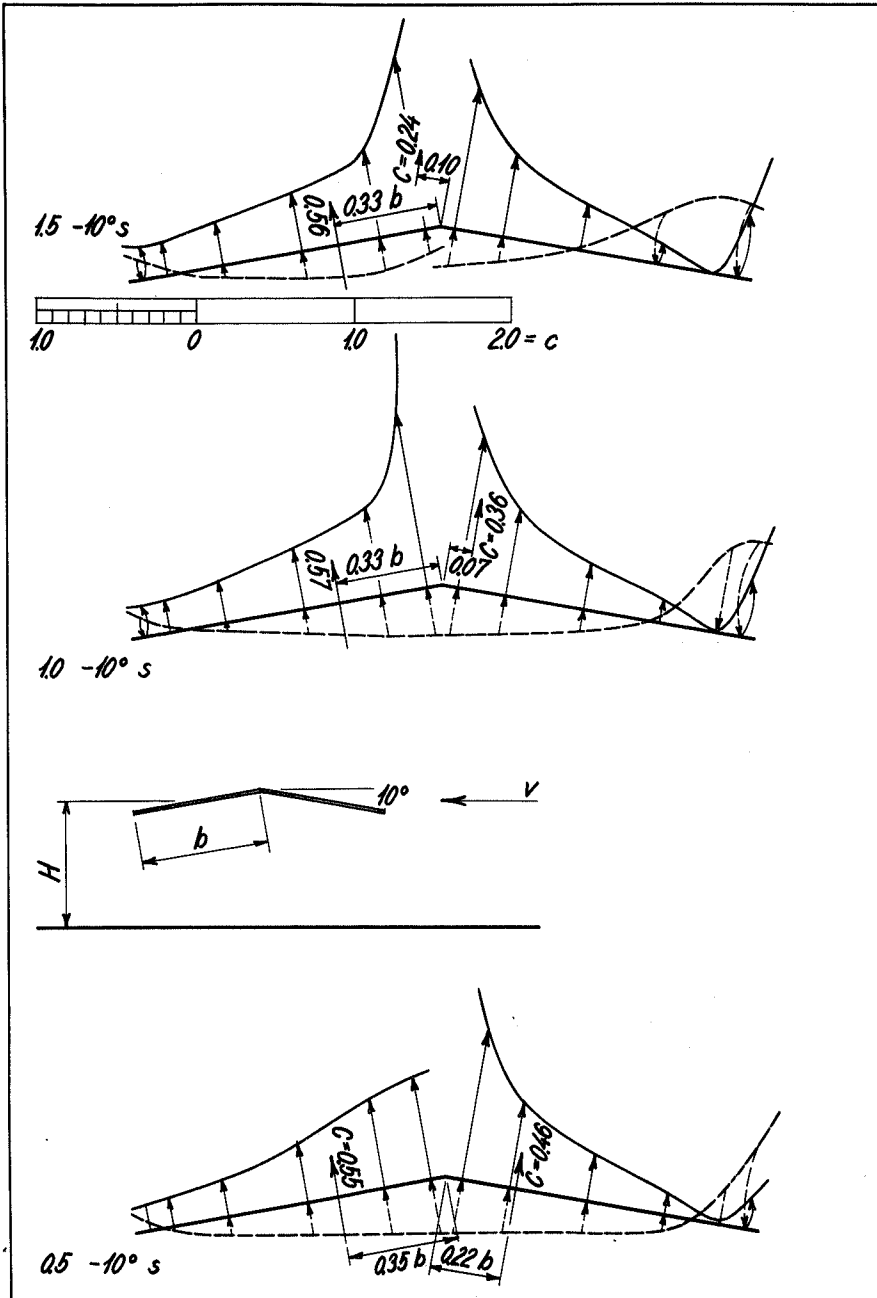
The key is  $H/b$ ,  $\alpha$ , turbulence.  $H$  is the mean height of the roof,  $b$  is the width of one part of the roof,  $\alpha$  is the roof slope, positive for trough roofs and negative for pitched roofs. The turbulence is in all cases small =  $s$  ( $z_0 = 1.8 \cdot 10^{-3}$  cm).

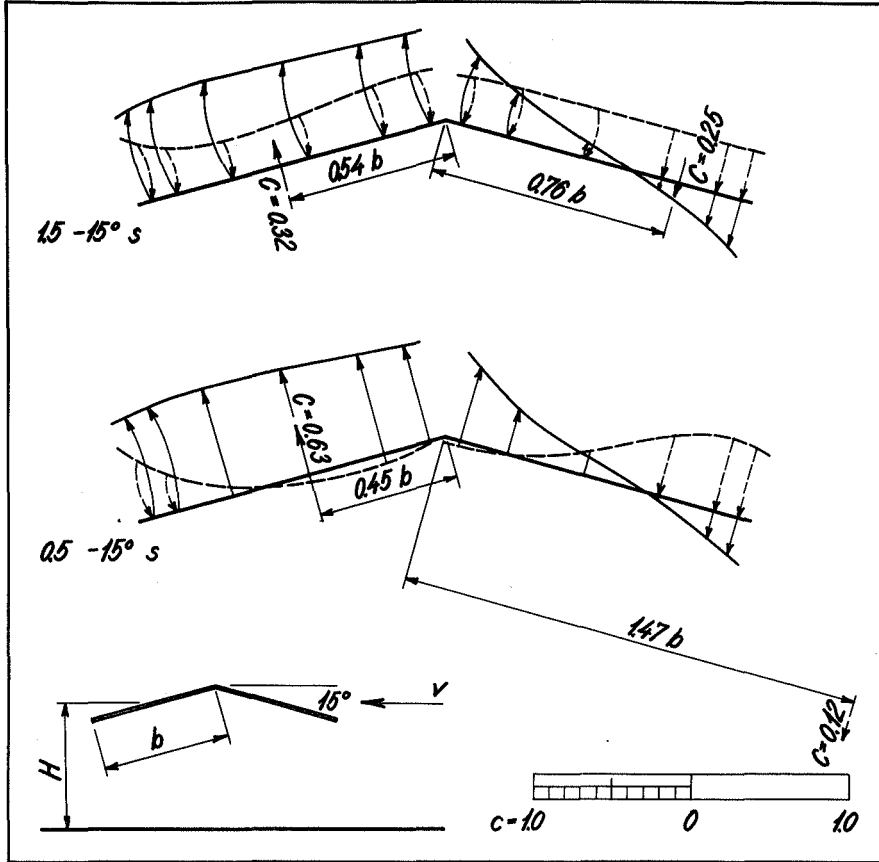
Full line curves and arrows correspond to the upper side of the roof. The arrows go from the roof surface to the curve. Broken line curves and arrows correspond to the under side of the roof. The arrows go from the curve to the roof surface.

The total load is equal in magnitude and direction to the distance from the broken line curve to the full line curve.

When the loads on the two sides of the roof are in opposite directions the arrows are curved for clarity.

$C$  is the factor for the resulting wind load on the roof, and  $e$  gives its distance from the centre line of the roof.





Figs. 157 to 166. Free trough and pitched roofs.

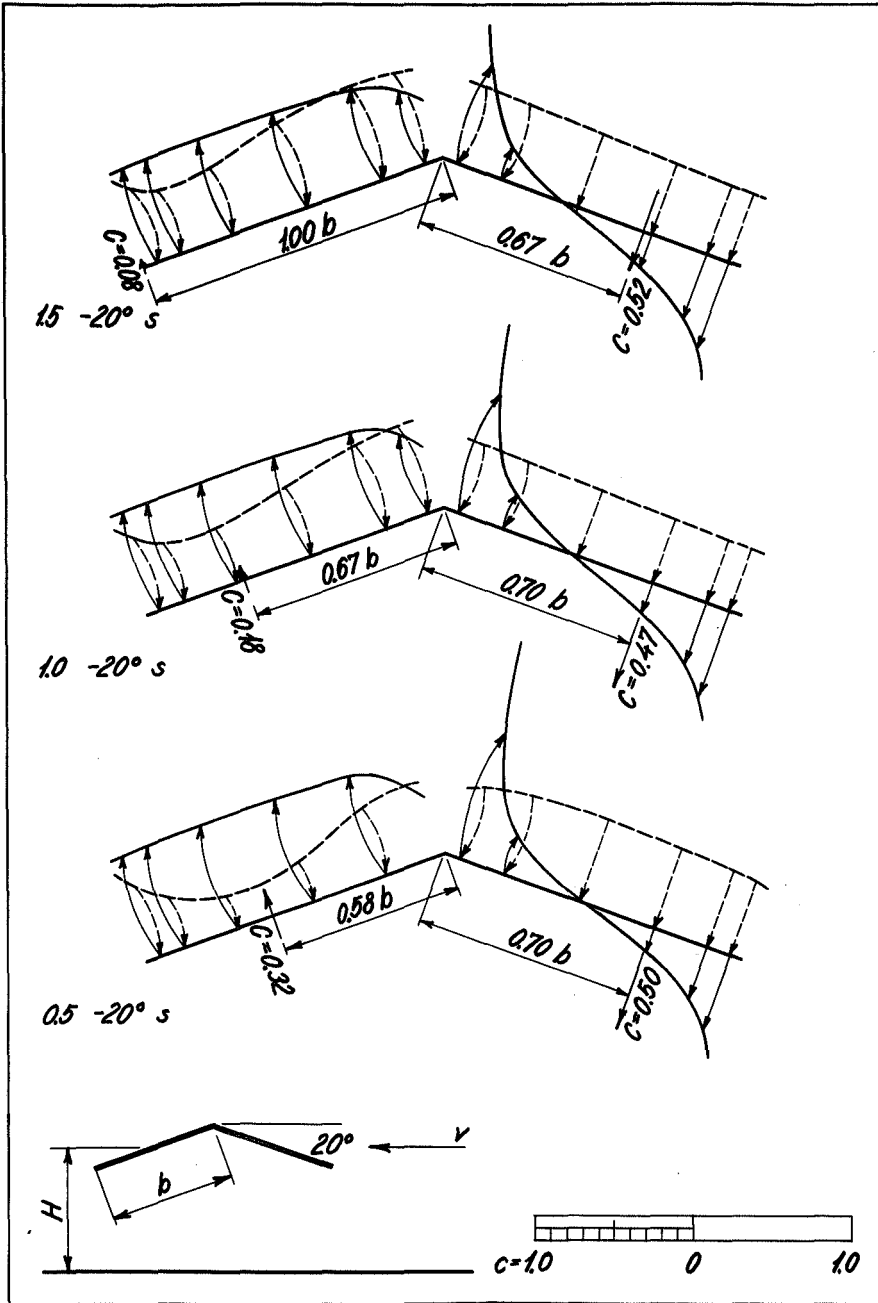
The key is  $H/b$ ,  $\alpha$ , turbulence.  $H$  is the mean height of the roof,  $b$  is the width of one part of the roof,  $\alpha$  is the roof slope, positive for trough roofs and negative for pitched roofs. The turbulence is in all cases small =  $s$  ( $z_0 = 1.8 \cdot 10^{-3}$  cm).

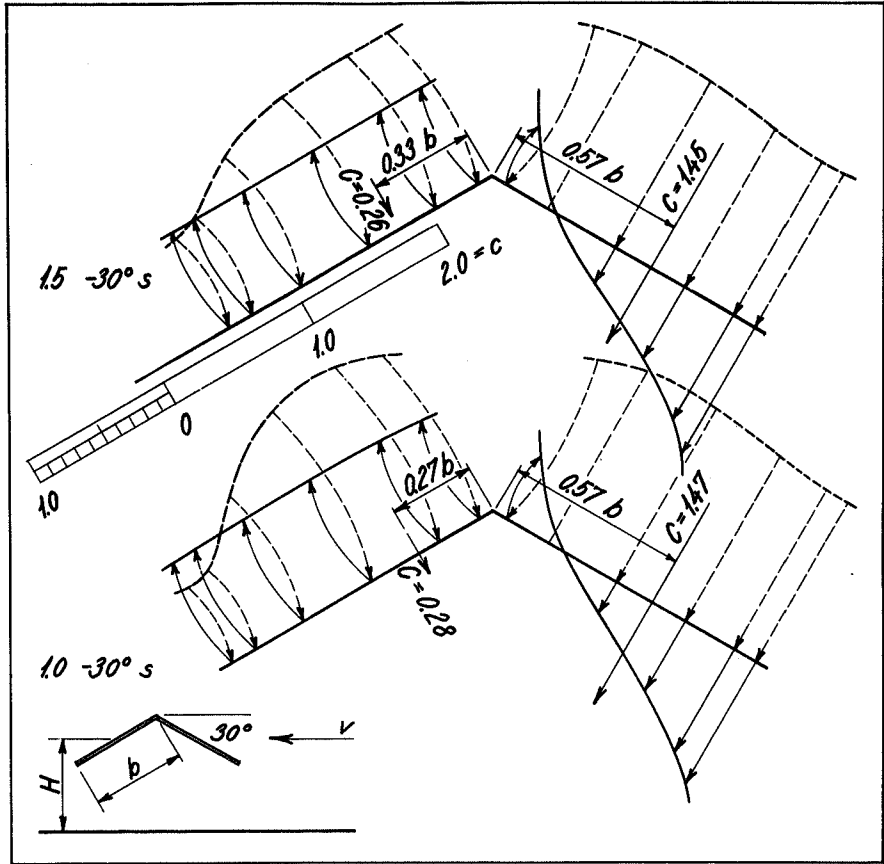
Full line curves and arrows correspond to the upper side of the roof. The arrows go from the roof surface to the curve. Broken line curves and arrows correspond to the under side of the roof. The arrows go from the curve to the roof surface.

The total load is equal in magnitude and direction to the distance from the broken line curve to the full line curve.

When the loads on the two sides of the roof are in opposite directions the arrows are curved for clarity.

$C$  is the factor for the resulting wind load on the roof, and  $e$  gives its distance from the centre line of the roof.





Figs. 157 to 166. Free trough and pitched roofs.

The key is  $H/b$ ,  $\alpha$ , turbulence.  $H$  is the mean height of the roof,  $b$  is the width of one part of the roof,  $\alpha$  is the roof slope, positive for trough roofs and negative for pitched roofs. The turbulence is in all cases small =  $s$  ( $z_0 = 1.8 \cdot 10^{-3}$  cm).

Full line curves and arrows correspond to the upper side of the roof. The arrows go from the roof surface to the curve. Broken line curves and arrows correspond to the under side of the roof. The arrows go from the curve to the roof surface.

The total load is equal in magnitude and direction to the distance from the broken line curve to the full line curve.

When the loads on the two sides of the roof are in opposite directions the arrows are curved for clarity.

$C$  is the factor for the resulting wind load on the roof, and  $e$  gives its distance from the centre line of the roof.

### 10.3 Conclusions

In Figures 168 and 169 the results are shown. The abscissa is the roof slope,  $\alpha$ , positive for trough roofs and negative for saddle roofs. The curves and the circular points correspond to  $H/b = 1.0$ . Square points correspond to  $H/b = 1.5$  and triangular points to  $H/b = 0.5$ .

In Figure 168 the factor  $C$  for the resulting wind load is ordinate.

In Figure 169 the ordinate is the factor  $E$  for the moment of the wind load about the centre line of the roof;  $E = Ce$  where  $e$  is the dimensionless distance of  $C$  from the centre. The moment is taken as positive, when it produces tension in the under side of the roof.

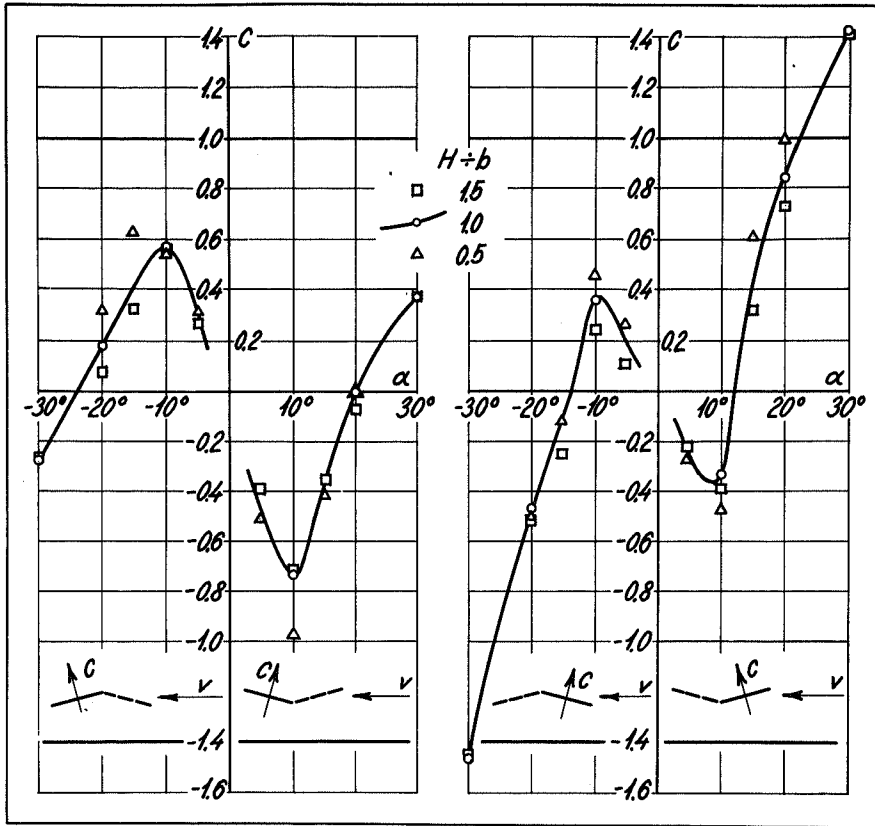


Fig. 168. Free trough and pitched roofs.

The abscissa is the roof slope  $\alpha$ , positive for trough roofs and negative for pitched roofs.

The ordinate is the factor  $C$  for the resulting wind load.  $C$  is positive when its vertical component acts upwards.

The diagram to the left shows the conditions at the leeward roof section. The diagram to the right corresponds to the windward roof section.

The curves and the circular points correspond to  $H/b = 1.0$ .  $H$  is the mean height of the roof. Square points correspond to  $H/b = 1.5$  and triangular points to  $H/b = 0.5$ .

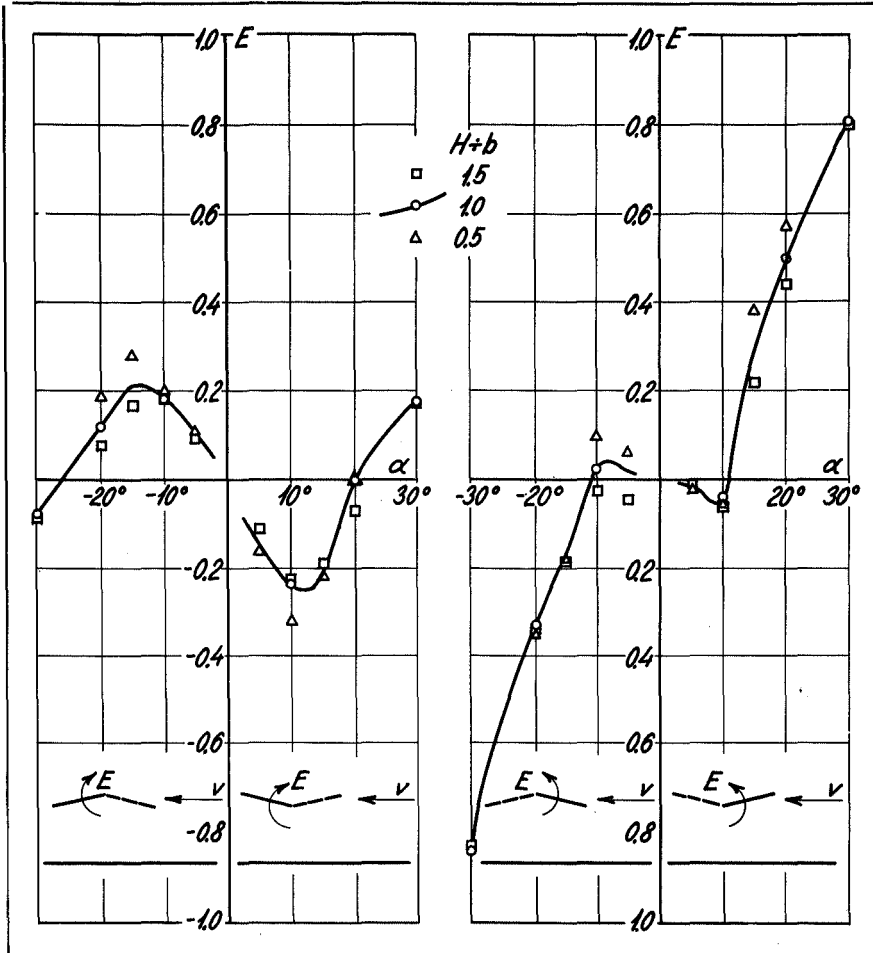


Fig. 169. Free trough and pitched roofs.

The abscissa is the roof slope  $\alpha$ , positive for trough roofs and negative for pitched roofs.

The ordinate is the factor  $E$  for the moment of the wind load about the centre line of the roof.  $E$  is positive when it produces tension in the under side of the roof.

The diagram to the left shows the conditions at the leeward roof section. The diagram to the right corresponds to the windward roof section.

The curves and the circular points correspond to  $H/b = 1.0$ .  $H$  is the mean height of the roof. Square points correspond to  $H/b = 1.5$  and triangular points to  $H/b = 0.5$ .

## **BIBLIOGRAPHY**

- JENSEN, MARTIN and NIELS FRANCK: Model-Scale Tests in Turbulent Wind, Part I. Copenhagen 1963.
- JENSEN, MARTIN: The Model-Law for Phenomena in Natural Wind. - Ingeniøren, International Edition, Vol. 2, No. 4, 1958.
- IRMINGER, J.O.V. and CHR. NØKKENTVED: Wind-Pressure on Buildings. 1. Series..- Ingeniørvidenskabelige Skrifter, A Nr. 23, København 1930.
- IRMINGER, J.O.V. and CHR. NØKKENTVED: Wind-Pressure on Buildings. 2. Series. - Ingeniørvidenskabelige Skrifter, A Nr. 42, København 1936.